

**An investigation of the mechanisms of
piperazine resistance in
Plasmodium falciparum malaria**



Megan Rose Ansbro
King's College
University of Cambridge

This dissertation is submitted for the degree of
Doctor of Philosophy

September 2019

Declaration

I hereby declare that this dissertation is the result of my own work and includes nothing which is the outcome of work done in collaboration except as specified in the text. It is not substantially the same as any work that I have submitted, or, is being concurrently submitted for a degree or diploma or other qualification at the University of Cambridge or any other University or similar institution. I further state that no substantial part of my dissertation has already been submitted, or, is being concurrently submitted for any such degree, diploma or other qualification at the University of Cambridge or any other University or similar institution. This dissertation does not exceed the prescribed 60,000 word limit for the Biology Degree Committee.

Abstract

An investigation of the mechanisms of piperazine resistance in *Plasmodium falciparum* malaria

Megan Rose Ansbro

Antimalarial drug resistance is an unrelenting obstacle to malaria control programs. In Southeast Asia (SEA), parasites have developed some degree of resistance to nearly every malaria drug currently available, with the most recent emergence to artemisinin combination therapies (ACTs). ACTs are the recommended front-line treatments for *Plasmodium falciparum* malaria worldwide and decreased susceptibility of parasites to both artemisinin and one of the widely used partner drugs, piperazine, have been reported in multiple locations in SEA. It is therefore necessary to have reliable methods for detecting and evaluating resistant phenotypes. The purpose of this study was to combine clinical data from Cambodia with findings from genomic studies to evaluate putative markers of piperazine resistance. The study first developed high-throughput assays to reliably detect one of these markers, a copy number variation (CNV) in the *plasmepsin 2* and *plasmepsin 3* (*PM2-PM3*) genes, in parasites likely to be PPQ-resistant. In addition to assay development, this study used gene overexpression techniques and CRISPR-Cas9 gene editing to examine the functional role of molecular markers of piperazine resistance, including the *PM2-3* CNV, and two gene candidates with nonsynonymous single nucleotide polymorphisms (SNPs): a putative exonuclease protein (*exo-E415G*) and a putative mitochondrial carrier protein (*mcp-N252D*). This research fills a knowledge gap in the lack of functional data for molecular markers of piperazine resistance by examining the phenotypic relevance of the genotypes observed in contemporary isolates. To complement these functional studies, this doctoral work has also used a *P. falciparum* hypermutator parasite line to select for a piperazine-resistant phenotype *in vitro*. Whole genome sequencing analysis (WGS) of the piperazine-resistant lines obtained through these experiments has identified nonsynonymous SNPs in gene candidates that have been reported to play a role in antimalarial drug resistance, including SNPs in the chloroquine resistance transporter gene (*pfert*) and the multidrug resistant protein 1 (*pfmdr1*) transporter. SNPs in *pfert* have been reported to confer piperazine resistance in the field and *in vitro* and our recent drug-pressure experiments provide additional evidence to support these findings. The WGS analysis also discovered novel SNPs in gene candidates not previously reported to modulate the piperazine-resistant phenotype that will require further evaluation. Such work has enabled the possibility of examining whether genetic changes observed in patient isolates can also be investigated and observed *in vitro*. By combining functional molecular approaches with genomic analyses, this study provides new insights into the mechanisms of piperazine resistance.

To my parents, grandparents, & Uncle Gene

Acknowledgements

I have been lucky enough to have support that spans three continents while performing my thesis work. In all the writing I have done these past couple of months (or years), this section has been the hardest to write because it feels like words cannot say “thank you” enough. Nevertheless, I will try.

To Marcus and Tom, the incredible mentors who did not have to be. Thank you for taking me on and for your mentorship and support. I have learned so much while in your labs and I will be forever grateful for the time I’ve been able to learn from you.

To Jeff Thompson and Stu Yuspa, two of my first advisors. Thank you for showing me what’s possible in the world of research and for always believing in me.

Chanaki, friend, colleague, and mentor in all things life. Thank you for showing me how to be an exemplary scientist and person.

Sophie, Brandy, Krittikorn, Manuela, and Alex: you are such inspiring scientists and people. I have learned so much from you all. Thank you for your guidance in lab and for your unending support.

To all of my lab mates in LMVR at the NIH (especially Erin, Kim, and Kristin) and on Teams 226 and 115 at Sanger, thank you for the comradery and for making cell culture enjoyable. Also, a special thank you to Liam Prestwood for ensuring all experiments can run smoothly and safely.

Thank you to all of the staff and patients in Cambodia from the field sites where this study has obtained clinical samples.

To the Gates Cambridge Scholarship, thank you for funding part of my time in Cambridge and also introducing me to an amazing community of fellow scholars and friends.

Many thanks to the amazing administrative support from the teams at LMVR and Sanger, notably Sam Moretz and Wendy Hamm, whose attention to detail is unmatched. To the NIH OxCam and Wellcome Sanger Institute graduate offices, especially Katie Soucy, Katie Stagliano, Annabel Smith, and Christina Hedberg-Delouka. Thank you also to the PaM administrative support team, especially Dee Toombs.

My friends from all over the world, notably Ash, Ingvild, Jess, Kenz, Matt, and Sandi. Thank you for always being there for me and for your optimism through it all!

My brother, Ryan, for his unwavering support, positive attitude, and sense of humor that has, and always will, remind me what is important in life.

To my husband, Levi. You have been with me every step of the way on this PhD journey. Two countries, four apartments, two cats, the highs and the lows—which have been intense on both ends. Through it all, you’ve never faltered and always believed in me and what I’m capable of. You have been a part of every word of this thesis (more literally than you may have liked). Thank you for being my partner in life. On to the next chapter!

Lastly, but certainly not least, thank you to my parents, grandparents, and Uncle Gene, for whom this thesis is dedicated. I wish my grandparents and uncle could be here to see this day, a day they helped make possible long before I even knew how big I could dream. To my mom and dad, you have given me the world. Thank you for everything.

Table of Contents

Declaration	<i>i</i>
Abstract	<i>ii</i>
Acknowledgements	<i>iv</i>
List of Figures	<i>viii</i>
List of Tables	<i>x</i>
Abbreviations	<i>xi</i>
Preface	<i>xiii</i>
Chapter 1: Introduction	<i>1</i>
1.1 Malaria: history, epidemiology, and biology	<i>1</i>
1.1.1 History of malaria	<i>1</i>
1.1.2 Malaria today: global burden and epidemiology.....	<i>3</i>
1.1.3 <i>P. falciparum</i> life cycle	<i>7</i>
1.1.4 Pathogenesis of <i>P. falciparum</i> malaria: asymptomatic, uncomplicated, severe disease	<i>10</i>
1.1.4.1 Uncomplicated <i>P. falciparum</i> malaria	<i>11</i>
1.1.4.2 Severe <i>P. falciparum</i> malaria	<i>13</i>
1.2 Antimalarial chemotherapy	<i>14</i>
1.2.1. Brief history of widely used antimalarial drugs: from monotherapies to combination therapies	<i>14</i>
1.2.1.1 Quinine.....	<i>14</i>
1.2.1.2 Chloroquine.....	<i>16</i>
1.2.1.3 Antifolates: sulfadoxine/pyrimethamine (SP), proguanil	<i>17</i>
1.2.1.4 Artemisinin.....	<i>18</i>
1.2.2.1 Combination therapies in malaria: ACTs.....	<i>19</i>
1.2.2.2 ACTs: dihydroartemisinin-piperaquine.....	<i>21</i>
1.3 Drug-resistance in <i>P. falciparum</i>	<i>23</i>
1.3.1 ACT failures: emergence of artemisinin and partner drug resistance in Cambodia	<i>23</i>
1.3.2 Assessing drug-resistance in <i>P. falciparum</i>	<i>24</i>
1.3.3 The genetic basis of resistance.....	<i>25</i>
1.3.4 The parasite digestive vacuole and antimalarial drugs	<i>26</i>
1.4 Genetic background and mechanisms of resistance in SEA	<i>28</i>
1.4.1 Chloroquine	<i>28</i>
1.4.2 Mefloquine: monotherapy and ACT.....	<i>29</i>
1.4.3 DHA-PPQ: piperaquine resistance in concert with decreased artemisinin susceptibility	<i>30</i>
1.4.4 Piperaquine resistance	<i>31</i>
1.5 Specific aims	<i>34</i>
Chapter 2: General Methodology	<i>35</i>
2.1 Cultivation of <i>Plasmodium falciparum</i>	<i>35</i>
2.1.1 <i>In vitro</i> culture maintenance	<i>35</i>
2.1.2 Determination of parasite culture hematocrit and parasitemia.....	<i>35</i>
2.1.3 Thawing and cryopreservation of parasites.....	<i>37</i>
2.1.4 Synchronization of parasites: sorbitol and Percoll gradients.....	<i>37</i>
2.1.5 Sorbitol synchronization.....	<i>38</i>
2.1.6 Percoll gradients for parasite synchronization	<i>38</i>
2.2 Parasite lines	<i>40</i>
2.2.1 Cambodian field isolates	<i>40</i>
2.2.2 Long-term laboratory-adapted parasite lines.....	<i>42</i>
2.3 Transfection of <i>P. falciparum</i> field isolates and laboratory lines	<i>43</i>
2.3.1 Transfection of <i>P. falciparum</i> using DNA-loaded red blood cells.....	<i>43</i>
2.3.2 Transfection of ring stage <i>P. falciparum</i>	<i>44</i>

2.4 Parasite cloning by limiting dilution	45
2.5 Saponin lysis and genomic DNA extraction from cultivated parasites	45
2.6 <i>In vitro</i> parasite survival assays.....	46
2.6.1 Antimalarial drug preparation.....	46
2.6.2 Drug sensitivity assays	46
2.6.3 Piperaquine survival assays (PSAs)	47
2.7 Quantification of viable parasites using flow cytometry	48
2.8 Molecular cloning techniques.....	50
2.8.1 Transformation of competent bacteria cells.....	50
2.8.2 Plasmid preparation: mini, midi, and maxi preparations	51
2.8.3 Polymerase chain reaction (PCR) protocols	51
2.8.4 DNA sequencing.....	51
<i>Chapter 3: Detection, surveillance, and evaluation of molecular markers of piperaquine resistance: plasmepsin 2-3 copy number assays and functional studies.....</i>	52
3.1 Declaration of work.....	52
3.1.1 Significance and purpose of study.....	52
3.1.2 Introduction.....	53
3.1.3 Objectives.....	55
3.2 Materials and methods	55
3.2.1 Parasite samples.....	55
3.2.2 <i>Plasmepsin 2-3</i> duplication breakpoint PCR assay	56
3.2.3 SYBR green validation of <i>plasmepsin 2-3</i> copy number using quantitative PCR.....	57
3.2.4 Overexpression of <i>PM2</i> and <i>PM3</i>	57
3.2.4.1 Gibson assembly of a <i>PM2</i> -only overexpression plasmid: pDC2-cam- <i>PM2</i> -2A- <i>GFP</i> -bsd-attP.....	58
3.2.4.2 Gibson assembly of the <i>PM2</i> -2A- <i>PM3</i> overexpression plasmid.....	59
3.2.4.3 Determination of drug selection concentration by IC ₅₀ assays	61
3.2.4.4 Use of flow cytometry to screen for pDC2-cam- <i>mRFP</i> -2A- <i>GFP</i> -bsd-attP plasmid in transfected parasites.....	62
3.3 Results.....	63
3.3.1 <i>PM2-3</i> breakpoint assay validation	63
3.3.2 <i>PM2-3</i> breakpoint assay utility in comparison with SYBR green assay.....	65
3.3.3 Analysis of <i>PM2-3</i> copy number in isolates from patients treated with artesunate-mefloquine	66
3.3.4 Overexpression of <i>PM2</i> and <i>PM3</i> in Cambodian isolates.....	67
3.3.4.1 Overexpression of <i>PM2</i> in Cambodian field isolate, 163-KH3-005	67
3.3.4.2 Confirmation of the pDC2-cam- <i>PM2</i> -2A- <i>PM3</i> plasmid and pDC2-cam- <i>mRFP</i> -2A- <i>GFP</i> -bsd-attP plasmid in transfected parasites by flow cytometry and PCR	68
3.4 Discussion and future work.....	70
<i>Chapter 4: Examination of the role of single nucleotide polymorphisms in an exonuclease protein and mitochondrial carrier protein in piperaquine resistance.....</i>	75
4.1 Declaration of work.....	75
4.1.1 Significance and purpose of study.....	75
4.1.2 Introduction.....	76
4.1.3 Objectives.....	81
4.2 Materials and methods	81
4.2.1 CRISPR-Cas9 mediated genome editing: two-plasmid system.....	81
4.2.1.1 Exonuclease <i>exo</i> -415 SNP editing plasmids	81
4.2.1.2 Two-plasmid system: cloning of the gRNA and donor plasmids.....	82
4.2.2 CRISPR-Cas9 mediated genome editing: single plasmid system.....	83
4.2.3 Transfection of CRISPR-Cas9 <i>exo</i> -415 and <i>mcp</i> -252 plasmids.....	84
4.2.4 Screening for integration of the <i>exo</i> - and <i>mcp</i> -SNPs in transfected parasites	85

4.2.4 Drug sensitivity assays	86
4.3 Results.....	86
4.3.1 CRISPR-Cas9 editing of the exonuclease-415 SNPs: low transfection efficiency in field isolates...	86
4.3.2 CRISPR-Cas9 editing of the mitochondrial carrier protein-252 SNPs: low transfection efficiency in field isolates and successful editing in Dd2 parasites	88
4.3.3 Drug susceptibility profiles of the edited exonuclease and mitochondrial carrier protein SNPs in Dd2-edited parasite lines.....	91
4.3.3.1 The exo-E415G SNP does not alter parasite susceptibility to common antimalarial drugs.....	91
4.3.3.2 The mcp-N252D SNP does not alter parasite susceptibility to common antimalarial drugs	92
4.3.3.3 The exo-E415G and mcp-N252D SNPs do not alter parasite survival in piperazine survival assays	92
4.4 Discussion and future work.....	95
<i>Chapter 5: Discovery of molecular markers of piperazine resistance by in vitro drug-pressure of a hypermutator Plasmodium falciparum line.....</i>	100
5.1 Declaration of work.....	100
5.1.1 Significance and purpose of study.....	100
5.1.3 Objectives.....	105
5.2 Materials and methods	105
5.2.1 Hypermutator parasites: <i>P. falciparum</i> Dd2-polymerase δ mutants.....	105
5.2.2 Experimental design for selection of piperazine resistant Dd2-hypermutator parasites: IC ₅₀ assays and selection procedures	106
5.2.3 Preparation of PPQ-pressured parasites for whole genome sequencing analysis: cloning and genomic DNA extraction	107
5.2.4 Whole genome sequencing analysis.....	107
5.3 Results.....	108
5.3.1 Selection of piperazine-resistant Dd2-hypermutator parasites.....	108
5.3.2 Phenotypic characterization of the piperazine-pressured Dd2-polymerase δ mutant parasites	110
5.3.2.1 IC ₅₀ survival assays of piperazine-pressured Dd2-polymerase δ mutant parasites	110
5.3.2.2 Morphological differences between the PPQ-pressured parasites and the parental hypermutator line	111
5.3.3 Whole genome sequencing analysis and genetic characterization of the PPQ-pressured Dd2-hypermutator parasites.....	112
5.4 Discussion and future work.....	113
<i>Chapter 6: What's next on the resistance front? Conclusions, reflections, and future work</i>	118
<i>References.....</i>	124

List of Figures

Figure 1. 1. The global distribution of malaria in the 20th century.....	5
Figure 1. 2. The global incidence of <i>P. falciparum</i> and <i>P. vivax</i> malaria in 2017.....	5
Figure 1. 3. The life cycle of <i>P. falciparum</i>	8
Figure 1. 4. The asexual and sexual intraerythrocytic life cycles of <i>P. falciparum</i> . A.) The 48-hour life cycle of <i>P. falciparum</i>	9
Figure 1. 5. Microscopy-based malaria diagnosis is the gold standard in all malaria endemic countries...13	
Figure 1. 6. Structural similarities of antimalarial drugs.....	21
Figure 1. 7. Antimalarial drugs depicted with their proposed mechanism of action in the erythrocytic (asexual) blood stage of <i>P. falciparum</i>	22
Figure 1. 8. Timeline of antimalarial drug use for the treatment of <i>P. falciparum</i> malaria in Cambodia... ..	24
Figure 1. 9. Transmission electron microscopy of <i>P. falciparum</i> infected erythrocytes.....	33
Figure 2. 1. Schematic of Percoll gradients.....	40
Figure 2. 2. Map of Cambodia highlighting the three provinces where samples were collected during clinical trials.....	42
Figure 2. 3. Schematic for IC ₅₀ drug assay 96-well plate layout.....	47
Figure 2. 4. PSA 48-well plate setup.....	48
Figure 2. 5. Flow cytometry quantification of parasitemia using SYBR Green I and MitoTracker Deep Red.....	50
Figure 3. 1. Whole genome sequencing data displaying average coverage on chromosome 14 for isolate 163-KH1-004 (PH1345_C) as viewed using the LookSeq browser.....	56
Figure 3. 2. Plasmid design and assembly for overexpression of <i>plasmepsin 2</i> (<i>PM2</i>).....	59
Figure 3. 3. Plasmid design and assembly for overexpression of <i>PM2</i> and <i>PM3</i>	61
Figure 3. 4. Dose-response curve for field isolate 163-KH3-005 after 72-hour exposure to blasticidin (BSD).....	62
Figure 3. 5. Schematic of <i>plasmepsin 2-3</i> gene duplication.....	64
Figure 3. 6. Comparison of the breakpoint PCR and qPCR assays for measuring <i>PM2-3</i> copy numbers.. ..	66
Figure 3. 7. Proportion of samples with >1 copy or 1 copy of <i>PM2-3</i> as determined by breakpoint PCR analysis in 3 Cambodian provinces from 2014-2015.....	67
Figure 3. 8. Transgenic piperazine-sensitive parasites (005) carrying the <i>PM2</i> overexpression plasmid showed no shift in PPQ IC ₅₀ values.....	68
Figure 3. 9. Flow cytometry assessment of transgenic parasites.. ..	69
Figure 3. 10. PCR confirmation of the <i>PM2-2A-PM3</i> plasmid in transfected 005 and Dd2 parasites. PCR confirmation that the pDC2- <i>cam</i> plasmid backbone was present in transfections.....	69
Figure 4. 1. Prevalence of the <i>PM2-3</i> copy number amplification and <i>exo-E415G</i> SNP in three provinces in Cambodia from 2012-2015.	79
Figure 4. 2. Two-plasmid system for CRISPR-Cas9 editing of the exonuclease SNP.....	83
Figure 4. 3. All-in-one pDC2- <i>cam</i> -coCas9-U6-hDHFR plasmid.	84
Figure 4. 4. Primers for PCR screening of transfectants for integration of the desired locus on chromosome 13.....	86
Figure 4. 5. Sequencing analysis of the <i>exo</i> -SNP field isolate transfections that recrudesced.. ..	88
Figure 4. 6. Sequencing analysis of the <i>mcp</i> -SNP field isolate transfection post-recrudescence.....	90
Figure 4. 7. Sequencing analysis of the Dd2- <i>mcp</i> -SNP transfections.....	91
Figure 4. 8. The <i>exo-E415G</i> SNP has no effect on IC ₅₀ values or susceptibility to PPQ and other commonly used antimalarial drugs.....	93
Figure 4. 9. The <i>mcp-N252D</i> SNP has no effect on IC ₅₀ values or susceptibility to PPQ and other commonly used antimalarial drugs.	94
Figure 4. 10. The Dd2 transgenic <i>exo-E415G</i> and <i>mcp-N252D</i> edited SNPs have no effect on parasite survival to PPQ in piperazine survival assays (PSAs).	95
Figure 5. 1. Alignment of the DNA polymerase δ amino acid sequence highlighting the conserved residues in the 3'→5'exonuclease domain.....	105

Figure 5. 2. Determination of PPQ concentration to use for selection of PPQ-resistant Dd2-polymerase δ mutant parasites	107
Figure 5. 3. Initial attempt (experiment 1) for selection of piperazine (PPQ)-resistant Dd2-hypermulator parasite lines	108
Figure 5. 4. Second attempt (experiment 2) for selection of piperazine (PPQ)-resistant Dd2-hypermulator parasite lines.....	109
Figure 5. 5. Comparison of PPQ susceptibility between the parental Dd2-polymerase δ hypermutator parasite and the PPQ-pressured lines.....	111
Figure 5. 6. Morphological difference between the parental Dd2-polymerase δ hypermutator parasite and a PPQ-pressured line	112

List of Tables

Table 2. 1 Summary of Cambodian field isolates and laboratory strains used in this study	41
Table 3. 1 Primers for the development of <i>PM2-PM3</i> overexpression plasmids.....	60
Table 4. 1 Top GWAS candidate SNPs associated with increased piperazine IC50 values	78
Table 4. 2 gRNA sequences in the donor plasmids for the <i>exo-415</i> and <i>mcp-252</i> CRISPR-Cas9 plasmids	82
Table 4. 3 Primers used to screen for integration of SNPs.....	86
Table 4. 4 CRISPR-Cas9 transfections and outcomes of <i>exo-415</i> SNP editing experiments in Cambodian field isolates.....	87
Table 4. 5 CRISPR-Cas9 transfections and editing efficiency of the <i>mcp-252</i> SNPs in Cambodian field isolates and <i>Dd2</i>	89
Table 5. 1 Non-synonymous SNPs discovered in the PPQ-pressured <i>Dd2</i> -hypermutator lines	113

Abbreviations

ACT	Artemisinin Combination Therapy
AQ	amodiaquine
AS	artesunate
bp	base pair
BSD	blasticidin
CNV	copy number variation
CPDA	citrate-phosphate-dextrose-adenine
CQ	chloroquine
CRISPR	Clustered Regularly Interspaced Short Palindromic Repeats
DHA	dihydroartemisinin
DV	digestive vacuole
exo-E415G	exonuclease SNP, E415G
FNT	formate-nitrite transporter
gRNA	guide RNA
GWAS	genome-wide association study
Hb	hemoglobin
hDHFR	human dihydrofolate reductase
IC50	inhibitory concentration assay
iRBCs	parasite-infected red blood cells
K13	kelch13
ldh	lactate dehydrogenase
LUM	lumefantrine
mcp-N252D	mitochondrial carrier protein SNP, N252D
MQ	mefloquine
MRP2	multidrug resistance-associated protein 2
NHEJ	non-homologous end joining
PCR	polymerase chain reaction
PfCRT	chloroquine resistance transporter
PfMDR1	multidrug resistance protein 1
PM2	plasmepsin 2
PM3	plasmepsin 3
PPQ	piperaquine
PPQ-R	piperaquine-resistant
PPQ-S	piperaquine-sensitive
pRBCs	packed red blood cells
PSA	piperaquine survival assay
RBC	red blood cell
RSA	ring stage survival assay
SD	standard deviation
SEA	Southeast Asia
SNP	single nucleotide polymorphism
TACT	Triple Artemisinin Combination Therapy
TRAC	Tracking Resistance to Artemisinin Collaboration

uRBCs
WGS
WWARN

uninfected red blood cells
whole genome sequencing
Worldwide Antimalarial Research Network

Preface

How does a disease that we have known about for thousands of years—for which we have cures—still cause nearly half a million deaths each year? This question has driven the entirety of this thesis project. By focusing on one facet of the complex problem, the intricate biology of the malaria parasite, this doctoral dissertation attempts to provide insight into the role that drug resistance plays in the treatment of *Plasmodium falciparum* malaria. Though the goal of this work was never to answer the overarching question explicitly, it continues to hold the larger perspective and impact of this devastating disease at the forefront of this research.

Chapter 1: Introduction

1.1 Malaria: history, epidemiology, and biology

Malaria is a parasitic infectious disease that has plagued humans, amongst other species, for millennia. Despite this long history and global efforts to eradicate the disease, 435,000 thousand people died of complications caused by malaria in 2017 and an estimated 3.2 billion people—roughly half of the people on earth—are at risk of infection (World Health Organization, 2018). Though these statistics might suggest otherwise, malaria is a *treatable* disease that can be cured. However, one of the greatest obstacles to malaria elimination is the ability of the malaria parasite, *Plasmodium*, to develop drug resistance and evade death by antimalarial chemotherapy (Menard and Dondorp, 2017). This thesis aims to provide insight into the biological mechanisms of drug resistance in the malaria parasite. With a focus on malaria in Southeast Asia, this work combines clinical and functional genetic studies to elucidate molecular modes of resistance to the widely-used antimalarial drug, piperazine.

1.1.1 History of malaria

Malaria is caused by a unicellular protozoan parasite of the genus, *Plasmodium*. The parasite is from a larger group of eukaryotic organisms in the phylum, *Apicomplexa*. *Plasmodium* are some of the most promiscuous parasites on our planet, with over a hundred *Plasmodium* species known to infect a diverse array of mammals, reptiles, and birds (Levine, 1988, Schlagenhauf, 2004). The malaria species that infect humans today are believed to have originated as zoonotic diseases that were transmitted from non-human primates to humans in Africa and spread with human migrations throughout the world (Carter and Mendis, 2002, Bruce-Chwatt, 1965). Today, more species of malaria infect primates than any other mammalian orders (Cox, 2010, Garnham, 1996). Six of those *Plasmodium* species infect humans: *P. falciparum*, *P. vivax*, *P. ovale* (recent work has distinguished two distinct species of *P. ovale* that infect humans (Sutherland et al., 2010)), *P. malariae*, and *P. knowlesi*. Though exact dates of transmission to humans is unknown, evidence of malaria-like symptoms have been present in human civilizations for centuries (Carter and Mendis, 2002) and more recently, detection of *Plasmodium* antigens in remains from antiquity have provided further affirmation of written accounts (Miller et al., 1994, Abbott, 2001).

Early descriptions of malaria can be found in writings and artifacts from civilizations in Mesopotamia, India, China, Egypt, Greece, and Rome (Bruce-Chwatt, 1988). Over 2,000 years ago in India, the *Atharvaveda* scripts described the periodic fevers of what was very likely malaria and bestowed upon it the title “king of diseases” (Kaur and Singh, 2017). The oldest book of medicine from China, the *Nei Ching* or “Canon of Medicine”, describes both the fevers and enlarged spleens of what was likely malaria-infected individuals. In 400 BC, Hippocrates was one of the first to write, in detail, about the paroxysmal fevers of malaria and associated malaria with the air—as were most ailments attributed at that time. Diseases that were then invisible to the naked eye were believed to be caused by “miasma,” a poisonous vapor in the air, often believed to emanate from swamps and decaying matter. Hippocrates associated certain environments and seasons with fevers that he described as “tertian” (*P. falciparum*/*P. vivax*/*P. ovale*, for which fevers recur every third day), “quartan” (*P. malariae*, fevers return every fourth day), or “intermittent.” He also recorded the strong association of splenomegaly with the disease (Bruce-Chwatt, 1988). This almost ethereal association of malaria with the air infiltrated civilizations for centuries, much like an actual noxious substance would, earning the disease its name, “*mal’aria*” or “bad air” amongst the citizens of Rome in the 1600s (Hempelmann and Krafts, 2013). Though incorrectly attributing malaria to vapors from foul-smelling swamp waters, they astutely connected the importance of stagnant water and time of year to the disease (Cunha and Cunha, 2008).

It was not until centuries later during the Golden Age of Microbiology in the 1800s, that the capabilities for identifying the causal agent of malaria emerged (Maloy and Schaechter, 2006). The long-searched for culprit of the disease was discovered in 1880 by French army doctor, Charles Louis Alphonse Laveran while stationed in Algeria, during the Franco-Prussian War (Bruce-Chwatt, 1981). In a fresh blood sample from an afflicted soldier, Laveran identified live *Plasmodium* parasites on a microscope slide by noticing moving filaments and pigment-containing cells. Laveran named the organism, *Oscillaria malariae* (Bruce-Chwatt, 1981). In 1885, two Italian scientists, Ettore Marchiafava and Angelo Celli, created a new genus for the malaria parasite called, *Plasmodium* (McFadden, 2012, Marchiafava, 1885). The nomenclature change was based on Marchiafava and Celli’s observations that the parasites, when inside of erythrocytes, or red blood cells (RBCs), had multiple-nuclei and an ameboid-like shape that resembled a slime-mold of the same name, plasmodium (McFadden, 2012, Marchiafava, 1885). During this same time period, a cohort of Italian scientists led by Camillo Golgi, Marchiafava, Celli, Grassi, among others, deduced

that the *Plasmodium* genus was made of distinct species that caused different forms of malaria (Cox, 2010).

Despite these insights into the biology of *Plasmodium*, it took over a decade from when the parasite was first discovered to determine how it was transmitted from person-to-person. In the early 1890s, Patrick Manson hypothesized that malaria was transmitted by mosquitoes (Manson, 1894). This theory was later confirmed in 1897 by Sir Ronald Ross (Cox, 2010, Manson, 1898). Under the mentorship of Manson, Ross had observed pigmented bodies (what we now know as oocysts) in the midgut of an *Anopheles* mosquito that had bitten a malaria-infected patient (Ross, 1897). It should be noted that at the same time, Grassi and colleagues had also documented the *Plasmodium* life cycle in the mosquito and demonstrated that the *Anopheles* mosquito was the only vector for the parasite (Cox, 2010).

1.1.2 Malaria today: global burden and epidemiology

When Laveran, Ross, and the other influential researchers mentioned above made their discoveries in the late 19th century, malaria existed on every continent except Antarctica (**Figure 1.1**). As can be seen on the map in Figure 1.1, malaria extended through both temperate and tropical regions, spreading as far north as Russia. Interventions by mankind from 1900-2002 substantially reduced the number of countries at risk of malaria from around 140 to 88, shrinking the land distribution of *Plasmodium* endemicity by half (Hay et al., 2004, Murray et al., 2012).

This reduction was made possible through national and global efforts in malaria endemic regions. Such strategies combined multidisciplinary approaches to reduce the malaria burden including, antimalarial drugs, insecticides, insecticide-treated bed nets, malaria surveillance tools, improved sanitation, and many other measures. This work has been achieved and sustained in the 21st century by many organizations and programs, including the Centers for Disease Control and Prevention (CDC) in the United States, the World Health Organization (WHO), the United Nations (UN), and the Bill & Melinda Gates Foundation, to name a few (World Health Organization, 2018). In spite of these efforts, the risk of malaria infection remains in approximately 100 countries and territories.

According to the most recent Malaria Report from the World Health Organization, malaria occurs in 87 countries with the majority of cases caused by *P. falciparum* and *P. vivax* (**Figure 1.2**) (World Health Organization, 2018). As seen in the maps in Figure 1.2, *P.*

falciparum and *P. vivax* have widespread global distributions with distinct regions of prevalence, with *P. falciparum* predominating in Sub-Saharan Africa and Southeast Asia (SEA), while *P. vivax* is most prominent in South America, SEA, and the Western Pacific. *P. falciparum* is the most dangerous malaria species and causes the highest rates of morbidity and mortality due to its ability to progress to severe malaria. *P. vivax* is sometimes referred to as “benign” malaria because it is often asymptomatic and progression to severe malaria is less common (Carter and Mendis, 2002, Price et al., 2007). However, benign is misleading because *P. vivax* also contributes to morbidity and mortality, though to a lesser extent than *P. falciparum* (Price et al., 2007). Furthermore, *P. vivax* and *P. ovale* have dormant liver stages that can relapse in infected individuals months or even years after initial infection. The less prevalent *P. malariae* and *P. ovale* have been identified in all malaria endemic regions, but their incidence rates are lower than *P. falciparum* and *P. vivax*, although studies suggest that it is likely these species are underreported due to missed detection, misdiagnosis, or co-infection with *P. falciparum* or *P. vivax* (Mueller et al., 2007, Doctor et al., 2016). *P. knowlesi*, a zoonotic parasite in macaque monkeys that also infects humans, has a less clearly delineated geographical distribution, but has been demonstrated in patients throughout SEA, with incidence rates recently reported on the rise in Malaysia (Barber et al., 2017, Cooper et al., 2019). Similar to *P. malariae* and *P. vivax*, it is hypothesized that *P. knowlesi* infections are underreported due to misdiagnosis as one of the other species (Shearer et al., 2016). It should also be acknowledged that *P. knowlesi* infections are currently being reported in countries that are making strides in eliminating the human malarias, so further studies are warranted and its prevalence should not be overlooked (Shearer et al., 2016).

From an epidemiological perspective, there were 219 million malaria cases in 2017 and 435,000 deaths (World Health Organization, 2018). The largest proportion of infections (92%) and deaths (93%) were in Sub-Saharan Africa. *P. falciparum* represented 99.7% of cases in Africa and 62.8% of malaria cases in SEA (World Health Organization, 2018). *P. vivax* was responsible for the majority of malaria infections outside of Africa, contributing to 74.1% of cases in the Americas and 37.2% of cases in SEA (World Health Organization, 2018). All individuals in malaria endemic regions are at risk of infection, but the severity and likelihood of illness is greatly increased for children under the age of five, pregnant women, and immunocompromised individuals. Children accounted for over half of the malaria deaths (61%) in 2017 (World Health Organization, 2018). These statistics show that this disease from antiquity is still very much a disease of the present.

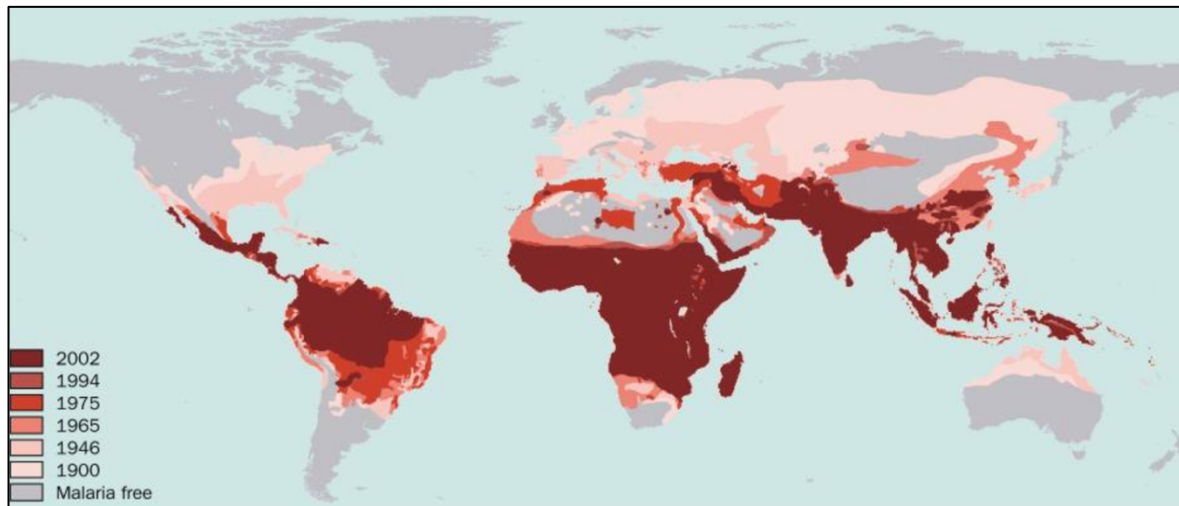


Figure 1. 1. The global distribution of malaria in the 20th century. The maps show the risk of malaria from *P. falciparum*, *P. vivax*, *P. malariae*, and *P. ovale* from circa 1900 to 2002, as estimated by Hay *et al.* (Hay *et al.*, 2004). The figure has been reprinted from Hay *et al.* (2004) with permission from Elsevier.

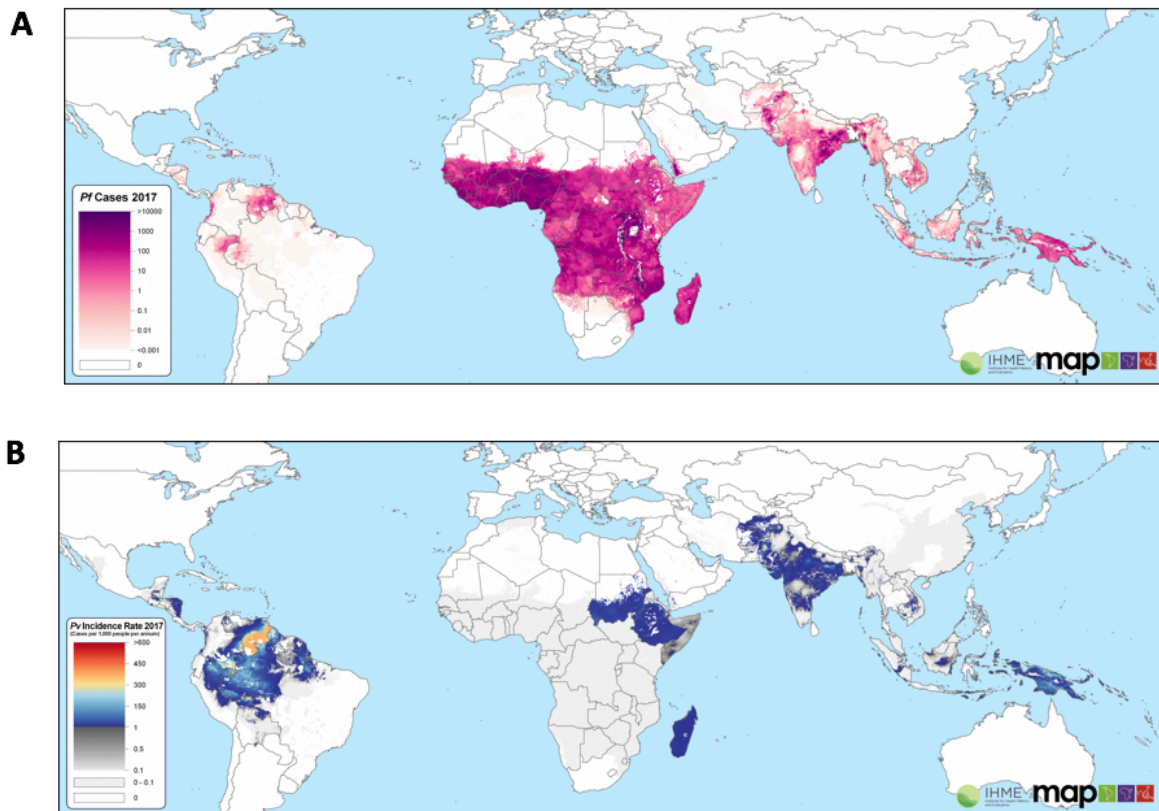


Figure 1. 2. The global incidence of *P. falciparum* and *P. vivax* malaria in 2017. A.) Incidence of *P. falciparum* malaria in all age groups in 2017. B.) Incidence of *P. vivax* malaria in all age groups in 2017. The maps are reprinted from The Malaria Atlas Project (2019) and are available in the public domain under the Creative Commons Attribution 3.0 Unported License.

Malaria disproportionately affects populations living in extreme poverty. The disease is both a cause of and result of poverty, and the cycle continues to repeat itself (Teklehaimanot and Mejia, 2008, Gallup and Sachs, 2001). For example in 2017, five countries with some of the

widest poverty gaps—Nigeria, the Democratic Republic of the Congo, Mozambique, India, and Uganda—comprised almost half of the total number of malaria cases globally (World Health Organization, 2018). This inextricable link between malaria and poverty has long been acknowledged (Teklehaimanot and Mejia, 2008, Feachem et al., 2019), but the steps for unravelling the two requires multidisciplinary approaches that remain complex. Economic, social, and political factors, amongst many other dynamics combined with ecological conditions in tropical regions, favors the continued transmission of malaria. Though progress has been made through the aid of the aforementioned programs (CDC, WHO, UN, Gates Foundation) the current World Malaria Report shows that no significant progress in reducing the malaria burden was made within the last three years from 2015-2017 (World Health Organization, 2018).

In spite of these issues, all hope for malaria elimination (reduction of the disease to zero new incidences in a distinct region) and eradication (permanent removal of disease pathogen) should not be quelled. There has been a considerable reduction of the malaria burden since 2010 and although overall global statistics from 2015-2017 have stalled, country specific advancements are numerable. Sri Lanka eradicated malaria in 2016. In 2017, Rwanda reported 430,000 less malaria cases than in 2016 and India had a 24% decrease in malaria infections. Furthermore, 46 countries had less than 10,000 cases of malaria in 2017 (World Health Organization, 2018). Continued reduction of the malaria burden and eventual eradication is possible in this century. Experts believe eradication could be possible by 2050 and have put forth the slogan, “malaria eradication within a generation” (Feachem et al., 2019).

In addition to the social, economic, and political factors that must be addressed, continued scientific advancements are imperative for the goals of eradication to be realized. Although malaria remains a curable disease, drug resistance and the potential for it to develop threatens the efficacy of the limited number of antimalarial drugs currently available. As endemic countries strive to reduce the burden caused by malaria, it is necessary to understand the mechanisms of drug resistance, which is the focus of this dissertation. Drug resistance has been reported in both *P. falciparum* and *P. vivax* malaria (Bloland, 2001, Cui et al., 2015, Blasco et al., 2017, Price et al., 2009, Dayananda et al., 2018). Due to the global burden of *P. falciparum* malaria and its resistance to currently available drugs in SEA, *P. falciparum* malaria is the focus of this dissertation. Investigation of the mechanisms of drug resistance in *P. falciparum* provides both fundamental insight into parasite biology and also into the

mechanisms through which resistance can develop. For these studies to be possible, it is necessary to understand both the life cycle and pathogenesis of *P. falciparum*.

1.1.3 *P. falciparum* life cycle

The life cycle of *P. falciparum* consists of three phases (**Figure 1.3**): a sexual stage in the mosquito vector (sporogonic cycle), an asexual stage in the liver of the human host (exo-erythrocytic cycle), and an asexual stage in the blood of the human host (intraerythrocytic cycle) (Cowman et al., 2016, Miller et al., 2013). The parasite is an obligate intracellular pathogen in liver hepatocytes and erythrocytes, which facilitates the parasite's ability to avoid detection by the host's immune system.

The life cycle begins when a *P. falciparum*-infected female *Anopheles* spp. mosquito takes a bloodmeal from a human host. Male mosquitoes do not bite, so are thus not able to spread malaria. When the female mosquito bites an individual, the contents of the mosquito's saliva, including anticoagulants and *P. falciparum* sporozoites, are injected into the human host's blood. The sporozoites enter the bloodstream and migrate to the liver (30-60 minutes) where they invade hepatocytes and take ~6 days to mature into schizonts that contain ~40,000 merozoites per hepatocyte (Miller et al., 2013, Phillips et al., 2017). This stage is clinically silent and the infected individual does not present with any symptoms. During *P. vivax* and *P. ovale* infections, it is during this exo-erythrocytic stage that some sporozoites differentiate to hypnozoites which can remain dormant in the liver for weeks to years before maturing to merozoites (Miller et al., 2013, Cowman et al., 2016).

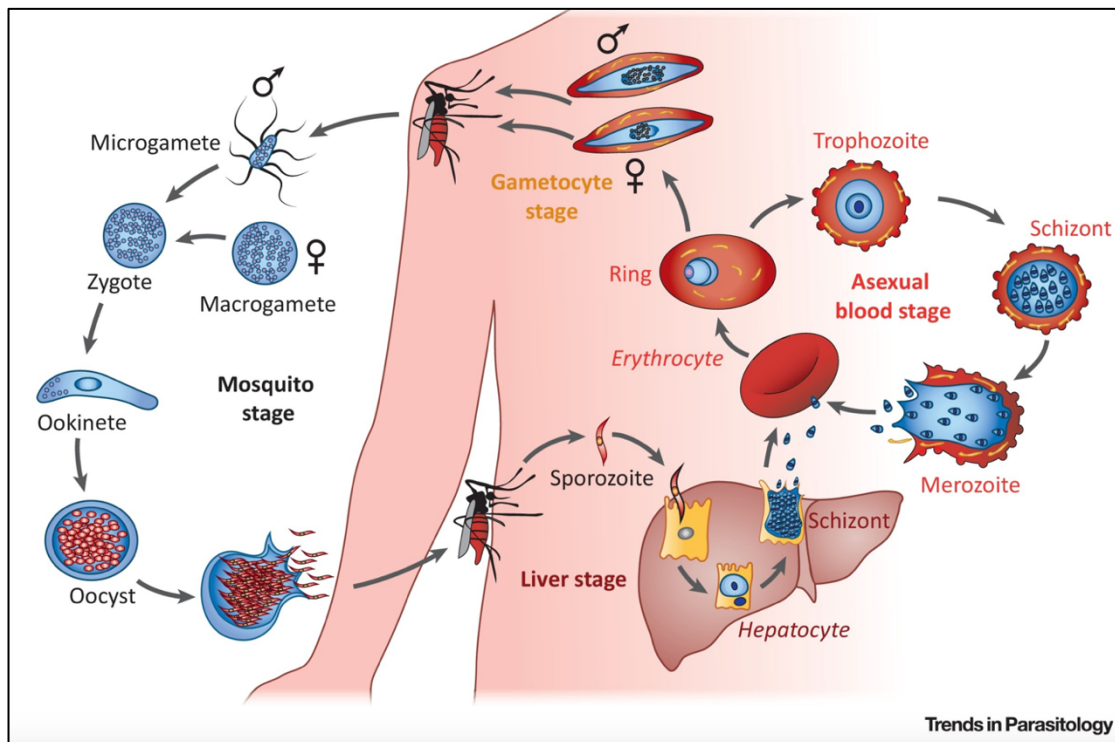


Figure 1. 3. The life cycle of *P. falciparum*. The life cycle begins when an infected female *Anopheles* mosquito bites a human host and sporozoites are inoculated into the host and migrate to the liver (liver/exo-erythrocytic stage) where they invade hepatocytes and form liver schizonts. When the liver schizonts rupture, they release merozoites that invade erythrocytes to start the asexual blood (intraerythrocytic) stage. When merozoites egress from the ruptured schizonts, they can reinvade erythrocytes to propagate the asexual cycle, or differentiate to sexual stage gametocytes. As gametocytes mature, they differentiate into male and female gametocytes that are taken up by a mosquito during a blood meal. Once inside the mosquito midgut (sporogonic/mosquito stage), the male and female gametes fuse to form a zygote that becomes an ookinete and then develops into an oocyst. When the matured oocyst ruptures, it releases sporozoites that migrate to the mosquito salivary glands to be transferred to a human host when the mosquito takes its next blood meal to repeat the cycle. The figure is reprinted from Maier *et al.* (2019) (Maier *et al.*, 2019) with permission from Elsevier.

The intraerythrocytic stage commences when an infected hepatocyte bursts and releases the hepatic merozoites into the bloodstream where they invade erythrocytes. Merozoite invasion into the erythrocyte takes about 1-2 minutes (Weiss *et al.*, 2015). The intraerythrocytic cycle is when clinical symptoms present and is marked by three distinct forms of parasite growth: ring, trophozoite, and schizont (**Figures 1.3-1.4**) (Bannister and Mitchell, 2003, Bannister *et al.*, 2000). Upon invading the host erythrocyte, the parasite enters the ring stage and begins to grow within the host cell over the course of 24 hours. The stage name is based on how the early ring stage parasite looks on a Giemsa-stained blood smear, with the nucleus off to one side and the disc-like cytoplasm adjacent (**Figure 1.4**). During the ring stage, the parasite begins to digest the host cell hemoglobin to obtain nutrients in the form of amino acids. Hemoglobin digestion enables the parasite to have space to grow (Bannister and Mitchell,

2003, Bannister et al., 2000, Cowman et al., 2016) and provides an osmotic balance within the erythrocyte (Lew et al., 2003). Following the ring stage the parasite enters the stage of highest metabolic activity, trophozoite (~24-36 hours), and continues to feed off of the host cell hemoglobin. As trophozoites mature and enter the schizont stage (~36-48 hours), they undergo asexual replication to yield ~16-32 daughter merozoites. When the schizont has fully matured after ~48 hours, the merozoites egress, or rupture, from the host erythrocyte (**Figure 1.4**). This process destroys the erythrocyte as the merozoites are released into the bloodstream where they can invade a new erythrocyte to continue the intraerythrocytic cycle (Cowman and Crabb, 2006, Cowman et al., 2016). This intraerythrocytic asexual cycle will continue until it is cleared by the host's immune system or an antimalarial drug, or until it causes severe disease and death of the host.

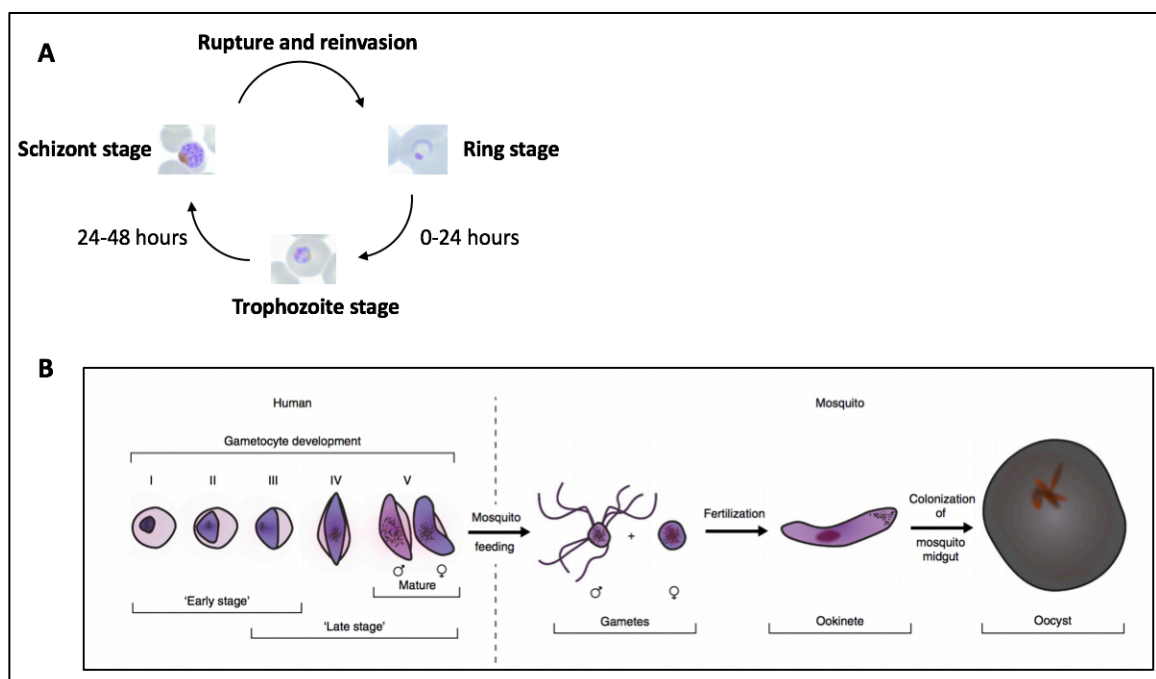


Figure 1. 4. The asexual and sexual intraerythrocytic life cycles of *P. falciparum*. A.) The 48-hour life cycle of *P. falciparum* asexual parasites as observed in Giemsa-stained blood smears. B.) A schematic of the sexual stages of *P. falciparum* gametocytes, including progression from sexual stage gametocytes in the human host to the mosquito vector. The image in part B was modified from Delves *et al.* (Delves et al., 2016) and reprinted with permission from Springer Nature Publishing.

During the asexual intraerythrocytic stages, a portion of merozoites will commit to the sexual stage by undergoing a process called gametocytogenesis (Baker, 2010, Ngotho et al., 2019). The time at which this developmental conversion occurs is the topic of much debate and remains to be fully elucidated, but studies have shown it is regulated by the transcription factor, AP2-G (Kafsack et al., 2014, Sinha et al., 2014). It was previously shown that following an increase in AP2-G expression, parasites complete an additional asexual life

cycle as committed parasites before reinvading as gametocytes in the next cycle (Baker, 2010). Recent studies have shown in addition to this pathway, parasites can undergo a developmental switch within the same asexual life cycle that increased AP2-G expression occurs (Bancells et al., 2019). Once committed to sexual development, gametocytogenesis consists of five stages (I-V), with the earliest stage (stage I) morphologically indistinguishable from asexual parasites (**Figure 1.4**) (Ngotho et al., 2019). Gametocytes require ~12 days to develop and the mature stages are identifiable by their “falciform” shape, from which falciparum earned its name (**Figure 1.4**). During development, the gametocytes are sequestered in the bone marrow to escape splenic clearance (Joice et al., 2014). In the final maturation stages, the gametocytes differentiate into haploid male (microgamete) or female (macrogamete) forms, which can remain in circulation for several days (Smalley and Sinden, 1977). The male and female gametocytes are the infective forms that are taken up by the mosquito during a blood meal (Ngotho et al., 2019). Once inside the mosquito midgut, the male gametocyte undergoes a process called exflagellation (induction) by which it becomes motile and fuses with the female macrogamete to form a diploid zygote (Phillips et al., 2017). In ~24 hours the zygote becomes an ookinete which enters the mosquito midgut epithelium and develops into an oocyst. When the oocyst is fully matured (after ~2 weeks), it releases thousands of haploid, motile sporozoites that travel to the mosquito’s salivary glands where they can be transferred by mosquito bite to the next host to restart the cycle (**Figure 1.3**) (Barillas-Mury and Kumar, 2005). Given that the *Anopheles* adult lifespan is 2-3 weeks in nature, this development cycle enables just enough time for the *P. falciparum* life cycle to be propagated (Clements, 1992, Centers for Disease Control, 2018).

The intraerythrocytic stage of *P. falciparum* malaria is the focus of this study. As will be discussed in later sections of this introduction, asexual *P. falciparum* isolates can be cultivated and maintained *in vitro* using human erythrocytes (Trager and Jensen, 1976). This enables the parasite to be studied using molecular biology techniques and tools.

1.1.4 Pathogenesis of *P. falciparum* malaria: asymptomatic, uncomplicated, severe disease

A malaria infection can be categorized as asymptomatic, uncomplicated, or severe. As described by the name, asymptomatic infections do not present with symptoms, due to the host’s immunity or other factors. However the infection can still be spread to mosquitoes because the host has circulating parasites in their blood (Chen et al., 2016). Uncomplicated

malaria is characterized by the classic malaria symptoms (described in the next section), but with no signs of severe disease. All species of *Plasmodium* can cause asymptomatic infections and uncomplicated malaria (Phillips et al., 2017). Severe malaria includes the symptoms of uncomplicated malaria in addition to multi-organ complications (Wassmer and Grau, 2017). Severe malaria is predominantly caused by *P. falciparum* but *P. vivax* and *P. knowlesi* can also cause severe disease (Phillips et al., 2017).

1.1.4.1 Uncomplicated *P. falciparum* malaria

The severity of *Plasmodium* spp. infection varies greatly depending on the species and a multitude of host factors, including inherited factors of resistance (such as sickle hemoglobin trait), age, prior exposure, and immunity levels (Bruce-Chwatt, 1985). In general, uncomplicated malaria is infamously recognized for its classic symptoms: acute fevers, sweats, headache, myalgia, fatigue, nausea, and vomiting. The symptoms are notorious for their paroxysmal, or sudden, onset.

The classic fevers observed in malaria infections correspond to the intraerythrocytic life cycle of the *Plasmodium* species. There are no clinical symptoms associated with the exoerythrocytic stage (liver stage), the sexual stage (gametocytogenesis), or when sporozoites are injected into the host bloodstream, aside from mild inflammation at the mosquito bite site (Bruce-Chwatt, 1985). In *P. falciparum*, *P. vivax*, and *P. ovale* infections, the intraerythrocytic life cycle is ~48 hours, which corresponds to fevers every third day (tertian). *P. malariae* has a 72 hour lifecycle with fevers every fourth day (quartan) and *P. knowlesi* has a 24 hour life cycle with fevers spiking daily (quotidian) (Bruce-Chwatt, 1985). The febrile episodes are the body's response to the rupture of infected erythrocytes. Although the *P. falciparum* life cycle is ~48 hours, the fevers are often irregular and do not adhere to the periodicity observed with respect to infection by the other *Plasmodium* species (Bartoloni and Zammarchi, 2012). All symptoms are also non-specific and could be caused by a plethora of other infectious diseases present in malaria endemic regions (for example, dengue, chikungunya, bacterial septicaemia and typhoid). The physical findings are also nonspecific and can include splenomegaly, hepatomegaly, jaundice, and abdominal pain. Therefore, malaria should be diagnosed by a laboratory test, particularly microscopy (Mathison and Pritt, 2017).

The gold standard for malaria diagnosis is to create a blood film, or smear, to directly examine patient blood for the presence of parasites (Mathison and Pritt, 2017). Blood smears

entail spreading a drop of malaria infected blood on a glass microscopy slide. The slides are then fixed in methanol and stained with a Giemsa solution. A component of Giemsa binds to the phosphate groups of DNA while other components in the Giemsa solution stain the nucleus and cytoplasm differently so they can be visualized by light microscopy. Since erythrocytes do not contain DNA, the only positively stained cells on a patient blood smear are white blood cells and malaria-infected erythrocytes. The microscopy examination can be performed immediately upon request and by any trained microscopist. As part of malaria control and elimination efforts, many countries have standardized training and protocols for performing microscopy-based malaria diagnoses. Figure 1.5 shows an example of a handbook for performing diagnostic malaria microscopy in Cambodia, for which the guidelines have been translated from English to Khmer, the official language.

Rapid diagnostic tests (RDTs) are another way to detect malaria infections quickly. These tests detect malaria-specific antigens in minutes, such as histidine-rich protein 2 (HRP2) (Wellems and Howard, 1986, Wellems and Howard, 1995), by using a drop of patient blood (Rock et al., 1987, Beadle et al., 1994, Shiff et al., 1993). Because RDTs can have false negatives, they should always be combined with microscopy. Additionally, multiple studies within the last three years have noted *P. falciparum* infections with deleted *HRP2/3* genes (Mathison and Pritt, 2017, World Health Organization, 2018, World Health Organization, 2017a), necessitating the need for microscopy to be jointly performed alongside RDTs and also demonstrating a need for new diagnostic tests to be developed.

There is also the possibility that malaria infections are undetectable by microscopy, as often seen with asymptomatic malaria infections. Many studies have developed various PCR, quantitative (qPCR), and droplet digital PCR (ddPCR) methods to detect lower limits of parasitemia (Tham et al., 1999, Lee et al., 2002, Koepfli et al., 2016). However, these methods do not offer the rapid results that RDTs and microscopy can provide and they also require more advanced laboratory equipment and materials that may not be available in the field. Advancements in diagnostic tests would greatly aid malaria elimination efforts and it will be interesting to see how the field changes in the next decade as countries push for malaria eradication.

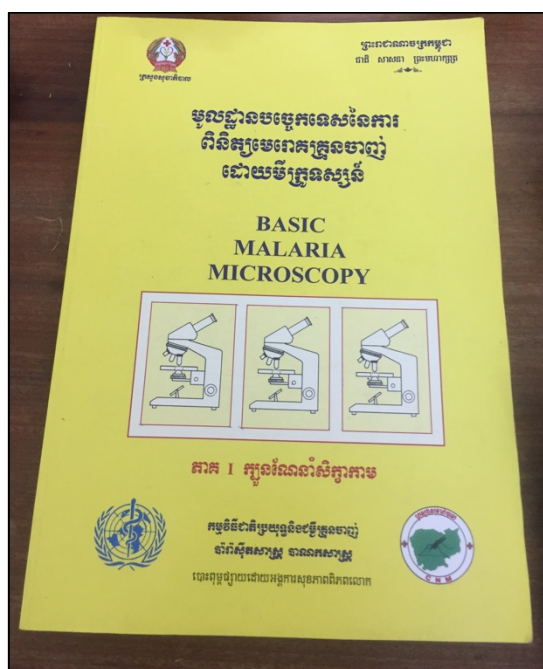


Figure 1. 5. Microscopy-based malaria diagnosis is the gold standard in all malaria endemic countries. This is a microscopy book that is used to train microscopists in Pursat Province, Cambodia. The *P. falciparum* isolates used in this dissertation were obtained from field sites in Cambodia and the photograph was taken during a field site visit to Pursat Province.

1.1.4.2 Severe *P. falciparum* malaria

P. falciparum is responsible for most cases of severe malaria, which often results in death. Young children are the population most impacted by severe disease but adults can progress to severe malaria as well. The pathophysiology of severe malaria is complex and not fully understood, but in general it is characterized by three coinciding conditions: severe anemia, metabolic acidosis, and cerebral malaria (Miller et al., 2013). Within the last two decades, research has also demonstrated that severe malaria results in multi-organ damage not limited to the brain and includes other organs such as the kidneys and pulmonary system (Miller et al., 2002, Wassmer and Grau, 2017, Wassmer et al., 2015).

One of the major causes of *P. falciparum* pathogenesis in severe malaria is its ability to cause infected erythrocytes to adhere to the endothelial lining of blood vessels, including those in the brain which results in cerebral malaria (Wassmer and Grau, 2017, Wassmer et al., 2015). This sequestration of infected erythrocytes drastically affects blood perfusion throughout the body. The effects of this cause different clinical presentation in children and adults, with complications in children predominantly resulting in cerebral malaria, seizures, hypoglycemia, and severe anemia. In adults, there is often kidney failure, jaundice, and pulmonary edema (Wassmer et al., 2015). Metabolic acidosis is a key symptom in both children and adults (Miller et al., 2002). Severe malaria is caused by the asexual

intraerythrocytic stages of the parasite and death often occurs within 48 hours after presentation of the disease (White, 2004). This means the parasites present at the onset of severe malaria symptoms will ultimately contribute to death, so preventing their maturation and reinvasion is vital.

In the context of severe malaria, it is important that the drugs are stage-specific to prevent the ring stages from progressing and the parasitemia from increasing. In the context of uncomplicated malaria, it is important to lower parasitemia as fast as possible, and prevent the likelihood that the disease will become severe (White, 2004). The way this is achieved is chemotherapy.

1.2 Antimalarial chemotherapy

The current frontline treatments for uncomplicated *P. falciparum* malaria worldwide are artemisinin combination therapies (ACTs) (World Health Organization, 2018, World Health Organization, 2015). ACTs combine a potent short-acting artemisinin derivative with a long-acting partner drug with a different mechanism of action. Severe malaria is treated with intramuscular (IM) or intravenous (IV) artesunate, an artemisinin derivative, for at least 24 hours followed by standard course of an ACT (World Health Organization, 2018).

P. falciparum has demonstrated resistance to nearly every antimalarial drug it has come in contact with and presently, decreased susceptibility of the parasite to both artemisinin and several commonly used partner drugs has been reported in multiple countries in SEA (Amaratunga et al., 2016, Dondorp et al., 2009, Denis et al., 2006, van der Pluijm et al., 2019, Blasco et al., 2017). This is of great concern as there are a limited number of drugs available to treat uncomplicated and severe malaria. In order to put antimalarial drug resistance into perspective, it is first necessary to delve into the history of antimalarial drug therapies.

1.2.1. Brief history of widely used antimalarial drugs: from monotherapies to combination therapies

1.2.1.1 Quinine

Extracted from the bitter bark of a cinchona tree, quinine was the first treatment discovered for malaria in the 1600s (**Figure 1.6**) (Tse et al., 2019, Butler et al., 2010, Arrow, 2004). The compound responsible for the bark's antimalarial action was first discovered by French

chemists, Joseph Pelletier and Jean Biename Caventou in 1820 and the structure of this compound from nature has inspired many synthetic treatments for malaria (Arrow, 2004).

Early anecdotal observations of quinine resistance were recorded in 1884 and 1910 (Talisuna et al., 2004). In the 1960s, quinine resistance was reported in human volunteers in SEA and Brazil, and later associated with treatment failures in SEA in the 1980s-90s (Peters, 1970, Peters, 1987, Pukrittayakamee et al., 1994). More recently, treatment failures were observed in Uganda when comparing quinine to the ACT, artemether-lumefantrine (Achan et al., 2009). In spite of intermittent periods of resistance, quinine is still an effective treatment for malaria in many regions and can still be used as a “drug of last resort” to treat severe malaria when an artemisinin derivative is unavailable (Achan et al., 2011, Schlitzer, 2007, Bloland, 2001). One reason for the continued efficacy of quinine is likely due to decreased use of the drug as newer drugs with higher therapeutic efficacy and less toxicities have become available (Achan et al., 2011). Quinine has severe side effects, both at standard therapeutic levels and when overdosed, which include tinnitus, blurred vision, confusion, vertigo, skin rashes, cardiotoxicity, nausea, and many additional symptoms referred to broadly as cinchonism (Achan et al., 2011). The mechanism of quinine action remains to be fully elucidated, but it is postulated to exert its antiparasitic effects by accumulating in the parasite’s digestive vacuole and interfering in heme detoxification (**Figure 1.7**) (Blasco et al., 2017, Greenwood et al., 2008).

Quinine remained the only available drug to treat malaria until the 20th century (Talisuna et al., 2004, Tse et al., 2019). This changed after the First World War when Germany made a push to develop synthetic antimalarial drugs after suffering huge losses to malaria during the war because of their inability to access quinine (Butler et al., 2010). The process to find quinine analogues that would be toxic to the malaria parasite began years before the war with the dye, methylene blue. Based on the compound’s similarity to quinine and its toxic effects on malaria parasites, it was used as a structural basis for synthesizing quinine-like compounds. (Presently, methylene blue is back in the spotlight and being considered in various combinations for malaria treatment (Tse et al., 2019). Shortly after the war in the early 1930s, mepacrine (also called quinacrine) and plasmochin (also called pamaquine) were the first synthetic antimalarial compounds synthesized as quinine analogues (Schlitzer, 2007). Plasmochin was not widely used due to toxicities, but mepacrine was used during the Second World War as an antimalarial prophylactic (Tse et al., 2019). Mepacrine also has severe side effects, including psychosis and yellow staining of the skin and eyes (Tse et al.,

2019). Both plasmochin and mepacrine are no longer used for malaria prophylaxis or treatment, however the aminoquinoline-based structures of both plasmochin and mepacrine led to two of the most commonly used antimalarial drugs: primaquine and chloroquine. Modifications of the plasmochin structure led to primaquine, and mepacrine helped to inspire the discovery of chloroquine (Schlitzer, 2007).

Chloroquine (originally called resoquin) was synthesized in 1934 by the group of German chemists employed to synthesize a new quinine-like compound (**Figure 1.6**), but it was believed to be too toxic. Sontoquin (3-methylchloroquine) followed after chloroquine and it was believed to have fewer side effects, so it was given to German troops during the Second World War. During the war, the Allies acquired ontoquin and when Americans tried to increase the drug's efficacy, they synthesized what they thought was a new drug, chloroquine. However, upon comparing resoquin and chloroquine, they realized they were the same drug (Arrow, 2004). Similar to quinine's proposed mechanism of action, chloroquine inhibits heme detoxification (Wellems and Plowe, 2001). Chloroquine has also been shown to accumulate in the parasite digestive vacuole (**Figure 1.7**) (Ridley, 1998, Sullivan et al., 1996).

1.2.1.2 Chloroquine

The deployment of chloroquine for the treatment of malaria had an enormous impact on the eradication of malaria in many countries in the first half of the 20th century. Chloroquine's potential was fully realized in the 1950s-1960s during WHO's Global Malaria Eradication Program (GMEP) (Wellems and Plowe, 2001, Croft, 1999). The GMEP (1955-1969) was immensely successful in eliminating malaria in multiple countries by combining the affordable chloroquine with the deployment of the insecticide, dichlorodiphenyltrichloroethane (DDT), and malaria case surveillance. The program eliminated malaria in North America, Europe, the Caribbean, parts of Asia, and Central America (Croft, 1999). However, many African countries were not included in the GMEP (the program did not involve these countries due to logistical/"technical" challenges) and thus no successes were observed in Africa (World Health Organization, 2001, Alonso et al., 2011). The GMEP ended in 1969 due to the emergence of both chloroquine resistance and insecticide resistance combined with the lack of organization for the necessary infrastructure and surveillance measures within individual countries—demonstrating that a single approach cannot be used globally long-term (Talisuna et al., 2004, Alonso et al., 2011).

Chloroquine resistance emerged from four independent locations (Wellems and Plowe, 2001, Talisuna et al., 2004). The first was in SEA on the Thai-Cambodian border in 1957 (Harinasuta et al., 1965). Around the same time period, another foci was reported in South America in Colombia and Venezuela (Payne, 1987). The last two emergences were in Papua New Guinea (1970s) and in Africa beginning in Kenya and Tanzania in 1978 (Peters, 1987, Talisuna et al., 2004). From these locations, chloroquine-resistant *P. falciparum* spread throughout endemic areas.

1.2.1.3 Antifolates: sulfadoxine/pyrimethamine (SP), proguanil

A combination of antifolate drugs were also used to treat malaria in response to the reduced efficacy of chloroquine. These drugs function by blocking steps in the folate synthesis pathway in bacteria, protozoa, and fungi. The pyrimidine analogue, proguanil (synthesized in 1945), was a product of the push to generate new drugs after the Second World War (Tse et al., 2019, Arrow, 2004). In the 1950s-1960s, pyrimethamine and sulfadoxine were also developed. When the drugs were introduced as monotherapies, it was quickly realized that they could not be used alone. Sulfadoxine and pyrimethamine (SP) were then combined to reduce the likelihood of drug resistance, but resistance continued to develop rapidly. In 1967, SP was introduced in Thailand and resistance was documented in the same year (Wernsdorfer and Payne, 1991). Today, SP is not used to treat malaria unless it is combined with an artemisinin derivative, most commonly with artesunate. SP is also used successfully as intermittent preventive treatment in pregnancy (IPTp) (World Health Organization, 2018, World Health Organization, 2015). IPTp is a public health measure designed to prevent malaria in pregnant women by administering antimalarial drugs during their pregnancy. It is recommended by WHO that pregnant women in moderate to high transmission areas in Africa receive IPTp at the beginning of their second trimester until the end of their pregnancy.

With widespread chloroquine resistance and the unreliable efficacy of SP, the pressure to find new antimalarial drugs was greatly increased (again at a time of war) during the Vietnam War, when all sides were subjected to the malaria scourge. During this time period, the US Army Medical Research and Development Command, the Walter Reed Army Institute of Research (WRAIR), and WHO sought to discover new drugs as well as promote research into parasitology and malariology, for which efforts had died down after the GMPEP (Alonso et al., 2011). Concurrently, the Chinese government, which was supporting the North Vietnamese in the war, launched Project 523 recruiting hundreds of chemists, scientists,

pharmacologists, doctors, and other biomedical experts to discover new antimalarial drugs (Butler et al., 2010). It was through this project that the next drug to revolutionize the malaria field was discovered: artemisinin (Tu, 2011).

1.2.1.4 Artemisinin

Artemisinin was discovered by Tu Youyou in 1972 as part of the efforts of Project 523. Tu extracted the compound from the *Artemisia annua* plant, commonly referred to as sweet wormwood or *qinghao* in Chinese (Tu, 2011). The plant had been used by Chinese herbalists for thousands of years as a treatment for a variety of maladies and around 300 AD, Ge Hong published the use of *qinghao* for fevers in the book, *A Handbook of Prescriptions for Emergencies* (Tu, 2011). Similar to quinine, another natural compound that had been known for its antipyretic properties, artemisinin was re-“discovered” and chemically isolated for the treatment of malaria. In contrast to quinine, artemisinins have few side effects and are well tolerated (White, 2008). Artemisinins are the fastest-acting, most potent malarial drugs available. The compounds are active against all erythrocytic asexual stages of parasite development and have also been shown to kill sexual stage gametocytes (Skinner et al., 1996, Adjalley et al., 2011), but they have no effect on liver stages (Meister et al., 2011). The mechanism of action of artemisinin is the topic of continued debate and remains a complex, to-be-continued story (Meshnick, 2002, Cui and Su, 2009). Artemisinins are prodrugs and one theory is when artemisinin is activated (some theories believe it is activated by heme in the erythrocyte (**Figure 1.7**) (Wang et al., 2015, Meshnick, 2002), it generates toxic free radicals or reactive oxygen species (ROS) that cause damage to any nearby cellular targets (Tilley et al., 2016, Blasco et al., 2017). Additional studies have also suggested that activated artemisinins have many targets they can bind resulting of alkylation of both lipids and proteins (Wang et al., 2015). Thus, artemisinin likely has many ways through which it exerts its antiparasitic effects.

Early clinical trials by Tu and colleagues in the 1970s showed that artemisinin was very effective at clearing parasites, however some recrudescences were observed (Cui and Su, 2009). Recrudescence means that the malaria infection has persisted at an undetectable level and when it reoccurs at a detectable level, it is termed a recrudescence infection. In spite of the recrudescences, the potency of artemisinin prompted the development of several artemisinin derivatives that are still recommended for malaria treatment today: dihydroartemisinin (which is the active metabolite of artemisinin), artemether, and artesunate (World Health Organization, 2015).

The short half-lives of artemisinin derivatives (~1 hour) are believed to be one of the main reasons why recrudescences are observed (Cui and Su, 2009). Because the Chinese scientists were aware of the pitfalls of artemisinin monotherapy early on, they performed multiple efficacy studies to optimize treatment regimens. In comparing 3-, 5-, and 7-day artemisinin monotherapy efficacy studies, Li *et al.* (Li et al., 1984) found that a 7-day course of artemisinin was most effective with only 5% treatment failures (Cui and Su, 2009, Li et al., 1984). Acknowledging that administering artemisinin monotherapy over the course of one week was neither feasible for patient compliance nor cost-efficient, Li and colleagues also tested artemisinin combination therapies (Li et al., 1984). Li *et al.* found the combination therapy artesunate-piperaquine to be most successful and after further optimization, artesunate was replaced with dihydroartemisinin and the two drugs, dihydroartemisinin-piperaquine, were co-formulated and first produced in Vietnam as CV8 in 1997 (Cui and Su, 2009). After slight changes of the drug dosages based on WHO recommendations, the combination therapy was marketed as Artekin® (Cui and Su, 2009). These early findings in the 1980s/90s set the stage for the current antimalarial regimens and combination therapies used today.

1.2.2.1 Combination therapies in malaria: ACTs

Combination therapies are common treatment regimens for many diseases, including tuberculosis, HIV, cancer, and autoimmune diseases (Ascierto and Marincola, 2011). The justification for combination therapies is that by using two or more drugs with different mechanisms of action, resistance is less likely to develop. Another potential advantage of a combination therapy is that the course of the disease is likely to be lessened in duration and/or severity as a result of more rapidly killing/inhibiting the causal agent. One of the classic examples of a disease in which multidrug therapies are standard course is tuberculosis. As early as the 1940s/50s, multiple drugs were used (and needed) to effectively cure patients infected with *Mycobacterium tuberculosis*, the causal agent of tuberculosis (Kerantzas and Jacobs, 2017).

If combination therapies were common in tuberculosis, why did it take decades after the emergence of chloroquine resistance for the malaria field to use combination therapies for the treatment of malaria? Perhaps it was the lack of available antimalarial drugs or the toxicities (quinine) that some drugs cause when used alone. Or, maybe it was the concern that using multiple drugs might cause the development of resistance to all currently available drugs? As seen in the case of tuberculosis, the disease is treated with four drugs, and multidrug

resistance to all four drugs, termed excessively drug-resistant tuberculosis (XDR-TB) has emerged and become a significant global health concern (Johnston et al., 2009).

Alternatively, perhaps the cost of multidrug therapies was the prohibitive barrier. Although SP, described above, was a combination of two drugs, it was not considered a combination therapy in the true sense of the regimen, for SP combined drugs with similar mechanisms of action. Of note, several studies also combined mefloquine with SP in the 1980s when SP was largely failing (Khim et al., 2005). However, the first regulated and recommended combination therapies for the treatment of malaria were ACTs.

In 2001, WHO recommended ACTs as the first-line treatment for uncomplicated *P. falciparum* malaria (World Health Organization, 2001). Currently, there are five ACTs recommended by WHO: artemether + lumefantrine; artesunate + mefloquine; artesunate + amodiaquine; dihydroartemisinin + piperaquine; and artesunate + sulfadoxine/pyrimethamine. A sixth ACT, artesunate + pyronaridine, has received positive reviews (Pryce and Hine, 2019) and is under consideration for being recommended by WHO (World Health Organization, 2018).

The rationale behind ACTs is that the potent artemisinin compound is responsible for clearing most parasites in the first several days of treatment while the partner drug, which has a different mechanism of action and a longer half-life, clears any remaining parasites. All ACTs are administered over a 3-day treatment course. This is designed to promote treatment efficacy and patient compliance as well as reduce the risk of resistance (World Health Organization, 2018, World Health Organization, 2015, World Health Organization, 2001). As mentioned above, the mode of action of artemisinin is still unknown but it has been suggested that the parasite rapidly kills parasites by actively damaging nearby proteins and other targets within the parasite (Wang et al., 2015). Similar to artemisinin, the exact mechanism of the partner drugs is unknown, but all are posited to target hemoglobin degradation or the detoxification of heme in the parasite digestive vacuole (Greenwood et al., 2008, Blasco et al., 2017) (**Figure 1.7**). This is not entirely surprising based on the chemical structures of the drugs. Piperaquine (PPQ) and amodiaquine (AQ) are 4-aminoquinilones, like chloroquine. Lumefantrine (LUM) and mefloquine (MQ) are aryl amino alcohols, like quinine (**Figure 1.6**). With the 3-day treatment course, any parasites that survive treatment and reinvade after 48 hours would still be exposed to a maximal dose of artemisinin on day 3 as well as to the partner drugs. After the artemisinin derivative has been rapidly cleared from the patient's system, the partner drugs are still at maximal concentration clear any additional

parasites over the next couple of days to weeks depending on the drug. The half-lives of the recommended partner drugs range from ~4 days to over 20 days. Mefloquine and piperazine have the longest half-lives around ~21-28 days (Tarning et al., 2008), the half-life of amodiaquine is ~7 days (Stepniewska et al., 2009), lumefantrine is ~5 days, and sulfadoxine and pyrimethamine half-lives are ~4 to ~8 days, respectively.

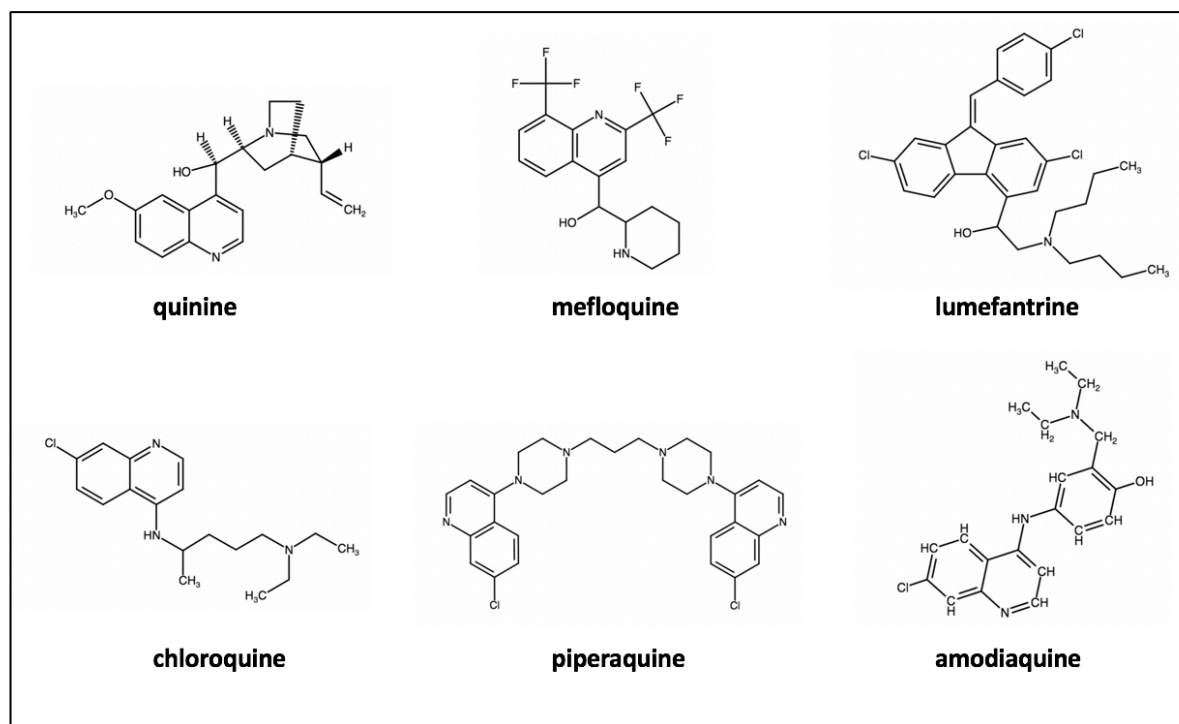


Figure 1.6. Structural similarities of antimalarial drugs.

1.2.2.2 ACTs: dihydroartemisinin-piperazine

The combination therapy that is the focus of this study is dihydroartemisinin-piperazine (DHA-PPQ). As mentioned above, DHA-PPQ was first co-formulated by Li *et al.* in the late 1980s/90s (Cui and Su, 2009), however piperazine was first synthesized in the 1960s (Davis et al., 2005). Piperazine is a bisquinoline drug that was synthesized independently in China at the Shanghai Research Institute of Pharmaceutical Industry and in France at Rhone-Poulenc. Structurally, it resembles two linked chloroquine molecules (**Figure 1.6**). In China, it was used as frontline antimalarial monotherapy and as prophylaxis starting in 1978. However, by the 1980s piperazine-resistant parasites emerged, so the monotherapy was discontinued (Davis et al., 2005). It was not until the studies by Li *et al.* with CV8 that piperazine re-emerged as an antimalarial drug contender in combination therapies (Davis et al., 2005).

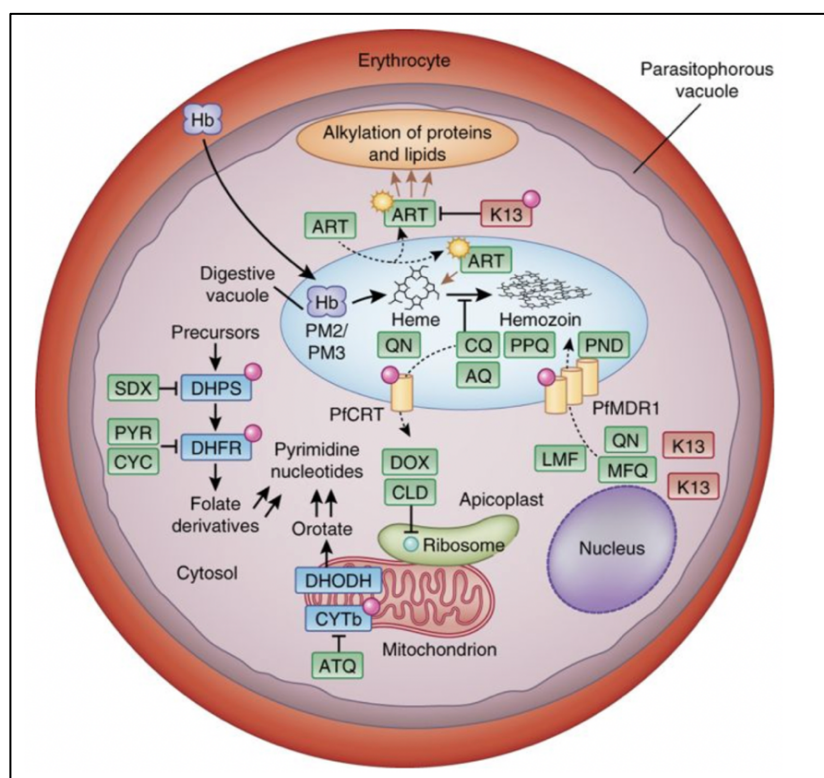


Figure 1. 7. Antimalarial drugs depicted with their proposed mechanism of action in the erythrocytic (asexual) blood stage of *P. falciparum*. The process of hemoglobin degradation is depicted in the parasite digestive vacuole (light blue) and common antimalarial drugs (green) are depicted near their proposed site of action. Of note, chloroquine (CQ) and piperaquine (PPQ) are shown interfering with heme detoxification. PfCRT (yellow) is shown on the digestive vacuole membrane with a mutation (red circle) that enables the efflux of CQ. PfMDR1 (yellow) is also shown on the digestive vacuole membrane (with increased copies) transporting mefloquine (MFQ) into the vacuole. Artemisinin (ART) is depicted in its proposed mode of action that causes oxidative stress and alkylation of proteins and lipids. This figure was reprinted from Blasco *et al.* (Blasco *et al.*, 2017) with permission from Springer Nature Publishing.

Since their implementation, ACTs have been responsible for the immense decline of *P. falciparum* malaria mortality and transmission worldwide (World Health Organization, 2018, World Health Organization, 2015). However, over the last decade, both artemisinin resistance and resistance to two commonly used partner drugs, mefloquine and piperaquine, has been reported in SEA (Blasco *et al.*, 2017, van der Pluijm *et al.*, 2019, Wongsrichanalai and Meshnick, 2008). Western Cambodia and the region along the Thai-Cambodian border are the sites where ACT treatment failures were first reported (Noedl *et al.*, 2008). SEA has long been regarded one of the prominent foci of drug-resistant malaria. As detailed above, resistance to many of the former frontline therapies (quinine, chloroquine, SP) emerged and spread throughout SEA, with all three treatment failures materializing first on the Thai-Cambodian border. Unlike the development of chloroquine resistance, which emerged in multiple independent locations (in South America at the same time as SEA), ACT treatment

failures are contained in SEA, at least for the time being. These failures severely threaten the disease's ability to be qualified as "treatable," for few other drugs are available as viable options. In order to understand the current setting of ACT resistance in SEA, it is necessary to understand the history of drug resistance in Cambodia and the genetic landscape through which parasites have developed resistance.

1.3 Drug-resistance in *P. falciparum*

1.3.1 ACT failures: emergence of artemisinin and partner drug resistance in Cambodia

In 2001, Cambodia was one of the first countries to implement ACTs with the inclusion of artesunate-mefloquine (AS-MQ) in their nationwide treatment guidelines (**Figure 1.8**) (World Health Organization, 2001). Less than four years after AS-MQ implementation, therapeutic efficacy studies reported >10% failure rates from 2001-2004 (Denis et al., 2006, Wongsrichanalai and Meshnick, 2008). Mefloquine was used as a monotherapy in Cambodia in the early 1990s (**Figure 1.8**) and was stopped due to resistance in the early 2000s, shortly before AS-MQ was introduced (Wongsrichanalai and Meshnick, 2008, Lim et al., 2009). It is therefore not entirely surprising that the combination treatment eventually failed. This caused a shift from AS-MQ to DHA-PPQ therapy in 2008 and DHA-PPQ was implemented nationwide in 2010 (**Figure 1.8**). By 2013, DHA-PPQ showed significant failure rates, specifically in Western Cambodia where rates were nearly 50% (Amaratunga et al., 2016, Leang et al., 2015, Saunders et al., 2014, Spring et al., 2015). This prompted an efficacy study by Amaratunga *et al.* in 2014-2015 to determine if AS-MQ could be reintroduced in Cambodia (Amaratunga et al., 2019). This study showed that AS-MQ was highly effective with recrudescence reported in only 1 patient out of 296 (Amaratunga et al., 2019). The continued reports of DHA-PPQ failures (van der Pluijm et al., 2019) and the demonstration that parasites returned to AS-MQ susceptibility prompted the reintroduction of AS-MQ and the use of triple-ACTs (TACTs) in Cambodia from 2015 to the present day (World Health Organization, 2017b). The triple therapy includes DHA-PPQ + mefloquine and has been shown to be efficacious in patients with negligible toxicities (van der Pluijm et al., 2019).

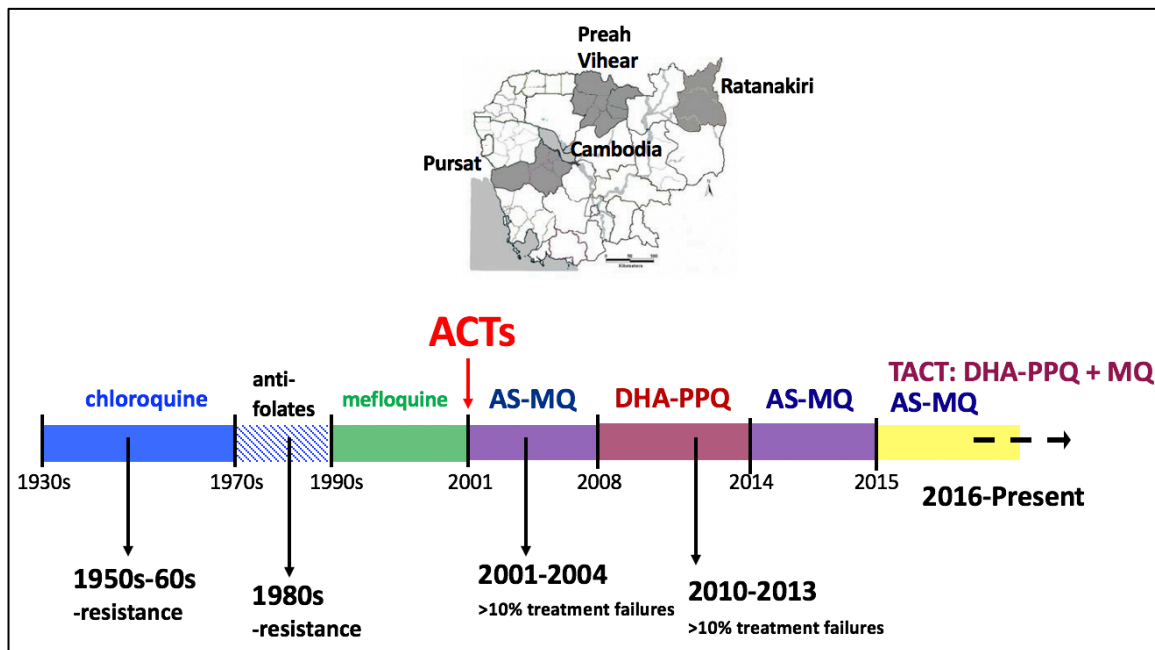


Figure 1. 8. Timeline of antimalarial drug use for the treatment of *P. falciparum* malaria in Cambodia. The period of time each drug has been used is indicated in color on the timeline. ACTs (red arrow) were introduced in 2001 in Cambodia. The approximate time widespread resistance developed (chloroquine and SP) or >10% treatment failures were first reported (AS-MQ (Denis et al., 2006) and DHA-PPQ (Amaratunga et al., 2016, Leang et al., 2013)) is indicated by the black arrows. Currently both triple ACTs (TACT) consisting of DHA-PPQ + MQ and AS-MQ are being used to treat uncomplicated *P. falciparum* malaria. A map of Cambodia is shown above the timeline and the shaded regions indicate three provinces where drug efficacy studies have been performed: from West to East, Pursat, Preah Vihear, and Ratanakiri. This dissertation has used parasite isolates from these three provinces and full details for the clinical sites will be discussed in Chapter 2 (General methodology).

In order to understand how piperazine resistance emerged and continues to spread in SEA, it is necessary to identify and characterize genetic changes in parasite populations that promote increased survival to piperazine.

1.3.2 Assessing drug-resistance in *P. falciparum*

Antimalarial drug resistance is defined as the ability of parasites to survive and/or multiply in the clinical setting despite treatment with the appropriate medication and dose. This definition necessarily includes that the parasite must have been exposed to the drug for the duration of time needed for the drug to exert its full antimalarial properties, ensuring drug compliance and proper absorption (taken with a fatty meal, etc.). This verifies that resistance is due to parasite adaptations and not due to the inability of the drug to “gain access to the parasite” (Bloland, 2001, Bruce-Chwatt, 1986). In such *in vivo* drug efficacy studies, true resistance is confirmed only after both remaining parasitemia and adequate serum drug concentrations are documented (Talisuna et al., 2004, Bloland, 2001).

Apart from the clinical setting, general ways to study and measure drug resistance include: surrogate *in vitro* assays, animal models, and detection of molecular markers (for example, by PCR assays or genomic studies) (Bloland, 2001). Surrogate *in vitro* assays test the effect of compounds on the parasites outside of the human host in cell culture, usually by a measure of survival. In *Plasmodium*, this is most easily performed with *P. falciparum* and *P. knowlesi*, since they have been adapted to grow in cell culture (Trager and Jensen, 1976, Moon et al., 2013). *In vitro* tests enable direct parasite biology to be assessed in response to specific drugs in a controlled environment outside of a host, however some notable disadvantages are also inherent because they are outside of the host. For example, if a prodrug needs to be cleaved within the host to its active metabolite (such as proguanil), it cannot be tested unless the compound is available and stable in its active form (as is the case with DHA). There is also no way to test the effects that host immunity may have on infection in *in vitro* settings. Nevertheless, *in vitro* work has provided much insight into the complex biology of the malaria parasite. Animal models (such as mice or non-human primates) can support both parasite biology studies and transmission studies under *in vivo* conditions. Lastly, molecular genomics studies encompass many techniques and approaches to enable molecular markers of resistance to be identified. In turn, they provide fundamental insight for highlighting the genetic candidates and pathways that *in vitro* studies can investigate. Candidate molecular markers can consist of any genetic variation including, single nucleotide polymorphisms (SNPs), copy number variations, insertions or deletions in the genome, and other such variations that are associated with the resistant-phenotype. It is then up to functional studies to verify if these markers are causal determinants of resistance.

1.3.3 The genetic basis of resistance

Drug resistance is the result of spontaneous and rare genetic mutations that alter genes directly or change the expression of genes (White, 2004). Sometimes a single genetic event is enough to produce a resistant phenotype, other times multiple genes may be involved. Furthermore, the resistance may be associated with the genetic background (epistasis) (White, 2004). *P. falciparum* has an approximate spontaneous mutation rate of $1.0\text{--}9.7 \times 10^{-9}$ mutations per base pair per generation in asexual culture (Bopp et al., 2013). Considering an average malaria infection can present with around $\sim 10^{12}$ parasites in the blood stream (which is about 2% parasitemia in the bloodstream), it is likely that random mutations will occur during several asexual life cycles (Cowell and Winzeler, 2019, White, 2004). These mutation rates are in the absence of selective drug pressure and are thought to be independent of the drug used (White, 2004). However, in the presence of drug pressure, mutations that confer

both a survival and fitness advantage would be favored. ACT partner drugs with long half-lives, such as mefloquine and piperazine offer a favorable selective environment because they remain in the bloodstream at suboptimal levels for weeks post initial infection.

There are many ways that parasites can develop resistance to antimalarial drugs. In general, two of the main mechanisms through which resistance is achieved are by: decreased availability of a drug at its target site (frequently due to mutations in transporter genes) and/or modification of the drug target (Paloque et al., 2016).

1.3.4 The parasite digestive vacuole and antimalarial drugs

Many antimalarial compounds, specifically ACT partner drugs, are believed to exert their effects in the parasite digestive vacuole by disrupting a crucial pathway: hemoglobin degradation (**Figure 1.7**). The digestive vacuole, located inside the parasite's cytosol and sometimes referred to as the food vacuole, is a membrane-bound organelle with an acidic pH. The digestive vacuole is the site of hemoglobin degradation (Wunderlich et al., 2012), during which 60-80% of the host cell hemoglobin is digested (Wunderlich et al., 2012). The parasite uses the degraded amino acids as a source of nutrients, since they have limited capabilities for *de novo* amino acid synthesis and exogenous uptake of amino acids (Goldberg et al., 1990).

Hemoglobin is the major protein in all erythrocytes that is responsible for carrying oxygenated blood throughout the body. Hemoglobin consists of four globin chains each containing a heme group, which consists of an iron ion in a heterocyclic ring surrounded by pyrrole molecules, called a porphyrin. In adults, hemoglobin A (HbA) is the most common form of hemoglobin and consists of two alpha globin chains and two beta globin chains. In SEA, hemoglobin E (HbE) is a very common variant and consists of two alpha globin chains and two mutant beta globin chains (Munkongdee et al., 2016). In Africa, hemoglobin S (HbS) consists of two alpha globin chains and two beta globin chains with a different mutation that results in sickle cell anemia. Individuals who are heterozygous for the sickle cell trait have protection from malaria infection (Weatherall and Clegg, 2001). In contrast, some studies have shown that HbE does not provide protective advantage against infection with *P. falciparum* malaria in studies in Thailand (Lithanatudom et al., 2016, Carter and Mendis, 2002) and in Cambodia (personal communication with Dr. Chanaki Amaratunga) where parasites may invade and develop normally in HbE erythrocytes. It is worth mentioning that some studies conducted in Thailand have found that it may be more difficult

for *P. falciparum* to invade HbE erythrocytes *in vitro* (Chotivanich et al., 2002). The authors suggest that although HbE does not prevent infection, it could prevent high parasitemias, however further *in vivo* and *in vitro* studies are necessary to further validate these findings.

When the parasite breaks down hemoglobin, heme is released as a toxic byproduct. To prevent oxidative damage from the reactive iron-heme groups, enzymes in the digestive vacuole convert (detoxify) the reactive heme to inert hemozoin crystals (Wunderlich et al., 2012). The hemozoin is what accounts for the characteristic brown pigment in malaria parasites that can be seen in the digestive vacuole when viewed by light microscopy. (This is the same pigment that Laveran and Ross distinguished when identifying *Plasmodium* in the blood and mosquitoes, respectively.) There are many different enzyme families that facilitate hemoglobin degradation and heme detoxification. Four plasmepsin enzymes (plasmepsins 1-4) are aspartic proteases that localize to the digestive vacuole and digest hemoglobin. Plasmepsins 1 and 2 initiate hemoglobin digestion and plasmepsins 3 and 4 aid in degradation after initial cleavage (Banerjee et al., 2002, Goldberg et al., 1991, Francis et al., 1997). Falcilysins and falcipains, cysteine proteases and metalloproteases, respectively, function downstream of the plasmepsins to further degrade hemoglobin (Subramanian et al., 2009, Eggleston et al., 1999). Another enzyme, heme detoxification protein (HDP) helps to generate inert hemozoin crystals from heme (Jani et al., 2008, Nakatani et al., 2014). Studies have also suggested a role for a glutathione-dependent process of heme degradation (Ginsburg et al., 1998). These are just a few examples of the various proteins and often overlapping processes that take place to achieve hemoglobin metabolism in the digestive vacuole. Such overlapping and redundant functions of many hemoglobin-degrading proteins may explain why many genes encoding these enzymes can be knocked out (Moura et al., 2009, Omara-Opyene et al., 2004, Bonilla et al., 2007) without compromising parasite viability.

Multiple transporters and ion pumps are also located on the membrane of the digestive vacuole. Two transporters that function in drug resistance are the chloroquine resistance transporter, PfCRT and the multidrug resistance protein 1 (PfMDR1). PfCRT has been shown to efflux substrates from the digestive vacuole into the parasite cytosol, while PfMDR1 has been shown to import substrates from the cytosol into the digestive vacuole (Bray et al., 2005, Ecker et al., 2012, Valderramos and Fidock, 2006, Reiling and Rohrbach, 2015).

In order to understand the mechanisms of drug resistance and prevent the emergence and spread of resistance, it is important to discover the genetic determinants of resistance and their corresponding markers.

1.4 Genetic background and mechanisms of resistance in SEA

1.4.1 Chloroquine

Chloroquine is a weak base and its mode of action is believed to be through its localization to the parasite's acidic digestive vacuole, where it disrupts heme detoxification (Wellems and Plowe, 2001). When chloroquine is inside the acidic vacuole, it becomes protonated and builds up inside the organelle (Homewood et al., 1972, Yayon et al., 1984). Once inside the digestive vacuole, it disrupts heme detoxification and results in parasite death due to the build-up of its own toxic byproduct (**Figure 1.7**) (Wellems and Plowe, 2001).

The mechanism of chloroquine resistance is through the parasite's ability to prevent the accumulation of chloroquine in the digestive vacuole. This is accomplished via the transporter, PfCRT (Wellems et al., 1991). PfCRT is a highly polymorphic protein with 10 transmembrane domains consisting of 424 amino acids located on chromosome 7 (PF3D7_0709000). Mutations in the *pfCRT* gene, specifically K76T, were found to play a role in chloroquine resistance *in vitro* and were also associated with clinical resistance in field studies across endemic regions (Fidock et al., 2000, Carlton et al., 2001, Bray et al., 2005, Picot et al., 2009). The switch from the positively charged lysine residue to the uncharged threonine residue enables protonated-chloroquine to be effluxed from the digestive vacuole (Lehane and Kirk, 2008, Martin and Kirk, 2004, Martin et al., 2009). The PfCRT K76T mutation is found in almost all chloroquine-resistant isolates, regardless of geographic location.

Mutations in the multidrug transporter, PfMDR1, have also been associated with decreased susceptibility to chloroquine. PfMDR1 is a transporter in the ATP-binding cassette (ABC) transporter family consisting of 1419 amino acids on chromosome 5 (PF3D7_0523000) encoding a predicted 12 transmembrane domain protein. The homologous protein in mammalian cells is often referred to as P-glycoprotein (P-gp). Several studies have found an N86Y mutation in *pfmdr1* that, when jointly present with PfCRT mutations, decreases parasite susceptibility to chloroquine (Foote et al., 1990, Babiker et al., 2001, Sa et al., 2009). Molecular studies have found that editing the *pfmdr1* N86Y mutation into chloroquine-resistant parasites decreases the parasites susceptibility to chloroquine (Veiga et al., 2016a).

However, additional work has shown that the N86Y mutation alone is not enough to confer chloroquine resistance (Djimde et al., 2001, Valderramos and Fidock, 2006) and further work is needed to assess the role of the *pfmdr1-N86Y* mutation in modulating chloroquine resistance in the field.

Recent studies have found that the PfCRT K76T mutation has reverted to a majority of wildtype after removal of chloroquine pressure in some countries in Africa (Mohammed et al., 2013, Mwanza et al., 2016) and China (Wang et al., 2005). However, the mutation remains at some level nearly everywhere (SEA, South America, and Africa). Residual persistence at low levels could be due to the continued use of chloroquine for symptomatic relief or for the treatment of presumed *P. vivax*. An alternative reason could be that the mutation is fixed in a population, because the sensitive parasites without the mutation did not survive (Cowell and Winzeler, 2019). Notably, studies by Pelleau *et al.* in French Guiana have found that in spite of the fixed PfCRT K76T allele, parasites are again chloroquine susceptible and they have identified a PfCRT C350R mutation that associates with the chloroquine-sensitive phenotype (Pelleau et al., 2015). This study also found that the PfCRT C350R mutation decreased parasite susceptibility to piperazine *in vitro*. They hypothesized that this mutation could be due to increased pressure from piperazine, as DHA-PPQ is available in the region (Pelleau et al., 2015).

In the context of chloroquine-resistance, mutations in PfCRT and PfMDR1 have both served as molecular markers of potential resistance, with PfCRT having the causal role in resistance. It was on this genetic background that mefloquine was introduced as a monotherapy and later as a partner of ACTs in Cambodia.

1.4.2 Mefloquine: monotherapy and ACT

Mefloquine is an aryl amino alcohol that was synthesized as a derivative of quinine at the Walter Reed Army Institute of Research (WRAIR) shortly after the Vietnam War during the push to discover new antimalarials in the 1960s-1970s (Arrow, 2004). Five years after its introduction in SEA, mefloquine resistance was reported in Thailand in the early 1980s (Nosten et al., 1991, Boudreau et al., 1982).

Resistance to mefloquine has been shown to be the result of a *pfmdr1* copy number variation (**Figure 1.7**). Rather than a point mutation as observed in chloroquine resistance, mefloquine resistance results from increased copies of *pfmdr1* both in the field and *in vitro* (Oduola et al.,

1988a, Cowman et al., 1994, Reed et al., 2000, Lim et al., 2009, Price et al., 2004). Furthermore, increasing the number of *pfmdr1* copies, increases the level of resistance *in vitro* (Sidhu et al., 2006). The *pfmdr1* amplification may also result in cross-resistance to the partner drug, lumefantrine, which is another aryl amino alcohol. Some studies have found an association of artemether-lumefantrine treatment failures and increased *pfmdr1* copy numbers (Price et al., 2006). However, increased *pfmdr1* copy numbers are infrequent in African countries, where artemether-lumefantrine is often used (Cheeseman et al., 2016).

As widespread AS-MQ treatment failures occurred throughout SEA and countries were switching to DHA-PPQ, the list of molecular markers of drug resistance continued to grow. In addition to monitoring PfCRT mutations, studies began tracking PfMDR1 mutations and copy numbers.

1.4.3 DHA-PPQ: piperazine resistance in concert with decreased artemisinin susceptibility

In 2008, decreased susceptibility of parasites to artemisinin *in vivo* was reported in Western Cambodia (Dondorp et al., 2009, Noedl et al., 2008). Over the next couple of years, decreased artemisinin susceptibility was documented at other sites in Cambodia, Thailand, Vietnam, Myanmar, Laos, and China (Fairhurst and Dondorp, 2016).

As briefly mentioned in the previous sections of this introduction, both the mechanism of action of artemisinin and the mechanism of artemisinin resistance have sparked continued debate and the discussion is ongoing. Multiple genome-wide association studies (GWAS) have been conducted to uncover molecular markers that associate with decreased artemisinin susceptibility *in vivo* and *in vitro* (Cheeseman et al., 2012, Takala-Harrison et al., 2013). Work by Arieu *et al.* identified mutations in the propeller domain of a kelch protein (K13) that associated with artemisinin resistance *in vivo* and *in vitro* (Arieu et al., 2014). The Tracking Resistance to Artemisinin Collaboration (TRAC) study further validated these studies in a multi-country collaboration that confirmed the association of several K13 mutations and decreased artemisinin susceptibility *in vivo* (Ashley et al., 2014). Genome editing studies also found an association between the K13 mutations and artemisinin resistance *in vitro*, as measured by a “ring-stage assay” that involves a short pulse of DHA on early ring stage parasites (Ghorbal et al., 2014, Straimer et al., 2015, Witkowski et al., 2013). Previous studies identified five K13 mutations that associated with the artemisinin-resistant phenotype (*K13-C580Y*; *K13-R539T*; *K13-Y493H*; *K13-I542T*; and *K13-P553L*) (Miotto et

al., 2015) and a more recent study by the Worldwide Antimalarial Research Network (WWARN) identified 20 *K13* mutations (WWARN, 2019).

The K13 protein (PF3D7_1343700) is postulated to serve a role in the parasite's response to oxidative stress through multiple protein-protein interactions (Ariey and Menard, 2019). The *P. falciparum* K13 protein is homologous to the human KLHL12 and KLHL2 proteins and Keap1, which function in ubiquitin-based degradation of proteins and oxidative stress responses, respectively (Dhanoa et al., 2013, Itoh et al., 1999). Recent findings have also raised the intriguing postulation that *P. falciparum* gametocytogenesis may be improved by certain K13 mutations, and thus promote transmission to mosquitoes as a parasite survival mechanism (Ashley et al., 2014, Lozano et al., 2018).

It should be emphasized there are multiple studies that have observed artemisinin-resistant phenotypes in the absence of K13 mutations, suggesting additional molecular determinants of resistance exist, and thus further work is necessary to determine if and how these may impact artemisinin resistance (Demas et al., 2018, Sa et al., 2018, Sutherland, 2017, Su et al., 2019).

1.4.4 Piperaquine resistance

Less than four years after the reports of decreased artemisinin susceptibility, DHA-PPQ treatment failures were reported in Western Cambodia (Spring et al., 2015, Amaratunga et al., 2016). Most recently, clinical studies have demonstrated very high treatment failures with an average of 50% treatment failures in parts of Cambodia, Vietnam, and Thailand (van der Pluijm et al., 2019).

Multiple GWAS studies were performed to identify potential molecular markers of piperaquine resistance. A GWAS of 297 Cambodian isolates revealed single-nucleotide polymorphisms (SNPs) on chromosome 13 in genes that encode a putative exonuclease (*exo-E415G*) (PF3D7_1362500) and a putative mitochondrial carrier protein (*mcp-N252D*) (PF3D7_1368700) that associate with reduced PPQ susceptibility *in vitro* and DHA-PPQ failures in patients (Amato et al., 2017). Additionally, a copy number variation (CNV) in the *plasmepsin 2* (*PM2*) and *plasmepsin 3* (*PM3*) genes on chromosome 14 associated with reduced susceptibility to piperaquine (Witkowski et al., 2017). Specifically, increased copies of *PM2-3* are associated with increased parasite survival under piperaquine pressure. Little is known about the putative exonuclease protein and mitochondrial carrier proteins on chromosome 13. However, as described above, previous work has determined a role for *PM2*

and PM3 in hemoglobin degradation in the parasite's digestive vacuole (Banerjee et al., 2002).

More recent studies have also demonstrated a role for mutations in the familiar transporter, PfCRT. Drug pressure experiments conducted over eight years ago identified a PfCRT-C101F mutation and a deamplification of *pfmdr1* in parasites that had been pressured with piperazine *in vitro*. Genome editing of the C101F mutation in parasites decreased parasite susceptibility to piperazine, but increased sensitivity to chloroquine (Dhingra et al., 2017). Another recent study identified three mutations in culture-adapted isolates from Cambodia that exhibited *ex vivo* piperazine resistance: PfCRT H97Y; PfCRT M343L; and PfCRT G353V (Duru et al., 2015). Genome editing of these three mutations and an additional mutation observed in patient isolates, PfCRT F145I, was found to confer piperazine resistance *in vitro* (Ross et al., 2018a). Additional GWAS studies have continued to find these mutations associated with piperazine failures in patients and have also reported two new mutations associated with PPQ-resistance, PfCRT T93S and PfCRT I218F (Hamilton et al., 2019). These piperazine resistance-associated mutations are all on the PfCRT K76T genetic background and the parasites still demonstrated reduced chloroquine susceptibility in *ex vivo* and *in vitro* survival assays (Amaratunga et al., 2016).

The piperazine-resistant parasites isolated from Cambodia have single copies of *pfmdr1*, indicating that the parasite population reverted back to a single copy of *pfmdr1* after the removal of mefloquine pressure from the region. One hypothesis is that piperazine gains access to the digestive vacuole through PfMDR1 (Witkowski et al., 2017), so reducing *pfmdr1* expression could reduce the amount of piperazine in the digestive vacuole. It is also possible that the *pfmdr1* copy number expansion results in a fitness cost, so in the absence of mefloquine pressure, there is no need (and is metabolically disadvantageous) for the parasites to maintain it.

It is hypothesized that increased tolerance to artemisinin facilitated the emergence of piperazine-resistant parasites. This is further supported by the genetic background of the parasites, as the majority piperazine-resistant parasites have K13-C580Y mutations (Amaratunga et al., 2016, van der Pluijm et al., 2019). Out of 2465 parasite genomes, 82% of parasites that highly associated with the piperazine-resistant phenotype were K13-C580Y, 5.4% were Y493H, and 5.3% were R539T (Hamilton et al., 2019).

Several studies have hypothesized that piperazine (like chloroquine and the other ACT partner drugs) interferes with heme detoxification and/or hemoglobin degradation. This is supported by transmission electron microscopy (TEM) studies by Sachanonta *et al.* that show distended digestive vacuoles with undigested hemoglobin and fewer hemozoin crystals than the untreated control after treatment with piperazine (**Figure 1.9**) (Sachanonta *et al.*, 2011). It is possible that increased *PM2-3* copy numbers could enable the parasite to circumvent any inhibition caused by the drug. In a similar fashion to the mechanism of chloroquine resistance, the PfCRT mutations could also enable efflux of piperazine from the digestive vacuole.

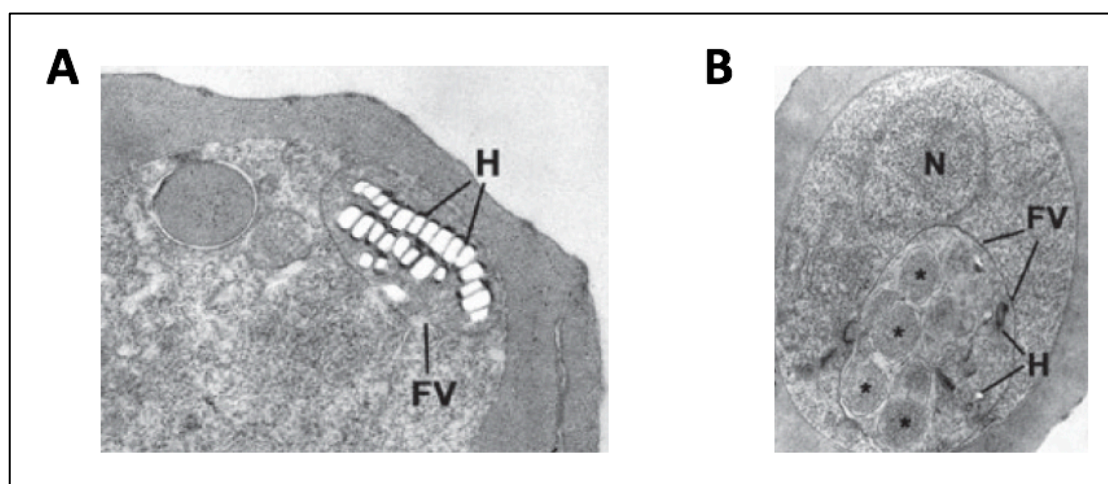


Figure 1. 9. Transmission electron microscopy of *P. falciparum* infected erythrocytes. A.) Low-power TEM of the control sample (no drug) in the trophozoite stage **B.)** Low-power TEM of treated sample after 4-hour exposure to piperazine in the trophozoite stage. The asterisks (*) indicate undigested hemoglobin in the distended digestive vacuole. Abbreviations indicate: nucleolus (N), food vacuole (FV), and hemozoin crystal (H). The images in this figure were modified and reproduced from Sachanonta *et al.* (Sachanonta *et al.*, 2011) with permission from Taylor & Francis Publishing.

1.5 Specific aims

The purpose of my thesis work has been to elucidate the molecular mechanisms of piperazine resistance. This dissertation has utilized molecular genomics, *in vitro* gene editing, and drug-pressure experiments to provide new insight into piperazine resistance in *P. falciparum*.

In the first research chapter (Chapter 3), I sought to design a high-throughput assay that could be utilized for analyzing copy number amplifications of the hemoglobin degrading proteases, *plasmepsin 2* and *plasmepsin 3*, using low quantities of genomic DNA. I developed methods to detect and monitor *plasmepsin 2-3* copy numbers using both traditional PCR and qPCR methods. I then examined the role of the *PM2-3* amplification in piperazine resistance by generating and transfecting a plasmid for overexpressing the *PM2-3* enzymes.

In the second research chapter (Chapter 4), I aimed to assess the effects of the putative *exonuclease* (PF3D7_1362500) and *mitochondrial carrier protein* (PF3D7_1368700) SNPs (*exo-E415G* and *mcp-N252D*) on susceptibility to piperazine and other commonly used antimalarial drugs. I used CRISPR-Cas9 genome editing to introduce the wildtype and mutant SNPs into the lab strain Dd2 and evaluate the phenotypes of piperazine response in these transformants.

In the final research chapter (Chapter 5), I aimed to select for a piperazine-resistant phenotype *in vitro* using a potential hypermutator *P. falciparum* parasite line. After generating piperazine-resistant parasites, I used whole genome sequencing to compare genetic differences between the parental parasites and the piperazine-pressured parasites. Through this analysis, I identify gene candidates that may play a role in the piperazine-resistant phenotype.

Chapter 2: General Methodology

2.1 Cultivation of *Plasmodium falciparum*

Parasites were cultivated *in vitro* following the methods developed by Trager and Jensen with minor modifications (Trager and Jensen, 1976). All cell culture work was conducted in a sterile biological safety cabinet and the mandatory safety precautions of each institution were followed (United States, Biosafety Level-2/BSL-2; United Kingdom, Containment Level-3/CL3).

2.1.1 *In vitro* culture maintenance

Asexual stages of *P. falciparum* isolates adapted for cell culture were grown in complete media (CM) consisting of Roswell Park Memorial Institute medium (RPMI)-1640 (Thermo Fisher Scientific) supplemented with 0.5-1% Albumax II (a serum substitute), GlutaMAX (Gibco, L-glutamine substitute), HEPES (20 mM, pH 7.0), 2.0 g/L sodium bicarbonate, and gentamicin (25 µg/ml) with 2-3% O+ human erythrocytes, more commonly referred to as red blood cells (RBCs). All parasite lines used in this study were adapted for continuous culture in Albumax II, a human serum substitute, but when specified, field isolates were also supplemented with 1.25-5% pooled human AB serum (Innovative Research). Unless noted otherwise, parasites were maintained in routine continuous culture at 0.5-2% parasitemia in CM at 2-3% hematocrit and stored at 37°C in non-vented tissue culture flasks (Corning) after addition of mixed gas containing 1% O₂, 3% CO₂, and 96% N₂.

2.1.2 Determination of parasite culture hematocrit and parasitemia

Hematocrit is defined as the proportion (% volume) of red blood cells per volume of blood or culture. For the purposes of this thesis and as widely standardized for *in vitro* cultivation of *P. falciparum* (Trager and Jensen, 1976), hematocrits ranged from 1-5% depending on the parasite line and experimental procedure. *P. falciparum* can invade and grow in all human blood types, but O+ RBCs were used preferentially due to their compatibility with any serum type (Jensen, 1988, Schuster, 2002). Leukocyte-depleted RBCs were obtained from healthy O+ donors weekly (Interstate Blood Bank, USA or National Health Service (NHS), UK) and added fresh to cultures at least once per week. Before use in cultures, the blood was aliquoted and washed twice with incomplete media (ICM) (RPMI-1640, with no additional supplements) by centrifugation at 3000 RPM for 10 minutes, without brake to ensure separation of the medium from the packed RBCs (pRBCs). After the final wash, the top layer

of ICM was aspirated and CM was added to dilute the packed cells to 50% hematocrit. Aliquots were stored at 4°C and used to maintain cultures for up to two weeks. When specified, 10% citrate-phosphate-dextrose-adenine (CPDA), an anticoagulant/whole blood preservative was added to the 50% hematocrit aliquot to prolong RBC integrity in long-term culture experiments (see **sections 2.3-2.4**).

Parasitemia denotes the quantification of parasites in the blood. Parasites can be measured in the blood using light microscopy or flow cytometry. The methods used for this study were based on the degree of quantitative accuracy required. Flow cytometry was utilized when more accurate parasite counts were necessary or to detect very low parasitemias (see section 2.7 on flow cytometry). Light microscopy was preferred for day-to-day culturing and accurate staging of the 48-hour *P. falciparum* life cycle.

To view and quantify *P. falciparum* parasitemia in cell cultures, medium was aspirated from the culture and ~1.5-2 µl of the pRBCs were spread on a glass microscope slide to create a thin film or “smear” of blood. Thin smears of every culture were made at least once weekly to quantify the percent parasitemia. The blood smears were fixed in 100% methanol, stained with 10% Giemsa (Sigma-Aldrich) for 10 minutes, then viewed with the 100X objective under oil immersion. Components in the Giemsa staining solution attach to DNA, making the stain particularly useful for detecting malaria parasites in cell culture, since their RBC hosts are devoid of a nucleus. Thus, any Giemsa stained cells on the blood smear can be viewed and counted as a parasite. (Note this restricted to *in vitro* parasite cultures or other samples depleted of leukocytes; in patient blood, leukocytes and any circulating reticulocytes (younger RBCs) contain DNA and would stain positive as well.) Parasitemia was calculated by dividing the number of parasite-infected red blood cells (iRBCs) by the total number of RBCs (iRBCs + uninfected RBCs) times one hundred (iRBCs/total RBCs*100= % parasitemia). For each smear, at least 500 cells were counted to obtain the % parasitemia.

Parasitemias of continuous cultures ranged between 0.5-5%, depending on the parasite line and experiment. For specific experimental protocols, parasitemias were grown above 5%, but culture medium was changed at least once daily to avoid nutrient depletion and stress. High parasitemias and other environmental conditions of *in vitro* cultures have been shown to stress asexual stage parasites and promote the irreversible conversion of asexual stages to gametocytes, the non-replicating, sexual stage of parasites (Carter and Miller, 1979).

Parasitemias of cultures were therefore monitored carefully and the higher the parasitemia,

the more frequent medium changes and blood replenishment occurred to prevent increased gametocyte production.

2.1.3 Thawing and cryopreservation of parasites

To minimize effects from long-term *in vitro* cultivation, parasites were grown in culture for up to 2-3 months then discarded after a fresh aliquot of the isolate was thawed. Parasite lines adapted for continuous culture were cryopreserved as described below and stored in a -80°C freezer or in liquid nitrogen. Frozen cryovials were thawed for 2-3 minutes in a 37°C incubator. All thawing solutions were warmed to 37°C before use. After thawing, the volume of the isolate was measured and transferred to a 50 mL centrifuge tube. Slowly, 0.1x the volume of 12% NaCl was added dropwise to the culture with gentle, intermittent shaking/swirling between drops. The tube was left standing at room temperature for 5 minutes. Next, 10x the volume of 1.6% NaCl was added to the isolate dropwise, while shaking/swirling. The mixture was left at room temperature undisturbed for an additional 5 minutes. Then the tube was centrifuged at 1500 RPM, room temperature for 5 minutes. The supernatant was aspirated and 10x the volume of 0.9% NaCl/0.2% dextrose was added dropwise to the pellet while slowly swirling the tube. The culture was centrifuged as before at 1500 RPM for 5 minutes. After aspirating the remaining thawing solution, the pellet was resuspended in pre-warmed CM and transferred to a culture flask and fresh RBCs were added, depending on the volume of thawed blood, for a final hematocrit of 1-3%.

Cryopreservation of the parasites was performed as soon as the cultures contained at least 1-2% of ring-stage parasites. Such ring-stage parasitemia is necessary because the method for freezing-down the cultures only preserves ring-stages. The culture was centrifuged at 2500 RPM for 5 minutes. The medium was aspirated and the volume of the packed culture was estimated and 1.66x the pellet volume of pre-warmed Glycerolyte 57 (Fenwal) solution was added to the pellet dropwise, with gentle shaking. The solution was transferred to a labelled cryovial (up to 1 mL per vial) and stored in a -80°C freezer or liquid nitrogen.

2.1.4 Synchronization of parasites: sorbitol and Percoll gradients

In *P. falciparum*-infected patients, the populations of parasite stages may be asynchronous or synchronous (Hawking et al., 1968, Hawking, 1970, Garcia et al., 2001). Ring stages predominate in circulation because mature trophozoite and schizont stages are sequester in the vasculature or are removed by splenic filtration (Miller et al., 2002). Ring stages survive

better than mature stages during cryopreservation, so that freshly established cultures tend to be synchronous, but these will become asynchronous after several life cycles (Trager and Jensen, 1976, Haynes et al., 1976). For many experimental procedures, stage-specificity is crucial, so two main methods of synchronization were employed by this study: sorbitol lysis and Percoll gradient separation.

2.1.5 Sorbitol synchronization

Sorbitol synchronization was used to obtain ring-stage populations of parasites (Lambros and Vanderberg, 1979). A stock solution of 5% D-sorbitol was prepared in deionized water and filtered (0.2 μm). Cultures containing mostly rings (less than 10-12 hours post-invasion) were centrifuged at 2500 RPM for 5 minutes, medium aspirated and the volume of the pellets/pRBCs was measured. The pellets were resuspended in 10x the pellet volume of pre-warmed 5% sorbitol, vigorously mixed and left at 37°C for 10-15 minutes. After incubation, the tubes were centrifuged at 2500 RPM for 5 minutes and resuspended in 10x volume of ICM. Cells were again centrifuged at 2500 RPM for 5 minutes, media was aspirated and cells were resuspended in CM to maintain the culture volume at 2-3% hematocrit.

2.1.6 Percoll gradients for parasite synchronization

Percoll gradients were used to separate late-stage parasites from early stages (Kramer et al., 1982, Stanley et al., 1982). Percoll enrichment was performed using either a 35%/65% gradient when at the National Institutes of Health (USA) or using a 63% single gradient when at the Wellcome Sanger Institute (UK). Variations in the protocols at each institute were based only on the availability of resources at each location and no differences were observed in experimental results from either Percoll procedure.

For the 35%/65% gradient procedure (Miao and Cui, 2011), a 90% stock of Percoll (GE Lifesciences) was made by diluting 9 volumes of Percoll in 1 volume of 10X PBS. The 90% Percoll stock was kept at 4°C for up to 1 month before making a fresh stock. On the day of synchronization, a solution of 7.5 U/mL heparin (Sigma) in ICM, referred to as heparinized RPMI, was prepared and warmed at 37°C. Aliquots of 35% and 65% Percoll were made by diluting the pre-warmed 90% Percoll stock with heparinized RPMI. Cultures to be synchronized were centrifuged at 2500 RPM for 5 minutes and resuspended in heparinized RPMI and left standing at 37°C for 15 minutes. While parasites were incubating, Percoll gradients were prepared in 15 mL centrifuge tubes by pipetting 65% Percoll into each tube,

then layering 35% Percoll on top, being careful not to create any bubbles or disturb the separation between the two solutions. The culture was then added on top of the 35% layer and a distinct separation between the culture and the Percoll layers was observed. The gradients were layered in 3's with 3 mL of 65% Percoll, followed by 3 mL of 35% Percoll, and 3 mL of culture consisting of ~300 μ L packed RBCs. After adding all three layers the tubes were centrifuged for 15 minutes at 1000g with no brake. After centrifugation the top layer containing debris was discarded (see **Figure 2.1**), the next layer containing the enriched, mature parasitized RBCs was saved and added to a tube containing 10 mL of pre-warmed ICM. The bottom pellet containing early stages and uRBCs was washed in 10 mL of ICM or discarded as necessary for the particular experiment. The tubes were centrifuged at 1000g for 5 minutes then resuspended in the desired volume of CM and/or RBCs.

The 63% Percoll procedure was performed by diluting Percoll to 63% with ICM and 10X PBS. This protocol does not use heparin. The culture was centrifuged at 800g for 5 minutes while 5-6 mL of pre-warmed 63% Percoll was added to 15 mL tubes. After centrifugation, the pellet (at least 1-1.5 mL of pRBCs) was resuspended in 5 mL of CM and layered on top of the 63% Percoll. The gradient was centrifuged at 1200g for 12 minutes, 0 break. After centrifugation, the layers were treated the same as for the aforementioned 35%/65% gradient, with the top debris layer aspirated and discarded, the middle late-stage layer saved and bottom pellet saved, if desired. The separated stages were washed in 10 mL of prewarmed CM by centrifugation at 800g for 5 minutes and resuspended in the volume of CM and RBCs needed for subsequent experiments.

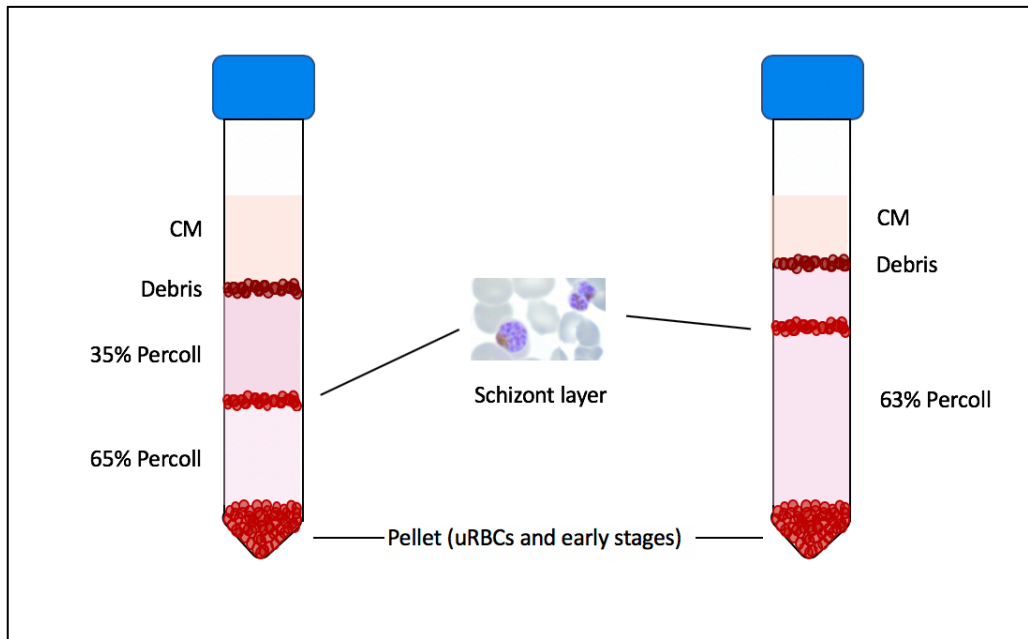


Figure 2. 1. Schematic of Percoll gradients. A.) Schematic of a 35%/65% Percoll gradient. The topmost cell suspension layer is aspirated, the distinct band in the middle between the 35% and 65% layers are enriched late-stage parasites, which can be seen in the Giemsa smear. The bottom pellet contains uninfected RBCs (uRBCs) and early-stage parasites. **B.)** Schematic of a 63% Percoll gradient.

2.2 Parasite lines

2.2.1 Cambodian field isolates

The patient isolates used for this study were obtained from cohort studies performed from September 2012 through December 2013 in three Cambodian provinces (ClinicalTrials.gov number, NCT01736319) (Amaratunga et al., 2016). All samples were collected from patients aged 2-65 years with acute, uncomplicated *P. falciparum* malaria. The isolates were adapted to *in vitro* parasite culture (Amaratunga et al., 2016) using previously published methods (Trager and Jensen, 1976, Haynes et al., 1976) and cultivated with the same culture conditions used for established parasite lab lines (**see Section 2.1**). The field isolates used during the course of this thesis research are summarized in Table 1.

The isolates referred to as piperazine-resistant (PPQ-R) in this study are from the Western Cambodian province of Pursat or the Northwestern province of Preah Vihear. Isolates referred to as piperazine-sensitive (PPQ-S) are from the Eastern province of Ratanakiri or Preah Vihear (**Figure 2.2**). Since PPQ-S parasites may recrudesce for various reasons and not all PPQ-R infections will recrudesce in immune patients, final categorization of lines as PPQ-R or PPQ-S was established by parasite susceptibility to piperazine as determined in *ex vivo*, *in vitro*, and piperazine survival assays (PSAs) (Duru et al., 2015, Amaratunga et al., 2016, Amato et al., 2017). Recrudescence vs. recurrent infections were determined by PCR

genotyping *msp1*, *msp2*, and *glurp*, the genetic markers used to distinguish recurrent infections from new infections (Snounou and Beck, 1998). Using both genotypic and phenotypic data, we were then further able to distinguish both the PPQ-R and PPQ-S populations of parasites (**Table 2.1**). The parasites referred to as PPQ-R have non-synonymous single nucleotide polymorphisms (SNPs) in the genes encoding the following proteins: K13 C580Y, MCP-N252D, *exo-E415G*, and several contain mutations in PfcRT including H97Y, M343L, and A366T. They also have two or more copies of *plasmepsin 2* and *plasmepsin 3* and one copy of *pfmdr1* (**Table 2.1**). In contrast the PPQ-S group of parasites are wildtype for: K13 C580, MCP-N252, *exo-E415*, and they have a single copy of *plasmepsin 2* and *plasmepsin 3*; similarly, they have one copy of *pfmdr1* (**Table 2.1**) but none of the PfcRT mutations noted in the PPQ-R parasites (Amaratunga et al., 2016). Details of these lines were published after whole genome sequencing in Amato *et al.* 2017 (Amato et al., 2017).

The Cambodian field isolate, PH-0212-C, was also used in this study and detailed in Table 2.1. It was obtained from Pursat, Cambodia in 2010 (Amaratunga et al., 2012) ClinicalTrials.gov, number NCT00341003) and has an intermediate resistance to PPQ and some of the mutations present in the isolates from 2012-2013 (**Table 2.1**).

Table 2. 1 Summary of Cambodian field isolates and laboratory strains used in this study

Oxford code (Sanger ID)	Code/Name	Region	PPQ status	Year	Recrudescence after DHA-PPQ treatment	Kelch13	mdr1 CN	PM2-3 CN	exo-E415G SNP	mcp-N252D SNP	PfcRT SNPs
PH1150-C	163-KH2-40	Preah Vihear	PPQ-S	2013	No	WT	1	1	E	N	WT
PH1034-C	163-KH2-007	Preah Vihear	PPQ-S	2012	No	WT	1	1	E	N	WT
PH1310-C	163-KH3-056	Ratanakiri	PPQ-S	2013	No	WT	1	1	E	N	WT
PH1058-C	163-KH3-012	Ratanakiri	PPQ-S	2012	No	WT	1	1	E	N	WT
PH0971-C	163-KH3-005	Ratanakiri	PPQ-S	2012	No	WT	1	1	E	N	WT
PH1097-C	163-KH2-033	Preah Vihear	PPQ-S	2012	No	WT	1	1	E	N	WT
PH1008-C	163-KH1-01RME	Pursat	PPQ-R	2012	Yes	C580Y	1	2	G	D	M343L
PH1345-C	163-KH1-004	Pursat	PPQ-R	2012	Yes	C580Y	1	3	G	D	WT
PH1224-C	163-KH1-081	Pursat	PPQ-R	2013	Yes	C580Y	1	2	G	D	A366T
PH1387-C	163-KH2-021	Preah Vihear	PPQ-R	2012	Yes	C580Y	1	2	G	D	H97Y
PH1265-C	163-KH1-060RME	Pursat	PPQ-R	2013	Yes	C580Y	1	3	G	D	H97Y
PH1263-C	163-KH1-059RME	Pursat	PPQ-R	2013	Yes	C580Y	1	3	G	D	H97Y
Dd2	Dd2	Southeast Asia	PPQ-S	N/A	N/A	WT	2	1	E	N	WT
3D7	3D7	Africa	PPQ-S	N/A	N/A	WT	1	1	E	N	WT

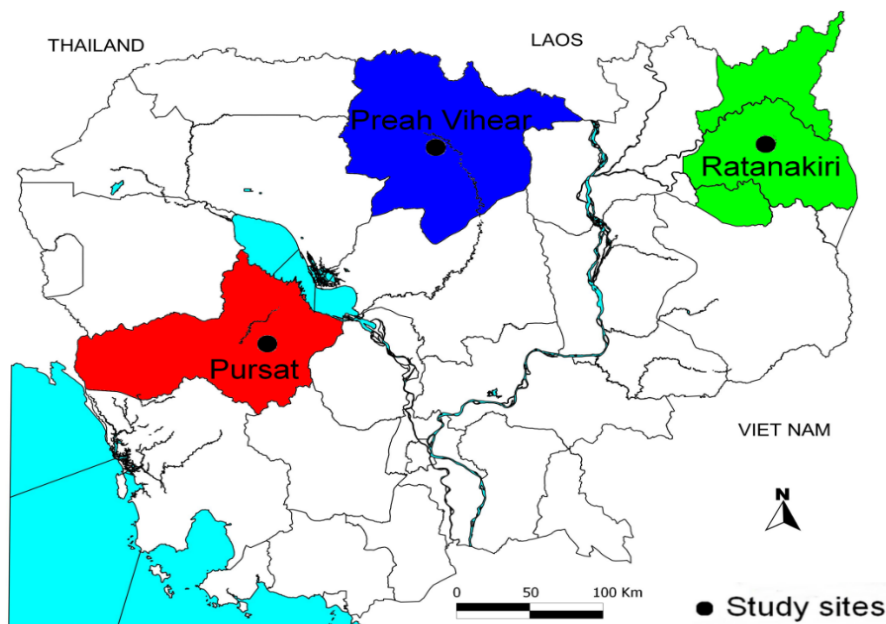


Figure 2. 2. Map of Cambodia highlighting the three provinces where samples were collected during clinical trials. From West to East, Pursat (red) is identified as “KH1” in the NIH sample identification code, Preah Vihear (blue) is “KH2,” and Ratanakiri (green) is “KH3.”

2.2.2 Long-term laboratory-adapted parasite lines

The laboratory strains (lab strains) used in this study are differentiated from the contemporary Cambodian isolates in that the lab lines are widely used parasite lines that have been maintained *in vitro* for many years. The lab strains, 3D7 and Dd2, were used for the purposes of this research and are included in Table 2.1.

The 3D7 parasite is a clone of NF54, which originated from a patient living near the Schiphol Airport, Amsterdam in the Netherlands, who had never been abroad (Ponnudurai et al., 1981, Walliker et al., 1987). The exact origin of the NF54 isolate is still unknown, but genetic studies suggest that it is from Africa (Preston et al., 2014, Su, 2014).

The Dd2 parasite is a Southeast Asian line derived as a clone from the W2-MEF line (a mefloquine pressured clone of W2) (Oduola et al., 1988a) which was obtained from an Indochina/CDC *P. falciparum*-infected patient isolate (Oduola et al., 1988b, Guinet et al., 1996).

2.3 Transfection of *P. falciparum* field isolates and laboratory lines

2.3.1 Transfection of *P. falciparum* using DNA-loaded red blood cells

Transfections of pre-loaded RBCs were performed using previously published methods (Wu et al., 1995, Deitsch et al., 2001) and based on the findings that *P. falciparum* takes up pre-loaded DNA from within its host RBC. Approximately 350 μL of 50% uninfected RBCs (uRBCs) or 175 μL of packed RBCs were aliquoted for each transfection and spun down in 15 mL centrifuge tubes for 5 minutes at 2500 RPM and washed twice with 5 mL of cytomix. During the washing steps, late-stage parasites (schizonts) to be transfected were enriched from cultures by Percoll gradient (**Section 2.1.4**) then gassed and incubated at 37°C. After the final wash of uRBCs, all cytomix was aspirated from the pellet and 50-100 μg of plasmid DNA in cytomix was added to each pellet for a final volume of 400 μL per tube. The contents of each 15 mL tube were transferred to 0.2 cm cuvettes and electroporated using a Bio-Rad GenePulser Xcell (Bio-Rad) set for 0.310 kV, 975 μFD , infinity resistance. Time constants were monitored with the desired range between 10-14 ms. Only 1-2 cuvettes were electroporated at a time and immediately following the pulse, contents were transferred to 15 mL culture tubes with 10 mL of CM and were incubated in the cell culture hood or at 37°C for 15-30 minutes. After recovering, the tubes of electroporated RBCs were centrifuged at 2500 RPM for 5 minutes and supernatant was aspirated. RBC lysis is expected in the supernatant, so it appears redder in color than normal. The cells were washed with ICM and then resuspended in ~ 5 mL CM. The Percoll enriched parasites (~ 30 -50 μL pellet) were resuspended in CM for a final concentration of ~ 10 μL pRBCs/mL and 1 mL was added to each transfection for a final 2-3% hematocrit culture. Cultures were gassed and incubated at 37°C. The next day (day 1 post-transfection), all transfections were smeared to ensure parasitemia was not too high (>4 -5%) or too low (unobservable or $<0.5\%$). If the parasitemia was too high, the cultures were cut and if parasitemia was too low, the cultures were watched closely or discarded. On day 1 or day 2 post-transfection, parasites were selected with drug-supplemented CM, containing either 1-10 nM WR99210 (Jacobus Pharmaceuticals) or 2 $\mu\text{g}/\text{mL}$ blasticidin (BSD) (Thermo-Fisher Scientific) depending on the plasmid used and parasite transfected. The drug concentrations used for selection were based on the IC_{50} values for the particular drug for each distinct parasite line. Optimally, parasites were selected with a drug concentration just above the IC_{50} value.

Transfections were smeared daily until they were observed to die off due to drug pressure (about 4-6 days post-transfection, depending on the drug). After that point, transfections were smeared only 1-2 times per week until around Day 18. If field isolates were not up by days 50-60, they were discarded.

Due to the challenges associated with the transfection of field isolates, variations of this general transfection protocol were performed to enhance transfection efficiency and are detailed within each data chapter when relevant.

2.3.2 Transfection of ring stage *P. falciparum*

Transfection of ring stage parasites was performed similar to DNA-loaded RBCs (**section 2.3.1**). In ring stage transfections, ring stage parasites (iRBCs) are directly electroporated. This procedure was predominantly performed using lab lines (Dd2), rather than field isolates, because this method causes direct stress to the parasites upon electroporation and lab lines are well-adapted to culture conditions and procedures.

Ring-stage parasites were collected at 5-6% ring-stage parasitemia, with earlier rings preferred. For every transfection, 3-5 mL of a culture at 2-3% hematocrit and 5-6% ring-stage parasitemia was centrifuged at 2500 RPM for 5 minutes and resuspended and washed in 5 mL cytomix. After the wash, 50-100 µg of plasmid DNA was added to each 15 mL tube in a total volume of 400 µL of cytomix and transferred to a 0.2 cm cuvette and electroporated under the same conditions described above (**section 2.3.1**). Immediately following electroporation, transfections were transferred to 15 mL tubes containing 10 mL of prewarmed CM then left in the 37°C incubator to recover for 1 hour. After recovery, transfections were centrifuged and washed in ICM at 2000 RPM for 5 minutes. Cultures were resuspended in medium for a final 2-3% hematocrit, gassed, and incubated overnight. As detailed above (**2.3.1**), cultures were smeared the following day and cut if parasitemias were too high. Drug was added on Day 1 post-transfection, using 1-5 nM WR99210 (Jacobus Pharmaceuticals) or 2 µg/mL blasticidin (BSD) (Thermo-Fisher Scientific) depending on the plasmid and parasite transfected.

Ring-stage transfections were supplemented with fresh blood containing 10% citrate-phosphate-dextrose-adenine (CPDA), an anticoagulant/whole blood preservative used to prolong RBC integrity since lab lines could take approximately 15-25 days to come up. If transfection experiments did not show parasites by days 40-45, they were discarded.

2.4 Parasite cloning by limiting dilution

To obtain isogenic parasite lines after positive transfections were confirmed, the bulk cultures were cloned by limiting dilution to obtain individual parasites (Rosario, 1981). Samples were plated in 96-well plates at 0.6 parasites per well and 1% hematocrit. For all cloning procedures, the cloning plates were set up in freshly washed blood prepared with 10% CPDA. Field isolates were plated at 0.8-1.2 parasites/well at 1% hematocrit in conditioned medium due to their slower growth rate. Conditioned medium was prepared by filtering spent medium from the specific isolate and diluting 1:2 or 1:4 with fresh CM. Conditioned medium was stored at 4°C for up to 3 days then discarded. Weekly, 0.5% fresh RBCs and CM or conditioned CM were added to each plate. Around days 17-18, plates were screened for parasite growth using a 1X SYBR Green I solution in lysis buffer. This technique takes advantage of the properties of SYBR to fluoresce upon intercalating between DNA bases. Since only parasitized RBCs contain DNA, only wells that contain living parasites will produce a measurable level of fluorescence when exposed to SYBR Green I. Aliquots from the cloning plates (~20 µl) were resuspended thoroughly in the lysis buffer solution (consisting of 10 mM Tris-HCl, 5 mM EDTA, 0.1% w/v saponin, and 1% v/v Triton X-100) and 1X SYBR Green I (Invitrogen, 10,000x stock) and incubated in the dark at 37°C for 20 minutes then read on a microplate reader (FLUOstar Omega) using a 485/535 nm excitation and emission filter. Positive wells with values higher than the background wells containing CM and RBCs-only were screened by smear. If parasites were observed, the clones were expanded and saved for genomic DNA (gDNA) extraction, cryopreservation, and continuous cultures were maintained for functional assays.

2.5 Saponin lysis and genomic DNA extraction from cultivated parasites

Parasites were collected for genomic DNA using a saponin solution to selectively permeabilize infected RBC membranes to remove host cell hemoglobin content. When cultures reached at least 2% parasitemia of late stages (trophozoites and schizonts) at 2-3% hematocrit in 10 mL-12 mL volume, cultures were spun down at 2500 RPM for 5 minutes and resuspended in 0.15% saponin (Sigma-Aldrich) in 1X phosphate buffered saline solution (PBS). Saponin solutions were made fresh on the day of the experiment from 1% or 10% stocks stored at 4°C for several months. Tubes were left to rest for 3-5 minutes at room temperature then were centrifuged at 4000 RPM, washed at least twice with 1X PBS, until the sample turned from red to a brownish/black color and the pellets were stored at -20°C or used immediately for DNA extraction. A DNeasy Blood & Tissue Kit (Qiagen) was used to

extract genomic DNA from thawed saponin pellets. DNA was eluted using the kit buffer (buffer AE) or water, depending on the experimental procedure.

2.6 *In vitro* parasite survival assays

2.6.1 Antimalarial drug preparation

Antimalarial drugs were obtained from the Worldwide Antimalarial Resistance Network (WWARN) and Sigma. Stocks were prepared according to solubility as follows: piperazine in 0.5% lactic acid in water; dihydroartemisinin (DHA) and lumefantrine (LUM) in dimethyl sulfoxide (DMSO); and chloroquine (CQ) and mefloquine (MQ) in water.

2.6.2 Drug sensitivity assays

The *in vitro* susceptibility of parasites to several commonly used antimalarial drugs was assessed using standard 72-hour dose-response SYBR Green I fluorescence-based assays (Bacon et al., 2007, Smilkstein et al., 2004). Drug stocks were prepared in CM at 2x the desired concentration and 1:2 serial dilutions were made by adding 50 μ l per well in duplicate in a 96-well plate (**Figure 2.3**). The second to last wells in column 11 served as a no drug control (CM only) to measure maximum parasite growth and the last wells in column 12 contained RBCs only (1.5% hematocrit) to measure background fluorescence of the RBCs (**Figure 2.3**). Synchronous ring-stage parasites (0-10 hours) were added (50 μ l per well at 3% hematocrit) to obtain a 1% parasitemia and 1.5% hematocrit in a final volume of 100 μ l per well. The concentrations for each drug were: PPQ and MQ: 400 nM; CQ: 10 μ M; DHA: 100-400 nM; and LUM: 100 nM. The drug assay plates were incubated in a chamber with mixed gas at 37°C for 72 hours. After the incubation period, parasites were lysed using a SYBR Green I solution. A 2x SYBR-lysis buffer solution was prepared by adding 2x SYBR (added fresh from a 10,000x stock) to a 2x solution of lysis buffer (20 mM Tris, pH 7.5, 5 mM EDTA, 0.016% w/v saponin, 0.08% v/v Triton X-100). After 72 hours, an equal volume of the SYBR-lysis buffer solution (100 μ L) was added directly to the volume in the drug assay plates and mixed thoroughly. Plates were incubated in the dark at 37°C for 20 minutes then measured on a microplate reader (FLUOstar Omega) using a 485/535 nm excitation and emission filter. For all experiments in this study, the half maximal inhibitory concentration (IC₅₀) was taken as the drug concentration at which the SYBR green fluorescence was 50% of the value measured in the no drug (control) wells. Parasite survival (% growth) was determined by comparing fluorescence of the parasites exposed to drug (exposed) to fluorescence of parasites in the no drug control (non-exposed). All values were normalized

by subtracting the background fluorescence of RBCs-only. GraphPad Prism 8 Version 8.0.2 was used to generate dose-response curves using a non-linear regression model for log(inhibitor) vs. normalized response(variable slope) to calculate IC₅₀ values with standard deviation (SD). All assays were performed in duplicate in three independent experiments. Statistical comparisons between parasite lines were performed using Mann-Whitney U tests.

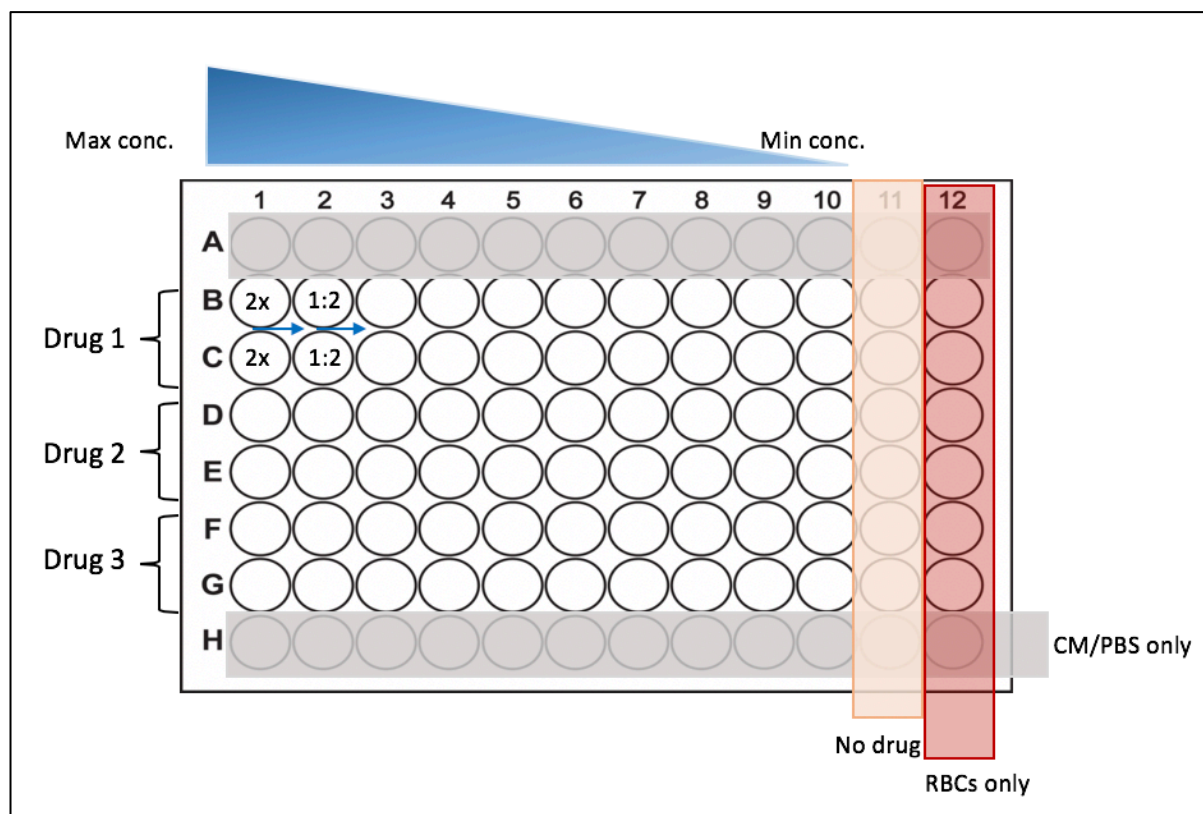


Figure 2. 3. Schematic for IC₅₀ drug assay 96-well plate layout. Maximum drug concentration is plated in column 12 (2x the desired concentration) and serial 1:2 dilutions are plated in the following wells up to column 10. Column 11 (orange) contains no drug (parasites only) and column 12 contains RBCs only. Rows A and B (grey) contain CM or PBS only to account for any edge effects due to evaporation. Up to three drugs can be assayed on one plate.

2.6.3 Piperaquine survival assays (PSAs)

Piperaquine survival assays (PSAs) were performed following the procedure detailed by Duru *et al.* 2015 (Duru et al., 2015). Parasite lines were tightly synchronized 1-2 weeks prior to the assay by 5% sorbitol lysis and when parasitemia reached 3-5%, a Percoll gradient was performed on ~45 hour schizonts (segmented schizonts) and allowed to invade fresh RBCs for up to 3 hours. After incubation, the parasites were immediately sorbitoled and adjusted to 0.8–1.5% parasitemia with a 2% hematocrit. The cultures were then plated in a 48-well plate (in triplicate) and exposed to 200 nM piperaquine (from the Worldwide Antimalarial Resistance Network (WWARN) or Sigma) or the control vehicle (0.5% lactic acid in water) (**Figure 2.4**). The plates were incubated for 48 hours in a chamber with mixed gas containing

1% O₂, 3% CO₂, and 96% N₂ at 37°C. After 48 hours, cultures were washed once with ICM (10 mL) resuspended in complete medium and placed in a new well and cultured for an additional 24 hrs (**Figure 2.4**). After 72 hours, smears of all samples were prepared and flow cytometry was performed to measure viability. The proportion of viable parasites in exposed and non-exposed cultures was evaluated by counting 250,000 events per sample. Based on the accuracy of flow cytometry for measuring parasitemia (Amaratunga et al., 2014), the flow cytometry data was taken to represent viable parasites per well rather than counting 10,000 RBCs per treatment (Duru et al., 2015). However, the slides for microscopy were still counted after performing flow cytometry (at least 1000 cells per slide) to ensure the values obtained via flow cytometry were similar to the number of viable cells viewed and counted by microscopy. The parasite growth rate was defined as the non-exposed (NE) parasitemia at 72 hours/initial parasitemia (INI) at time zero (growth rate= NE/INI). The percent survival was defined as the number of viable parasites in PPQ-exposed (PPQ)/# of viable parasites in non-exposed (NE) x 100 (% survival=PPQ/NE*100). The % survival data was graphed and analysed using GraphPad Prism Version 8.0.2. Statistical comparisons between parasite lines were performed using Mann-Whitney U tests.

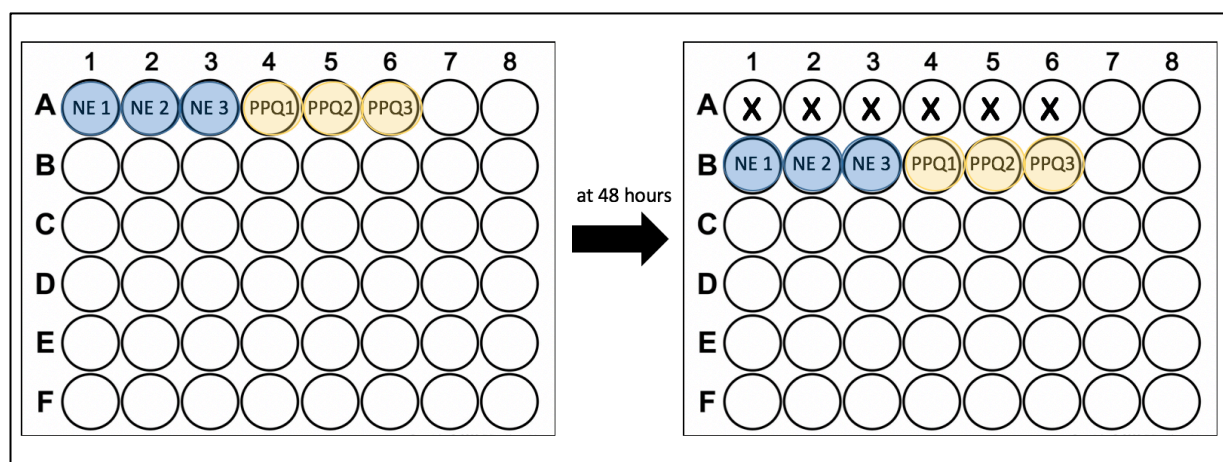


Figure 2. 4. PSA 48-well plate setup. Each treatment condition non-exposed (NE) and treated (PPQ) is performed in triplicate. After 48 hour incubation with PPQ, the drug is washed off and the cultures are plated in a new well in the 48-well plates.

2.7 Quantification of viable parasites using flow cytometry

Flow cytometry was utilized to measure parasitemia following the methods described by Amaratunga *et al.* (Amaratunga et al., 2014). This procedure utilizes two fluorescent dyes: SYBR green I, which binds DNA (as described above) and MitoTracker Deep Red (Thermo

Fisher Scientific), which stains mitochondria and is a marker for actively metabolizing (live) cells.

For quantification of viable parasites in PSAs, 100 μ L of culture from each treatment condition was collected in a 96-well plate and washed twice with 1X PBS. For measuring the parasitemia of other cell cultures, at least 20 μ L of packed iRBCs were collected. Two controls were included for each flow cytometry assay: a stained-RBC only sample (2% hematocrit) and an unstained-RBC only sample to control for background fluorescence. After aspirating the final wash for all samples, the cells (except for the unstained-RBC only control) were resuspended in 100 μ L of a SYBR Green I (0.4x)/MitoTracker Deep Red (0.6 μ M) solution and incubated for 20 minutes at 37°C in the dark. After incubation, the cells were washed twice in 1X PBS and resuspended in 200 μ L of 1X PBS. A 1:10 dilution of the stained samples was made in a final volume of 200 μ L PBS and read on a flow cytometer (BD Accuri, NIH and CytoFLEX and Beckman Coulter CytoFLEX, Sanger).

The excitation and emission spectra for SYBR Green I is 497/520 nm and MitoTracker Deep red is 644/665 nm enabling the fluorescent dyes to be measured using the FITC (FL1) and APC (FL4) filters, respectively. A range of 200,000-250,000 events were recorded for each sample and subsequent data was analyzed and gated using FlowJo (Version 10.5.3).

Samples that stained positive with both SYBR and MitoTracker were recorded as live cells. Samples that stained with only SYBR green were counted as dead and only the percentage from the SYBR + MitoTracker gate was used to calculate the parasitemia for each culture (**Figure 2.5**). Samples were gated using the side scatter (SSC) vs. forward scatter (FSC) view (**Figure 2.5A**) of all events to obtain a population of “non-debris” by removing all debris outside of the gate (**Figure 2.5B**). Using the non-debris population, a single cell (singlet) population was obtained by gating the population in the forward scatter-area (FSC-A) by forward scatter-height (FSC-H) view (**Figure 2.5C**). Parasitemias were then quantified by gating the quadrants in FL1 (FITC/SYBR) vs. FL4 (APC/MitoTracker) (**Figure 2.5 D-E**). Quadrant 1 (Q1, upper left) shows cells that are SYBR positive only and counted as dead since SYBR fluorescence only indicates the presence of DNA. Quadrant 2 (Q2, upper right) shows SYBR + MitoTracker positive cells, which is taken to be the parasitemia or percentage of all live cells (**Figure 2.5 D-E**).

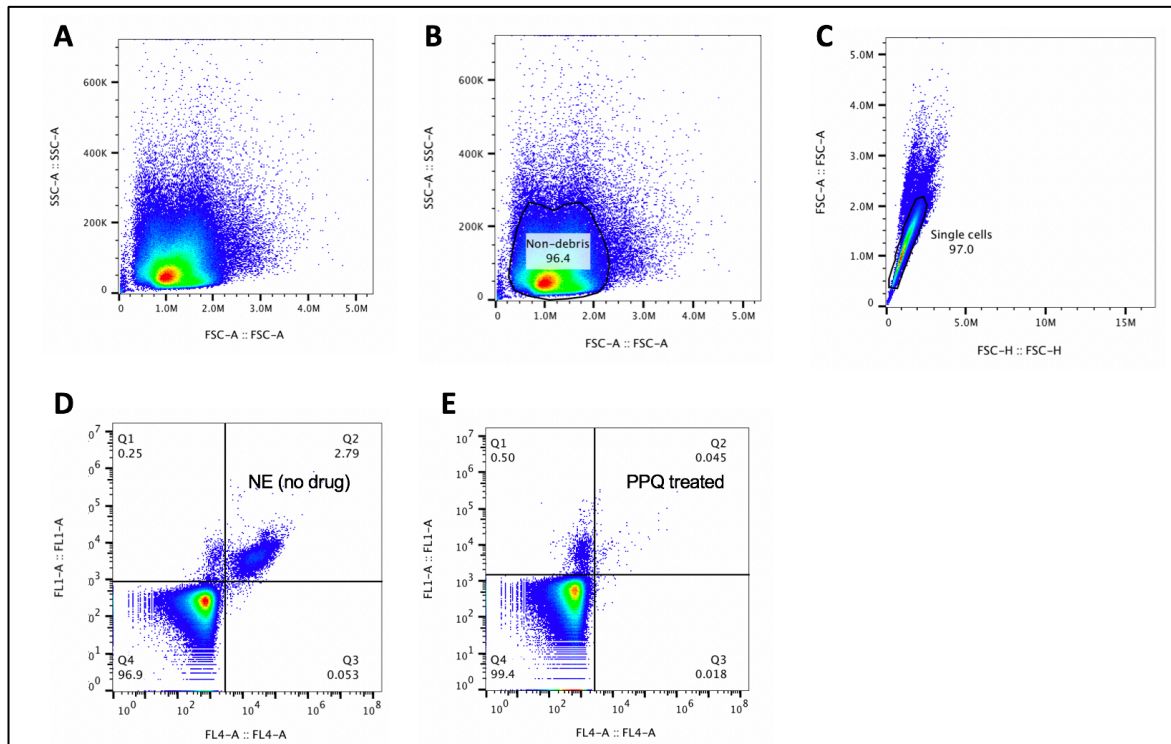


Figure 2. 5. Flow cytometry quantification of parasitemia using SYBR Green I and MitoTracker Deep Red. A.) Side-scatter (SSC) and forward scatter (FSC) view of all 250,000 events. B.) The population of cells was gated to remove debris. C.) The non-debris population was further gated to obtain single cells only (singlets). D.) Example of a non-exposed (NE) sample from a PSA. The parasitemia is represented in the top right corner of quadrant 2 (Q2). Q2 contains cells that stained positively for SYBR and MitoTracker. E.) Example of a PPQ-treated sample from a PSA with a PPQ-sensitive isolate. The population in Q1 (upper left) represents SYBR-positive parasites and the population in Q2 shows few live cells, as expected in a PPQ-sensitive isolate. The flow cytometry data was analyzed using FlowJo (Version 10.5.3).

2.8 Molecular cloning techniques

2.8.1 Transformation of competent bacteria cells

Bacterial transformations were carried out using competent *E. coli* cells (XL10-Gold Ultracompetent cells, Agilent Technologies or 10-beta Electrocompetent *E. coli*, NEB). Plasmid DNA (~1-50 ng of DNA in 2-10 μ L) was added directly to competent cells on ice and incubated for 30 minutes. After incubation, the transformations were heat-shocked at 42°C for 30 seconds, placed back on ice for 2 minutes then recovered in 1 mL of SOC broth for 1-2 hours at 37°C. The transformations were plated on LB agar plates containing 100 μ g/mL ampicillin (LB + ampicillin plates) and incubated at 37°C overnight. The following day, colonies were inoculated in LB broth supplemented with 100 μ g/mL ampicillin and incubated overnight, at 37°C, shaking (~180 RPM). Cultures were harvested the next day at 4000 RPM for 20 minutes at 4°C and plasmids were isolated.

2.8.2 Plasmid preparation: mini, midi, and maxi preparations

Plasmids for all experiments were prepared using mini, midi, or maxi preparation (prep) kits (Qiagen, NIH; Macherey-Nagel, Sanger). For molecular cloning work, less plasmid DNA was needed, so mini preps were performed and DNA was eluted using water or the elution buffer supplied with the kit. For transfections, large amounts of plasmid DNA were required and were obtained via maxi preps. Plasmid DNA for use in transfections was resuspended in cytomix. Glycerol stocks of bacterial cultures were made by combining a 1:1 mixture of glycerol and the bacteria culture in a cryovial. Stocks were stored at -80°C.

2.8.3 Polymerase chain reaction (PCR) protocols

PCR reactions were performed using SapphireAmp Fast PCR Master Mix (Takara Bio Inc) or CloneAmp HiFi PCR Premix (Takara Bio Inc) and reaction conditions were set based on the manufacturer's recommendations. Each reaction contained 10 µM of the forward and reverse primers, 2x SapphireAmp Fast PCR Master Mix or CloneAmp HiFi PCR, the DNA template (1-2 µl for approximately ~20 ng DNA), and up to 10 or 20 µL of water. For the Sapphire mix, the thermocycler (GeneAmp 9700 PCR machine, Thermo Fisher) conditions were as follows: 92°C for 2 minutes, followed by 30 cycles of 92°C for 30 seconds, 55-59°C for 30 seconds (temperature was dependent on primers), 66°C for 1.5 minutes, followed by a 1 minute extension at 66°C. For CloneAmp: denaturation at 98°C for 2 minutes, followed by 30-35 cycles of 98°C for 10 seconds; 55°C for 30 seconds, and elongation at 68°C for one minute.

2.8.4 DNA sequencing

PCR products were purified using a PCR purification kit (Qiagen or Macherey-Nagel) and sent for sequencing by Genewiz (USA) when at the NIH or to Eurofins (Europe) when at the Sanger Institute.

Chapter 3: Detection, surveillance, and evaluation of molecular markers of piperazine resistance: *plasmepsin 2-3* copy number assays and functional studies

3.1 Declaration of work

The following chapter includes excerpts of data from a manuscript in which I am co-first author submitted for pre-print publication on bioRxiv on 4th July 2019 (Jacob et al., 2019). This chapter also contains copy number data that was performed for a manuscript in preparation in which I am a contributing author (Amaratunga et al., 2019). The content included in this chapter is my own work and does not include work done in collaboration with others unless directly stated.

3.1.1 Significance and purpose of study

Antimalarial drug resistance is an unrelenting obstacle to malaria control programs. As countries push toward malaria elimination, drug resistance and the potential for resistance to develop pose constant threats to treatment efforts which rely solely on chemotherapy. In Southeast Asia (SEA), parasites have developed some degree of resistance to nearly every malaria drug currently available, with the most recent emergence to artemisinin combination therapies (ACTs) (World Health Organization, 2018). ACTs are the recommended front-line treatments for *Plasmodium falciparum* malaria worldwide (World Health Organization, 2018) and decreased susceptibility of parasites to both artemisinin and one of the widely used partner drugs, piperazine (PPQ), have been reported in multiple locations throughout SEA (Duru et al., 2015, Leang et al., 2015, Spring et al., 2015, Saunders et al., 2014, Amaratunga et al., 2016, Chaorattanakawee et al., 2015, Imwong et al., 2017). It is therefore necessary to have reliable methods for detecting and evaluating resistant phenotypes. The purpose of this study was to combine clinical data from Cambodia with genomic studies to develop assays for detecting one of the molecular markers of piperazine (PPQ) resistance, a copy number variation (CNV) in the *plasmepsin 2* and *plasmepsin 3* (*PM2-PM3*) genes. In addition to assay development, this study designed and performed *in vitro* functional studies to examine the role of the *PM2-3* CNV in PPQ resistance.

3.1.2 Introduction

In 2008, dihydroartemisinin-piperaquine (DHA-PPQ) was deployed as frontline treatment for uncomplicated *P. falciparum* malaria in Cambodia and implemented nationwide in 2010 (Amaratunga et al., 2016). Since that time, drug efficacy studies have monitored for treatment failures, which are defined as greater than 10% recrudescence (persistence of the infection). As soon as 2010 in Western Cambodia, approximately 25% and 11% failure rates to DHA-PPQ treatment were observed in Pailin and Pursat provinces, respectively (Leang et al., 2013). By 2013—less than 3 years after nationwide drug implementation—widespread failure rates were observed throughout Cambodia, reaching as high as 50% (Duru et al., 2015, Leang et al., 2015, Spring et al., 2015, Saunders et al., 2014, Amaratunga et al., 2016, Chaorattanakawee et al., 2015). Genomic studies (Amato et al., 2017, Witkowski et al., 2017) on parasite samples collected from patients in three Cambodian provinces from 2012-2013 (Amaratunga et al., 2016) found several regions of the parasite genome that associated with treatment failures in patients and reduced PPQ susceptibility *in vitro*. Specifically, genome-wide association studies (GWAS) revealed copy number variations (CNVs) in the *plasmepsin 2* (*PM2*) and *plasmepsin 3* (*PM3*) genes on chromosome 14 as well as nonsynonymous single-nucleotide polymorphisms (SNPs) on chromosome 13 in genes encoding a putative exonuclease, PF3D7_1362500 (*exo-E415G*), and a putative mitochondrial carrier protein, PF3D7_1368700 (*mcp-N252D*) (Amato et al., 2017, Witkowski et al., 2017). Further work also reported mutations in the *chloroquine resistance transporter* gene (*pfcr1*) that confer varying levels of resistance to PPQ in both field isolates and the lab-adapted strain, Dd2 (Ross et al., 2018a, Agrawal et al., 2017, Duru et al., 2015). These molecular markers are on a mutant kelch13 (K13) propeller domain background, the genetic marker for artemisinin resistance, so it is hypothesized that the rapid decline of piperaquine efficacy was due to widespread artemisinin resistance in Western Cambodia, which put increased pressure on the partner drug, allowing parasites to quickly develop resistance to piperaquine.

Copy number variations or polymorphisms describe an amplification (increase) or decrease in the number or copies of a gene in the genome. CNVs are common in many eukaryotes, including humans, mice, and malaria parasites and are often associated with drug resistant phenotypes (Freeman et al., 2006, Anderson et al., 2009). In *P. falciparum*, the significant role CNVs could play in drug resistance was seen in the *multidrug resistant-1* gene (*pfmdr1*) (Anderson et al., 2009). An increase in the copy number of the *pfmdr1* gene was found to confer resistance to the ACT partner drug, mefloquine (Wilson et al., 1989, Wilson et al.,

1993, Price et al., 2004). Mefloquine was used in Cambodia from 2001 as the ACT, artesunate-mefloquine (AS-MQ) until 2008, when the partner drug failed with widespread amplification of *pfmdr1*. Since the introduction of DHA-PPQ in 2008, the *pfmdr1* amplification has declined with parasite populations predominantly reverting back to single copies of *pfmdr1* and increased copies of *PM2-3* (Amaratunga et al., 2016, Amato et al., 2017, Witkowski et al., 2017).

The *PM2-3* CNV observed in Cambodian parasite isolates exposed to DHA-PPQ treatment consists of an amplification of both the *PM2* and *PM3* genes. Whole genome sequencing (WGS) data shows that the breakpoint of parasites with at least two copies of *PM2-3* lies in the ends of the *plasmepsin 1* and *plasmepsin 3* genes, creating a duplication of the full *plasmepsin 2* gene and a chimeric *plasmepsin 3* in which the 3' end of *PM3* is replaced with the 3' end of *plasmepsin 1* (depicted in **Figure 3.5**) (Amato et al., 2017). Plasmepsins 1-4 (PM1-PM4) are enzymes located in the digestive vacuole of the parasite that function as proteases during the intraerythrocytic stages of the parasite lifecycle by degrading hemoglobin (Banerjee et al., 2002). Hemoglobin degradation also generates heme, which is a toxic by-product that causes oxidative stress to the parasite, so it is converted to inert hemozoin crystals (Wunderlich et al., 2012). Though the mechanism of piperazine action is unknown, one hypothesis is that it interferes with the hemoglobin degradation pathway, similar to chloroquine, and prevents hemoglobin degradation or heme detoxification. Thus a potential role for the *PM2-3* gene amplification could be to overcome any inhibitory effects that piperazine may have on the process. It should also be noted that the plasmepsins are redundant enzymes, and additional proteases such as falcilysins and falcipains also facilitate hemoglobin degradation (Liu et al., 2006), so it is possible that piperazine is affecting earlier stages of the degradation pathway in which the plasmepsins are involved. However, these are speculations that have yet to be tested in molecular studies.

The emergence of DHA-PPQ resistance greatly threatens the efficacy of the remaining ACTs worldwide. With the availability of molecular markers of piperazine resistance, it is imperative to have robust assays that can be used to monitor the presence and frequency of these markers in contemporary parasite isolates across endemic regions. Functional studies are also necessary for providing insight into the biological mechanisms of resistance. This study has developed quantitative PCR (qPCR) assays to measure the copy number of *PM2* and *PM3* using genomic DNA. I have also developed a PCR-based breakpoint assay to detect the presence of the chimeric *PM3-PM1* hybrid created by the duplication. The two copy

number assays are sensitive, reliable, and cost-efficient methods for detecting the breakpoint quickly. In addition to assays for monitoring the *PM2-3* CNV, I performed functional studies to test for the effects of increased copies of *PM2-3*.

3.1.3 Objectives

Examine the role of the amplification of hemoglobin degrading proteases, *PM2* and *PM3* (*PM2-PM3*), in piperazine resistance

- (1) Development of qPCR and breakpoint PCR-based assays to detect *PM2-3* resistance-associated copy number variation
 - a. Breakpoint PCR validation and comparison with SYBR-based qPCR assay using samples from DHA-PPQ study (Amaratunga et al., 2016)
 - b. Analysis of *PM2-3* copy numbers in samples from AS-MQ study (Amaratunga et al., 2019)
- (2) Study the functional role of the *PM2-3* amplification by genetic modulation of *PM2-3* copy numbers *in vitro*
 - a. Overexpression of *PM2* and both *PM2-3* in a piperazine-sensitive Cambodian field isolate with a single copy of the *PM2-3* genes

3.2 Materials and methods

3.2.1 Parasite samples

Field isolates used in breakpoint PCR and qPCR assays were obtained from clinical trials conducted in 3 sites (**Ch. 2, Figure 2.2**) in Cambodia: Pursat, Preah Vihear, and Ratanakiri between 2012-2015 (clinicaltrials.gov ID: NCT01736319) (Amaratunga et al., 2016). In the clinical trial from 2012-2013, patients presenting with uncomplicated *P. falciparum* malaria were treated with DHA-PPQ at all sites (Amaratunga et al., 2016). In the clinical trial from 2014-2015, patients were treated with artesunate-mefloquine (AS-MQ) at all sites (Amaratunga et al., 2019). Genomic DNA (gDNA) was obtained from 200 μ L of whole-blood taken at the time of diagnosis. Control samples used for validation and assay optimization were obtained from gDNA extracted from the lab strains, 3D7 and Dd2, and from field isolates (**Ch. 2, Table 2.1**) growing in continuous culture for which WGS data was available (**Figure 3.1**).

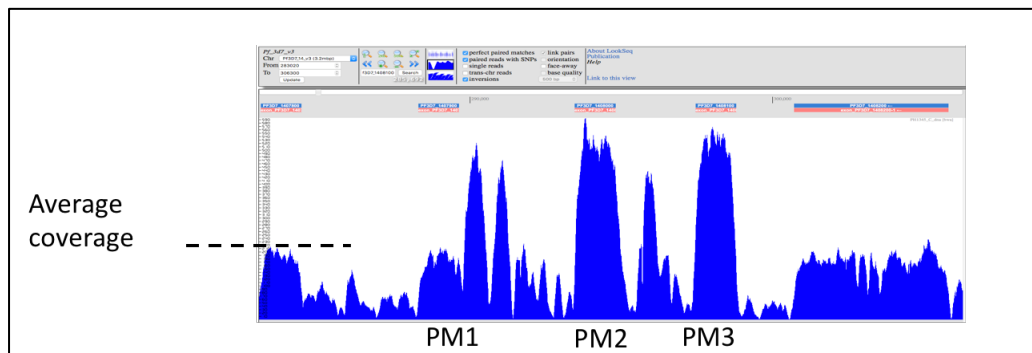


Figure 3. 1. Whole genome sequencing data displaying average coverage on chromosome 14 for isolate 163-KH1-004 (PH1345_C) as viewed using the LookSeq browser. (Manske and Kwiatkowski, 2009). The dashed line represents the average coverage and the blue represents the number of reads at the approximate positions on chromosome 14: 283100-300550, encompassing the genes of *plasmepsins 1, 2, and 3*, PF3D7_1407900-PF3D7_1408100. All field isolates used for copy number controls were validated for increased *PM2-3* copy number using the LookSeq browser.

3.2.2 *Plasmepsin 2-3* duplication breakpoint PCR assay

Whole genome sequencing data from piperazine-resistant *P. falciparum* isolates obtained from clinical trials in Cambodia were used to identify the breakpoint of the *PM2-3* amplification. PCR primers were manually designed to amplify the region surrounding the breakpoint (Amaratunga et al., 2016, Amato et al., 2017, Witkowski et al., 2017). Primers AF (forward 5'-CCACGATTTATATTGGCAAGTTGATTTAG-3') and AR (reverse 5'-CATTTCTACTAAAATAGCTTTAGCATCATTACAG-3') amplify a 623 base pair (bp) product surrounding the breakpoint located at the 3' end of *plasmepsin 1* (*PM1*). Primers BF (forward - 5'-CGTAGAATCTGCAAGTGT TTTCAAAG-3') and BR (reverse 5'-AATGTTATAAATGCAATATAATCAAACGACATCAC-3') amplify a 484 bp product surrounding the breakpoint located at the 3' end of *PM3*. BF + AR amplify the junction between the breakpoint and produce a 497 bp product in isolates with *PM2-3* amplifications. These primers face opposite directions in samples without duplications and are not expected to amplify a product in single copy isolates. Both control (AF + AR; BF+ BR) and duplication (BF + AR) primer sets were used with all samples and single copy isolates were only noted if the control primer sets amplified a product and duplication PCR was negative. Two or more copies were annotated as >1 copy of *PM2-3* only if both the control and duplication primer sets produced a product. PCR reactions contained 10 µl SapphireAmp Fast PCR Master Mix (Takara Bio Inc), 0.3 µl of each primer (Integrated DNA Technologies), 1 µl of genomic DNA up to 20 µl final volume with water. PCR conditions were: 92°C for 2 minutes, followed by 30 cycles of 92°C for 30 seconds, 59°C for 30 seconds, 66°C for 1.5 minutes, followed by a 1 minute extension at 66°C.

3.2.3 SYBR green validation of *plasmepsin 2-3* copy number using quantitative PCR

PCR primers for estimating *PM2* copy number amplification were designed manually inside the *PM2* gene (forward - 5'-CTTATACTGCTTCAACATTTGATGGTATCCTTGG-3'; reverse - 5'-GGTTAAGAATCCTGTATGTTTATCATGTACAGGTAAG-3'). Previously described primers for *P. falciparum* lactate dehydrogenase (*ldh*) (Lim et al., 2013), were used as the control for a single copy gene (forward - 5'-AGGACAATATGGACTCCGAT-3'; reverse - 5'-TTTCAGCTATGGCTTCATCAA-3'). Similar to the assays performed by Jacob *et al.* (Jacob et al., 2019), assays for amplifying *PM2* and *PM3* individually were compared to determine if each gene could be used as a marker of duplication and no major differences were observed (data not shown). *PM2* primers only were used for higher throughput in SYBR green assays, since each gene, *PM2* and *ldh* must be analyzed in separate reactions. Real-time PCR reactions were carried out in 20 μ l volumes in a 96-well plate (Bio-Rad) containing 10 μ l SensiFAST SYBR No-ROX mix (2x) (Bioline Inc.), 300 nM of each primer, and 2 μ l genomic DNA. Reactions were performed using a CFX Connect Real-Time PCR Detection System (Bio-Rad) using the following conditions: 5 minutes at 95°C, followed by 40 cycles of 10 seconds at 95°C, 20 seconds at 58°C, and 20 seconds at 60°C. Relative copy number was calculated on the basis of the $2^{-\Delta\Delta C_t}$ method for relative quantification. $\Delta\Delta C_t$ was calculated as $(C_{t_{ldh}} - C_{t_{pfplasmepsin2}}) - (C_{t_{ldh\ cal}} - C_{t_{pfplasmepsin2\ cal}})$, where cal is the calibration control of genomic 3D7 DNA with one copy of both *ldh* and *PM2*. DNA from an isolate with two copies of *PM2-3* (PH1387-C) (Amaratunga et al., 2016) was used as an internal plate control. All samples were analyzed in triplicate and each plate was replicated in triplicate. A relative copy number of 1.5 or greater was recorded as 2 copies.

3.2.4 Overexpression of *PM2* and *PM3*

For overexpression of both the *PM2* and *PM3* genes, I used the pDC2-*cam-mrfp-2A-gfp*-bsd-attP plasmid (Straimer et al., 2012). This plasmid was selected to enable stoichiometric amounts of both *PM2* and *PM3* to be expressed by utilizing the same promoter and a 2A-“skip” peptide to separate the two genes. Gibson assembly for all plasmids was performed using the HiFi DNA Assembly reagent and accompanying protocol from New England Biolabs (NEB).

3.2.4.1 Gibson assembly of a *PM2*-only overexpression plasmid: pDC2-*cam-PM2-2A-gfp-bsd-attP*

Before assembling a *PM2* and *PM3* overexpression plasmid, a single *PM2*-only expression plasmid was made by inserting the *PM2* gene into the pDC2-*cam-mrfp-2A-gfp-bsd-attP* plasmid. The *mrfp* segment was excised from the pDC2-*cam-mrfp-2A-gfp-bsd-attP* plasmid using the enzymes, *AvrII* and *BglIII* (NEB) (**Figure 3.2A**). The *PM2* gene was PCR-amplified from genomic 3D7 DNA using the primers, *PM2_OE_F* and *PM2_OE_R* (**Table 3.1**), which included overlap (lowercase letters) with the plasmid for Gibson assembly. No stop codon was included after the *PM2* gene to ensure translation would carry on through the 2A-skip peptide to the 2A-*gfp* segments (**Figure 3.2A**).

The reverse primer (*PM2_OE_R*) used to amplify the *PM2* gene contains a *BglIII*-2A overlap region (**Figure 3.2A**) by including the *BglIII* restriction site (AGATCT), but uses the “T” from the end of *PM2* and this T is highlighted in red in primer, *PM2_OE_R* (**Table 3.1**). Because of this, the plasmid generated by Gibson assembly was missing this nucleotide (read as an “A” in the forward sequence) (**Figure 3.2B**). This does not affect *PM2* expression, but changes the reading frame downstream of *PM2*, so *gfp* is not translated. The shift in the reading frame causes the nearest stop codon to be located in the 2A-skip peptide and no longer at the end of *gfp*, as originally designed. Since the reading frame was shifted after the full length *PM2* gene, this study was able to use this plasmid to examine the role of *PM2*-only gene overexpression (since it would be translated) but needed to use a different approach to generate a *PM2-2A-PM3* overexpression plasmid, described below.

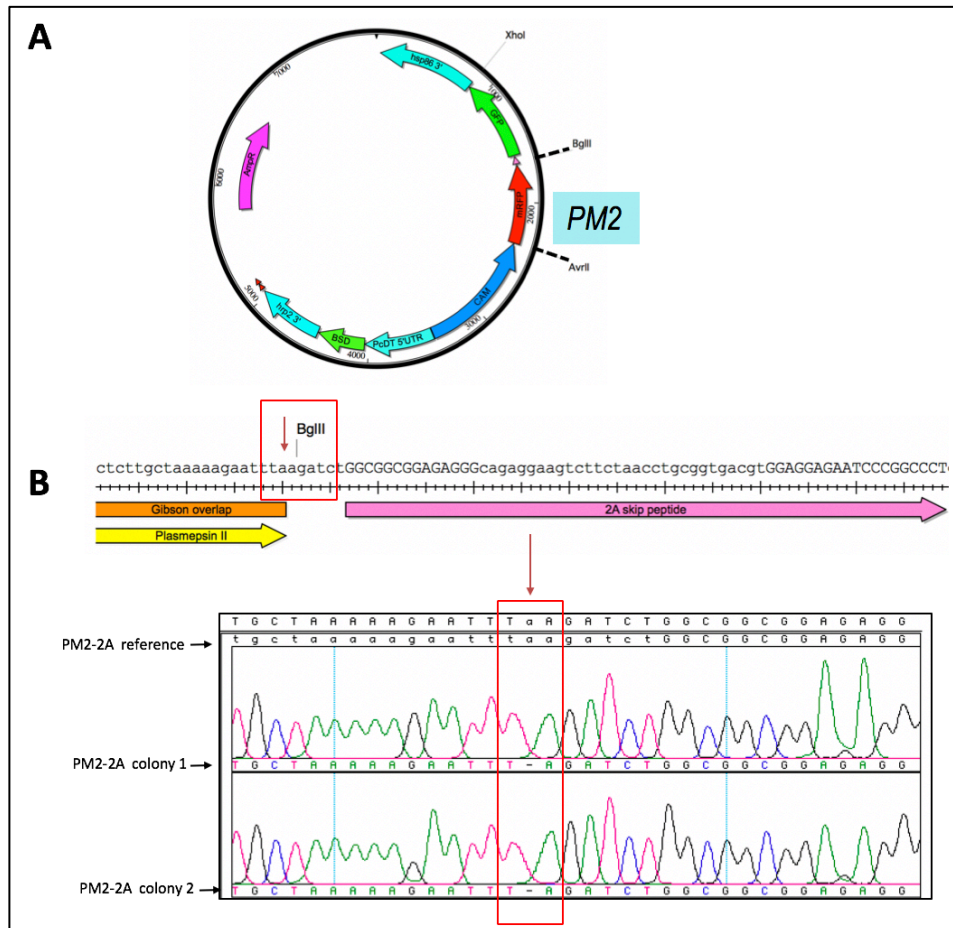


Figure 3.2. Plasmid design and assembly for overexpression of *plasmepsin 2* (*PM2*). A.) The pDC2-*cam-mrfp-2A-gfp-bsd-attP* plasmid was digested with AvrII and BglII to obtain the plasmid backbone and the *PM2* gene (light blue) was inserted via Gibson assembly. B.) Sequence chromatograms of pDC2-*cam-PM2-2A-gfp* colonies (colonies 1 and 2) aligned with the reference sequence of the inserted *PM2* through the 2A peptide sequence. A red box highlights the region missing the “A” nucleotide (indicated with a red arrow) in the forward sequence. This missing nucleotide does not affect *PM2* expression, but shifts the reading frame downstream of *PM2* so that the nearest stop codon is located in the 2A-skip peptide and *gfp* is not translated.

3.2.4.2 Gibson assembly of the *PM2-2A-PM3* overexpression plasmid

Briefly, the *mrfp-2A-gfp* segment was excised from the pDC2-*cam-mrfp-2A-gfp-bsd-attP* plasmid using the enzymes, AvrII and XhoI (NEB) (Figure 3.3A). The *PM2* gene was PCR-amplified from the *PM2-2A-gfp* plasmid made by this study and described above (3.2.4.1, Figure 3.2) using the primers, p1632 (forward - 5'-ACCTAATAGAAATATATCACCTAGG - 3') and p1633 (forward - 5'-GCCAGATCTTAAATTCTTTTAGCAAGAGC - 3') (Table 3.1). The reverse primer, p1633 includes the “T” (highlighted in red) that was not included in the previous plasmid to correct the shift in the reading frame (Table 3.1). A *2A-PM3* fragment was synthesized (Life Technologies) including regions for overlap with the pDC2 plasmid backbone and the *PM2* fragment. The three fragments (Figure 3.3A): *PM2*, *2A-PM3*, and digested pDC2 plasmid

(100 ng) were assembled using a ratio of 2:1 = insert:vector and incubated at 50°C for 20 minutes. A no insert control with digested plasmid only was tested using an equivalent amount of plasmid and no insert. After assembly, 5 µl of the reactions were transformed into competent *E. coli* (Ch. 2, Section 2.8.1) and LB + ampicillin plates were screened for colonies the next day.

Correct insertion of *PM2* and *PM3* into the pDC2 plasmid was confirmed by sequencing (Figure 3.3C-D), using the primers: p364 (5'- GGGCCCCGCATGCTTAGCTAATTCG - 3') and p648 (5'- GATTCTTCTTGAGACAAAGGC - 3'), which produce a 649 bp product. Following sequence confirmation, the plasmid was midi-prepped (Ch.2, Section 2.8.2) and parasites were transfected (Ch.2, Section 2.3.2).

Table 3. 1 Primers for the development of *PM2-PM3* overexpression plasmids

Primer name	Primer (5' - 3') sequence	Description
PM2_OE_F	acctaataagaaatatatcacctaggATGGATATTACAGTAA GAGAACATG	PM2 forward primer with Gibson overlap
PM2_OE_R	ctctgccctctccgccgagatcTAAATTCTTTTAGCA AGAGCAATAC	PM2 reverse primer with Gibson overlap
p1632	ACCTAATAGAAATATATCACCTAGG	PM2-2A forward primer, binds CAM promoter upstream of <i>PM2</i> insertion site in the pDC2-cam-PM2-2A-GFP-bsd-attP plasmid
p1633	GCCAGATcTAAATTCTTTTAGCAAGAGC	PM2-2A reverse primer, binds 2A region downstream of <i>PM2</i> insertion site in the pDC2-cam-PM2-2A-GFP-bsd-attP plasmid

The “T” highlighted in red in p1633 is the nucleotide that was not included in the *PM2*-only plasmid reverse primer (PM2_OE_R). This corrected the shift in the reading frame in the *PM2-2A-PM3* plasmid

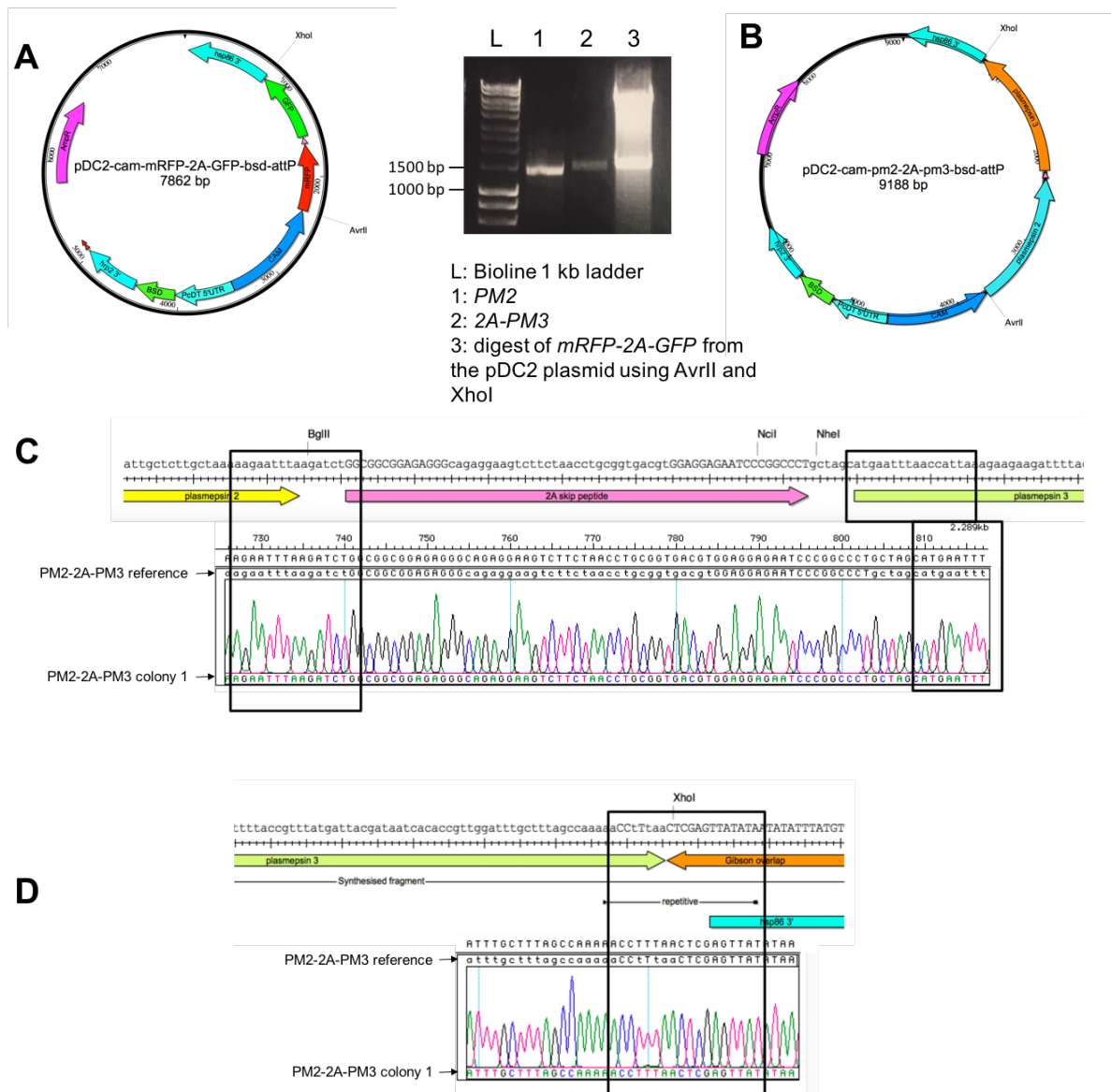


Figure 3.3. Plasmid design and assembly for overexpression of *PM2* and *PM3*. **A.)** The pDC2-*cam-mrffp-2A-gfp-bsd-attP* plasmid was digested with AvrII and XhoI to obtain the plasmid backbone. The fragments for Gibson assembly: *PM2* (1384 bp), *2A-PM3* (1487 bp), and digested plasmid (6380 bp) with an excised *mrffp-2A-gfp* fragment (1482 bp) were run on a 1% agarose gel to confirm sizes. **B.)** The pDC2-*cam-PM2-2A-PM3-bsd-attP* plasmid after Gibson assembly. **C.)** Sequence of *PM2-2A-PM3* colony 1 aligned with the reference sequence of the inserted *PM2* through the 2A peptide to *PM3*. Black boxes indicate regions of overlap with the sequence alignment and plasmid map. **D.)** Sequence chromatogram of *PM2-2A-PM3* colony 1 aligned with the reference sequence through the end of the inserted *PM3* gene. Black boxes indicate regions of overlap with the reference sequence alignment and plasmid map. The top sequence above the reference is the consensus sequence for all reads.

3.2.4.3 Determination of drug selection concentration by IC_{50} assays

Successful transfection of the episomal plasmid was verified by drug selection with blasticidin (BSD). To determine the concentration of BSD to use on the transfected field isolate, 163-KH3-005 (005), (a “PPQ-sensitive” parasite, **Ch. 2, Table 2.1**) an IC_{50} assay was performed (**Figure 3.4**). Based on the IC_{50} results, it was determined that 2 μ g/ml BSD,

which is the same concentration used for lab strains, could be used for the 005 isolate. The transfected parasites were kept under constant drug selection in order to maintain the episomal plasmid.

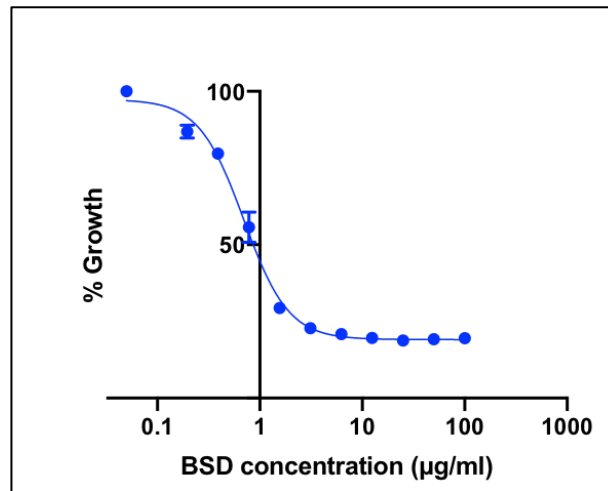


Figure 3. 4. Dose-response curve for field isolate 163-KH3-005 after 72-hour exposure to blasticidin (BSD). The curve represents 4 technical replicates with an IC_{50} value of 0.697 Error bars represent SD.

3.2.4.4 Use of flow cytometry to screen for pDC2-*cam-mrfp-2A-gfp-bsd-attP* plasmid in transfected parasites

The transfected 005 and Dd2 parasites were screened for the presence of GFP using flow cytometry as described in Chapter 2 (**Ch. 2, section 2.7**). Approximately 50 µl of a 3% hematocrit culture transfected with the pDC2-*cam-mrfp-2A-gfp-bsd-attP* plasmid was added to 200 µl of PBS and washed twice, then resuspended in 200 µl of PBS and 10 µl of this dilution was added to a further 200 µl of PBS. No stain was added to any of the samples. A non-transfected 005 parent line was analyzed as a control along with the transfected 005 and Dd2 lines. Each sample was read on a CytoFLEX (Beckman Coulter) flow cytometer using the channels: FITC (to detect GFP) and PE (to detect RFP).

3.3 Results

3.3.1 *PM2-3* breakpoint assay validation

In order to develop a method for detecting the *PM2-3* copy number variations, I designed PCR primers that amplify the breakpoint of the *PM2-3* amplification observed in Cambodian isolates (**Figure 3.5A**). The breakpoint assay identifies copy number amplification in isolates that contain 2 or more copies of *PM2* and *PM3* (**Figure 3.5B**). As expected, no PCR products were observed in samples with a single copy of *PM2-3* (**Figure 3.5B**). Control primers confirmed that the regions surrounding the *PM2-3* amplification were present in all isolates (**Figure 3.5C**) and verified that absence of amplification using the duplication primer sets was not due to lack of DNA or low quality DNA.

Further verification of the breakpoint assay was performed via sequence analysis of the BF + AR PCR product. Sequence data revealed the same breakpoint location as observed by WGS (**Figure 3.5D**). All Cambodian samples that were positive for *PM2-3* amplifications as detected by the breakpoint assay (>1 copy) were in 100% concordance with qPCR and WGS data that called 2 or more copies of *PM2*. Sequencing chromatogram review of PCRs representing 2 and 3 copy samples showed that the breakpoints for representative 2 and 3 copy samples were identical. These sequencing results combined with the identical PCR sizes for all isolates indicates that the breakpoint is identical in all Cambodian isolates tested to date.

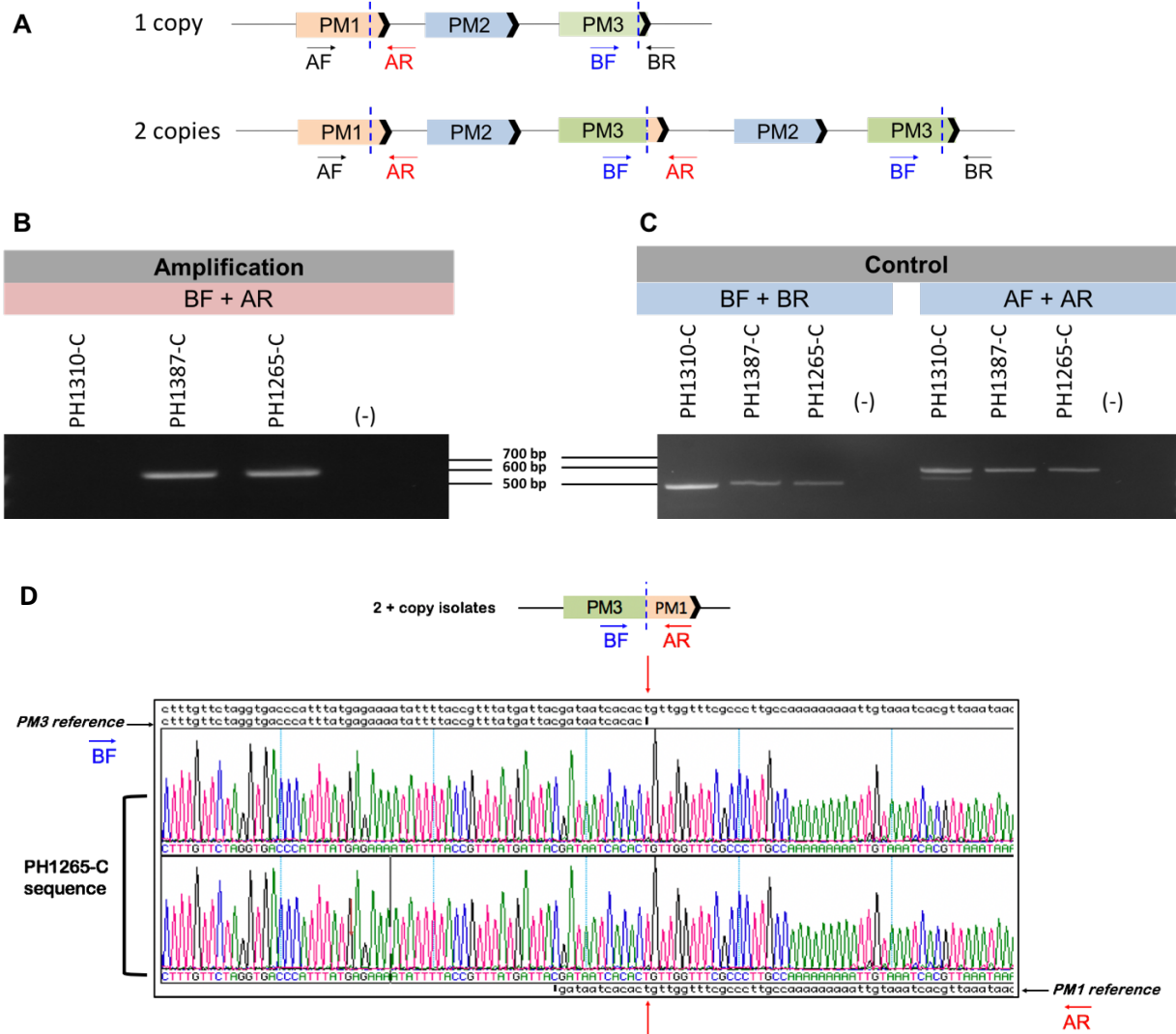


Figure 3.5. Schematic of *plasmepsin 2-3* gene duplication. A.) Gene model depicting the *PM2-3* breakpoint (dashed blue lines) observed in Cambodian isolates. Primer positions are labeled in the single copy (top) and multi-copy (bottom) isolates. B.) Amplification primer set BF + AR amplifies a product in an isolate with two copies (PH1387-C) and three copies (PH1265-C) of *PM2-3*. No product is observed for the single copy (PH1310-C) isolate or in the DNA-negative control (-). C.) Control primers amplify a product in the single copy (PH1310-C) and multi-copy isolates (PH1387-C; PH1265-C). No product is observed in the DNA-negative control (-). D.) Sequence chromatograms of the breakpoint PCR product of primer set BF + AR using 3 copy isolate, PH1265-C. The primers sequence through the breakpoint between the 3' end of *PM3* and the 3' end of *PM1*. The sequence of isolate, PH1265-C is represented in color with the chromatograms. The reference sequences for *PM3* and *PM1* are shown in black and indicated with the black arrow. Viewed from the top, the *PM3* sequence stops (red arrows) and aligns with the *PM1* sequence due to the formation of the chimeric *PM3-PM1* gene. The sequence proceeds through the breakpoint (red arrows) to align with the sequence of *PM1* (bottom).

3.3.2 *PM2-3* breakpoint assay utility in comparison with SYBR green assay

To test the utility of using the breakpoint assay for rapid surveillance of large sample sizes for which WGS data is not yet completed or available, I performed breakpoint PCR on 99 samples from patients treated with DHA-PPQ in Cambodia from 2012-2013 (Amaratunga et al., 2016). I found that 90% of samples from Pursat had increased copies of *PM2-3*, 22% of samples from Preah Vihear had increased copies, and 3.2% of samples from Ratanakiri had increased *PM2-3* copies (**Figure 3.6A**).

The qPCR-based assay results for the same 99 samples from patients treated with DHA-PPQ showed approximately 90% of samples from Pursat had increased *PM2-3* copy numbers, while 16% of samples from Preah Vihear had increased copies and Ratanakiri samples were all single copy *PM2-3* by the qPCR method (**Figure 3.6B**).

I compared the results of the breakpoint assay with the qPCR SYBR green assay and found that 93/99 samples tested with the breakpoint PCR assay matched qPCR data for the same samples, a 94% concordance. The six non-concordant samples were determined to be >1 copy by breakpoint PCR (**Figure 3.6A**), but qPCR read them as single copy isolates (**Figure 3.6B**). This included 1 sample from Ratanakiri, 2 samples from Preah Vihear, and 3 samples from Pursat that had >1 copy by breakpoint PCR but single copy by qPCR (**Figure 3.6**). The six non-concordant samples were repeated, always producing the same results. These results could suggest that the breakpoint PCR assay is more sensitive than the qPCR assay for detecting the breakpoint in samples that are polyclonal. Minor clones containing the duplication in field isolates would not be detected in the qPCR assay, however, they would be detected by the breakpoint assay. One limitation of the breakpoint assay is that there is no high-throughput way to determine if these samples are false positives. The best way to check would be to examine WGS data for each sample, however these samples were selected for breakpoint PCR because WGS data for the samples either failed or was not chosen for WGS analysis due to insufficient or low-quality DNA. Another way to assess if the six non-concordant breakpoint PCR samples were false positives would be to sequence the PCR product and see if the *PM3-PM1* chimeric sequence is present, which would provide evidence that the CNV is likely present.

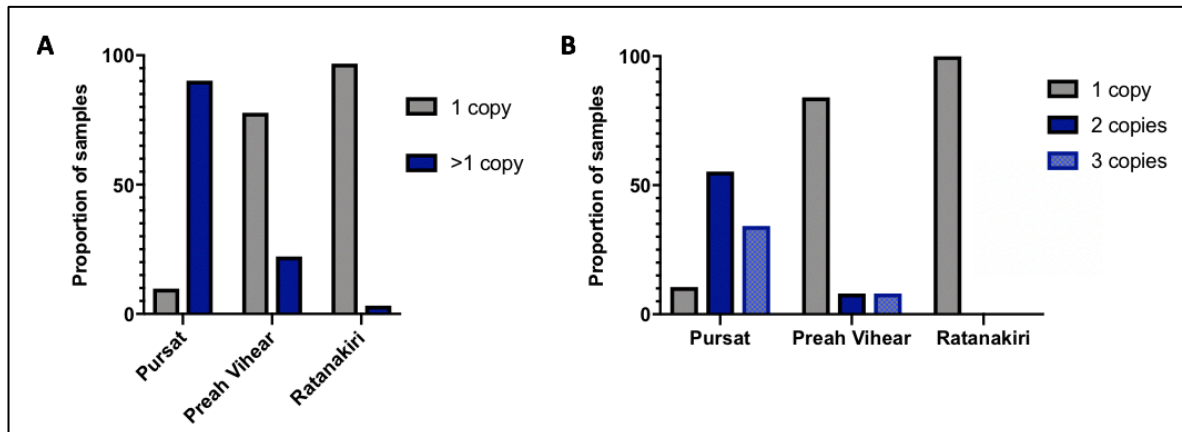


Figure 3.6. Comparison of the breakpoint PCR and qPCR assays for measuring *PM2-3* copy numbers. A.) Proportion of samples with 1 copy or >1 copy of *PM2-3* as determined by breakpoint PCR. B.) Proportion of samples with 1, 2, or 3 copies of *PM2* as determined by qPCR analysis. For both breakpoint PCR (A) and qPCR (B) assays a total of 99 isolates were analyzed from 3 Cambodian provinces during 2012-2013 after treatment with DHA-PPQ.

3.3.3 Analysis of *PM2-3* copy number in isolates from patients treated with artesunate-mefloquine

The breakpoint PCR assay was utilized to detect the *PM2-3* breakpoint in samples from a clinical trial conducted in 3 provinces in Cambodia from 2014-2015 to test the efficacy of artesunate-mefloquine (AS-MQ) (clinicaltrials.gov ID: NCT01736319) (Amaratunga et al., 2019). The prevalence of *PM2-3* amplifications in 295 total patient isolates from Pursat, Preah Vihear, and Ratanakiri were 96%, 93%, and 24%, respectively (**Figure 3.7**). As seen in Figures 3.6-3.7, the proportion of multi-copy parasites is continuing to increase in the 3 Cambodian provinces from 2012 to 2015 (**Figures 3.6-3.7**).

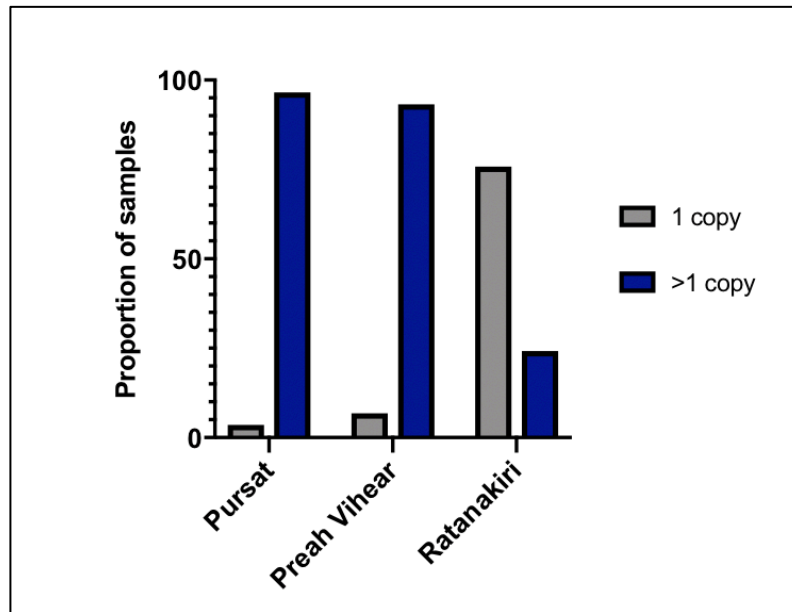


Figure 3. 7. Proportion of samples with >1 copy or 1 copy of *PM2-3* as determined by breakpoint PCR analysis in 3 Cambodian provinces from 2014-2015. A total of 295 patient isolates from 3 Cambodian provinces were analyzed after treatment with AS-MQ.

3.3.4 Overexpression of *PM2* and *PM3* in Cambodian isolates

It was hypothesized that the increased *PM2-3* copy numbers are not only associated with piperazine resistance, but could also serve a causal role in the resistant phenotype. To test this hypothesis directly, this study used transgenic approaches to generate isogenic parasite lines that overexpressed *PM2* and *PM3* in stoichiometric amounts. The best way to do this was to link expression of both genes to a single promoter, with the genes separated by a 2A viral skip peptide. The peptide results in translation that continues to the downstream gene with a break in the peptide bond, and has been used when 1:1 stoichiometric expression of two genes is desired, such as for immunoglobulin heavy and light chains or T-cell receptors (Szymczak et al., 2004). The plasmid used by this study was codon-optimized for *P. falciparum* and used successfully by Straimer *et al.* for dual protein expression of RFP and GFP (Straimer et al., 2012).

3.3.4.1 Overexpression of *PM2* in Cambodian field isolate, 163-KH3-005

This study first assessed if overexpression of *PM2*-only had any effect on susceptibility to piperazine. I transfected the *PM2* overexpression plasmid into a PPQ-sensitive isolate from Cambodia, 005, and found little to no differences in parasite susceptibility to piperazine in the transgenic lines compared to the control (not transfected) parasites in IC₅₀ assays (**Figure 3.8**).

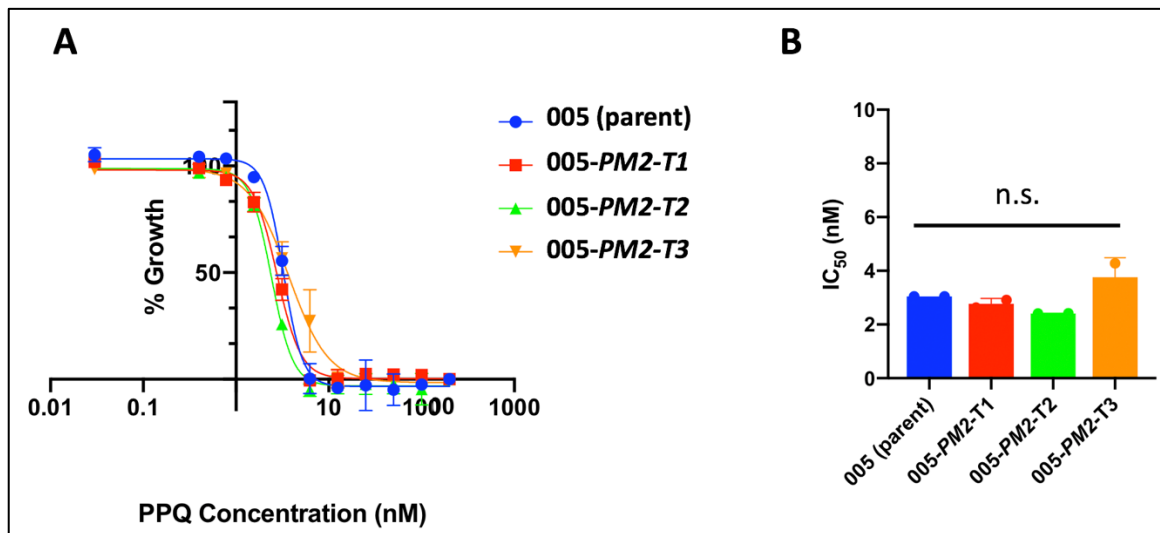


Figure 3. 8. Transgenic piperazine-sensitive parasites (005) carrying the *PM2* overexpression plasmid showed no shift in PPQ IC₅₀ values. A.) Dose-response curves for three 005-transfectants with the *PM2* overexpression plasmid (T1, T2, T3) compared to the parental line (005). Error bars represent SD (n=2). B.) Significance was determined using Mann-Whitney U tests comparing the PPQ IC₅₀ values of the three 005-*PM2* transfectants with the 005 parent line. n.s. indicates not significant (p>0.05).

3.3.4.2 Confirmation of the pDC2-cam-*PM2*-2A-*PM3* plasmid and pDC2-cam-*mrfp*-2A-*gfp*-bsd-attP plasmid in transfected parasites by flow cytometry and PCR

To fully recapitulate the *PM2*-3 CNV observed in clinical isolates, I next aimed to overexpress both *PM2* and *PM3* in the 005 field isolate and Dd2.

Field isolate, 005 and lab strain, Dd2 were transfected with the *PM2*-2A-*PM3* overexpression plasmid and the pDC2-cam-*mrfp*-2A-*gfp*-bsd-attP plasmid as a transfection control.

As soon as there was a detectable parasitemia (around days 14-15 post-transfection for both lines), the 005 isolate and Dd2 transfectants with the control pDC2-cam-*mrfp*-2A-*gfp*-bsd-attP plasmid were screened for the presence of GFP and RFP by flow cytometry (**Figure 3.9**). Fluorescence was detected in the Dd2 transfected parasite, as demonstrated by the presence of a population of cells positive in the FITC (GFP) and PE (RFP) channels (**Figure 3.9**, right panel). However, no fluorescence in the FITC or PE channels was observed for the 005 transfected parasite (**Figure 3.9**, middle panel), which showed a similar profile to the non-transfected 005 parent line (**Figure 3.9**, left panel). The experiment was repeated twice and detection of GFP and RFP was only observed in the Dd2 transfected parasites.

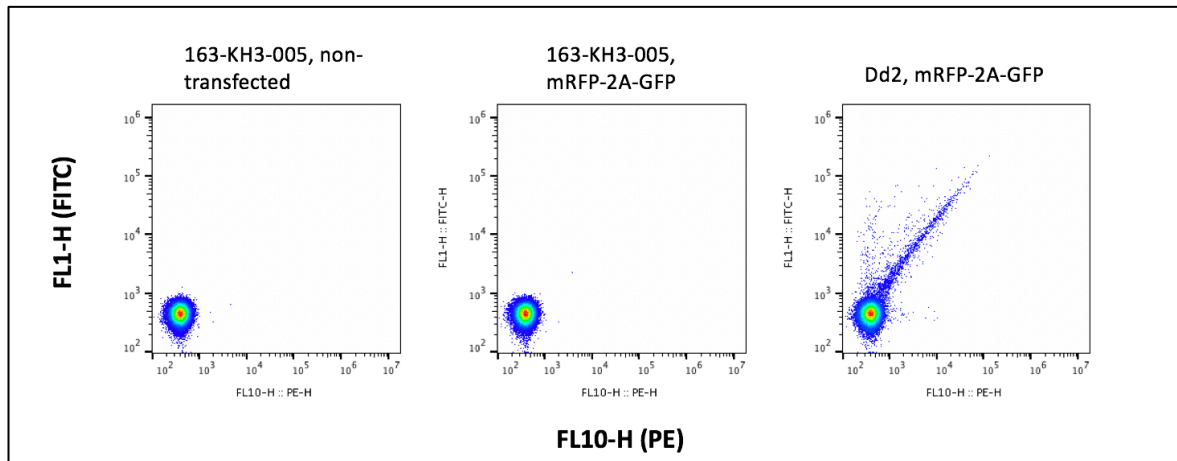


Figure 3. 9. Flow cytometry assessment of transgenic parasites. Flow cytometry assessment of GFP transgene expression (FITC channel) and RFP transgene expression (PE channel) in transfected parasite lines 005 and Dd2, compared with a non-transfected control line (left panel).

Although the *pDC2-cam-mrpf-2A-gfp-bsd-attP* plasmid was transfected as a control to monitor transfection success by measuring GFP/RFP fluorescence, it could have no relationship to whether or not the *PM2-2A-PM3* plasmid was successfully transfected. Therefore, to determine if the 005 and Dd2 parasite lines were successfully transfected with the both the *PM2-2A-PM3* plasmid and *pDC2-cam-mrpf-2A-gfp-bsd-attP*, the transfections were screened using plasmid-specific primers (**Figure 3.10**). As seen in Figure 3.10, both plasmids are present in the 005 and Dd2 transfected lines. Due to time constraints the PPQ response of the *PM2-3* transgenic lines was not yet tested (as well as RNA and protein expression) but will be prioritized in future work.

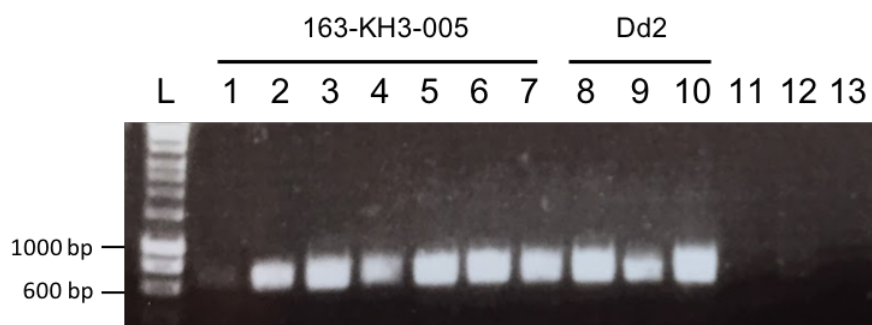


Figure 3. 10. PCR confirmation of the *PM2-2A-PM3* plasmid in transfected 005 and Dd2 parasites. PCR confirmation that the *pDC2-cam* plasmid backbone was present in transfections. Lane L is the 1 kb ladder (Bioline); lanes 1-2 and 5-7 are field isolate 005 transfected with the *pDC2-cam-PM2-2A-PM3* plasmid and lanes 3-4 are field isolate 005 transfected with the control *pDC2-cam-mrpf-2A-gfp-bsd-attP* plasmid. Lane 8 is Dd2 transfected with the control *pDC2-cam-mrpf-2A-gfp-bsd-attP* plasmid and lanes 9-10 are Dd2 transfected *pDC2-cam-PM2-2A-PM3* plasmid. Lanes 11 and 12 are the non-transfected parental lines 005 and Dd2, respectively. Lane 13 is the no template control.

3.4 Discussion and future work

The novel breakpoint and qPCR assays developed by this study are sensitive, reliable, and cost-efficient methods for detecting the *PM2-3* gene amplifications. They can be used in place of WGS or in areas where sequencing is not feasible, as they require considerably less time and facilities, allowing for copy number analysis within the same day of sample collection. Both assays can be performed with very little genomic DNA (2-5 ng of gDNA) which is useful in many endemic regions where only filter paper blood spots are available. The qPCR and breakpoint assays are also high-throughput, with the possibility of using 96-well plate analysis, making them ideal for surveillance throughout malaria endemic regions.

The qPCR-based *PM2-3* CNV assay measures discrete number of copies, which is especially useful in determining if the number of *PM2-PM3* copies is increasing in parasite populations throughout countries where DHA-PPQ was previously used or is still currently in use. One disadvantage of the qPCR method is the arbitrary relative assignment of 1 vs. 2 copies. For the purposes of this study, a value of “2 copies” was set as a relative copy number of 1.5 or greater. This leaves the potential that a sample read as 1.44 copies in the qPCR assay, for example, would be counted as single copy, when it actually had two copies of *PM2-3*. The same could be said for a 1.5 relative copy number actually being a single copy parasite, rather than multicopy. In spite of the inherent potential errors with relative copy number, because qPCR methods do not rely on the primer location in reference to an estimated breakpoint, they can be used broadly.

The breakpoint PCR assay (**Figure 3.4**) also effectively determines increased *PM2-3* copy number in field isolates and can be used in areas where qPCR is infeasible. Since the assay detects the presence of the breakpoint, it does not have the same problems as WGS and qPCR with calling average or relative copy numbers and is positive only if the breakpoint is present. The sensitivity of this assay also enables the detection of minor clones, which proves advantageous, given the potential for polyclonal infections. The basic laboratory equipment needed for breakpoint-PCR makes it possible for analysis to be conducted at field sites, rather than shipping the samples to another laboratory within the country or outside of the country to wait for results. However, a notable disadvantage of this method is that the breakpoint assay was designed with primers specific to the *PM2-3* breakpoint observed in Cambodian field isolates (Amato et al., 2017). The PCR primers used to detect the Cambodian breakpoint observed to date may not amplify a product in samples that contain different breakpoints. As previous studies have shown (Menard et al., 2013, Hostetler et al., 2016),

copy number variations in the same gene can arise independently on different genetic backgrounds and result in distinct molecular breakpoints of amplification. Though this study has observed over 300 samples from Cambodia with the same breakpoint (**Figures 3.6-3.7**), Witkowski *et al.* (Witkowski et al., 2017) have reported different breakpoints in Cambodian isolates. Therefore, both breakpoint and qPCR assays should be performed for the most accurate results, when possible.

This thesis (**Figures 3.6-3.7**) and other studies (Amato et al., 2017, Jacob et al., 2019, Witkowski et al., 2017) have shown that parasites with the *PM2-3* copy number expansion are increasing in prevalence in Cambodia. The breakpoint and qPCR assays have shown that the proportion of parasites with more than one copy of *PM2-3* has increased in the 3 Cambodian provinces where samples were collected from 2012 to 2015 (**Figures 3.6-3.7**). These parasite samples have been obtained from clinical studies carried out by Amaratunga *et al.* in 2012-2013 (Amaratunga et al., 2016) and 2014-2015 (Amaratunga et al., 2019). From these clinical trials, we know that the patients in all 3 provinces (Pursat, Preah Vihear, and Ratanakiri, **Ch. 2 Figure 2.2**) were treated with the same drug regimens, specifically DHA-PPQ in the 2012-2013 trial followed by AS-MQ in the 2014-2015 trial. As discussed in Chapter 2 (**Section 2.2.1**), field isolates from these three Cambodian provinces from 2012-2013 varied in their susceptibility to PPQ, with parasites from Ratanakiri (Eastern Cambodia), being largely susceptible to PPQ and also containing single copies of *PM2-3*. It will be important to determine if the parasites with increased *PM2-3* copy numbers from Ratanakiri in 2014-2015 (**Figure 3.7**) remain susceptible to PPQ, since the parasite samples from this study were successfully treated with AS-MQ, but not exposed to DHA-PPQ. The 2014-2015 parasite samples were the most recent samples this thesis had access to, but recent studies by van der Pluijm *et al.* reported that *PM2-3* amplifications were present in 72% of samples from Ratanakiri collected from 2015-2018 (van der Pluijm et al., 2019). Continued and future work is thus needed to monitor if and how the *PM2-3* copy number expansion changes in this region. In areas where WGS is not possible, the breakpoint and qPCR methods designed by this study can provide efficient, cost-effective methods for real-time analysis of *PM2-3* copy numbers.

In addition to assays for monitoring the *PM2-3* CNV, I developed methods to test for the effects of increased copies of *PM2-3* on piperazine response. To mimic the CNV observed in field isolates encompassing both *PM2* and *PM3*, I generated both a *PM2*-only overexpression vector (**Figure 3.2**) and a *PM2-2A-PM3* vector to co-express stoichiometric

amounts of both genes using the 2A skip peptide (**Figure 3.3**). Initial comparisons of *PM2*-only overexpression in PPQ-sensitive isolate, 005, showed no significant difference in parasite survival to piperazine (**Figure 3.7**). This could indicate that both genes, *PM2* and *PM3*, are needed to obtain a resistant phenotype. To test this hypothesis, I transfected the same PPQ sensitive isolate, 005, and the Dd2 lab strain with the *PM2-2A-PM3* vector. Confirmation of the presence of the plasmid in the PPQ-sensitive field isolate 005 and Dd2 lab strain was demonstrated via PCR (**Figure 3.10**). I also transfected the unmodified pDC2-*cam-mrffp-2A-gfp-bsd-attP* plasmid as a transfection control (**Figure 3.10**). Curiously, the study was only able to detect GFP and RFP fluorescence in the Dd2 transfectants (**Figure 3.9**) and not the 005 isolate, although both the Dd2 and 005 transfectants were PCR-positive for the plasmids and maintained on the appropriate BSD selection pressure to maintain the episomal plasmid (**Figure 3.10**). Since the pDC2-*cam-mrffp-2A-gfp-bsd-attP* plasmid was used as a transfection control to determine if the parasites could be successfully transfected, the lack of GFP and RFP fluorescence in the 005 transfectants will not be pursued further, since the PCR results and the growth of the parasites on BSD pressure show that both plasmids (*mrffp-2A-gfp* and *PM2-2A-PM3*) are present in the transfected parasites. However, plasmid-rescue of the episomal plasmid from the 005 parasites, and sequencing of the *mrffp-2A-gfp* cassette would be the first step in determining why expression of the reporter genes is not observed.

Future work will now prioritize further characterization of the *PM2-3* transfected lines. Before performing further parasite survival assays to assess the impact of *PM2-3* overexpression on PPQ sensitivity, it is necessary to examine both *PM2-3* RNA and protein levels to determine if the overexpression plasmids have resulted in increased RNA and protein in the transfected parasites compared to the non-transfected parent lines. Samples have been saved for qPCR analysis to compare *PM2-3* transcript expression levels and preliminary Western blots to compare protein expression in the parental non-transfected and transfected lines have been performed but must be optimized.

Recent functional studies have provided insight into the role of the *PM2-3* amplification in response to antimalarial drug pressure. Loesbanluechai *et al.* 2019 (Loesbanluechai *et al.*, 2019) demonstrated that overexpression of either *PM2* or *PM3* individually in the 3D7 parasite background had no effect on parasite susceptibility to piperazine, artemisinin, and chloroquine. Consistent with this result, I did not observe any survival difference in response to piperazine in initial studies on the PPQ-sensitive isolate, 005 overexpressing only *PM2*

(Figure 3.7). Interestingly, Bopp *et al.* 2018 found that increased *PM2-3* copy numbers in PPQ-resistant field isolates enhanced survival to PPQ (Bopp *et al.*, 2018). It should be noted that the isolates with increased *PM2-3* copy numbers and survival under PPQ pressure in the study by Bopp *et al.* were *kelch13* C580Y or Y493H mutants, and were not generated by transgenic methods but were naturally multicopy for *PM2-3* (Bopp *et al.*, 2018). Additional studies on *PM2* and *PM3* knockouts in 3D7 parasites showed decreased survival to PPQ, though the differences in PPQ IC₅₀ survival assays appeared minor (Mukherjee *et al.*, 2018). It is therefore possible that the *PM2-3* amplification needs to be present in the same genetic background of artemisinin resistance (K13 mutant or other potential genetic variants). Furthermore, it may be necessary for the *PM2-3* amplification to be in the presence of other molecular markers of PPQ resistance for the effects of the amplification to manifest. In subsequent chapters, I will explore other potential markers of piperazine resistance, including SNPs in the putative exonuclease protein, PF3D7_1362500 (exo-E415G), putative mitochondrial carrier protein, PF3D7_1368700 (MCP-N252D), and PfCRT. It is also necessary to further examine the role of knocking out or knocking down *PM2* and *PM3*, thus future functional work is critical.

I have made over four separate attempts (in duplicate) to transfect the *PM2-2A-PM3* plasmid into multiple field isolates with K13 C580Y mutations, one of the molecular markers of artemisinin resistance. Additional attempts were made with the generous help of my lab colleague, Dr. Sophie Adjalley. All attempts to date have been unsuccessful. Studies have shown that laboratory strains such as Dd2 and 3D7 are genetically different from more recently adapted field isolates (Mackinnon *et al.*, 2009), which could contribute to difficulties experienced in field isolate transfections. Due to the lack of additional field isolates transfected with the *PM2-2A-PM3* plasmid, my studies in field isolates with various genetic backgrounds (K13, exo-E415G, MCP-N252D, PfCRT) are ongoing. Transfection protocols have been optimized using different machines (Bio-Rad electroporator and Amaxa electroporator) and conditions (pre-loading RBCs versus direct transfection of ring-stage parasites and use of conditioned media) but these changes have yet to result in transfected field isolates. Transfections of schizonts rather than loaded RBCs or ring-stage parasites has also been widely used for transfections of *P. knowlesi* (Moon *et al.*, 2013) and could be attempted with the field isolates used in this study. Additional transfection attempts with field isolates could also vary the concentrations of BSD used for plasmid selection (increasing the BSD concentration) or perhaps different drug resistance genes could be used. Nevertheless,

progress has been made in transfecting the 005 isolate with the dual *PM2-2A-PM3* overexpression plasmids and future work on RNA and protein expression is forthcoming.

As antimalarial drug resistance continues to thwart treatment efforts, it is imperative to have assays and functional studies to assess molecular markers of drug resistance. This thesis has developed two novel assays that can be used to monitor for the *PM2-3* molecular marker of piperazine resistance. In a proof of concept of assay reliability and ease of use, I spent one month in Cambodia (April 2017) teaching our NIH-based team in Phnom Penh how to perform the assays, where the procedures were quickly introduced without any technical issues. In addition to the copy number assays, I have also developed a *PM2-3* overexpression plasmid that can be used to assess the effects of stoichiometric overexpression of both *PM2* and *PM3*. Though future work is necessary, the tools developed by this study have formed a fundamental basis for monitoring and determining the role of the *PM2-3* amplification in piperazine resistance.

Chapter 4: Examination of the role of single nucleotide polymorphisms in an exonuclease protein and mitochondrial carrier protein in piperazine resistance

4.1 Declaration of work

The following chapter includes data obtained from plasmids designed by Dr. Marcus Lee and edited parasite lines obtained from Dr. Manuela Carrasquilla. Dr. Lee provided all plasmids used for CRISPR-Cas9 editing in this study. Dr. Carrasquilla generated Dd2-edited parasite lines that contained the wildtype and mutant exonuclease SNPs. Both Drs. Lee and Carrasquilla are cited accordingly in the relevant sections of this chapter for their generous contributions to this work.

4.1.1 Significance and purpose of study

Advances in genetic studies and technologies have greatly enhanced our current understanding of malaria parasites. Whole genome sequencing (WGS) technologies allow for real-time monitoring and detection of genetic changes in parasite populations throughout widespread endemic areas. These technologies enable us to track genetic changes as they occur and provide useful information for both control efforts and the potential elimination of the disease (Ariey et al., 2014, Miotto et al., 2015, Manske et al., 2012, Wootton et al., 2002, Dondorp et al., 2009). With the use of genome wide association studies (GWAS), we can identify potential molecular markers of drug resistance by comparing single nucleotide polymorphisms (SNPs), copy number variations, insertion and deletion polymorphisms (indels), and other genetic changes in parasite populations. However, the identified molecular markers of resistance may have no phenotypic relevance or causal relationship to the resistance observed. Alternatively, the molecular marker could have a more indirect impact on resistance, for example to compensate for the fitness cost of another mutation. In order to understand how drug resistance develops, and definitively test whether a marker is necessary and sufficient to confer resistance, it is necessary to perform functional studies. We can harness the clues GWAS provides and use them as a roadmap for assessing the mechanisms of resistance of various antimalarial drugs. The purpose of this study was to use CRISPR-Cas9 gene editing to investigate the role of two nonsynonymous SNPs associated with piperazine resistance: a putative exonuclease protein SNP, PF3D7_1362500 (*exo-E415G* SNP), and a putative mitochondrial carrier protein. SNP, PF3D7_1368700 (*mcp-N252D*

SNP) (Amato et al., 2017). This study fills a knowledge gap in the lack of functional data for molecular markers of piperaquine resistance by examining phenotypic and functional relevance of the genotypes observed.

4.1.2 Introduction

The ability of the *P. falciparum* parasite to adapt to the selective pressure of antimalarial drugs is a major impediment to treatment regimens. The use of specific antimalarial drugs in distinct geographic regions can also have an immense effect on the evolution of parasite populations in different areas. It is therefore necessary to have a means to detect and track these genetic changes as they occur. Whole genome sequencing (WGS) of *P. falciparum* was first published in 2002 (Gardner et al., 2002, Hall et al., 2002) and such technologies have revolutionized malaria control and treatment programs by enabling widespread surveillance of malaria parasite populations throughout the globe. When combined with clinical studies and *in vitro* drug susceptibility profiles, genome wide association studies (GWAS) enable identification and genetic tracking of molecular markers of resistance (Ariey et al., 2014, Miotto et al., 2015, Manske et al., 2012, Wootton et al., 2002, Dondorp et al., 2009, Amato et al., 2017, Witkowski et al., 2017, Imwong et al., 2017). This information can provide clues for uncovering mechanisms of resistance, though molecular markers may eventually be found to play little to no causal role in the drug-resistant phenotype. As artemisinin and partner drug resistance continue to spread throughout Southeast Asia (SEA), it is crucial to elucidate and understand mechanisms of antimalarial drug resistance in order to aptly inform current and future malaria treatment strategies.

As detailed in Chapter 1, artemisinin combination therapies (ACTs) are the first line treatment for *P. falciparum* malaria and function by combining a potent short-acting artemisinin derivative with a long-acting partner drug with a different mechanism of action (World Health Organization, 2018). Over the last decade, dihydroartemisinin-piperaquine (DHA-PPQ) has been the ACT commonly used in many countries in SEA, including Cambodia, Thailand, Myanmar, and Vietnam, among others (World Health Organization, 2015). However, both artemisinin and piperaquine resistance have been reported at multiple sites in Cambodia and neighboring countries (Cui et al., 2015), with the most recent reports from 2015-2018 documenting an even further decline of DHA-PPQ efficacy, with efficacy rates of 12%, 38%, and 47% in Northeastern Thailand, Western Cambodia, and Southwestern Vietnam, respectively (van der Pluijm et al., 2019).

In order to monitor and investigate the causes of DHA-PPQ resistance, multiple studies have reported independent molecular markers of resistance for both artemisinin and piperazine resistance. Several mutations in the *kelch 13* (K13) gene have been accepted as markers of artemisinin resistance (Ariey et al., 2014, Miotto et al., 2013) and multiple studies (outside the scope of this doctoral thesis) have focused on determining the mechanism of artemisinin resistance (Meshnick et al., 1991, Tilley et al., 2016, Bridgford et al., 2018, del Pilar Crespo et al., 2008, Klonis et al., 2013, Heller and Roepe, 2019, Mok et al., 2015, Mok et al., 2011, Rocamora et al., 2018, Sa et al., 2018, Straimer et al., 2015), which is a complex and unfinished story. Molecular markers of piperazine resistance were first reported in 2017 (Amato et al., 2017, Witkowski et al., 2017) and have emerged on a K13 mutant background (Imwong et al., 2017, Amato et al., 2018). As discussed in Chapter 3, amplification of the *plasmepsin 2* and *plasmepsin 3* (*PM2-3*) genes on chromosome 14 associates with DHA-PPQ failures in patients (Witkowski et al., 2017, Amato et al., 2017) and the amplification is currently used as a reliable marker of piperazine resistance (Chapter 3) (Jacob et al., 2019, van der Pluijm et al., 2019, Hamilton et al., 2019). Additional *in vitro* studies (Agrawal et al., 2017, Dhingra et al., 2017, Ross et al., 2018a) have reported mutations in the *chloroquine resistance transporter* gene (*pfcr*) that confer variable degrees of piperazine resistance. Following these reports, more recent genetic studies (Hamilton et al., 2019) have identified an increased frequency of previously reported (Agrawal et al., 2017, Ross et al., 2018a) and novel mutations in PfCRT that have arisen on an amplified *PM2-3* background that significantly associate with decreased piperazine susceptibility. However, before these PfCRT mutations were prevalent, piperazine treatment failures and parasites with decreased *in vitro* piperazine susceptibility were present on PfCRT backgrounds lacking these mutations (Amato et al., 2017) (**Chapter 2, Table 2.1**). Consequently, many questions remain in the pursuit to discover the genetic determinants of piperazine resistance.

At the time this thesis commenced, a genome-wide association study (GWAS) (Amato et al., 2017) of 297 parasite isolates exposed to DHA-PPQ identified SNPs that strongly associate with reduced PPQ susceptibility *in vitro* and DHA-PPQ failures in patients detailed in Table 4.1. The top most significant nonsynonymous SNPs are located on chromosome 13 in a putative exonuclease (*exo-E415G*) and a mitochondrial carrier protein (*mcp-N252D*) (**Table 4.1**). Unlike the above-mentioned markers of piperazine resistance, no *in vitro* work has been reported on the role of the *exo-E415G* or *mcp-N252D* SNPs in the piperazine-resistant phenotype.

Table 4. 1 Top GWAS candidate SNPs associated with increased piperazine IC₅₀ values

Chr.	Position	Gene ID	Gene Description	N/S	Alteration	p value
13	2,504,560	PF3D7_1362500	exonuclease, putative	N	p.Glu415Gly	2.69× 10 ⁻⁹
12	418,346	PF3D7_1208900	conserved <i>Plasmodium</i> protein, unknown function	S	p.981Pro	4.80× 10 ⁻⁸
13	2,728,402	PF3D7_1368700	mitochondrial carrier protein, putative	N	p.Asn252Asp	2.33× 10 ⁻⁷
13	2,512,415	PF3D7_1362700	conserved <i>Plasmodium</i> protein, unknown function	S	p.687Asn	6.25× 10 ⁻⁷
13	2,519,091	PF3D7_1362800	conserved <i>Plasmodium</i> protein, unknown function	N	p.Gly202Asp	2.12× 10 ⁻⁶
13	2,447,146	PF3D7_1361000	arginine methyltransferase 5, putative (PRMT5)	N	p.Asn40Ser	3.96× 10 ⁻⁶
4	904,088	PF3D7_0420000	zinc finger protein, putative	S	p.213Leu	7.67× 10 ⁻⁶
14	2,411,942	PF3D7_1458700	conserved <i>Plasmodium</i> protein, unknown function	N	p.Arg25Lys	1.27× 10 ⁻⁵
14	2,395,752	PF3D7_1458300	conserved <i>Plasmodium</i> protein, unknown function	N	p.Ile301Phe	2.03× 10 ⁻⁵
13	2,542,366	PF3D7_1363300	mitochondrial ribosomal protein L9 precursor, putative	N	p.Thr28Ile	2.48× 10 ⁻⁵

Table 4.1, adapted from Amato *et al.* 2017 (Amato et al., 2017), displays the top ten GWAS candidate SNPs associated with increased piperazine IC₅₀ values in order of increasing p-value. Each gene is listed with: chromosome number (chr.); nucleotide position (position); gene ID and description; type of SNP: nonsynonymous (N) or synonymous (S); the amino acid difference (alteration); and p-value.

The nonsynonymous SNP in the putative exonuclease protein, PF3D7_1362500, encodes a glutamic acid (E) to glycine (G) substitution at position 415 and the prevalence of this SNP has increased along with the *PM2-3* amplification in Cambodia from the time period of 2012-2015 (**Figure 4.1**) (Amaratunga et al., 2019). Though sparse information is known about this protein in *P. falciparum*, the putative exonuclease contains domains with sequence similarity to 3'-5' exonucleases from other organisms including both prokaryotes and eukaryotes (PlasmoDB; NCBI BLAST). However, sufficient data is currently not available for generating a proposed model for the domain structures of the putative exonuclease, PF3D7_1362500.

As implied by their name, exonucleases are enzymes that cleave nucleotides from DNA at the 3' or 5' ends by hydrolyzing the phosphodiester bonds between nucleic acids (Shevelev and Hübscher, 2002, Lovett, 2011). This is a common feature of some polymerases that have “exo activity” or proofreading activity and is distinguished from endonuclease activity because exonucleases excise from the end of the DNA chain as opposed to internally (Lovett, 2011). Prior research has shown that 3'-5' exonuclease activity is also needed in double-stranded break repair and in non-homologous end joining (NHEJ) showing a role for exonucleases not only in DNA replication but also in distinct repair processes (Shevelev and Hübscher, 2002).

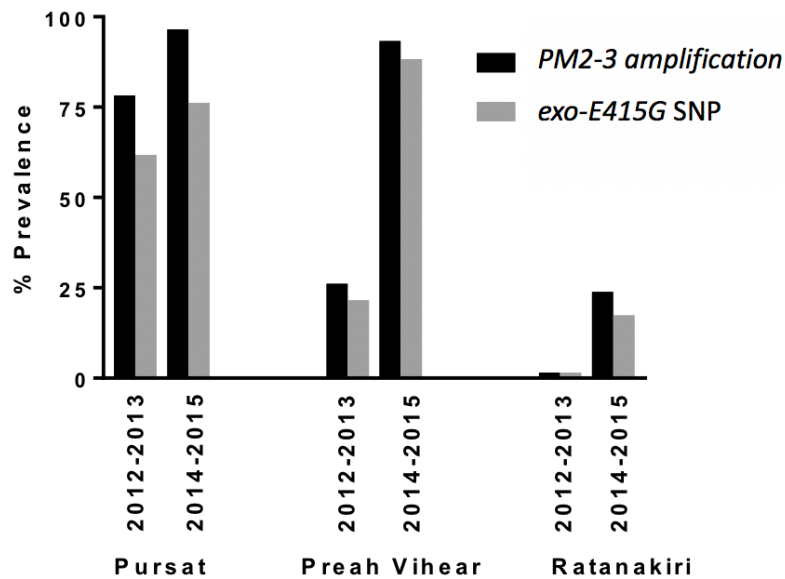


Figure 4. 1. Prevalence of the *PM2-3* copy number amplification and *exo-E415G* SNP in three provinces in Cambodia from 2012-2015. (Adapted from Amaratunga *et al.* (Amaratunga *et al.*, 2019) with *PM2-3* CNV data obtained from Chapter 3.)

This study hypothesized that the *P. falciparum* putative exonuclease plays a 3'-5' proofreading role during DNA replication and perhaps even DNA repair. It is uncertain what role, if any, the *exo-E415G* SNP plays in piperazine-resistant *P. falciparum*, however one possibility is that the SNP affects the proofreading or repair ability of the putative protein, leading to significant differences (increases or decreases) in the overall mutations in the parasite, which might aid in the resistant phenotype. Studies by Lee and Fidock (2016) examined mutator rates of Cambodian isolates with mutations in repair genes in comparison to reference laboratory strains without mutations and showed only a mild increase in overall mutations in Cambodian isolates possessing the mutant repair genes (Lee and Fidock, 2016). The role of the *exo-E415G* SNP could thus be directly related to survival or fill a milder, indirect role in resistance via fitness or compensatory measures. This thesis therefore hopes to provide insight into the role the *exo-E415G* SNP plays in the parasite response to piperazine.

Similar to the exonuclease, little is currently known about the putative mitochondrial carrier protein (MCP). The nonsynonymous SNP in the putative MCP, PF3D7_1368700, encodes an asparagine (N) to aspartic acid (D) substitution at position 252 (*mcp-N252D*). Mitochondria are vital organelles in all eukaryotic organisms, serving key roles in metabolism, apoptosis, the breakdown of amino acids, and many other processes. MCPs are a large family of

proteins that mediate transport of molecules across the mitochondrial membranes. MCPs thus enable mitochondrial activities and connect processes in the cytosol with those in the mitochondrial matrix (Wohlrab, 2009). MCPs are nuclearly encoded and contain inner targeting signals that direct them to the inner mitochondrial membrane, where MCPs transport molecules such as adenosine triphosphate (ATP) or protons (H⁺) to establish membrane gradients (Kunji, 2004). Sequence analysis of the PF3D7_1368700 putative MCP using PlasmoDB and BLAST, shows that this molecule shares amino acid sequence similarity with other MCPs, specifically with the yeast ADP/ATP carriers, Aac2p and Aac3p (Ruprecht et al., 2014). Conserved motifs for MCPs consist of a PX(D/E)XX(K/R) motif (Ferramosca and Zara, 2013, Robinson and Kunji, 2006, Kunji, 2004), called the carrier signature and sequence analysis by this study suggests the motif is present in the PF3D7_1368700 MCP as PGD TVR. Similar to the putative exonuclease protein, not enough information is available to generate a model for the domain structures of the MCP, PF3D7_1368700.

Antimalarial drug resistance in *P. falciparum* has long been associated with genetic variation in malaria transporters (PfCRT, PfMDR1, PfMDR2) (Ecker et al., 2012, Eastman et al., 2011, Kirk, 2001, Sauvage et al., 2009) but no studies have yet reported a role for the putative MCP PF3D7_1368700 in resistance. However, studies by Cowell *et al.* (Cowell et al., 2018) have identified mutations in another mitochondrial protein on chromosome 1, PF3D7_0108400, after *in vitro* drug selection experiments with several different compounds. Due to the significant correlation of DHA-PPQ failures and the presence of this *mcp-N252D* SNP, I decided to test if the putative MCP, PF3D7_1368700, could also have a functional role in facilitating piperazine resistance. It should be stated that like the *exo-E415G* SNP, it is possible the *mcp-N252D* SNP could have a modest role in resistance and instead serve a compensatory role in modulating parasite fitness. It is also entirely plausible that both SNPs are unrelated to piperazine resistance. Furthermore, the putative proteins could behave very differently in *P. falciparum* when compared to the homologous proteins in other organisms from which they inherited their putative names due to sequence similarities. Thus, further genetic studies are imperative to shed light on these questions and postulations.

The goal of this study is to evaluate the potential role of the resistance-associated SNPs, *exo-E415G* and *mcp-N252D*, in susceptibility to piperazine. To examine these genetic associations, I used CRISPR-Cas9-based genome editing to dissect out the potential individual contributions of each of these candidates in an isogenic parasite background, the

Southeast Asian lab-adapted line Dd2 and in piperazine-sensitive and resistant Cambodian isolates that contain the wildtype and mutant SNPs, respectively. I then examined if there were any phenotypic differences in the transgenic parasites by analyzing the drug susceptibility profiles of each edited line in response to piperazine and other commonly used antimalarial drugs.

4.1.3 Objectives

Investigate the role of the putative exonuclease (PF3D7_1362500) and mitochondrial carrier protein (PF3D7_1368700) single nucleotide polymorphisms (SNPs) in piperazine resistance

- (1) Investigate whether the exonuclease nonsynonymous SNP on chromosome 13, *exo-E415G* SNP, confers piperazine resistance and characterize any additional phenotypes
 - a. Use CRISPR-Cas9 to insert the *exo-E415G* SNP into the lab strain, Dd2 and Cambodian field isolates
 - b. Characterize the *exo-E415G* SNP in phenotypic assays
- (2) Evaluate the role of the putative mitochondrial carrier protein (PF3D7_1368700) nonsynonymous SNP on chromosome 13, *mcp-N252D*, in piperazine resistance
 - a. Use CRISPR-Cas9 to insert the *mcp-N252D* SNP into the lab strain, Dd2 and Cambodian field isolates
 - b. Characterize the *mcp-N252D* SNP in phenotypic assays

4.2 Materials and methods

4.2.1 CRISPR-Cas9 mediated genome editing: two-plasmid system

Initial attempts at CRISPR-Cas9-based gene editing (Jiang and Doudna, 2017, Sander and Joung, 2014) of the exonuclease SNPs were made using a two-plasmid system (**Figure 4.2**). All plasmids were designed and generously provided by Dr. Marcus Lee.

4.2.1.1 Exonuclease *exo-415* SNP editing plasmids

For the exonuclease *exo-415* wildtype (E) and mutant (G) SNP two-plasmid editing system, one plasmid (**Figure 4.2A**, plasmid one) contained the gRNA and Cas9 (pDC2-cam-Cas9-U6-*hdhfr*, 11.9 kb) and the second plasmid (plasmid two) contained a 1 kb donor region with either the *exo-E415* wild-type SNP or with the *exo-G415* mutant SNP (pDC2-cam-*egfp*-BSD-attP, 5.602 kb) (**Figure 4.2B**, plasmid two). Briefly, identification of an appropriate gRNA was performed using the online resources at Benchling (benchling.com) and Cas-OFFinder (<http://www.rgenome.net/cas-offinder>) to find a unique sequence of 20 base pairs followed

by the NGG motif, located near the SNP at the amino acid position 415 in the *exonuclease* gene, PF3D7_1362500, near the SNP location at amino acid position 415 followed by NGG. The Cas9 endonuclease encoded by plasmid one (**Figure 4.2A**) is from *Streptococcus pyogenes* which recognizes and will create a double stranded DNA break at the protospacer adjacent motif (PAM) sequence, 5'-NGG-3' (Anders et al., 2014). The exonuclease donor sequence in the donor plasmid (plasmid two) (**Figure 4.2B**) was synthesized to include several synonymous SNPs at the gRNA recognition site (**Table 4.2**, lowercase letters) to prevent Cas9 from cleaving the plasmid and the edited genome. It should also be noted that for the *exo*-415 guide, the SNP of interest (415) is located within the gRNA sequence. For the wildtype codon, the sequence "GAG" encodes a glutamic acid (E) at position 415 (**Table 4.2**, in bold), for the mutation, the sequence, "GgG" encodes the mutant glycine (G) (**Table 4.2**, in bold).

Table 4. 2 gRNA sequences in the donor plasmids for the *exo-415* and *mcp-252* CRISPR-Cas9 plasmids

Gene	SNP position	Guide RNA (5' - 3') in donor template
exonuclease, E415	415	AAGAGGAAGTgAACAAcCAc
exonuclease, G415	415	AAGgGGAAGTgAACAAcCAc
mitochondrial carrier protein	252	CGATATTTTATTGATGCtTC

4.2.1.2 Two-plasmid system: cloning of the gRNA and donor plasmids

To clone the gRNA into plasmid one, pDC2-cam-Cas9-U6-*hdhfr*, two complementary primers including the specific gRNA sequence and overhangs for ligation into the BbsI site were generated (**Figure 2A**). The pDC2-cam-Cas9-U6-*hdhfr* plasmid was digested with BbsI followed by dephosphorylation of the vector using an alkaline phosphatase (NEB). At the same time, the complementary guide oligos were resuspended to 100 μ M in water and phosphorylated in 10 μ L total using: 1 μ L of each oligo, 1 μ L 10X ligation buffer (NEB) and 0.5 μ L T4 polynucleotide kinase (NEB), and 6.5 μ L water. Guide oligos were then incubated in a thermocycler for 30 minutes at 37°C, followed by denaturation at 94°C for 5 minutes, then annealing in decreasing steps of 5°C every 5 minutes to 25°C. After annealing, the oligos were ligated into the BbsI digested pDC2-cam-Cas9-U6-*hdhfr* vector. A 1:200 dilution of the oligo mix was made and 1 μ L of oligos was added to 1 μ L of digested plasmid (50 ng), 1 μ L 10x ligase buffer (NEB) and 1 μ L T4 ligase (NEB) in water up to 10 μ L total. The ligation mix was incubated for 10 minutes at room temperature then transformed into XL10 gold competent cells (**section 2.8.1**) and plated on LB-ampicillin plates. Donor regions were cloned into plasmid two, the pDC2-cam-*egfp*-BSD-attP plasmid (**Figure 2B**), following a

similar procedure using the enzymes AatII and EcoRI to digest the plasmid at the donor site. Following confirmation of the correct insertion of the guide and donor sequences, the plasmids were prepared by midi or maxi preps (**section 2.8.2**) and transfected into field isolates.

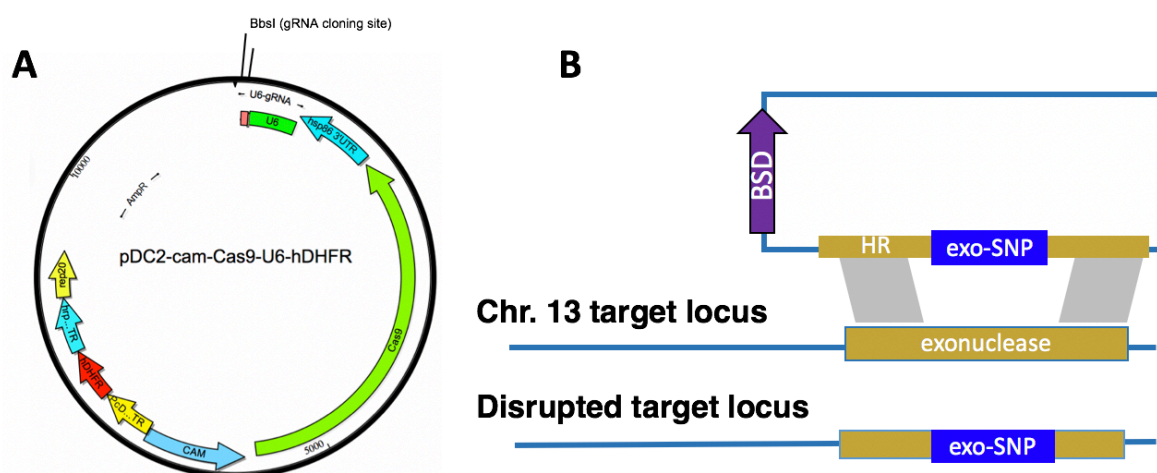


Figure 4. 2. Two-plasmid system for CRISPR-Cas9 editing of the *exonuclease* SNP. A.) Plasmid one: the pDC2-cam-Cas9-U6-*hdhfr* plasmid with Cas9 expression cassettes. The gRNA cloning site is flanked by BbsI digestion sites (labeled) B.) Plasmid two: the pDC2-cam-*egfp*-BSD-attP donor plasmid containing the homology region (HR) and the desired exonuclease SNP for editing parasites to either the wild-type (E) or mutant (G) exonuclease SNP on Chromosome 13. The donor cloning site outside of the homology region (gold) includes EcoRI and AatII digestion sites.

4.2.2 CRISPR-Cas9 mediated genome editing: single plasmid system

The pDC2-cam-coCas9-U6-*hdhfr* single plasmid editing system (**Figure 4.3**) designed by Dr. Marcus Lee was also used in this study. In this vector, Cas9 has been codon optimized for expression in *P. falciparum*, and in addition to the gRNA cassette, contains cloning sites for insertion of the donor region (**Figure 4.3**). This enabled the pDC2-cam-coCas9-U6-*hdhfr* plasmid (~11 kb, depending on donor size) to be used as a backbone for generating both the *exo*-E415G and *mcp*-N252D editing plasmids, both of which were also generated by Dr. Marcus Lee for use in this study. The procedure for inserting both the gRNA and donor sites was similar to the methods described above in **section 4.2.1.2**. The gRNA sequences used for the *exo*-415 single plasmid system were the same gRNAs used for the two-plasmid system and listed in **Table 4.2**.

The *mcp*-252 editing plasmids for the mitochondrial carrier protein, PF3D7_1368700, were generated in a similar manner to the above *exo*-415 two-plasmid system (**section 4.2.1.2**).

Selection of gRNA (**Table 4.2**) and molecular cloning of the donor and gRNA regions into the vector plasmids was performed as described for the *exo-415* plasmids. The gRNA sequence in the donor region (**Figure 4.3**) was modified to introduce a synonymous SNP (**Table 4.2**, lowercase letters) to prevent Cas9 from cutting the plasmid and the edited region in the genome. The SNP was located 87 bp from the gRNA site and the mutant N252D plasmid changes the wildtype “AAT” (N) sequence to the mutant “gAT” codon (D), whereas the silent N-252N plasmid maintains the wildtype (N) sequence.

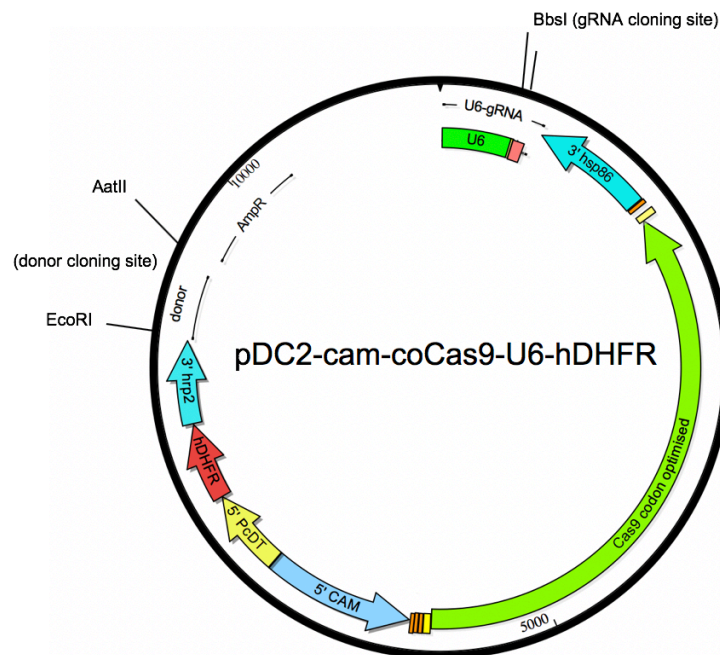


Figure 4. 3. All-in-one pDC2-cam-coCas9-U6-hdhfr plasmid. Schematic of the all-in-one pDC2-cam-coCas9-U6-hdhfr plasmid (~11 kb) design for CRISPR-Cas9 editing contains codon optimized Cas9 for expression in *P. falciparum*, and includes the cloning sites for inserting the donor (using EcoRI and AatII) and gRNA (using BbsI).

4.2.3 Transfection of CRISPR-Cas9 *exo-415* and *mcp-252* plasmids

The plasmids were transfected into field isolates and Dd2 parasites (**Chapter 2, Table 1**) following the protocols detailed in Chapter 2, **sections 2.3.1-2.3.2**. Both pre-loaded red blood cells (RBCs) and ring stage transfections were performed. As mentioned in Chapter 2, the pre-loaded RBC transfection method was preferred for field isolates because it does not involve direct electroporation of the parasites and as a result, is likely to be less harsh to these parasites. Ring stage transfections were always performed for the laboratory strain, Dd2, but were also attempted with field isolates. Both the PPQ-sensitive and resistant isolates (**Chapter 2, Table 1**) were transfected with the plasmids containing the SNP they already contain (i.e. only introducing the silent gRNA site mutations) to serve as an editing control, ensuring that the CRISPR-Cas9 system did not cause any additional genome disruption.

For the two-plasmid system (**Figure 4.2**), both the gRNA/Cas9 plasmid and donor plasmid were transfected at the same time using 50 µg of each plasmid. The pDC2-cam-Cas9-U6-*hdhfr* contains a human dihydrofolate resistance gene (*hdhfr*) so transfectants were selected with 2 nM WR99210, a DHFR inhibitor. The pDC2-cam-*egfp*-BSD-attP donor encodes a blasticidin (BSD) resistance gene and 2 µg/mL of blasticidin (BSD) was used to select for this plasmid (**Figure 4.2**). Drug selection was started on day 1 or 2 post-transfection depending on parasitemia on day 1 and parasites were maintained on drug for at least 8 days and up to 2 weeks following transfection.

For the single plasmid system (**Figure 4.3**), the pDC2-cam-coCas9-U6-*hdhfr* transfectants were selected with 5-10 nM WR99210 on day 1 post-transfection and parasites were maintained with drug for 10-12 days. The Cambodian isolates have a moderate level of resistance to DHFR inhibitors, due to the quadruple pyrimethamine-resistance mutations in *dhfr*, so 5-10 nM WR99210 was used for the transfected parasites while 5 nM WR99210 was used for Dd2.

To increase transfection efficiency in field isolates, some of the transfected isolates were cultured in parasite-conditioned media (**Tables 4.4-4.5**), consisting of complete media (CM) supplemented with drug (WR or BSD) and 25-50% of spent media from the specific parasite line (called conditioned media), prepared as described in **section 2.4**.

4.2.4 Screening for integration of the *exo*- and *mcp*-SNPs in transfected parasites

As soon as the parasites recrudesced after transfection, an aliquot of the culture was saved for genomic DNA extraction as described in **section 2.5**. The parasites were screened for integration of the *exo-E415G* and *mcp-N252D* SNPs using the primers listed in **Table 4.3**. PCR amplification and sequencing protocols were performed as described in **sections 2.8.3-2.8.4**. At least one primer was designed outside of the donor homology region to ensure that the region amplified was from the genome and not the episomal donor plasmid (**Figure 4.4**).

After initial screening, the parasites with confirmed edits were cloned by limiting dilution (**section 2.4**) and collected for sequencing (**section 2.8.4**) to confirm the genotype in each clone. Following confirmation, clones were cryopreserved (**section 2.1.3**; at least two vials per edited line) and phenotypes were examined in parasite survival assays.

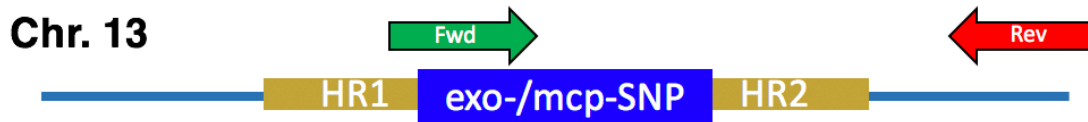


Figure 4. 4. Primers for PCR screening of transfectants for integration of the desired locus on chromosome 13 (blue line) to capture the *exo-415* or *mcp-252* SNPs. The gold HR1 and HR2 regions represent the homology regions surrounding the SNP included in the donor region. The forward (Fwd) primer includes the region with the SNP and the reverse (Rev) primer is outside of the donor homology region so that only regions integrated into the genome will be amplified.

Table 4. 3 Primers used to screen for integration of SNPs

Gene	SNP	Plasmid system	Primer name	Primer (5' - 3') sequence	Description
exo	exo-415	two	exo_fwd1	CTGACCCCTTTATAGG AATGTGC	fwd inside donor region; for sequencing
			exo_rev1	CTTGGTTAAGTGGTCT TATATCCAGTTAGC	rev flanking donor region
mcp	mcp-252	single	p1580	GATGACAAAACAAAG TTACGCTTCC	fwd flanking donor; for sequencing
			p1581	CTTAATAAATCTAATG GATATGAGAGAG	rev flanking donor

4.2.4 Drug sensitivity assays

Drug susceptibility profiles of the wildtype and mutant *exo-415* and *mcp-252* edited parasite lines were assessed according to the protocols detailed in Chapter 2 (**section 2.6**). Standard IC₅₀ assays (**section 2.6.2**) were performed using piperazine (PPQ) and other commonly used antimalarial drugs including: dihydroartemisinin (DHA), lumefantrine (LUM), chloroquine (CQ), and mefloquine (MQ). Piperazine survival assays (PSAs) (**section 2.6.3**) were also performed on the wildtype and mutant edited *exo-415* and *mcp-252* parasite lines. All IC₅₀ assays and PSAs were performed in duplicate and triplicate, respectively, with three independent experiments (biological replicates) performed for each assay.

4.3 Results

4.3.1 CRISPR-Cas9 editing of the *exonuclease-415* SNPs: low transfection efficiency in field isolates

CRISPR-Cas9 gene editing of the exonuclease, *exo-415* SNP, to the wildtype (E) and mutant (G) SNPs observed in piperazine-sensitive (PPQ-S) and resistant (PPQ-R) isolates from Cambodia was attempted in culture-adapted Cambodian field isolates (**Ch. 2, Table 2.1**). All field isolate transfections for both plasmid systems (two-plasmid and single-plasmid) were

performed using pre-loaded RBCs. The two-plasmid was used at the commencement of this study because this system had been used successfully by the Lee Lab and many other labs for CRISPR-Cas9 editing (Ghorbal et al., 2014). During the course of this study, Dr. Marcus Lee designed the all-in-one CRISPR-Cas9 plasmid and due poor transfection efficiencies with the two-plasmid system, I switched to the single-plasmid system.

Transfection efficiency for all isolates was low with only five transfections out of 158 total transfections recrudescing post-drug selection, two of which were cultured with parasite-conditioned media (**Table 4.4**). Amplified PCR products from transfected parasites that recrudescenced were screened for edits and sequencing data showed that none of these transfectants contained the desired edits (**Figure 4.5**). The parasite lines 033 and 056 are PPQ-S isolates that should have been edited to the mutant G amino acid codon (“GGG”) but they remained the wildtype (“GAG”). The parasite line 021 is a PPQ-R isolate that should have been edited to the wildtype E amino acid codon (“GAG”) but also remained unedited (“GGG”) (**Figure 4.5**).

Table 4. 4 CRISPR-Cas9 transfections and outcomes of *exo-415* SNP editing experiments in Cambodian field isolates

Parasite line	PPQ status	Plasmid system	SNP	exo-SNP transfections			Conditioned media*
				No. of transfections	Recrudescence	Edited SNP	
163-KH2-033 (PH1097-C)	PPQ-sensitive	two	<i>exo-E415E (wt)</i>	10	0	0	Y (5)
			<i>exo-E415G (mutant)</i>	16	2*	0	Y (6)
		single	<i>exo-E415E (wt)</i>	4	0	0	N
			<i>exo-E415G (mutant)</i>	6	0	0	N
163-KH3-056 (PH1310-C)	PPQ-sensitive	two	<i>exo-E415E (wt)</i>	10	0	0	N
			<i>exo-E415G (mutant)</i>	14	1	0	Y (6)
		single	<i>exo-E415E (wt)</i>	4	0	0	N
			<i>exo-E415G (mutant)</i>	4	0	0	N
163-KH3-005 (PH0971-C)	PPQ-sensitive	two	<i>exo-E415E (wt)</i>	0	N/A	N/A	
			<i>exo-E415G (mutant)</i>	0	N/A	N/A	
		single	<i>exo-E415E (wt)</i>	0	N/A	N/A	
			<i>exo-E415G (mutant)</i>	6	0	0	Y (4)
163-KH1-081 (PH1224-C)	PPQ-resistant	two	<i>exo-E415E (wt)</i>	14	0	0	Y (6)
			<i>exo-E415G (mutant)</i>	10	0	0	
		single	<i>exo-E415E (wt)</i>	0	N/A	N/A	
			<i>exo-E415G (mutant)</i>	0	N/A	N/A	
163-KH2-021(PH1387-C)	PPQ-resistant	two	<i>exo-E415E (wt)</i>	16	2	0	Y (6)
			<i>exo-E415G (mutant)</i>	10	0	0	Y (5)
		single	<i>exo-E415E (wt)</i>	0	N/A	N/A	
			<i>exo-E415G (mutant)</i>	0	N/A	N/A	
163-KH1-060RME (PH1265-C)	PPQ-resistant	two	<i>exo-E415E (wt)</i>	12	0	0	Y (6)
			<i>exo-E415G (mutant)</i>	10	0	0	N
		single	<i>exo-E415E (wt)</i>	6	0	0	N
			<i>exo-E415G (mutant)</i>	6	0	0	N
Total				158	5	0	

Table 4.4 Details of the field isolate transfections with *exo-415* SNP plasmids, categorized by parasite line (field isolate name), PPQ susceptibility status (sensitive or resistant), and the plasmid system used for CRISPR-Cas9 gene editing (two-plasmid or single-plasmid). The transfections are further sorted based on whether conditioned media was used (Y= yes N= no) with the number of transfections exposed to conditioned media indicated in parentheses. Recrudescence transfections are highlighted in yellow and are denoted with an asterisk (*) if the transfections that recrudescenced were cultured with conditioned media. All transfections were performed using pre-loaded RBCs.

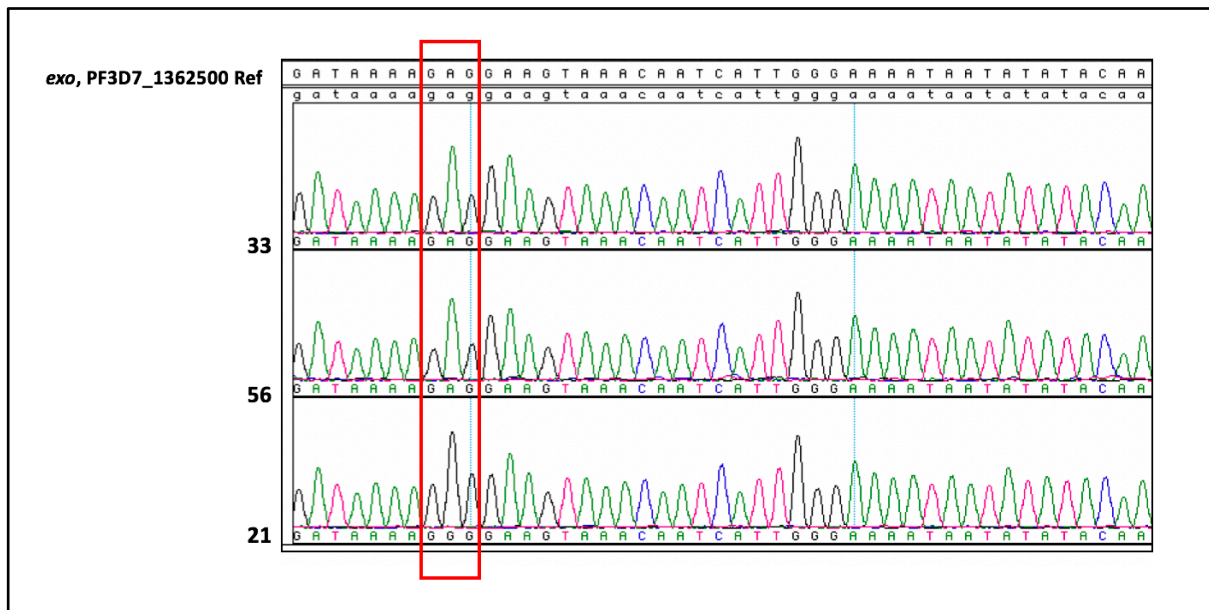


Figure 4. 5. Sequencing analysis of the *exo*-SNP field isolate transfections that recrudesced. The top *exo*, PF3D7_1362500 Ref is the wildtype reference sequence. The red box highlights the location of the codon 415 SNP in the reference and isolates. Parasite isolates 033 and 056 are PPQ-S *exo*-E415 isolates that should have been edited to G415. Parasite isolate 021 is a PPQ-R *exo*-G415 isolate that should have been edited to the wildtype E415 SNP. Primers used to screen the *exo*-SNP two-plasmid transfectants are listed in Table 4.3.

Due to the lack of editing success in Cambodian field isolates, the *exo* editing plasmids were transfected into the Southeast Asian lab strain, Dd2, in parallel by Dr. Manuela Carrasquilla. Both the wildtype (silent) and mutant (G) *exo*-415 SNPs were edited in the Dd2 parasite using the single-plasmid system (**Figure 4.3**). Dr. Carrasquilla confirmed the edits using PCR and sequencing (data not shown).

4.3.2 CRISPR-Cas9 editing of the *mitochondrial carrier protein-252* SNPs: low transfection efficiency in field isolates and successful editing in Dd2 parasites

CRISPR-Cas9 gene editing of the mitochondrial carrier protein, *mcp-252* SNP, yielding the wildtype N codon (AAT) or the mutant D codon (GAT), observed in PPQ-sensitive and resistant isolates respectively, was attempted in lab-adapted Cambodian field isolates (**Ch. 2, Table 2.1**) and the Dd2 parasite strain. Both pre-loaded RBC and ring stage transfections were performed and are detailed in **Table 4.5**. Similar to the *exo*-415 plasmid transfections, efficiency of field isolate transfections with the *mcp-252* single plasmid was low with one field isolate out of 120 total transfections recrudescing (**Table 4.5**). The line 033-*mcp*-N252D transfectant that recrudesced (**Table 4.5, Figure 4.6**) was screened for edits and sequencing data showed that the SNP remained unedited although the silent mutation in the gRNA donor region was introduced (**Figure 4.6C**).

Transfection efficiency of the Dd2 strain was much higher with two of four total transfections recrudescing and one of the transfections containing the edited SNP (**Table 4.5**). The two Dd2-*mcp-N252D* transfectants that recrudesced were screened for edits and the sequencing data showed that one of the transfections carried approximately 30% of the edited SNP in the bulk culture (**Figure 4.7A**). The culture was cloned by limiting dilution and clone H5 was shown to contain the edited SNP (**Figure 4.7B**). Clone D2 did not contain the mutant SNP and remained wildtype (N252) (**Figure 4.7C**) but did contain the edit of the silent mutation in the gRNA region (**Table 4.2**). Since this indicates that clone D2 was edited, I used this clone as the *mcp-N252N* silent editing control for subsequent phenotypic assays.

Table 4. 5 CRISPR-Cas9 transfections and editing efficiency of the *mcp-252* SNPs in Cambodian field isolates and Dd2

					<i>mcp</i> -SNP transfections			
Parasite line	PPQ status	Plasmid system	SNP	Type	No. of transfections	Recrudescence	Edited SNP	Conditioned media*
163-KH2-033 (PH1097-C)	PPQ-sensitive	single	<i>mcp-N252N</i> (wt)	loaded	8	0	0	Y (4)
				ring	4	0	0	N
			<i>mcp-N252D</i> (mutant)	loaded	16	1*	0	Y (8)
				ring	4	0	0	N
163-KH3-056 (PH1310-C)	PPQ-sensitive	single	<i>mcp-N252N</i> (wt)	loaded	0	N/A	N/A	
				ring	0	N/A	N/A	
			<i>mcp-N252D</i> (mutant)	loaded	10	0	0	N
				ring	0	N/A	N/A	
163-KH3-005 (PH0971-C)	PPQ-sensitive	single	<i>mcp-N252N</i> (wt)	loaded	8	0	0	N
				ring	0	N/A	N/A	
			<i>mcp-N252D</i> (mutant)	loaded	12	0	0	Y (4)
				ring	6	0	0	
163-KH2-021(PH1387-C)	PPQ-resistant	single	<i>mcp-N252N</i> (wt)	loaded	0	N/A	N/A	
				ring	0	N/A	N/A	
			<i>mcp-N252D</i> (mutant)	loaded	6	0	0	N
				ring	0	N/A	N/A	
163-KH1-060RME (PH1265-C)	PPQ-resistant	single	<i>mcp-N252N</i> (wt)	loaded	14	0	0	Y (6)
				ring	0	N/A	N/A	
			<i>mcp-N252D</i> (mutant)	loaded	10	0	0	Y
				ring	0	N/A	N/A	
163-KH1-001RME (PH1008-C)	PPQ-resistant	single	<i>mcp-N252N</i> (wt)	loaded	8	0	0	N
				ring	4	0	0	N
			<i>mcp-N252D</i> (mutant)	loaded	6	0	0	N
				ring	0	N/A	N/A	
Dd2	PPQ-sensitive	single	<i>mcp-N252N</i> (wt)	loaded	0	N/A	N/A	
				ring	2	0	0	N
			<i>mcp-N252D</i> (mutant)	loaded	0	N/A	N/A	
				ring	2	2	1	N
Total					120	3	1	

Table 4.5 Details of the field isolate transfections with *mcp-252* SNP editing plasmids categorized by parasite line (field isolate name), PPQ susceptibility status (sensitive or resistant), and the plasmid system used for CRISPR-Cas9 gene editing (single-plasmid), and the method for transfection, pre-loaded RBCs (loaded) or directed electroporation (rings). The transfections are further sorted based on whether conditioned media was used (Y= yes; N= no) with the number of transfections exposed to conditioned media indicated in parentheses. Recrudescence transfections are highlighted in yellow and are denoted with an asterisk (*) if the transfections that recrudesced were cultured with conditioned media.

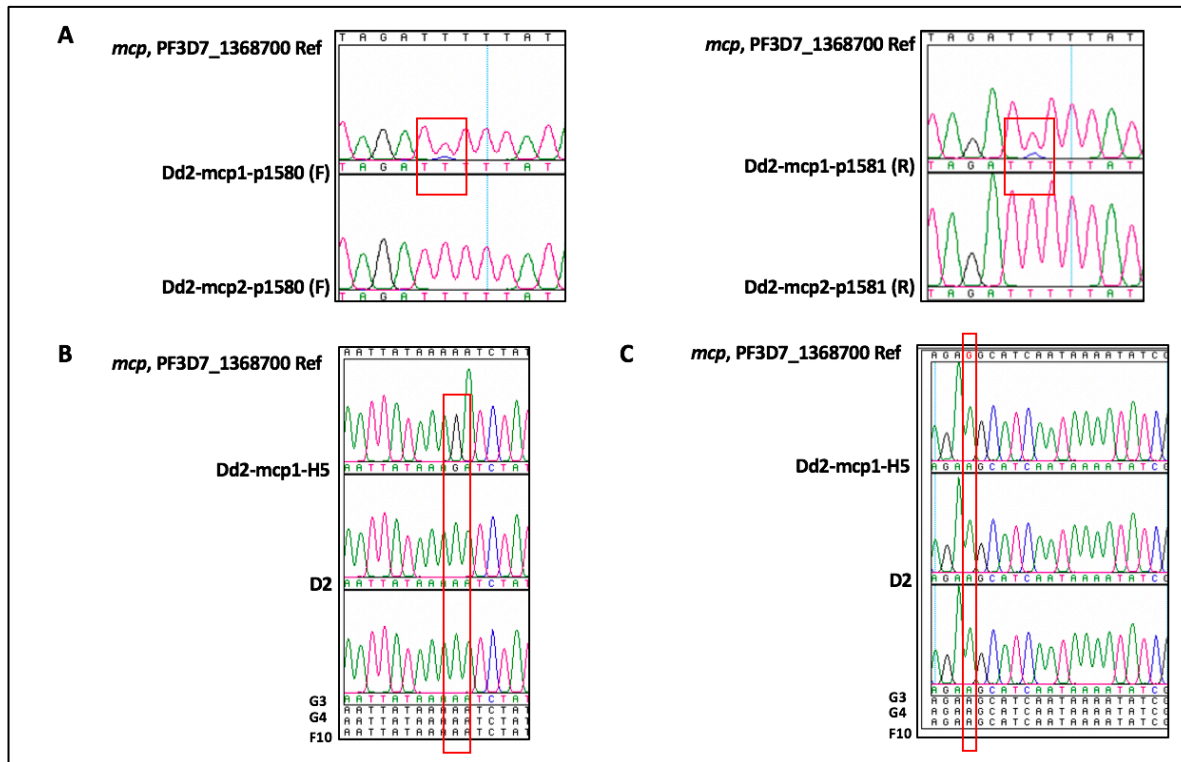


Figure 4.7. Sequencing analysis of the Dd2-*mcp*-SNP transfections. A.) The top Ref sequence is the wildtype reference sequence. The chromatogram shows the region of the *mcp*-252 SNP in the reference and the two Dd2 transfections that recrudesced: Dd2-*mcp*1 and Dd2-*mcp*2. The Dd2-*mcp*1 chromatogram shows a mixed peak (red box) around position 252, displaying both a wildtype “T” and a small blue peak on the chromatogram that is the mutant “C”. Chromatograms for both the forward p1580 (F) and reverse p1581 (R) primers are displayed. Dd2-*mcp*2 did not show mixed peaks or any signs of editing. B.) Sequence analysis of Dd2-*mcp*1-N252D clones. Dd2 clone H5 contains the edited SNP “G” (highlighted in the red box) and the other clones (D2, G3, G4, and F10) are unedited and remain the wildtype “A”. Note: the sequence in panel (B) is the reverse sequence of the sequence displayed in panel (A). In the sequence in panel (A), the edited nucleotide is a C and in the reverse sequence in panel (B), the edited nucleotide is a G. C.) Sequence analysis of Dd2 clones shows that although the mutant D SNP is not edited in every clone, the silent mutation in the gRNA site is edited in all Dd2-*mcp*1 clones. Clone Dd2-D2 was used as the silent-edited wildtype line for all drug assays. Primers used to screen the *mcp*-SNP transfectants are listed in Table 4.3.

4.3.3 Drug susceptibility profiles of the edited exonuclease and mitochondrial carrier protein SNPs in Dd2-edited parasite lines

4.3.3.1 The *exo*-E415G SNP does not alter parasite susceptibility to common antimalarial drugs

The transgenic *exo*-E415G mutant and wildtype (silent *exo*-E415E) parasites were tested in 72-hour survival assays to compare susceptibility to piperazine (PPQ) and several other antimalarial drugs: chloroquine (CQ), dihydroartemisinin (DHA), mefloquine (MQ), and lumefantrine (LUM). MQ, LUM, and CQ were selected based on their structural similarity to piperazine, as they are quinolone drugs, and DHA, MQ, and LUM are all currently recommended antimalarial drugs in ACT regimens. The dose response curves for all five

antimalarial drugs showed that the *exo-E415G* mutant SNP had little to no effect on parasite susceptibility to the five drugs compared to the wildtype control (Figure 4.8). This was further supported by the IC₅₀ values for each drug condition (Figure 4.8F).

4.3.3.2 The *mcp-N252D* SNP does not alter parasite susceptibility to common antimalarial drugs

The transgenic *mcp-N252D* mutant and wildtype (silent *mcp-N252N*) parasites were also tested in 72-hour survival assays to compare susceptibility to the same drugs as described for the *exo*-SNP lines: PPQ, CQ, DHA, MQ, and LUM. The dose response curves for all five antimalarial drugs showed that the *mcp-N252D* mutant SNP had little to no effect on parasite susceptibility to the five drugs compared to the wildtype control (**Figure 4.9**). This was further supported by the IC₅₀ values for each drug condition (**Figure 4.9F**).

4.3.3.3 The *exo-E415G* and *mcp-N252D* SNPs do not alter parasite survival in piperazine survival assays

I further assessed the phenotype of the transgenic *exo-E415G* and *mcp-N252D* parasites in piperazine survival assays (PSAs). After 48 hour exposure to piperazine and then a further incubation period of 24 hours (as described in **section 2.6.3**), little to no differences were again observed between the edited *exo-415* and *mcp-252* SNP edited parasite lines (**Figure 4.10**).

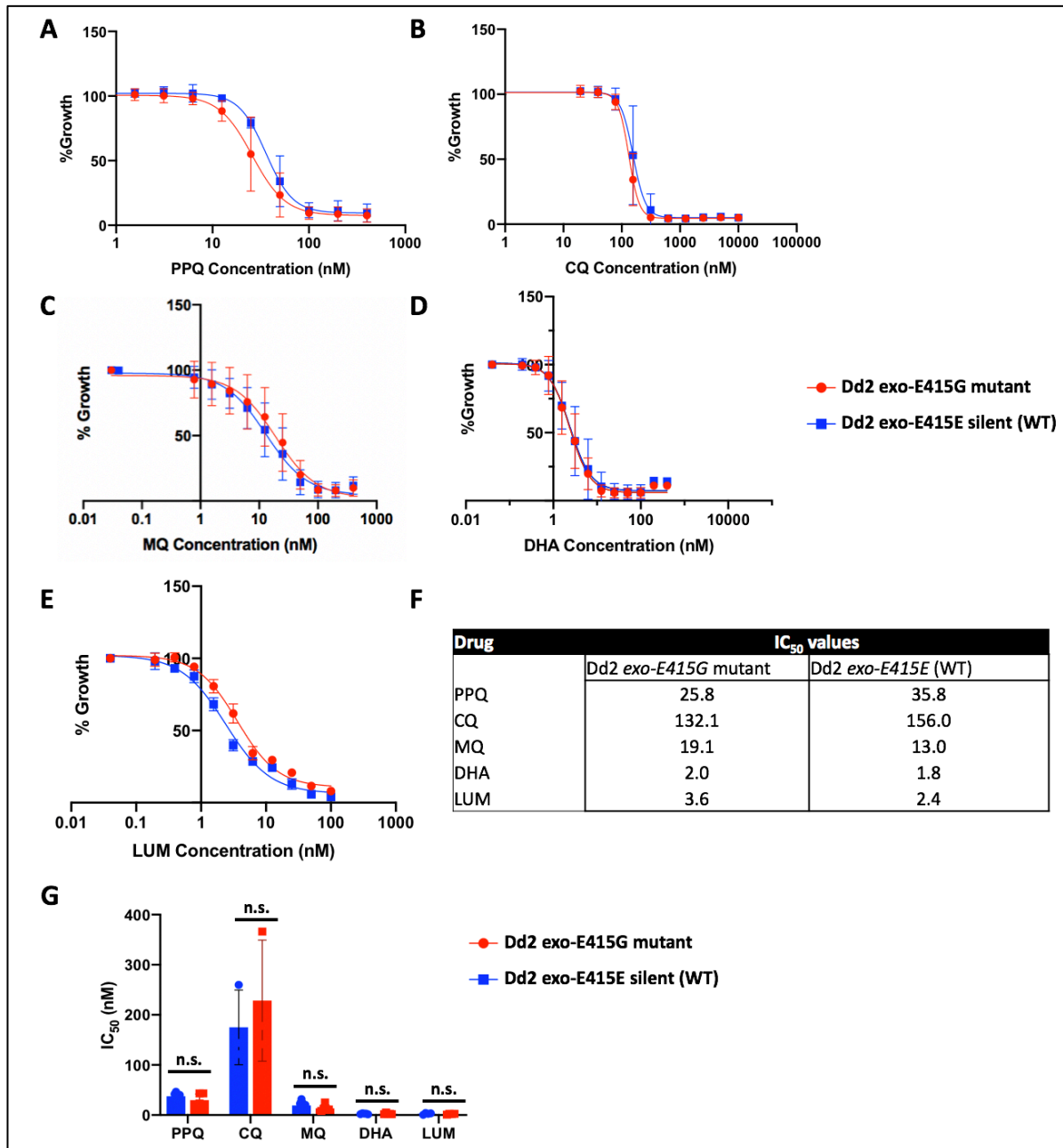


Figure 4. 8. The *exo-E415G* SNP has no effect on IC₅₀ values or susceptibility to PPQ and other commonly used antimalarial drugs. A.-E.) Dose-response curves for Dd2 edited parasites containing the mutant *exo-E415G* SNP (red) or the wildtype *exo-E415E* control (blue) exposed to: piperazine (PPQ) (A), chloroquine (CQ) (B), mefloquine (MQ) (C), dihydroartemisinin (DHA) (D), and lumefantrine (LUM) (E). Error bars represent SD (n=3 biological replicates). **F.)** Table showing the average IC₅₀ values for the mutant and wildtype (WT) *exo-415* SNP transgenic Dd2 lines calculated using GraphPad Prism Version 8.0.2. **G.)** Mean IC₅₀ values ± SD for each drug (PPQ, CQ, MQ, DHA, LUM) tested on the *exo-E415G* SNP (red) and the wildtype *exo-E415E* control (blue) lines. Significance was determined using Mann-Whitney U tests comparing the mutant and silent edited lines. n.s. indicates not significant (p>0.05). No significant differences were observed between the WT and mutant SNP edited lines for any of the drug treatments.

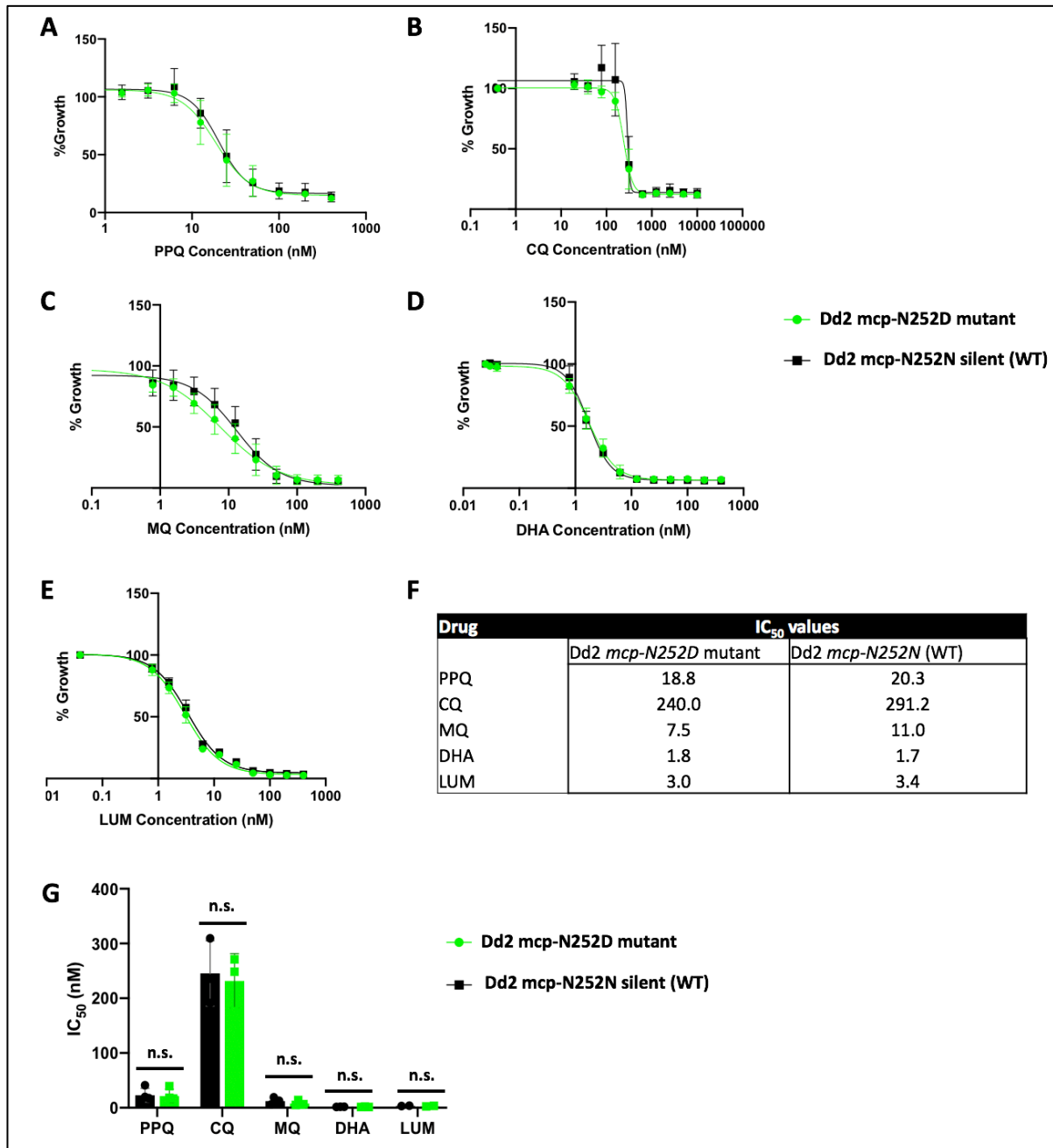


Figure 4. 9. The *mcp-N252D* SNP has no effect on IC₅₀ values or susceptibility to PPQ and other commonly used antimalarial drugs. A.-E.) Dose-response curves for Dd2 edited parasites containing the mutant *mcp-N252D* SNP (green) or the wildtype *mcp-N252N* control (black) exposed to: piperavaquine (PPQ) (A), chloroquine (CQ) (B), mefloquine (MQ) (C), dihydroartemisinin (DHA) (D), and lumefantrine (LUM) (E). Error bars represent SD (n=3 biological replicates). **F.)** Table showing the average IC₅₀ values for the mutant and wildtype (WT) *mcp-252* SNP transgenic Dd2 lines calculated using GraphPad Prism Version 8.0.2. **G.)** Mean IC₅₀ values ± SD for each drug (PPQ, CQ, MQ, DHA, LUM) tested on the *mcp-N252D* SNP (green) and the wildtype *mcp-N252N* control (black) lines. Significance was determined using Mann-Whitney U tests comparing the mutant and silent edited lines. n.s. indicates not significant (p>0.05). No significant differences were observed between the WT and mutant SNP edited lines for any of the drug treatments.

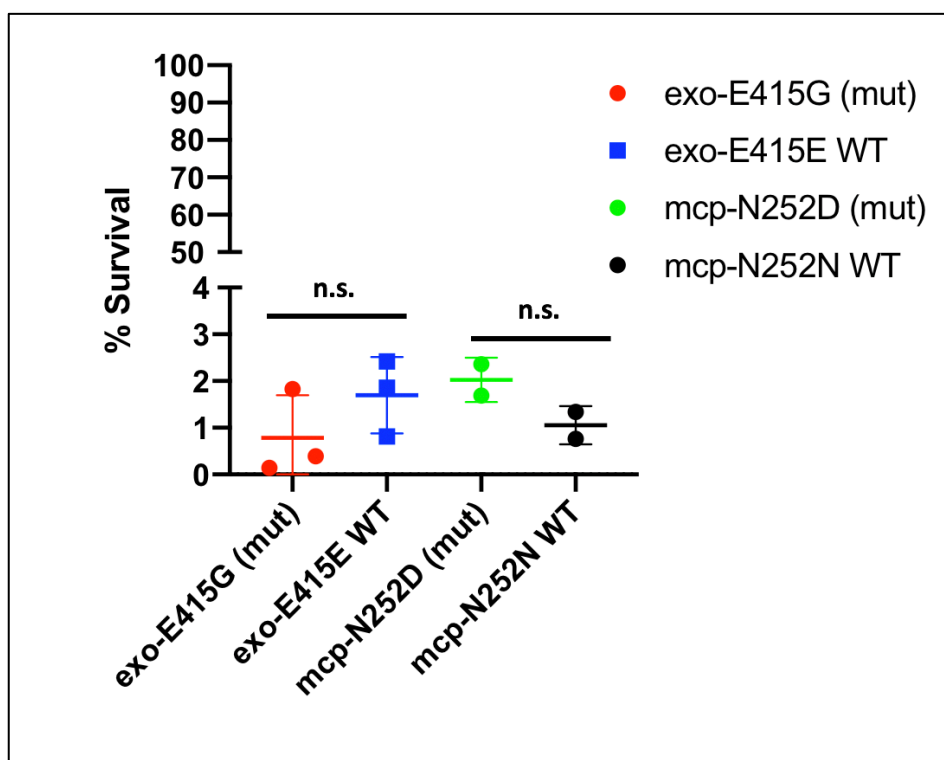


Figure 4. 10. The Dd2 transgenic *exo-E415G* and *mcp-N252D* edited SNPs have no effect on parasite survival to PPQ in piperazine survival assays (PSAs). PSAs comparing parasite susceptibility to piperazine. Parasites were exposed to 200 nM PPQ for 48 hours and measured at 72 hours. Error bars represent SD (for *exo*, n=3 biological replicates; for *mcp*, n=2). Significance was determined using Mann-Whitney U tests comparing PSA values for the mutant and silent edited lines for each SNP, *exo-415* and *mcp-252*. n.s. indicates not significant ($p > 0.05$).

4.4 Discussion and future work

The studies by Amato *et al.* and Witkowski *et al.* (2017) were the first reports to independently identify molecular markers of piperazine resistance that associated with DHA-PPQ failures in patients and decreased PPQ susceptibility *in vitro* (Amato *et al.*, 2017, Witkowski *et al.*, 2017). The top two nonsynonymous SNPs (**Table 4.1**) discovered by the GWAS performed by Amato *et al.*, but not reported by Witkowski *et al.*, were in a putative exonuclease protein, PF3D7_13625000, and a mitochondrial carrier protein, PF3D7_1368700 (Amato *et al.*, 2017). These findings laid the groundwork for this thesis, which aimed to characterize the potential functional roles of the *exo-E415G* and *mcp-N252D* SNPs in piperazine resistance. In order to investigate the molecular mechanisms of piperazine resistance and to validate these two molecular markers of resistance, the study began with the initial questions: do these genes play a causal or compensatory role, if any, in the piperazine resistance phenotype? Could these genes play a role in resistance to other antimalarial drugs?

This study used parasites generated by CRISPR-Cas9 gene editing to elucidate phenotypic effects of the *exo-E415G* and *mcp-N252D* SNPs in response to piperazine pressure. One of the main objectives was to insert the wildtype and mutant SNPs into both piperazine-resistant (PPQ-R) and PPQ-sensitive (PPQ-S) isolates to examine if reverting PPQ-R parasites to the wildtype SNP and changing the PPQ-S to the mutant SNP would alter susceptibility of the isolates to piperazine. Though over a hundred transfections of culture-adapted lines from various Cambodian field sites were attempted for both the *exo*- and *mcp*-SNPs (**Tables 4.4-4.5**), only five *exo-415* SNP transfectants from three different isolates recrudescenced; but sequencing showed that none of the desired editing events occurred (**Table 4.4, Figure 4.5**). For the *mcp-252* transfections, one transfectant recrudescenced, but sequencing showed only a silent mutation present in the donor region of the gRNA and no change in the desired SNP (**Table 4.2, Figure 4.6**). Though the gRNA selected for the *mcp-252* editing plasmid was close to the *mcp-252* SNP (87 bp downstream) and contained all features of a suitable gRNA candidate with no predicted off-target sites (**Table 4.2**), it is possible that it was too far from the region of the SNP to be edited. It should also be noted that the genomic sequences of the field isolates were compared to the reference sequences of Dd2 from which the gRNA sequences were designed to ensure there were no additional SNPs in the field isolates that may have interfered with the editing processes for both the *exo* and *mcp* genes. Transformation of the Dd2 strain, however, proved successful with both *exo*- and *mcp*-SNPs, raising the intriguing question of other possible differences that might account for the editing successes with Dd2 but not with the more recently lab-adapted Cambodian lines.

Transfections in *P. falciparum* asexual stage parasites are notorious for their low efficiency (de Koning-Ward et al., 2000, Carvalho and Menard, 2005). Prior notable studies have shown that transfections in the rodent malaria parasite, *P. berghei* are much higher than *P. falciparum*, with efficiency rates of 10^{-2} to 10^{-3} (Janse et al., 2006) compared to 10^{-6} to 10^{-9} in *P. falciparum*. Further studies in *P. knowlesi* have demonstrated even higher success rates, reporting 30-40% transfection efficiency (Moon et al., 2013). Due to these known transfection obstacles in *P. falciparum*, this study attempted to increase chances of transfection success in field isolates by favoring pre-loaded RBC transfection methods, which are shown to be ~5-180 fold more efficient than direct parasite electroporation methods (Hasenkamp et al., 2012). Additionally, about half of field isolate transfections were supplemented with parasite-conditioned media (**Tables 4.4-4.5**) to try to reduce parasite stress and promote favorable growth conditions. Several transfectants cultured with conditioned media, did recrudescence to parasitemias greater than 1%, (**Tables 4.4-4.5**) however,

as seen in the parasite transfection efficiency Tables 4.4-4.5, these additional procedures did not produce edited parasites. Further comparisons of transfection efficiency with conditioned media and without are therefore necessary to determine if the supplemented media has any effect on transfection success. Furthermore, parasite-conditioned media is widely used to promote conversion of asexual stage parasites to gametocytes (Williams, 1999), based on the findings from Carter and Miller (Carter and Miller, 1979) which showed that the environmental culture conditions affect gametocytogenesis. Since field isolates already have a higher proportion of gametocytes and greater likelihood of parasites to commit to sexual stages than lab reference strains, it is possible that rather than promoting parasite growth, the conditioned media used in the field isolate transfections maintained stress in cultures that were already stressed, post-electroporation. However, conditioned media was only used for 28% of the *exo* transfections and 18% of the *mcp* (Tables 4.4-4.5) field isolate transfections, so this would not explain why the other transfections did not recrudesce. Continued optimization of transfection efficiency in *P. falciparum* in general, and especially in lab-adapted field isolates, is required.

Successful editing of the lab strain, Dd2, with the single-plasmid system for both the *exo* and *mcp* SNPs was achieved (Figures 4.- 4). This indicates that the single-plasmid systems for the *exo*- and *mcp*- were able to produce the desired edits in *P. falciparum*. Since the two-plasmid editing system for the *exo*-SNP was not attempted in Dd2, it is unclear if the low editing success was due to the plasmids or the low transfection efficiency in the field isolates. However, this cannot explain why the single-plasmid system for both the *exo* and *mcp* SNPs worked in Dd2 but not in the field isolates. As mentioned, the Dd2-*exo*-415 mutant and silent edited (wildtype) parasites were obtained from Dr. Carrasquilla and no data on transfection efficiency are available for those lines. However, for the Dd2-*mcp*-252 mutant and silent parasites, two out of two total Dd2 transfections (100% transfection efficiency) recrudesced with one of the transfections (50% editing success) carrying the desired *N252D* mutation. For the silent editing plasmid, *mcp*-*N252N*, 0 of 2 transfections recrudesced and further transfections of this plasmid in Dd2 were not performed because field isolate transfections were prioritized. As mentioned in section 4.3.2, one of the clones, Clone D2, transfected with the mutant *mcp*-*N252D* plasmid did not contain the mutant SNP and remained wildtype (*N252*) but did contain the edit of the silent mutation that was in the *mcp*-252 editing donor plasmid in the gRNA region (Table 4.2; Figure 4.7). Since this indicates that clone D2 was edited, it was used as a silent editing control for the wildtype *N252N* SNP in all phenotypic assays.

Analysis of the drug susceptibility profile of the Dd2 transgenic parasites revealed that neither the *exo-E415G* nor *mcp-N252D* SNPs altered susceptibility to PPQ based on IC₅₀ survival assays and PSAs (**Figures 4.8-4.10**). My findings indicate that the mutations observed in the exonuclease and mitochondrial carrier protein are not the primary genetic determinants of PPQ resistance, suggesting, in line with other studies, that mutations elsewhere in the *P. falciparum* genome are responsible for resistance. The Dd2-edited *exo-415* and *mcp-252* lines also showed no difference in susceptibility to other quinolone drugs, CQ and MQ, and additional antimalarial drugs, DHA and LUM in 72 hour IC₅₀ survival assays (**Figures 4.8-4.9**). Based on these results, this study further indicates that the *exo-E415G* and *mcp-N252D* SNPs do have a causal role in resistance to several commonly used antimalarial drugs. It remains possible that the SNPs may affect parasite fitness. Drug resistance mutations are often accompanied by fitness costs (Rosenthal, 2013), so the *exo-E415G* and *mcp-N252D* SNPs could serve in these roles. Further studies would be required to compare fitness between the wildtype and mutant SNP transgenic parasites.

It must be noted that Dd2 is lab strain that has been cultivated for many years *in vitro* and although it comes from a Southeast Asian lineage, it is genetically different from the more recently adapted field isolates from Cambodia used in this study (Mackinnon et al., 2009). The phenotypic effects of SNPs observed in the *exo* and *mcp* genes could be dependent on the genetic background of the Cambodian isolates. Therefore continued efforts to edit field isolates with both the *exo*- and *mcp*-SNP plasmids is necessary. If editing of the Cambodian isolates continues to prove difficult, it could also be interesting to further genetically modify Dd2-transgenic parasites obtained by this study. For example, the *PM2-2A-PM3* episomal plasmid generated by this study in Chapter 3 could be transfected into the Dd2 parasites to evaluate if increase *PM2-3* copy numbers are needed for the *exo*- and or *mcp*- SNPs to have a measurable phenotypic effect. Or perhaps a mutant *kelch13* background is necessary for the effects to be observed.

Although Amato *et al.* performed stringent tests in their GWAS analysis to ensure the signal on chromosome 13 was not due to confounding or batch effects (Amato et al., 2017), it is still possible that the *exo-E415G* and *mcp-N252D* SNPs are associated with piperazine resistance because of linkage to other functional mutations in the Cambodian isolates, such as the *PM2-3* CNV (Amato et al., 2017). Further studies of Cambodian parasites may shed light on these and other possibilities.

Though outside the scope of this study, it would be very interesting to examine the functions of both the exonuclease and mitochondrial carrier proteins in *P. falciparum*.

Aside from preliminary transcriptomics and sequencing work, it is also important to acknowledge that no studies have confirmed or refuted whether the putative exonuclease protein and mitochondrial carrier protein in *P. falciparum* are actually homologous to the proteins to which they share sequence similarity. Therefore, future studies into the exonuclease and mitochondrial carrier protein, including localization, should help to evaluate their potential roles in drug resistance and in the biology of the malaria parasite.

In order to fully understand the causes of drug resistance and inform drug development and treatment strategies, it is necessary to complement genetic studies with functional assays. This study has enabled the possibility of examining whether genetic changes observed in patient isolates can also be investigated and observed in *in vitro* settings. This study successfully edited a molecular marker of piperaquine resistance, an *mcp-N252D* SNP, in Dd2 parasites. Additionally, this work assessed the phenotypes of the resistance-associated *exo-E415G* and *mcp-N252D* SNPs in response to piperaquine and other commonly used antimalarial drugs. The results from this study of transgenic Dd2 parasites indicates that the *exo-E415G* and *mcp-N252D* SNPs are not genetic determinants of piperaquine resistance and likely do not play a significant role in piperaquine resistance. Though future work is needed, this study provides novel insight into the roles of these genetic markers in piperaquine resistance and suggests additional genetic determinants remain to be uncovered.

Chapter 5: Discovery of molecular markers of piperazine resistance by *in vitro* drug-pressure of a hypermutator *Plasmodium falciparum* line

5.1 Declaration of work

The hypermutator parasite line used in this study was generated by Dr. Krittikorn Kumpornsini. All bioinformatic analyses were performed by Dr. Frank Schwach. Both Drs. Kumpornsini and Schwach are cited in the relevant sections of this chapter for their invaluable contributions to this work.

5.1.1 Significance and purpose of study

The current frontline treatments for *Plasmodium falciparum* malaria, artemisinin combination therapies (ACTs), are designed to increase treatment efficacy and prevent the development of drug resistance. These therapies combine potent, short-acting artemisinin derivatives with partner drugs with different mechanisms of action and longer half-lives to clear any remaining parasites. However, the development of artemisinin resistance in Southeast Asia has placed increased pressure on partner drugs. Continued treatment failures of the ACT dihydroartemisinin-piperazine (DHA-PPQ) have prompted multiple reverse genetic studies that have identified several candidate molecular markers of piperazine resistance (Amato et al., 2017, Witkowski et al., 2017, Hamilton et al., 2019). Further studies, including work in this doctoral thesis, have performed functional analyses to assess the phenotypic relevance of these genetic markers (Ross et al., 2018a, Loesbanluechai et al., 2019, Bopp et al., 2018) (Chapters 3-4). With limited drug alternatives available, it is imperative to have diverse approaches to study the malaria parasite biology and the molecular mechanisms through which drug resistance can emerge. In comparison to reverse genetics approaches, forward genetics methods in *P. falciparum* have been largely hindered due to the slow spontaneous mutation rates of *P. falciparum* (Bopp et al., 2013). Recent elegant studies in the rodent malaria parasite, *Plasmodium berghei* (Honma et al., 2014, Honma et al., 2016) have designed “hypermutator” parasites that are able to rapidly develop mutations which can be used to obtain resistant phenotypes for drug-pressured lines. Studies by Kumpornsini *et al.* (*in preparation*) used this work as a model to generate a hypermutator parasite line in *P. falciparum*. The purpose of this thesis study was to use a forward genetics approach to elucidate genetic determinants of piperazine resistance. I was able to select for

piperazine-resistant parasites in a feasible experimental timespan by utilizing a hypermutator *P. falciparum* parasite line. Through whole genome sequencing (WGS) analyses of these piperazine-resistant parasites this study identifies several gene candidates that have already been reported to play a role in piperazine resistance and resistance to other antimalarial compounds. This study also identifies multiple new gene candidates that may play a causal role in piperazine resistance. These include mutations never identified before in transmembrane domain (TMD) 10 of PfCRT, a domain that is thought to have a critical role in the homo-dimer structure of the trans-membrane channel (Summers et al., 2012). By combining forward genetics tools with the reverse genetics approaches detailed in the previous chapters, this study aims to combine functional and genomic approaches to further drive the quest to uncover the mechanism of piperazine resistance.

5.1.2 Introduction

The ability of the malaria parasite, *Plasmodium falciparum*, to develop resistance to nearly all approved treatments remains a severe challenge for disease prevention and elimination efforts. For almost two decades, ACTs have been the standard treatment for *P. falciparum* malaria because they maximize therapeutic efficacy by combining two drugs with different mechanisms of action while also reducing the potential for resistance to develop (World Health Organization, 2018, World Health Organization, 2015, World Health Organization, 2001, Arrow, 2004). The ACT dihydroartemisinin-piperazine (DHA-PPQ) combines the fast-acting artemisinin compound with a half-life of approximately one hour with a partner drug with a half-life of around 23 days (Hoglund et al., 2017, Batty et al., 1998). The inherent contradiction in this combination is that the mismatched pharmacokinetic profiles of the drugs means that any recrudescence or new infection is exposed to suboptimal levels of piperazine monotherapy. With the failures of two different ACTs in Southeast Asia, artesunate-mefloquine (AS-MQ) in 2004 (Denis et al., 2006) and most recently, DHA-PPQ (Leang et al., 2013, Saunders et al., 2014, Spring et al., 2015, Amaratunga et al., 2016), the question is no longer *if* resistance will develop, but *when* and *how*? To inform and improve treatment methods, it is essential to understand the mechanisms through which malaria parasites can respond and adapt to the diverse pressures in their environment.

Similar to many other diseases, antimalarial drug resistance can be caused by a plethora of complex environmental and molecular interactions. Thus, multiple approaches may be needed to identify mechanisms of resistance. Both reverse (target-based) and forward genetics (phenotype-based) approaches are useful methods for identifying mechanisms of

resistance (Mitchison, 1994, Schenone et al., 2013). In previous chapters of this thesis (Chapters 3-4), I made use of genetic information provided by genome wide association studies (GWAS) to examine potential genetic determinants of piperazine resistance. In addition to these reverse genetics approaches, I also employed a forward genetics approach to complement these studies in *P. falciparum* by using a “hypermulator” parasite line to select for a piperazine-resistant phenotype. Combining forward and reverse genetics has the potential to provide insight into both the mechanism of resistance and the potential mechanism of action of piperazine.

In many eukaryotic organisms, forward genetics studies are hindered by the slow occurrence of spontaneous mutations. The estimated mutation rate of human cells is 1×10^{-8} per base pair (bp) per generation (Genomes Project et al., 2010). In *P. falciparum*, the mutation rate of asexual *in vitro* cultures is approximately $1.0\text{--}9.7 \times 10^{-9}$ per bp per generation (Bopp et al., 2013). For the parasite, this slow mutation rate is desirable as it reduces the potential for deleterious mutations that may negatively affect survival. However, for the researcher performing *in vitro* drug-selection experiments—where obtaining a phenotype of interest is the primary goal—the ability to generate mutations rapidly under selective pressure is advantageous.

The low spontaneous mutation rate in eukaryotes is largely due to the proofreading functions of the high fidelity replication and repair enzymes, DNA polymerases (Shevelev and Hübscher, 2002). There are four nuclear DNA polymerases in eukaryotic cells, α , β , δ , and ϵ . Both DNA polymerases δ and ϵ have 3'→5' exonuclease activity and these proofreading domains are highly conserved amongst prokaryotes and eukaryotes (Hubscher et al., 2002, Shevelev and Hübscher, 2002, Swan et al., 2009). Studies in yeast have shown that disruption of the exonuclease domain of polymerase δ has a strong effect on proofreading ability, causing a “hypermulator” phenotype characterized by at least a 10-100-fold increase in spontaneous mutations (Morrison and Sugino, 1994, Fortune et al., 2005). Interestingly, the proofreading domain of polymerase δ is also highly conserved in *Plasmodium* (Ridley et al., 1991). Recent studies in *P. berghei*, the causative agent of rodent malaria, have mutated two highly conserved residues in polymerase δ (D311A and E313A) to obtain a hypermutator parasite line with 86 to 90-fold higher mutation rates than the wildtype parasite (Honma et al., 2014, Honma et al., 2016).

Modelled after the novel studies with hypermutator *P. berghei* parasite lines, Kumpornsin *et al.* (*in preparation*) generated a mutant *P. falciparum* polymerase δ parasite line by mutating the two conserved residues (D308A and E310A) in the exonuclease domain reported to affect proofreading ability (Morrison and Sugino, 1994, Honma *et al.*, 2014, Honma *et al.*, 2016). Based on the similarity of the *P. falciparum* polymerase δ to its homologues in other eukaryotes (Ridley *et al.*, 1991), it is hypothesized that mutations of the conserved exonuclease domain will also have a profound effect on mutation rates, as was observed in *P. berghei* (Honma *et al.*, 2014, Honma *et al.*, 2016). Though measurements of the spontaneous mutation rate of the *P. falciparum* polymerase δ mutant compared to the wildtype parasite are in progress, preliminary data by Dr. Kumpornsin indicated that the mutant parasite line had a higher propensity to yield drug resistance, observations that stimulated my use of this line for drug-pressure experiments with piperazine.

Hypermutator lines can rapidly generate mutations under various environmental conditions, which can be useful in determining if certain conditions produce measurable phenotypes. The use of hypermutator lines enable forward genetics approaches to gather data in more feasible experimental timelines. Such lines also enable the possibility of examining whether genetic changes observed *in vivo* can be observed in *in vitro* settings. As discussed in the previous chapters, multiple independent studies (Agrawal *et al.*, 2017, Ross *et al.*, 2018a, van der Pluijm *et al.*, 2019, Hamilton *et al.*, 2019) have reported a role for mutations in the chloroquine resistance transporter (PfCRT) in the piperazine-resistant phenotype. Early *in vitro* drug-pressure studies by Eastman *et al.* found a SNP in *pfert* (encoding a C101F mutation) and an amplification event upstream of the *pfmdr1* gene on chromosome 5 as well as a deamplification of *pfmdr1* (also on chromosome 5) to be associated with piperazine-resistant parasites (Eastman *et al.*, 2011), though the same mutations have not been identified in field isolates, to date. Recent studies by Agrawal *et al.*, van der Pluijm *et al.*, and Hamilton *et al.* have identified *pfert* SNPs in patient isolates from Southeast Asia that strongly associated with DHA-PPQ failures in patients (Hamilton *et al.*, 2019, van der Pluijm *et al.*, 2019, Agrawal *et al.*, 2017). Ross *et al.* have used genetic editing techniques to demonstrate a role for several of these *pfert* SNPs in piperazine resistance *in vitro* (Ross *et al.*, 2018a). The ability to gather multiple lines of evidence for the role of various genes in resistant phenotypes greatly aids in surveillance of drug resistance. Such extensive confirmation also influences current treatment regimens and the development of new drugs.

As mentioned in Chapter 4, piperazine treatment failures and reduced PPQ susceptibility *in vitro* was observed in patient isolates lacking the more recently reported mutations, for example the recently prevalent PfCRT T93S mutation (Hamilton et al., 2019) (**Chapter 2, Table 2.1**) (Amaratunga et al., 2016, Amato et al., 2017, Witkowski et al., 2017). However, most of the isolates used by our study from 2012-2013 (Amaratunga et al., 2016) contained at least one PfCRT mutation (H97Y, M343L, and one isolate with no PfCRT mutations) (**Chapter 2, Table 2.1**), though the GWAS study by Amato *et al.* did not find an association of mutations in PfCRT and the piperazine resistant phenotype (Amato et al., 2017, Witkowski et al., 2017). The role of the other molecular markers of piperazine resistance (*PM2-3* copy number amplification) in the resistant-phenotype also remains unclear. It is therefore necessary to combine forward and reverse genetic approaches to gain further insight into the mechanisms of piperazine resistance.

The aim of this study was to elucidate the genetic determinants of piperazine resistance by using *in vitro* drug selection methods. I used a hypermutator *P. falciparum* line to select for piperazine-resistant parasites. Through WGS analyses of these piperazine-resistant parasites, this study identifies nonsynonymous SNPs in multiple gene candidates that have not been previously linked to piperazine resistance, including the *formate-nitrite transporter (FNT)*, the *multidrug resistance protein 1 (pfmdr1)*, and the *multidrug resistance-associated protein 2 (mrp2)*. The study also identifies mutations in PfCRT, including an A366T mutation that is present in a piperazine-resistant isolate used in this study (**Chapter 2, Table 2.1**) (Amaratunga et al., 2016). Additionally, this study identifies a *pfprt* SNP resulting in a point mutation at position G353C, which is at the same position as a G353V mutation observed in field isolates and reported to demonstrate a piperazine-resistant phenotype *in vitro* (Ross et al., 2018a). By combining these forward genetics tools with the reverse genetics approaches detailed in the previous chapters, this study aims to combine functional and genomic studies to investigate the mechanism of piperazine resistance.

5.1.3 Objectives

Use a hypermutator *P. falciparum* line to select for a piperazine-resistant phenotype *in vitro*

- (1) Examine the phenotype of piperazine-pressured parasites in comparison to the parental hypermutator line
- (2) Use whole genome sequencing analysis to compare genetic differences between the parental hypermutator parasites and the piperazine-pressured parasites
 - a. Identify potential gene candidates that may play a role in the piperazine-resistant phenotype

5.2 Materials and methods

5.2.1 Hypermutator parasites: *P. falciparum* Dd2-polymerase δ mutants

All experiments were performed with a hypermutator *P. falciparum* line generated by Dr. Krittikorn Kumpornsin (*manuscript in preparation*). The generation of this hypermutator was based on studies in *Saccharomyces cerevisiae* (yeast) and *P. berghei* that have shown that mutation of the conserved aspartic acid (D) and glutamic acid (E) residues in the exonuclease domain of DNA polymerase δ (**Figure 5.1**) significantly disrupts proofreading ability, causing a hypermutator phenotype (Morrison and Sugino, 1994, Fortune et al., 2005, Ridley et al., 1991, Honma et al., 2014, Honma et al., 2016).

To obtain a hypermutator *P. falciparum* line, Kumpornsin *et al.* used CRISPR-Cas9 gene editing to mutate two conserved residues (D308A and E310A, **Figure 5.1**) in the proofreading domain of DNA polymerase δ (PF3D7_1017000) in the laboratory line, Dd2. After confirmation of the desired edits in a clonal population of Dd2-polymerase δ D308A-E310A parasites, Dr. Kumpornsin kindly provided the line to be used in this study, referred to as “Dd2-hypermutator.” Any description of a “parental line” in this study refers to the Dd2-hypermutator without drug-pressure.

<i>S. cerevisiae</i> pol δ	DIHYENIEPMALENEYQKIPKLRILSFDIECIKLDGKGFPEAKTDPIIQISSILYLQGD
<i>H. sapiens</i> pol δ	DISYEHVEPITLENEYQQIPKLRILSFDIECIKLDGKGFPEAKNDPIIQISSILYFQGE
<i>P. berghei</i> pol δ	SINYRNLIHPAEGDWSHTAPLRIMSFDIECAGRIG-VFPEPEYDPVIQIANVVSIIAGAK
<i>P. falciparum</i> pol δ	DVLWSDVVSHPPEGPWQRIAPLRVLSFDIECAGRKG-IFPEPERDPVIQICSLGLRWGEP

Figure 5. 1. Alignment of the DNA polymerase δ amino acid sequence highlighting the conserved residues in the 3' \rightarrow 5' exonuclease domain. Yeast (*S. cerevisiae*), human (*H. sapiens*), *P. berghei*, and *P. falciparum* all share the aspartic acid (D) and glutamic acid (E) residues in DNA polymerase δ exonuclease active site. The alignment was generated using the CLUSTAL O (1.2.4) multiple sequence alignment tool.

5.2.2 Experimental design for selection of piperazine resistant Dd2-hypermutator parasites: IC₅₀ assays and selection procedures

Previous work has selected for PPQ-resistant parasites using a clone of the Dd2 parasite line (Eastman et al., 2011). Eastman *et al.* pressured the parasite with 47 nM and 140 nM PPQ based on the peak plasma levels of PPQ following a low-fat or high-fat meal, respectively (Ashley et al., 2004, Sim et al., 2005, Tarning et al., 2005). They observed that no parasites recrudesced after 80 days of continuous 140 nM PPQ-pressure but did observe one flask (of triplicate flasks) that recrudesced under 47 nM PPQ-pressure at day 54 (Eastman et al., 2011).

Based on this prior work, my study was designed to avoid a PPQ concentration that would be too high to obtain recrudescing parasites. In order to tip the drug-selection balance in our favor, I decided to base the PPQ concentration on the standard PPQ IC₅₀ values of the Dd2-hypermutator line. IC₅₀ assays were performed as previously described (**Chapter 2, section 2.6.2**) to assess the PPQ half maximal inhibitory concentration for the Dd2-hypermutator line in comparison to the Dd2 wildtype line (Dd2). Significance was determined using Mann-Whitney U tests comparing the IC₅₀ values of wildtype Dd2 with the Dd2-hypermutator line and no significant differences were observed between the IC₅₀ values for the two lines ($p > 0.05$) (**Figure 5.2**). As seen in Figure 5.2B, the PPQ IC₅₀ values were between 16 nM-20 nM for both Dd2 and the Dd2-hypermutator line. I therefore decided to start PPQ-pressure at various increments of the lower of the two IC₅₀ values, 16 nM.

Two PPQ-selection attempts were made during the course of this study. The initial selection attempt was set up with 5×10^8 parasites per flask (in triplicate) at $3 \times \text{PPQ IC}_{50}$ (48 nM) in 50 mL. As mentioned above, since spontaneous mutation rates of *P. falciparum* are quite low, in the second selection attempt, we increased the number of parasites to 1×10^9 parasites per flask (in triplicate) at $2 \times \text{PPQ IC}_{50}$ (32 nM) in 100 mL. Parasites were grown as described previously (**Chapter 2, section 2.1.1**) in complete media (CM) supplemented with the desired concentration of PPQ at 3% hematocrit. During the first week of drug pressure, media was changed daily and fresh red blood cells (RBCs) were added as needed for cutting the flasks, since the parasitemia was quite high and piperazine clearance of parasites took several days. Parasitemia was maintained below 8% and preferably maintained around 3% until the parasites cleared (no parasites were observed by smear). Continuous drug pressure was maintained for at least 21 days unless otherwise noted.

To account for spontaneous mutations that could be generated in the PPQ-pressured lines that are the result of the hypermutator line and not PPQ-pressure, the Dd2-hypermutator line was maintained in continuous culture for the duration of all experiments and was never pressured with PPQ.

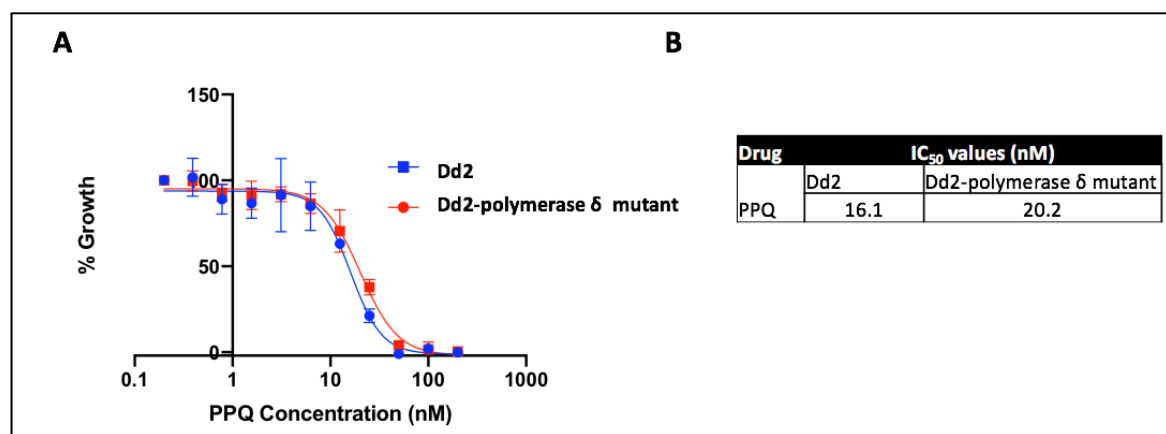


Figure 5. 2. Determination of PPQ concentration to use for selection of PPQ-resistant Dd2-polymerase δ mutant parasites. A.) Dose-response curve for Dd2 (wildtype) and Dd2-polymerase δ mutant (Dd2-hypermutator) parasites after exposure to PPQ. Error bars represent SD (n=2 biological replicates). B.) Table showing the average IC₅₀ values for Dd2 and the Dd2-polymerase δ mutant calculated using GraphPad Prism Version 8.0.2. Significance was determined using Mann-Whitney U tests comparing the IC₅₀ values of wildtype Dd2 with the Dd2-hypermutator line. No significant differences were observed between the two lines (p>0.05).

5.2.3 Preparation of PPQ-pressured parasites for whole genome sequencing analysis: cloning and genomic DNA extraction

Any parasites that recrudescenced following PPQ-selection were expanded and the lines were cloned by limiting dilution (Chapter 2, section 2.4). Genomic DNA (gDNA) from the bulk cultures and the clones was extracted as described previously and all lines were cryopreserved (Chapter 2, sections 2.1.3 and 2.5). The control parental parasite line (Dd2-hypermutator parent) at the start of the experiment was also sent for sequencing analysis. The DNA concentration and quality were measured using a Qubit 2.0 Fluorometer (Thermo Fisher Scientific). DNA from the bulk PPQ-pressured cultures, clones, and the two parental controls was sent for WGS analysis at the Wellcome Sanger Institute.

5.2.4 Whole genome sequencing analysis

All WGS analyses were performed by Dr. Frank Schwach. Illumina sequence reads were mapped to *P. falciparum* genome version 3.1 using the Burrows-Wheeler Aligner (Li and Durbin, 2009) and the Picard toolkit. Local realignment by assembly as well as variant data calibration on known variants was performed using the GATK toolkit, following published

recommendations for the GATK toolkit (DePristo et al., 2011), and the MalariaGEN project (<https://www.malariagen.net/>). Known *P. falciparum* variants were obtained from the MalariaGEN project. The SNPeff software (Cingolani et al., 2012) was used to annotate functional implications of variants and variants that did not have an impact on a protein product were filtered out. In addition, a minimum coverage of 30 reads was required for the final set of high quality variants. Variants that were observed in the parental line were disregarded in order to exclude differences between Dd2 and the 3D7 reference genome. Variants in known highly variable gene families were also excluded from further analysis. The Dd2-hypermulator parental line was used as the reference sequence for identifying variations present in the PPQ-pressured parasite lines.

5.3 Results

5.3.1 Selection of piperazine-resistant Dd2-hypermulator parasites

Two PPQ-selection experiments using the Dd2-hypermulator line were performed as outlined in **Figures 5.3-5.4**. The first selection experiment (Exp. 1, Figure 5.3), was started at 3xPPQ IC_{50} and when parasitemia was still high on day 4, the parasites were brought up to 60 nM PPQ and then to 90 nM on day 6. By day 9 the parasites were starting to clear and no parasites were visible by microscopy on day 12. On day 22, the cultures were split and one set of flasks was maintained at 90 nM PPQ and the other set was taken off drug. No recrudescence was observed after 65 days (**Figure 5.3**). We hypothesized that the lack of recrudescence was due to the number of starting parasites or the rapid ramping up of the concentration of PPQ.

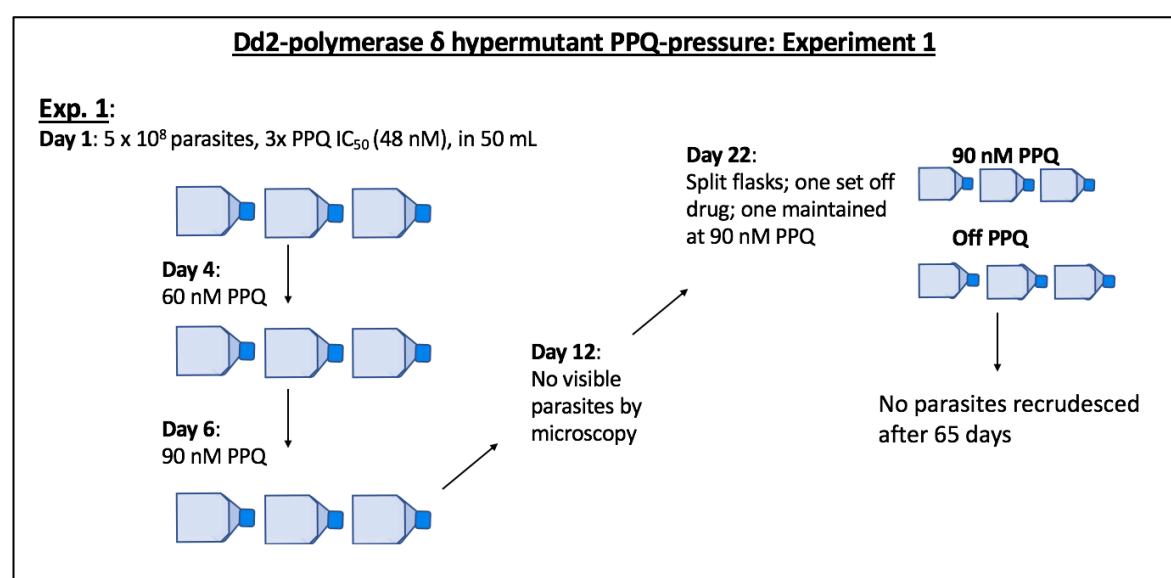


Figure 5.3. Initial attempt (experiment 1) for selection of piperazine (PPQ)-resistant Dd2-hypermulator parasite lines. No recrudescence was observed.

The second selection experiment (Exp. 2) was set up with a higher number of parasites and a lower concentration of PPQ (**Figure 5.4**). As seen in Figure 5.4, the parasites were still surviving well on 2xPPQ IC₅₀ on day 6, so the flasks were split to 50 mL and one set was maintained at 2xPPQ IC₅₀ and the other set was brought up to 3xPPQ IC₅₀ (called 3x-day 6). On day 9, the 2xPPQ IC₅₀ parasites were still not clearing, so they were also brought to 3xPPQ IC₅₀ (called 3x-day 9). On day 13, there were no visible parasites by microscopy in any flasks but flasks were maintained and checked every 2-3 days for parasites (**Figure 5.4**). On day 21, recrudescence was observed in a 3x-day 9 flask (PPQ#1) (**Figure 5.4**). On day ~24 all flasks were taken off drug pressure including the PPQ#1 flask for which recrudescence was already observed. On day ~45, another 3x-day 9 flask (PPQ#2) recrudescenced and on day 59 a 3x-day 6 flask recrudescenced. The remaining flasks with no observed parasites were maintained in CM until days 65-70, but no parasites were observed.

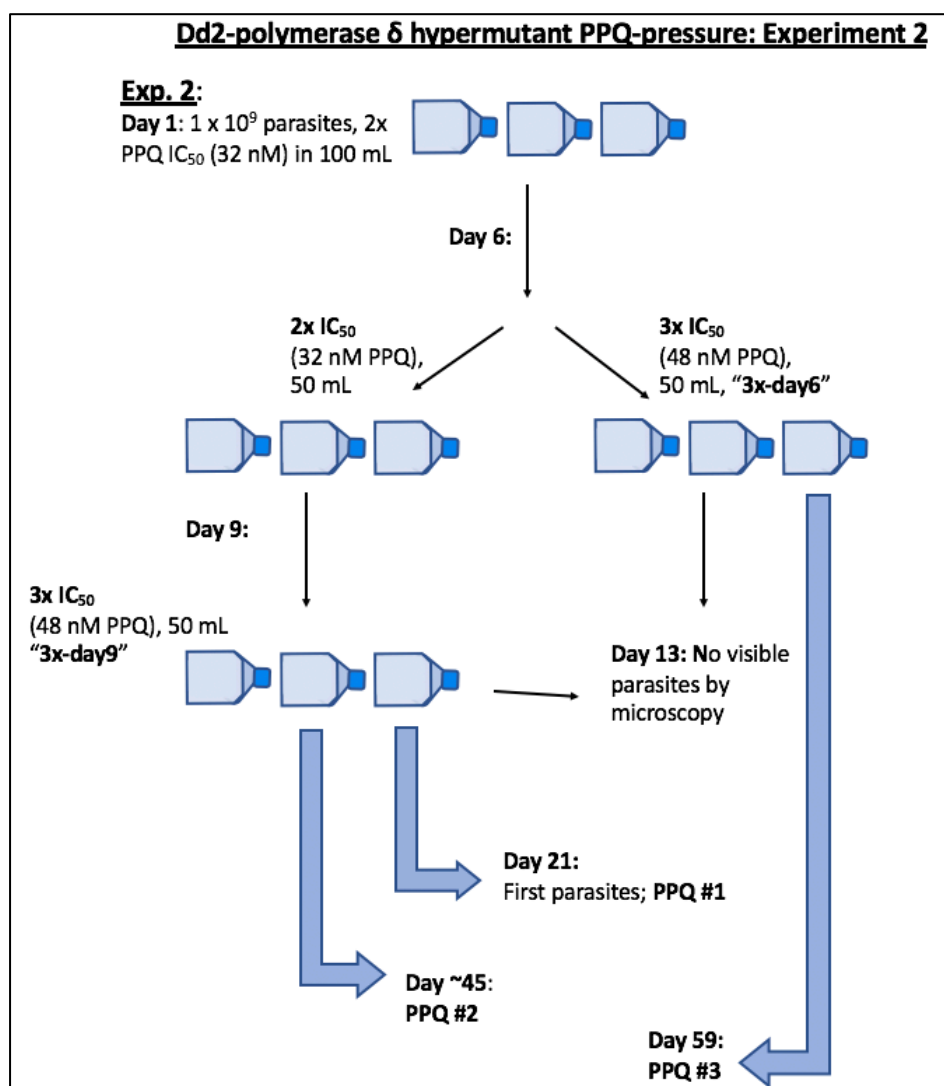


Figure 5. 4. Second attempt (experiment 2) for selection of piperazine (PPQ)-resistant Dd2-hypermutator parasite lines.

Of the three parasite lines that came up on PPQ-pressure (PPQ#1-3), PPQ#1 and PPQ#3 were cloned and a total of 23 clones from PPQ-pressured parasites and all three bulk cultures (PPQ#1-3), were whole genome sequenced. As described by Honma *et al.*, the clones were also referred to as “PPQ-pressured lines” since presumably, these isogenic clones would also acquire mutations while in continuous culture (Honma *et al.*, 2014).

5.3.2 Phenotypic characterization of the piperazine-pressured Dd2-polymerase δ mutant parasites

5.3.2.1 IC₅₀ survival assays of piperazine-pressured Dd2-polymerase δ mutant parasites

In order to determine if there were any phenotypic differences between the PPQ-pressured lines (PPQ#1-#3) and the parental Dd2-hypermutator line, IC₅₀ assays were performed to compare PPQ susceptibility (**Figure 5.5**). The dose-response curves show differences in susceptibility of the PPQ-pressured lines compared to the parental line. The parental line has an IC₅₀ similar to the value observed at the beginning of the drug-selection experiments, as expected (**Figure 5.2**) while the PPQ-pressured lines have IC₅₀ values that are shifted approximately 6-fold or more (**Figure 5.5**). Due to time constraints, IC₅₀ assays were only performed on the bulk PPQ-pressured lines, but analysis of the cloned PPQ-pressured lines is forthcoming. Also due to time constraints, determination of the optimal concentration of PPQ that results in complete death of the PPQ-pressured lines (PPQ#1-#3) is ongoing, therefore the dose response curves shown in Figure 5.5 are only intended to show the relative differences between the parental hypermutator line and the PPQ-pressured lines. As can be seen in Figure 5.5, without complete killing of the PPQ-pressured lines, the dose-response curves do not plateau and thus accurate IC₅₀ values cannot be calculated and statistical significance cannot be determined.

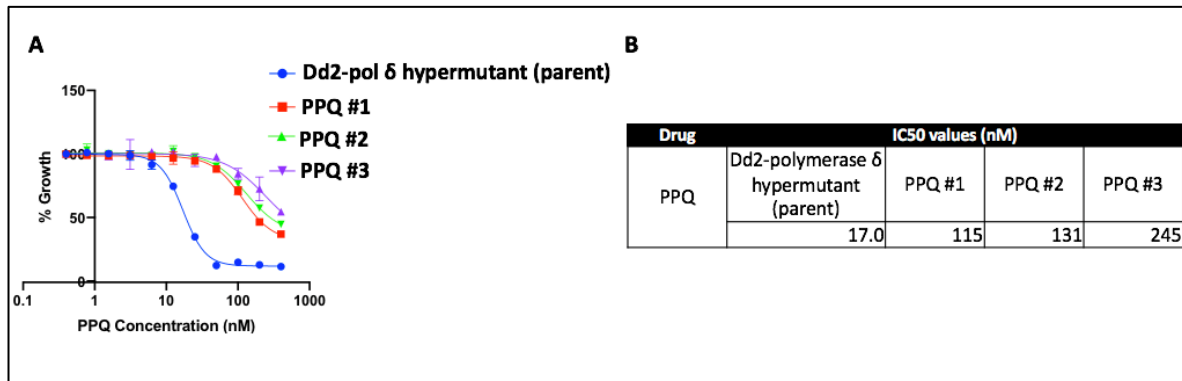


Figure 5.5. Comparison of PPQ susceptibility between the parental Dd2-polymerase δ hypermutator parasite and the PPQ-pressured lines. A.) Estimated dose-response curve of Dd2-hypermutator (parent) line and PPQ-pressured lines (PPQ#1-#3). Error bars represent SD (n=2 technical replicates). B.) Table showing the estimated average IC₅₀ values for Dd2-hypermutator parent and PPQ-pressured lines. IC₅₀ values were calculated using GraphPad Prism Version 8.0.2. The concentration of PPQ was not high enough to result in complete killing of the three PPQ-pressured lines (PPQ#1-#3) so the dose-response curves and IC₅₀ values shown here are only estimates used to show the relative differences between the lines. Accurate IC₅₀ values and statistical significance cannot be determined from the data currently available, but continued assays with the PPQ-pressured lines are in progress.

5.3.2.2 Morphological differences between the PPQ-pressured parasites and the parental hypermutator line

Further analysis of the PPQ-pressured lines also indicated a starkly different morphological phenotype. Figure 5.6 shows Giemsa stained microscopy slides (**Chapter 2, section 2.1.2**) for both the Dd2-hypermutator parent and a PPQ-pressured line (**Figure 5.6**). As seen in the parental images, the parasites have the normal morphology of a mixed, asynchronous culture, with early ring stages and later trophozoites and schizonts (**Figure 5.6A**). In the PPQ-pressured parasite line, the late stage trophozoites and schizonts strikingly show large, distended digestive vacuoles (**Figure 5.6B**). This phenotype is noted in the presence and absence of drug, and the pictures included in Figure 5.6 are from a parasite that had been off PPQ-pressure for at least two weeks. The parasites have not been synchronized and ongoing work to compare stage-specific images for the parental and PPQ-pressured parasites is necessary.

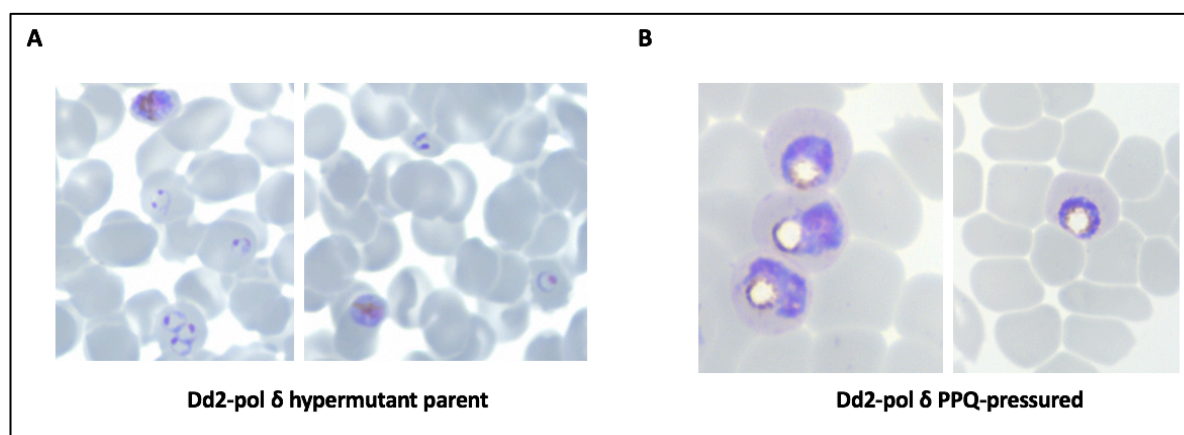


Figure 5. 6. Morphological difference between the parental Dd2-polymerase δ hypermutator parasite and a PPQ-pressured line. A.) Dd2-polymerase δ hypermutator parental line B.) PPQ-pressured line showing large digestive vacuoles in the absence of PPQ. Slides were viewed with a light microscope using a 100X immersion field. Pictures were taken with a Leica EC4 Digital Microscope camera.

5.3.3 Whole genome sequencing analysis and genetic characterization of the PPQ-pressured Dd2-hypermutator parasites

Whole genome sequencing was performed for the parental Dd2-hypermutator line, the bulk PPQ-pressured cultures (**Figure 5.4**), and the cloned PPQ-pressured lines (23 total clones) obtained from bulk cultures “PPQ#1” and “PPQ#3” Two controls were sequenced (section 5.2.3), the Dd2-hypermutator line at the beginning for the experiment and the same parent line at the end of the experiment at the time the clones and bulk cultures were collected for sequencing. Preliminary alignments mapped the PPQ-pressured lines to the parental line at the start of the experiment as the reference.

Initial analyses of the 23 PPQ-pressured lines in comparison to the Dd2-hypermutator parent have revealed multiple non-synonymous SNPs in genes previously reported to play a role in antimalarial drug resistance (**Table 5.1**): *pfprt*, *pfmdr1*, *formate-nitrite transporter (FNT)*, and *multidrug resistance-associated protein 2* (**Figure 5.7**). The study identified *pfprt* SNPs that resulted in the following mutations: N295T, G353C, A366T, D377Y, and T380S. The PfCRT A366 and G353 residues have been previously implicated in piperaquine resistance (Ross et al., 2018a). SNPs were found in other genes but due to time constraints, the study was specifically interested in looking at SNPs in transporter genes. Additionally, the SNPs listed in Table 5.1 are not present in each clone and vary by line. Future work dissecting out the various mutations in each clone and analyzing the full read-out of SNPs from the WGS analysis is necessary and planned.

The WGS analyses also identified a PfMDR1-N86I mutation in the PPQ-pressured lines (**Figure 5.7**) which is the same residue of a N86Y natural variant previously reported by multiple studies to affect susceptibility to various antimalarial drugs (Veiga et al., 2016b, Sisowath et al., 2005, Duraisingh and Cowman, 2005). SNPs were also discovered in two genes coding for transporters that have been implicated in antimalarial drug resistance, *FNT-A224T* and *FNT-S17F* (Hapuarachchi et al., 2017) and *pfmrp2-D1028Y* (Cowell et al., 2018, Veiga et al., 2014).

Table 5. 1 Non-synonymous SNPs discovered in the PPQ-pressured Dd2-hypermutator lines

Chr.	Position	Gene ID	Gene Description	Alteration	Reported in field
7	405005	PF3D7_0709000	chloroquine resistance transporter (CRT)	p.Asn295Thr	N
7	405590	PF3D7_0709000	chloroquine resistance transporter (CRT)	p.Gly353Cys	Y, G353V
7	405629	PF3D7_0709000	chloroquine resistance transporter (CRT)	p.Ala366Thr	Y
7	405855	PF3D7_0709000	chloroquine resistance transporter (CRT)	p.Asp377Tyr	N
7	405864	PF3D7_0709000	chloroquine resistance transporter (CRT)	p.Thr380Ser	N
5	958146	PF3D7_0523000	multidrug resistance protein 1 (<i>mdr1</i>)	p.Asn86Ile	Y, N86Y
3	669939	PF3D7_0316600	formate nitrite transporter	p.Ala224Thr	N
3	670824	PF3D7_0316600	formate nitrite transporter	p.Ser17Phe	N
12	1196133	PF3D7_1229100	multidrug resistance-associated protein 2 (<i>mrp2</i>)	p.Asp1028Tyr	N

Table 5.1. Representation of several non-synonymous SNPs discovered in the PPQ-pressured Dd2-hypermutator lines. The SNPs in each of the 23 clones were different and this table shows a general subset of genes with the SNPs discovered in each. Further analysis of the WGS data is planned for assessing and comparing the genotypes of all clones. All genes included in this table have previously been reported to be involved in antimalarial drug resistance. Each gene is listed with: chromosome number (chr.); nucleotide position (position); gene ID and description; type and the amino acid difference (alteration). The last column includes if the SNP has been previously reported in field isolates.

5.4 Discussion and future work

The purpose of this study was to employ a forward genetics approach to gain further insight into the mechanisms of piperazine resistance. This study has utilized a *P. falciparum* hypermutator line to select for a piperazine-resistant phenotype *in vitro*. I was able to generate piperazine-resistant parasites in a feasible experimental timespan with the first parasites demonstrating a PPQ-resistant phenotype by day 21 (**Figure 5.4**). The other two PPQ-resistant lines recrudesced within two months from the start of the experiment (days 40 and 59, **Figure 5.4**). The use of the hypermutator *P. falciparum* polymerase δ mutant parasite appears to have greatly reduced the amount of time it took to generate parasites with a resistant phenotype. Though studies directly comparing the unedited Dd2 line (wildtype polymerase δ) (**Figure 5.2**) to the Dd2-hypermutator under PPQ pressure would be able to confirm if this suggestion holds in practice. Previous work by Eastman *et al.* pressured a Dd2 clone (Dd2 1pa) and 7G8 isolate and obtained only one recrudescing Dd2 flask (of triplicate

flasks) after 54 days (Eastman et al., 2011). This is likely due to the slow spontaneous mutation rate of *P. falciparum* (Bopp et al., 2013) and the concentration of PPQ used. As shown through the studies of Oduola *et al.* in obtaining a mefloquine resistant *P. falciparum* line, generation of a mutant parasite can require continuous culture for over a year, depending on the drug and protocol used (Oduola et al., 1988a). Drug selection experiments often entail a bit of trial and error, based on what seems most appropriate for the particular parasite line and the specific drug of interest. However, hypermutator lines may tip the balance in favor of selecting a resistant-phenotype.

WGS of the piperazine-resistant lines obtained through these experiments have identified nonsynonymous SNPs in gene candidates that have previously been reported to play a role in antimalarial drug resistance (**Table 5.1**), including SNPs in the transporter genes: *chloroquine resistance transporter* (*pfcr* PF3D7_0709000), *multidrug resistance protein 1* (*pfmdr1*, PF3D7_0523000), *formate-nitrite transporter* (*FNT*, PF3D7_0316600), and *multidrug resistance-associated protein 2* (*mrp2*, PF3D7_1229100).

Recent studies have discovered SNPs in *pfcr* that confer piperazine resistance *in vitro* and strongly associate with DHA-PPQ failures in patients (Agrawal et al., 2017, Ross et al., 2018a, van der Pluijm et al., 2019, Hamilton et al., 2019). Interestingly, two of the *pfcr* SNPs discovered by this study, *pfcr* A366T and *pfcr* G353C have been observed in field isolates and associated with PPQ-resistance *in vitro*. The *pfcr* A366T SNP discovered in our WGS analysis is present in a PPQ-resistant field isolate from Pursat, Cambodia that has been used by this study (**Chapter 2, Table 2.1**) and has been reported in Cambodian isolates by other studies (Ross et al., 2018a). The *pfcr* G353C SNP from our study results in a point mutation at residue G353, which has previously been found to harbor a G353V mutation in field isolates. Gene editing of the *pfcr* G353V SNP was shown to confer PPQ-resistance *in vitro* (Ross et al., 2018a). Further work by Ross *et al.* edited several other *pfcr* SNPs present in field isolates, H97Y, F145I, M343L, into Dd2 parasites and found that the gene-edited *pfcr* mutations alone could confer PPQ-resistance *in vitro*, though a fitness cost was noted for all SNPs but the PfCRT M343L variant (Ross et al., 2018a).

As noted in **Figure 5.6**, I observed large, distended digestive vacuoles in the PPQ-pressured lines. Ross *et al.* also reported this phenotype in their *pfcr*-edited parasites, including the G353V edited line (Ross et al., 2018a). Previous studies by Pulcini *et al.* have also reported distended vacuoles in parasites pressured with amantadine or blasticidin that contain PfCRT

C101F or L272F mutations (Pulcini *et al.*, 2015). Intriguingly, the light microscopy images published by Ross *et al.* and Pulcini *et al.* display striking similarity to the images shown in this thesis, pictured in Figure 5.6 (Pulcini *et al.*, 2015, Ross *et al.*, 2018a). It is acknowledged that the parasites shown in Figure 5.6 are asynchronous and the parental and PPQ-resistant lines are not showing the same stage parasites. However, this preliminary indication of a distinct morphological phenotype will guide future work to demonstrate this vacuole phenotype in synchronised parasites. Intriguingly, Ross *et al.* noted that the distended vacuole phenotype was not observed in the field isolates containing these mutations (Ross *et al.*, 2018a). PPQ-resistant isolates may have compensated for this effect through other genetic pathways and that the observed phenotype may be dependent on the genetic background of the parasite. Future work planned by this study will examine if the *plasmepsin 2-3* (*PM2-3*) copy number amplification has any effect on the PPQ-pressured hypermutator lines. We plan to transfect the PPQ-pressured lines with the *PM2-3* overexpression plasmid generated in Chapter 3. This will enable us to see if the *PM2-3* amplification, and consequent increase in abundance of these vacuolar proteases, has any effect on the PPQ-resistant phenotype and will enable us to see if this amplification may reduce the distended vacuole phenotype.

The other transporters with nonsynonymous SNPs discovered by this study: PfMDR, FNT, and PfMRP2 have all previously been shown to play a role in antimalarial drug resistance and could have a role in PPQ-resistance. The N86Y mutation in PfMDR1 is associated with chloroquine and amodiaquine resistance, but reported to increase susceptibility to lumefantrine, mefloquine, and dihydroartemisinin and moderately to piperazine (Veiga *et al.*, 2016b). Recent drug-pressure experiments used to screen new compounds with antiplasmodial activity found mutations in the lactate/H⁺ transporter, FNT, specifically FNT-G107S, to reduce susceptibility to two of these novel, structurally similar compounds, MMV007839 and MMV000972 (Hapuarachchi *et al.*, 2017). The study by Hapuarachchi *et al.* (Hapuarachchi *et al.*, 2017) is the first to report compounds that target FNT, which is located on the parasite cell membrane and functions to remove lactic acid, a waste product from glycolysis (Marchetti *et al.*, 2015, Wu *et al.*, 2015). Prior work assessing *mrp2* polymorphisms reported a high frequency of SNPs within the gene as well as microindels, which have been shown to reduce parasite susceptibility to quinolone drugs (Veiga *et al.*, 2014, Mok *et al.*, 2014). It is not clear what role these SNPs could play in PPQ resistance, but ability of *pfmdr1* and *pfmrp2* SNPs to have an effect on quinolone drugs could also apply to piperazine.

The intriguing results of selection pressure experiments and WGS analyses have clearly demonstrated the need for future studies. Continued examination of the WGS data is in progress. Importantly, analysis of copy number variations (CNVs) is ongoing. It will be interesting to learn if any CNVs are present in the *PM2-3* genes or any other genes. In most PPQ-resistant isolates observed to date, the parasites have a single copy of *pfmdr1* (Amato et al., 2017, Witkowski et al., 2017). The Dd2 wildtype parasite has two copies of *pfmdr1* and presumably the Dd2 polymerase δ hypermutator line used by this study has two copies of *pfmdr1*. However, it is important to check if the increased copy numbers have been retained in the PPQ-resistant lines. Studies have hypothesized that PfMDR1 could facilitate PPQ entry into the digestive vacuole (Witkowski et al., 2017), which could explain the presence of single *pfmdr1* copy numbers in field isolates from regions where DHA-PPQ has been used. Other *in vitro* studies have reported a deamplification on chromosome 5 in the region with *pfmdr1* after exposure to piperazine (Eastman et al., 2011), thus there is precedence for further investigation of the role of PfMDR1 in the PPQ-resistant phenotype.

Further analysis of the WGS data will also enable us to determine which gene candidates to target for further study. CRISPR-Cas9 gene editing can be used to evaluate non-synonymous SNPs. It is also necessary to compare growth rates of the parasites and conduct competition assays to determine if there are any fitness effects of the acquired mutations. Cross-resistance studies with different antimalarial drugs will also provide vital insight into the characterization of the PPQ-pressured lines.

It is imperative to discuss that there are inherent caveats when using hypermutator parasites. The ability of the parasite to develop mutations more rapidly would mean that drug-pressured parasites may also rapidly acquire mutations that have nothing to do with the drug pressure. This can add unnecessary noise when trying to filter out the genetic variants that play a causal role in the resistant phenotype. It is also possible that while cloning to obtain isogenic parasites, the parasites are acquiring further mutations that have nothing to do with the resistance observed. However, this can be controlled for by performing multiple independent drug-pressure selections. I have performed the piperazine pressure experiments in triplicate flasks, thus hits obtained across multiple independent selections adds confidence that the variations identified are due to drug pressure, and are not random. We have also included a control in this study to assuage, not solve, these limitations. The parental-hypermutator line from the start of the experiment was maintained in culture for as long as the other drug-pressured lines, but it was never pressured with PPQ. In addition to sequencing the parental

line at the start of the experiment, we also sequenced this parental line that was grown for the duration of the experiment. As mentioned, due to time constraints, we have only been able to compare the PPQ-pressured lines to the parental line from the start of the experiment. However, comparison of both parental lines parental-start and parental-end will be performed. When we are able to compare the parental-start and parental-end genotypes, we will be able to estimate the spontaneous mutation rate of the parasite and this information can provide insight into how long the PPQ-pressured cloned lines can be kept in continuous culture. We will also be able to compare mutation rates of the PPQ-pressured lines. This information can inform future drug selection experiments.

Through the use of a hypermutator line, this study provides new insights into the PPQ-resistant phenotype while providing experimental evidence that supports previously reported markers of PPQ resistance. This study may also serve as a proof-of-concept study for using a hypermutator line for *in vitro* drug selection. Though the data presented here is preliminary, it offers promising potential and clearly defines future work needed in the quest to understand the mechanisms of PPQ resistance.

Chapter 6: What's next on the resistance front? Conclusions, reflections, and future work

Antimalarial drug resistance came into the spotlight with the first documented reports of chloroquine resistance in the 1950s-1960s (Harinasuta et al., 1965, Payne, 1987, Talisuna et al., 2004, Wellems and Plowe, 2001). Since then, drug resistance has impeded malaria prevention, control, and elimination efforts—with no signs of leaving the world's stage. The most recent development in this saga is the failure of dihydroartemisinin-piperaquine (DHA-PPQ), one of the recommended frontline artemisinin combination therapies (ACT) in Southeast Asia (SEA) (World Health Organization, 2018, van der Pluijm et al., 2019). By combining functional molecular approaches with genomic studies, this dissertation has investigated the molecular mechanisms of piperaquine resistance in *P. falciparum* malaria.

In the first research chapter (chapter 3), I developed copy number assays for detecting the *plasmepsin 2* and *plasmepsin 3* (*PM2-3*) copy number variation (CNV) associated with piperaquine resistance using genomic DNA from patient blood or dried blood spots. In order to mitigate the effects and spread of resistance, it is critical to have reliable methods to detect and monitor potential markers of drug resistance. The breakpoint PCR and qPCR-based assays for determining *PM2-3* copy numbers developed by this study are robust, timely, and cost-efficient methods for measuring *PM2-3* copy numbers in comparison to whole genome sequencing (WGS) techniques. Additionally, these assays can be performed in the field as long as a PCR or qPCR machine is present. While these new methods have many advantages, one limitation of the breakpoint PCR is its specificity for the predominant *PM2-3* breakpoints observed in Cambodian isolates (Amaratunga et al., 2016, Amato et al., 2017). The PCR primers designed for the breakpoint PCR would fail if used for samples with a different breakpoint. Cambodian isolates that have different *PM2-3* breakpoints were reported by Witkowski *et al.* (Witkowski et al., 2017) in 2017, and additional analyses of the *PM2-3* breakpoints in isolates from 2017 to the present day have not been reported. Further research will be needed to determine if the *PM2-3* breakpoints have remained the same or if they have changed in the last couple of years.

It will also be important to track if the *PM2-3* amplification will persist in parasite populations as the frontline treatments shift from DHA-PPQ to artesunate-mefloquine (AS-MQ) and triple ACTs (TACTs) with DHA-PPQ plus MQ. The majority of contemporary

isolates from SEA have increased *PM2-3* copies and single *pfmdr1* copies. As AS-MQ is reintroduced in the region, samples should be monitored for increased copies of *pfmdr1*, which was found to be the molecular marker and mechanism of mefloquine resistance (Price et al., 2004). Since piperazine is a component of the TACT regimens, it is possible that the *PM2-3* amplification will remain or that copies may increase, as seen in samples from 2014-2015 with increased numbers of parasites with three *PM2-3* copies (Jacob et al., 2019). However, the role this amplification plays in antimalarial drug resistance remains to be elucidated. Will the *pfmdr1* copy number increase in the presence of increased *PM2-3* copy numbers? Can parasites become resistant to both mefloquine and piperazine? Would the genetic alterations cause fitness disadvantages? Continued surveillance of parasite populations for these markers is necessary and it is crucial to understand what functional role (if any) the *PM2-3* CNV serves.

Although the *PM2-3* CNV is currently used as a molecular marker of piperazine resistance, it has yet to be validated as a causal genetic determinant of piperazine resistance. Initial attempts by this dissertation to evaluate the functional role of the *PM2-3* amplification have found that overexpression of *PM2*-only in a Cambodian field isolate (163-KH3-005) does not have any effect on parasite response to piperazine. This study has also synthesized a *PM2-2A-PM3* plasmid for overexpressing stoichiometric amounts of *PM2-3* in transfected parasites to more closely mimic the CNV observed in the field. I confirmed that the plasmid was transfected into a piperazine-sensitive field isolate from Cambodia (163-KH3-005) and Dd2, but similar to the *PM2*-only transfectants, it is necessary to confirm RNA and protein levels in the transfected parasites compared to the parent lines. Once overexpression of both the *PM2* and *PM3* genes is confirmed, I will be able to perform functional assays on these parasites to determine if the *PM2-3* amplification results in increased survival or plays a more compensatory role in fitness. One drawback of this study was the lack of successful transfections in isolates with *kelch13* (K13) mutations, one of the molecular markers of artemisinin resistance. Piperazine resistance emerged on an artemisinin-tolerant background, thus it is hypothesized that the presence of K13 mutations or other molecular markers of artemisinin resistance and/or piperazine resistance (PfCRT mutations) may be needed for the *PM2-3* amplification to demonstrate its role in parasite survival. Future work will be able to use the *PM2-2A-PM3* plasmid generated by this study to transfect isolates with different genetic backgrounds to evaluate if the *PM2-3* amplification has an effect on piperazine susceptibility.

The importance of examining the role of the *PM2-3* amplification in piperazine resistance has been further demonstrated by recent studies by Leroy *et al.* (Leroy *et al.*, 2019) that have detected increased *PM2* copies in Burkina Faso and Uganda (>30% of samples in both countries) and in Mozambique and Gabon (12.5% and 11.3%, respectively). This was one of the first studies to report increased *PM2-3* copy numbers in Africa, but several earlier reports also reported low levels of increased *PM2* copy numbers in Mozambique (1.1% of isolates) (Gupta *et al.*, 2018) and Mali (10.8% of isolates) (Inoue *et al.*, 2018).

The discovery of increased *PM2* copy numbers in African countries suggests that this marker of piperazine resistance may be the same across endemic countries, which supports a functional role for the variation. In the context of chloroquine, resistance independently emerged due to mutations in PfCRT throughout malaria endemic areas where the drug was used. It is possible that the *PM2-3* CNV will be found in other regions where piperazine has been used as a partner drug. It is also possible that due to the different genetic backgrounds of parasites in South America, Africa, and other malaria endemic regions, mechanisms of piperazine resistance will involve different genetic pathways, if resistance occurs. The environment that *P. falciparum* evolves in is very different throughout endemic regions that have various climates, *Anopheles* species, other *Plasmodium* species, insecticides, antimalarial drug use/history, transmission rates, and many other conditions. With so many different factors it is possible that piperazine resistance may emerge differently in different areas. It is thus necessary to not only monitor for known markers of resistance, but to continue surveillance for other genetic markers of resistance throughout endemic regions.

In chapter 4, I evaluated the functional relevance of two additional candidate markers of piperazine resistance: a putative exonuclease protein SNP, PF3D7_1362500 (*exo-E415G*), and a putative mitochondrial carrier protein SNP, PF3D7_1368700 (*mcp-N252D*). Although these non-synonymous SNPs were identified in a GWAS by Amato *et al.* (Amato *et al.*, 2017) as the top signals associated with decreased piperazine susceptibility *in vivo*, this dissertation found no difference in the responses of wildtype and mutant transgenic Dd2 parasites responses to piperazine. This suggests the *exo-415* and *mcp-252* candidates are not causal determinants of piperazine resistance. As discussed for the *PM2-3* overexpression plasmids, it is necessary to examine if the *exo-E415G* and *mcp-N252D* SNPs have any effect in the presence of other molecular markers of piperazine resistance (PfCRT mutations or the *PM2-3* amplification) or markers of artemisinin resistance (K13).

Low transfection efficiency of field isolates in chapters 3 and 4 are limitations of these studies. Though multiple field isolates, different conditions, and different plasmids were tested, these variations did not have an effect on transfection efficiency. In future studies, it will be essential to survey more culture-adapted field isolates to test which isolates tolerate growth at very low parasitemia (as would be expected after transfection while on drug pressure and during cloning by limiting dilution). Another alternative would be to suppress conversion of asexual parasites to gametocytes by use of the lipid compound, lysophosphatidylcholine or LysoPC. Studies in *P. falciparum* have found that a reduction in LysoPC triggers an environmental cue that causes asexual parasites to differentiate to gametocytes (Brancucci et al., 2017). This pathway could be used as a method to increase transfection efficiency by supplementing transfected cultures with LysoPC to prevent unwanted conversion of the parasites to gametocytes during the stress of transfection. Such modifications will be tested in future transfection attempts.

In chapter 5, I used a hypermutator *P. falciparum* parasite line to generate piperazine-resistant parasites in a feasible experimental timeline of six months rather than years. The use of the hypermutator line allowed this dissertation to complement the reverse genetics studies in chapters 3 and 4 with a forward genetics approach. Rather than starting with candidate gene markers of resistance and performing functional studies to assess their potential role in resistance, I selected for a piperazine-resistant phenotype *in vitro*. Initial WGS analyses of the piperazine-pressured parasites identified mutations in PfCRT and PfMDR1, among others. As discussed, this is of particular relevance as mutations in PfCRT have been reported to confer piperazine resistance *in vitro* (Eastman et al., 2011, Ross et al., 2018a, Dhingra et al., 2017) and are increasingly prevalent in field isolates. The WGS analysis is ongoing and additional gene candidates and variations present in the piperazine-pressured parasites will be examined. It has not been determined if these parasites have any copy number variations, including the *PM2-3* CNV, but these parasites do not have mutations in the genes encoding the putative exonuclease (PF3D7_1362500) or mitochondrial carrier protein (PF3D7_1368700). Analysis of the WGS data will shape the course of continued studies with these parasite lines (competition assays, growth assays, gene-editing, and more).

Currently, DHA-PPQ treatment failures have been confined to SEA. If such treatment failures were to occur in African countries where malaria transmission is high, it would have devastating effects on the ability to cure malaria-infected patients. With only five recommended ACTs currently available (World Health Organization, 2018), it is crucial to

understand how drug resistance develops. Additionally, the partner drugs in use today are believed to have the same site of action in the digestive vacuole, so resistance to one drug could promote resistance to another. An understanding of the mechanism of resistance to antimalarial drugs will provide knowledge that can be used to prolong the lifespan of the limited drugs that are currently available. This should be prioritized, for the same drugs continued to be recycled and rotated in the face of treatment failures (AS-MQ to DHA-PPQ back to AS-MQ).

Advanced understanding of the mechanisms of drug resistance informs the development of new drugs. Recent studies have used knowledge of antimalarial drug resistance to select for new compounds that specifically select against known antimalarial drug resistance alleles (Lukens et al., 2014, Ross et al., 2018b). New antimalarial drugs are also being discovered through large high-throughput screens that select for compounds based on anti-*Plasmodial* properties and not on structural similarity to quinine or chloroquine, as done in the past (Fidock et al., 2004, Cowell et al., 2018). These studies also prioritize drugs that can target different stages of the parasite lifecycle (liver stage, sexual stage, and asexual stage), which will be the best way to fight malaria going forward. Drug discovery, development, and regulation takes time, however, several organizations in recent years have been created to discover and develop new antimalarial drugs. One example is the product development partnership (PDP), Medicines for Malaria Venture. Such organizations combine basic science, pharmaceutical industries, economic assets and more—multidisciplinary approaches—with the same purpose of discovering and producing new antimalarial drugs.

Before the World Summit on Malaria in April 2018, Bill Gates (who committed another \$1 billion dollars to the fight against malaria in 2018 through the Bill & Melinda Gates Foundation) said that there is no standing idle with malaria. “If we stand still, the insecticides we use stop working, the drugs stop working because the parasite itself evolves around that, so this is a game where you are either falling behind or getting ahead (BBC, 2018).” Malaria eradication is possible. Understanding how resistance develops is one facet of the problem that will aid in defeating the disease, and this doctoral dissertation has shed light on drug resistance to one commonly used antimalarial drug. In the battle against malaria, there must be new innovations from all sides. Basic science can provide much insight through understanding parasite and mosquito biology and through the development of new drugs and vaccines. In addition to this, there must be innovative solutions to the social, economic, environmental, and operational challenges that are present in malaria endemic regions.

Through these combined efforts, the slogan “eradication within a generation (Feachem et al., 2019)” could come to fruition. To stay in the game, the path to elimination and eradication must be holistic and it must be global.

References

- ABBOTT, A. 2001. Earliest malaria DNA found in Roman baby graveyard. *Nature*, 412, 847.
- ACHAN, J., TALISUNA, A. O., ERHART, A., YEKA, A., TIBENDERANA, J. K., BALIRAIN, F. N., ROSENTHAL, P. J. & D'ALESSANDRO, U. 2011. Quinine, an old anti-malarial drug in a modern world: role in the treatment of malaria. *Malaria Journal*, 10, 144.
- ACHAN, J., TIBENDERANA, J. K., KYABAYINZE, D., WABWIRE MANGEN, F., KAMYA, M. R., DORSEY, G., D'ALESSANDRO, U., ROSENTHAL, P. J. & TALISUNA, A. O. 2009. Effectiveness of quinine versus artemether-lumefantrine for treating uncomplicated falciparum malaria in Ugandan children: randomised trial. *BMJ*, 339, b2763.
- ADJALLEY, S. H., JOHNSTON, G. L., LI, T., EASTMAN, R. T., EKLAND, E. H., EAPPEN, A. G., RICHMAN, A., SIM, B. K., LEE, M. C., HOFFMAN, S. L. & FIDOCK, D. A. 2011. Quantitative assessment of Plasmodium falciparum sexual development reveals potent transmission-blocking activity by methylene blue. *Proc Natl Acad Sci U S A*, 108, E1214-23.
- AGRAWAL, S., MOSER, K. A., MORTON, L., CUMMINGS, M. P., PARIHAR, A., DWIVEDI, A., SHETTY, A. C., DRABEK, E. F., JACOB, C. G., HENRICH, P. P., PAROBK, C. M., JONGSAKUL, K., HUY, R., SPRING, M. D., LANTERI, C. A., CHAORATTANAKAWEE, S., LON, C., FUKUDA, M. M., SAUNDERS, D. L., FIDOCK, D. A., LIN, J. T., JULIANO, J. J., PLOWE, C. V., SILVA, J. C. & TAKALA-HARRISON, S. 2017. Association of a Novel Mutation in the Plasmodium falciparum Chloroquine Resistance Transporter With Decreased Piperaquine Sensitivity. *J Infect Dis*, 216, 468-476.
- ALONSO, P. L., BROWN, G., AREVALO-HERRERA, M., BINKA, F., CHITNIS, C., COLLINS, F., DOUMBO, O. K., GREENWOOD, B., HALL, B. F., LEVINE, M. M., MENDIS, K., NEWMAN, R. D., PLOWE, C. V., RODRIGUEZ, M. H., SINDEN, R., SLUTSKER, L. & TANNER, M. 2011. A research agenda to underpin malaria eradication. *PLoS Med*, 8, e1000406.
- AMARATUNGA, C., LIM, P., SRENG, S., MAO, M., SOPHA, C., SAM, B., DEK, D., ANSBRO, M. R., AMATO, R., MIOTTO, O., KWIAKOWSKI, D., TARNING, J., TULLO, G., FAY, M., ANDERSON, J. M., SEILA, S. & FAIRHURST, R. M. 2019. Artesunate-mefloquine effectively treats dihydroartemisinin-piperaquine-resistant Plasmodium falciparum malaria in Cambodia. *in preparation*.
- AMARATUNGA, C., LIM, P., SUON, S., SRENG, S., MAO, S., SOPHA, C., SAM, B., DEK, D., TRY, V., AMATO, R., BLESSBORN, D., SONG, L., TULLO, G. S., FAY, M. P., ANDERSON, J. M., TARNING, J. & FAIRHURST, R. M. 2016. Dihydroartemisinin-piperaquine resistance in Plasmodium falciparum malaria in Cambodia: a multisite prospective cohort study. *Lancet Infect Dis*, 16, 357-65.
- AMARATUNGA, C., NEAL, A. T. & FAIRHURST, R. M. 2014. Flow cytometry-based analysis of artemisinin-resistant Plasmodium falciparum in the ring-stage survival assay. *Antimicrob Agents Chemother*, 58, 4938-40.

- AMARATUNGA, C., SRENG, S., SUON, S., PHELPS, E. S., STEPNIEWSKA, K., LIM, P., ZHOU, C., MAO, S., ANDERSON, J. M., LINDEGARDH, N., JIANG, H., SONG, J., SU, X. Z., WHITE, N. J., DONDORP, A. M., ANDERSON, T. J., FAY, M. P., MU, J., DUONG, S. & FAIRHURST, R. M. 2012. Artemisinin-resistant *Plasmodium falciparum* in Pursat province, western Cambodia: a parasite clearance rate study. *Lancet Infect Dis*, 12, 851-8.
- AMATO, R., LIM, P., MIOTTO, O., AMARATUNGA, C., DEK, D., PEARSON, R. D., ALMAGRO-GARCIA, J., NEAL, A. T., SRENG, S., SUON, S., DRURY, E., JYOTHI, D., STALKER, J., KWIATKOWSKI, D. P. & FAIRHURST, R. M. 2017. Genetic markers associated with dihydroartemisinin-piperaquine failure in *Plasmodium falciparum* malaria in Cambodia: a genotype-phenotype association study. *Lancet Infect Dis*, 17, 164-173.
- AMATO, R., PEARSON, R. D., ALMAGRO-GARCIA, J., AMARATUNGA, C., LIM, P., SUON, S., SRENG, S., DRURY, E., STALKER, J., MIOTTO, O., FAIRHURST, R. M. & KWIATKOWSKI, D. P. 2018. Origins of the current outbreak of multidrug-resistant malaria in southeast Asia: a retrospective genetic study. *Lancet Infect Dis*, 18, 337-345.
- ANDERS, C., NIEWOEHNER, O., DUERST, A. & JINEK, M. 2014. Structural basis of PAM-dependent target DNA recognition by the Cas9 endonuclease. *Nature*, 513, 569-73.
- ANDERSON, T. J., PATEL, J. & FERDIG, M. T. 2009. Gene copy number and malaria biology. *Trends Parasitol*, 25, 336-43.
- ARIEY, F. & MENARD, D. 2019. An Update on Artemisinin Resistance. *Methods Mol Biol*, 2013, 141-149.
- ARIEY, F., WITKOWSKI, B., AMARATUNGA, C., BEGHAIN, J., LANGLOIS, A. C., KHIM, N., KIM, S., DURU, V., BOUCHIER, C., MA, L., LIM, P., LEANG, R., DUONG, S., SRENG, S., SUON, S., CHUOR, C. M., BOUT, D. M., MENARD, S., ROGERS, W. O., GENTON, B., FANDEUR, T., MIOTTO, O., RINGWALD, P., LE BRAS, J., BERRY, A., BARALE, J. C., FAIRHURST, R. M., BENOIT-VICAL, F., MERCEREAU-PUIJALON, O. & MENARD, D. 2014. A molecular marker of artemisinin-resistant *Plasmodium falciparum* malaria. *Nature*, 505, 50-5.
- ARROW, K. J., PANOSIAN, C.B. AND GELBAND, H. 2004. *Saving Lives, Buying Time: Economics of Malaria Drugs in an Age of Resistance*, Washington, D.C., The National Academies Press.
- ASCIERTO, P. A. & MARINCOLA, F. M. 2011. Combination therapy: the next opportunity and challenge of medicine. *J Transl Med*, 9, 115.
- ASHLEY, E. A., DHORDA, M., FAIRHURST, R. M., AMARATUNGA, C., LIM, P., SUON, S., SRENG, S., ANDERSON, J. M., MAO, S., SAM, B., SOPHA, C., CHUOR, C. M., NGUON, C., SOVANNAROTH, S., PUKRITTAYAKAMEE, S., JITTAMALA, P., CHOTIVANICH, K., CHUTASMIT, K., SUCHATSOONTHORN, C., RUNCHAROEN, R., HIEN, T. T., THUY-NHIEN, N. T., THANH, N. V., PHU, N. H., HTUT, Y., HAN, K. T., AYE, K. H., MOKUOLU, O. A., OLAOSEBIKAN, R. R., FOLARANMI, O. O., MAYXAY, M., KHANTHAVONG, M., HONGVANTHONG, B., NEWTON, P. N.,

- ONYAMBOKO, M. A., FANELLO, C. I., TSHEFU, A. K., MISHRA, N., VALECHA, N., PHYO, A. P., NOSTEN, F., YI, P., TRIPURA, R., BORRMANN, S., BASHRAHEIL, M., PESHU, J., FAIZ, M. A., GHOSE, A., HOSSAIN, M. A., SAMAD, R., RAHMAN, M. R., HASAN, M. M., ISLAM, A., MIOTTO, O., AMATO, R., MACINNIS, B., STALKER, J., KWIATKOWSKI, D. P., BOZDECH, Z., JEEYAPANT, A., CHEAH, P. Y., SAKULTHAEW, T., CHALK, J., INTHARABUT, B., SILAMUT, K., LEE, S. J., VIHOKHERN, B., KUNASOL, C., IMWONG, M., TARNING, J., TAYLOR, W. J., YEUNG, S., WOODROW, C. J., FLEGG, J. A., DAS, D., SMITH, J., VENKATESAN, M., PLOWE, C. V., STEPNIIEWSKA, K., GUERIN, P. J., DONDORP, A. M., DAY, N. P., WHITE, N. J. & TRACKING RESISTANCE TO ARTEMISININ, C. 2014. Spread of artemisinin resistance in *Plasmodium falciparum* malaria. *N Engl J Med*, 371, 411-23.
- ASHLEY, E. A., KRUDSOOD, S., PHAIPHUN, L., SRIVILAIRIT, S., MCGREADY, R., LEOWATTANA, W., HUTAGALUNG, R., WILAIRATANA, P., BROCKMAN, A., LOOAREESUWAN, S., NOSTEN, F. & WHITE, N. J. 2004. Randomized, controlled dose-optimization studies of dihydroartemisinin-piperaquine for the treatment of uncomplicated multidrug-resistant *falciparum* malaria in Thailand. *J Infect Dis*, 190, 1773-82.
- BABIKER, H. A., PRINGLE, S. J., ABDEL-MUHSIN, A., MACKINNON, M., HUNT, P. & WALLIKER, D. 2001. High-level chloroquine resistance in Sudanese isolates of *Plasmodium falciparum* is associated with mutations in the chloroquine resistance transporter gene *pfcr1* and the multidrug resistance Gene *pfmdr1*. *J Infect Dis*, 183, 1535-8.
- BACON, D. J., LATOUR, C., LUCAS, C., COLINA, O., RINGWALD, P. & PICOT, S. 2007. Comparison of a SYBR green I-based assay with a histidine-rich protein II enzyme-linked immunosorbent assay for in vitro antimalarial drug efficacy testing and application to clinical isolates. *Antimicrob Agents Chemother*, 51, 1172-8.
- BAKER, D. A. 2010. Malaria gametocytogenesis. *Mol Biochem Parasitol*, 172, 57-65.
- BANCELLS, C., LLORA-BATLLE, O., PORAN, A., NOTZEL, C., ROVIRA-GRAELLS, N., ELEMENTO, O., KAFSACK, B. F. C. & CORTES, A. 2019. Revisiting the initial steps of sexual development in the malaria parasite *Plasmodium falciparum*. *Nat Microbiol*, 4, 144-154.
- BANERJEE, R., LIU, J., BEATTY, W., PELOSOF, L., KLEMBA, M. & GOLDBERG, D. E. 2002. Four plasmepsins are active in the *Plasmodium falciparum* food vacuole, including a protease with an active-site histidine. *Proc Natl Acad Sci U S A*, 99, 990-5.
- BANNISTER, L. & MITCHELL, G. 2003. The ins, outs and roundabouts of malaria. *Trends Parasitol*, 19, 209-13.
- BANNISTER, L. H., HOPKINS, J. M., FOWLER, R. E., KRISHNA, S. & MITCHELL, G. H. 2000. A brief illustrated guide to the ultrastructure of *Plasmodium falciparum* asexual blood stages. *Parasitol Today*, 16, 427-33.
- BARBER, B. E., RAJAHRAM, G. S., GRIGG, M. J., WILLIAM, T. & ANSTEY, N. M. 2017. World Malaria Report: time to acknowledge *Plasmodium knowlesi* malaria. *Malar J*, 16, 135.

- BARILLAS-MURY, C. & KUMAR, S. 2005. Plasmodium-mosquito interactions: a tale of dangerous liaisons. *Cell Microbiol*, 7, 1539-45.
- BARTOLONI, A. & ZAMMARCHI, L. 2012. Clinical aspects of uncomplicated and severe malaria. *Mediterr J Hematol Infect Dis*, 4, e2012026.
- BATTY, K. T., THU, L. T., DAVIS, T. M., ILETT, K. F., MAI, T. X., HUNG, N. C., TIEN, N. P., POWELL, S. M., THIEN, H. V., BINH, T. Q. & KIM, N. V. 1998. A pharmacokinetic and pharmacodynamic study of intravenous vs oral artesunate in uncomplicated falciparum malaria. *Br J Clin Pharmacol*, 45, 123-9.
- BBC, B. B. C. 2018. *Malaria experts fear disease's resurgence* [Online]. online: BBC. Available: <https://www.bbc.co.uk/news/health-43786343> [Accessed].
- BEADLE, C., LONG, G. W., WEISS, W. R., MCELROY, P. D., MARET, S. M., OLOO, A. J. & HOFFMAN, S. L. 1994. Diagnosis of malaria by detection of Plasmodium falciparum HRP-2 antigen with a rapid dipstick antigen-capture assay. *Lancet*, 343, 564-8.
- BLASCO, B., LEROY, D. & FIDOCK, D. A. 2017. Antimalarial drug resistance: linking Plasmodium falciparum parasite biology to the clinic. *Nat Med*, 23, 917-928.
- BLOLAND, P. B. 2001. Drug resistance in malaria. Geneva, Switzerland: World Health Organization.
- BONILLA, J. A., BONILLA, T. D., YOWELL, C. A., FUJIOKA, H. & DAME, J. B. 2007. Critical roles for the digestive vacuole plasmepsins of Plasmodium falciparum in vacuolar function. *Mol Microbiol*, 65, 64-75.
- BOPP, S., MAGISTRADO, P., WONG, W., SCHAFFNER, S. F., MUKHERJEE, A., LIM, P., DHORDA, M., AMARATUNGA, C., WOODROW, C. J., ASHLEY, E. A., WHITE, N. J., DONDORP, A. M., FAIRHURST, R. M., ARIEY, F., MENARD, D., WIRTH, D. F. & VOLKMAN, S. K. 2018. Plasmepsin II-III copy number accounts for bimodal piperazine resistance among Cambodian Plasmodium falciparum. *Nat Commun*, 9, 1769.
- BOPP, S. E., MANARY, M. J., BRIGHT, A. T., JOHNSTON, G. L., DHARIA, N. V., LUNA, F. L., MCCORMACK, S., PLOUFFE, D., MCNAMARA, C. W., WALKER, J. R., FIDOCK, D. A., DENCHI, E. L. & WINZELER, E. A. 2013. Mitotic evolution of Plasmodium falciparum shows a stable core genome but recombination in antigen families. *PLoS Genet*, 9, e1003293.
- BOUDREAU, E. F., WEBSTER, H. K., PAVANAND, K. & THOSINGHA, L. 1982. Type II mefloquine resistance in Thailand. *Lancet*, 2, 1335.
- BRANCUCCI, N. M. B., GERDT, J. P., WANG, C., DE NIZ, M., PHILIP, N., ADAPA, S. R., ZHANG, M., HITZ, E., NIEDERWIESER, I., BOLTRYK, S. D., LAFFITTE, M. C., CLARK, M. A., GRURING, C., RAVEL, D., BLANCKE SOARES, A., DEMAS, A., BOPP, S., RUBIO-RUIZ, B., CONEJO-GARCIA, A., WIRTH, D. F., GENDASZEWSKA-DARMACH, E., DURAISINGH, M. T., ADAMS, J. H., VOSS, T. S., WATERS, A. P., JIANG, R. H. Y., CLARDY, J. & MARTI, M. 2017. Lysophosphatidylcholine Regulates Sexual Stage Differentiation in the Human Malaria Parasite Plasmodium falciparum. *Cell*, 171, 1532-1544 e15.

- BRAY, P. G., MARTIN, R. E., TILLEY, L., WARD, S. A., KIRK, K. & FIDOCK, D. A. 2005. Defining the role of PfCRT in Plasmodium falciparum chloroquine resistance. *Mol Microbiol*, 56, 323-33.
- BRIDGFORD, J. L., XIE, S. C., COBBOLD, S. A., PASAJE, C. F. A., HERRMANN, S., YANG, T., GILLETT, D. L., DICK, L. R., RALPH, S. A., DOGOVSKI, C., SPILLMAN, N. J. & TILLEY, L. 2018. Artemisinin kills malaria parasites by damaging proteins and inhibiting the proteasome. *Nat Commun*, 9, 3801.
- BRUCE-CHWATT, L. J. 1965. Paleogenesis and Paleo-Epidemiology of Primate Malaria. *Bull World Health Organ*, 32, 363-87.
- BRUCE-CHWATT, L. J. 1981. Alphonse Laveran's discovery 100 years ago and today's global fight against malaria. *J R Soc Med*, 74, 531-6.
- BRUCE-CHWATT, L. J. 1985. *Essential Malariology. 2nd Ed.*, New York, John Wiley and Sons.
- BRUCE-CHWATT, L. J. 1988. *History of malaria from prehistory to eradication*, Edinburgh, United Kingdom: Churchill Livingstone.
- BRUCE-CHWATT, L. J. E. A. 1986. *Chemotherapy of malaria*. World Health Organization. Geneva, Switzerland.
- BUTLER, A. R., KHAN, S. & FERGUSON, E. 2010. A brief history of malaria chemotherapy. *J R Coll Physicians Edinb*, 40, 172-7.
- CARLTON, J. M., FIDOCK, D. A., DJIMDE, A., PLOWE, C. V. & WELLEMS, T. E. 2001. Conservation of a novel vacuolar transporter in Plasmodium species and its central role in chloroquine resistance of P. falciparum. *Curr Opin Microbiol*, 4, 415-20.
- CARTER, R. & MENDIS, K. N. 2002. Evolutionary and historical aspects of the burden of malaria. *Clin Microbiol Rev*, 15, 564-94.
- CARTER, R. & MILLER, L. H. 1979. Evidence for environmental modulation of gametocytogenesis in Plasmodium falciparum in continuous culture. *Bull World Health Organ*, 57 Suppl 1, 37-52.
- CARVALHO, T. G. & MENARD, R. 2005. Manipulating the Plasmodium genome. *Curr Issues Mol Biol*, 7, 39-55.
- CENTERS FOR DISEASE CONTROL. 2018. *Biology: Anopheles Mosquitoes* [Online]. Available: <https://www.cdc.gov/malaria/about/biology/index.html#tabs-1-5> [Accessed].
- CHAORATTANAKAWEE, S., SAUNDERS, D. L., SEA, D., CHANARAT, N., YINGYUEN, K., SUNDRAKES, S., SAINGAM, P., BUATHONG, N., SRIWICHAI, S., CHANN, S., SE, Y., YOM, Y., HENG, T. K., KONG, N., KUNTAWUNGINN, W., TANGTHONGCHAIWIRIYA, K., JACOB, C., TAKALA-HARRISON, S., PLOWE, C., LIN, J. T., CHUOR, C. M., PROM, S., TYNER, S. D., GOSI, P., TEJA-ISAVADHARM, P., LON, C. & LANTERI, C. A. 2015. Ex Vivo Drug Susceptibility Testing and Molecular Profiling of Clinical Plasmodium falciparum Isolates from Cambodia from 2008 to 2013 Suggest Emerging Piperaquine Resistance. *Antimicrob Agents Chemother*, 59, 4631-43.

- CHEESEMAN, I. H., MILLER, B., TAN, J. C., TAN, A., NAIR, S., NKHOMA, S. C., DE DONATO, M., RODULFO, H., DONDORP, A., BRANCH, O. H., MESIA, L. R., NEWTON, P., MAYXAY, M., AMAMBUA-NGWA, A., CONWAY, D. J., NOSTEN, F., FERDIG, M. T. & ANDERSON, T. J. 2016. Population Structure Shapes Copy Number Variation in Malaria Parasites. *Mol Biol Evol*, 33, 603-20.
- CHEESEMAN, I. H., MILLER, B. A., NAIR, S., NKHOMA, S., TAN, A., TAN, J. C., AL SAAI, S., PHYO, A. P., MOO, C. L., LWIN, K. M., MCGREADY, R., ASHLEY, E., IMWONG, M., STEPNIIEWSKA, K., YI, P., DONDORP, A. M., MAYXAY, M., NEWTON, P. N., WHITE, N. J., NOSTEN, F., FERDIG, M. T. & ANDERSON, T. J. 2012. A major genome region underlying artemisinin resistance in malaria. *Science*, 336, 79-82.
- CHEN, I., CLARKE, S. E., GOSLING, R., HAMAINZA, B., KILLEEN, G., MAGILL, A., O'MEARA, W., PRICE, R. N. & RILEY, E. M. 2016. "Asymptomatic" Malaria: A Chronic and Debilitating Infection That Should Be Treated. *PLoS Med*, 13, e1001942.
- CHOTIVANICH, K., UDOMSANGPETCH, R., PATTANAPANYASAT, K., CHIERAKUL, W., SIMPSON, J., LOOAREESUWAN, S. & WHITE, N. 2002. Hemoglobin E: a balanced polymorphism protective against high parasitemias and thus severe *P falciparum* malaria. *Blood*, 100, 1172-6.
- CINGOLANI, P., PLATTS, A., WANG LE, L., COON, M., NGUYEN, T., WANG, L., LAND, S. J., LU, X. & RUDEN, D. M. 2012. A program for annotating and predicting the effects of single nucleotide polymorphisms, SnpEff: SNPs in the genome of *Drosophila melanogaster* strain w1118; iso-2; iso-3. *Fly (Austin)*, 6, 80-92.
- CLEMENTS, A. N. 1992. *The Biology of Mosquitoes: Development, Nutrition and Reproduction*, London, Chapman & Hall.
- COOPER, D. J., RAJAHRAM, G. S., WILLIAM, T., JELIP, J., MOHAMMAD, R., BENEDICT, J., ALAZA, D. A., MALACOVA, E., YEO, T. W., GRIGG, M. J., ANSTEY, N. M. & BARBER, B. E. 2019. Plasmodium knowlesi Malaria in Sabah, Malaysia, 2015–2017: Ongoing Increase in Incidence Despite Near-elimination of the Human-only Plasmodium Species. *Clinical Infectious Diseases*.
- COWELL, A. N., ISTVAN, E. S., LUKENS, A. K., GOMEZ-LORENZO, M. G., VANAERSCHOT, M., SAKATA-KATO, T., FLANNERY, E. L., MAGISTRADO, P., OWEN, E., ABRAHAM, M., LAMONTE, G., PAINTER, H. J., WILLIAMS, R. M., FRANCO, V., LINARES, M., ARRIAGA, I., BOPP, S., COREY, V. C., GNADIG, N. F., COBURN-FLYNN, O., REIMER, C., GUPTA, P., MURITHI, J. M., MOURA, P. A., FUCHS, O., SASAKI, E., KIM, S. W., TENG, C. H., WANG, L. T., AKIDIL, A., ADJALLEY, S., WILLIS, P. A., SIEGEL, D., TANASEICHUK, O., ZHONG, Y., ZHOU, Y., LLINAS, M., OTTILIE, S., GAMO, F. J., LEE, M. C. S., GOLDBERG, D. E., FIDOCK, D. A., WIRTH, D. F. & WINZELER, E. A. 2018. Mapping the malaria parasite druggable genome by using in vitro evolution and chemogenomics. *Science*, 359, 191-199.
- COWELL, A. N. & WINZELER, E. A. 2019. The genomic architecture of antimalarial drug resistance. *Brief Funct Genomics*.
- COWMAN, A. F. & CRABB, B. S. 2006. Invasion of red blood cells by malaria parasites. *Cell*, 124, 755-66.

- COWMAN, A. F., GALATIS, D. & THOMPSON, J. K. 1994. Selection for mefloquine resistance in *Plasmodium falciparum* is linked to amplification of the *pfmdr1* gene and cross-resistance to halofantrine and quinine. *Proc Natl Acad Sci U S A*, 91, 1143-7.
- COWMAN, A. F., HEALER, J., MARAPANA, D. & MARSH, K. 2016. Malaria: Biology and Disease. *Cell*, 167, 610-624.
- COX, F. E. 2010. History of the discovery of the malaria parasites and their vectors. *Parasit Vectors*, 3, 5.
- CROFT, A. M. 1999. World Health Organization "Roll Back Malaria" Campaign--report on a visit to the Central Drug Research Institute, Lucknow, India. *J R Army Med Corps*, 145, 104.
- CUI, L., MHARAKURWA, S., NDIAYE, D., RATHOD, P. K. & ROSENTHAL, P. J. 2015. Antimalarial Drug Resistance: Literature Review and Activities and Findings of the ICEMR Network. *Am J Trop Med Hyg*, 93, 57-68.
- CUI, L. & SU, X. Z. 2009. Discovery, mechanisms of action and combination therapy of artemisinin. *Expert Rev Anti Infect Ther*, 7, 999-1013.
- CUNHA, C. B. & CUNHA, B. A. 2008. Brief history of the clinical diagnosis of malaria: from Hippocrates to Osler. *J Vector Borne Dis*, 45, 194-9.
- DAVIS, T. M., HUNG, T. Y., SIM, I. K., KARUNAJEEWA, H. A. & ILETT, K. F. 2005. Piperaquine: a resurgent antimalarial drug. *Drugs*, 65, 75-87.
- DAYANANDA, K. K., ACHUR, R. N. & GOWDA, D. C. 2018. Epidemiology, drug resistance, and pathophysiology of *Plasmodium vivax* malaria. *J Vector Borne Dis*, 55, 1-8.
- DE KONING-WARD, T. F., JANSE, C. J. & WATERS, A. P. 2000. The development of genetic tools for dissecting the biology of malaria parasites. *Annu Rev Microbiol*, 54, 157-85.
- DEITSCH, K., DRISKILL, C. & WELLEMS, T. 2001. Transformation of malaria parasites by the spontaneous uptake and expression of DNA from human erythrocytes. *Nucleic Acids Res*, 29, 850-3.
- DEL PILAR CRESPO, M., AVERY, T. D., HANSEN, E., FOX, E., ROBINSON, T. V., VALENTE, P., TAYLOR, D. K. & TILLEY, L. 2008. Artemisinin and a series of novel endoperoxide antimalarials exert early effects on digestive vacuole morphology. *Antimicrob Agents Chemother*, 52, 98-109.
- DELVES, M. J., STRASCHIL, U., RUECKER, A., MIGUEL-BLANCO, C., MARQUES, S., DUFOUR, A. C., BAUM, J. & SINDEN, R. E. 2016. Routine in vitro culture of *P. falciparum* gametocytes to evaluate novel transmission-blocking interventions. *Nature Protocols*, 11, 1668.
- DEMAS, A. R., SHARMA, A. I., WONG, W., EARLY, A. M., REDMOND, S., BOPP, S., NEAFSEY, D. E., VOLKMAN, S. K., HARTL, D. L. & WIRTH, D. F. 2018. Mutations in *Plasmodium falciparum* actin-binding protein coronin confer reduced artemisinin susceptibility. *Proc Natl Acad Sci U S A*, 115, 12799-12804.

- DENIS, M. B., TSUYUOKA, R., PORAVUTH, Y., NARANN, T. S., SEILA, S., LIM, C., INCARDONA, S., LIM, P., SEM, R., SOCHEAT, D., CHRISTOPHEL, E. M. & RINGWALD, P. 2006. Surveillance of the efficacy of artesunate and mefloquine combination for the treatment of uncomplicated falciparum malaria in Cambodia. *Trop Med Int Health*, 11, 1360-6.
- DEPRISTO, M. A., BANKS, E., POPLIN, R., GARIMELLA, K. V., MAGUIRE, J. R., HARTL, C., PHILIPPAKIS, A. A., DEL ANGEL, G., RIVAS, M. A., HANNA, M., MCKENNA, A., FENNELL, T. J., KERNYTSKY, A. M., SIVACHENKO, A. Y., CIBULSKIS, K., GABRIEL, S. B., ALTSHULER, D. & DALY, M. J. 2011. A framework for variation discovery and genotyping using next-generation DNA sequencing data. *Nat Genet*, 43, 491-8.
- DHANOVA, B. S., COGLIATI, T., SATISH, A. G., BRUFORD, E. A. & FRIEDMAN, J. S. 2013. Update on the Kelch-like (KLHL) gene family. *Hum Genomics*, 7, 13.
- DHINGRA, S. K., REDHI, D., COMBRINCK, J. M., YEO, T., OKOMBO, J., HENRICH, P. P., COWELL, A. N., GUPTA, P., STEGMAN, M. L., HOKE, J. M., COOPER, R. A., WINZELER, E., MOK, S., EGAN, T. J. & FIDOCK, D. A. 2017. A Variant PfCRT Isoform Can Contribute to Plasmodium falciparum Resistance to the First-Line Partner Drug Piperaquine. *MBio*, 8.
- DJIMDE, A., DOUMBO, O. K., CORTESE, J. F., KAYENTAO, K., DOUMBO, S., DIOURTE, Y., COULIBALY, D., DICKO, A., SU, X. Z., NOMURA, T., FIDOCK, D. A., WELLEMS, T. E. & PLOWE, C. V. 2001. A molecular marker for chloroquine-resistant falciparum malaria. *N Engl J Med*, 344, 257-63.
- DOCTOR, S. M., LIU, Y., ANDERSON, O. G., WHITESELL, A. N., MWANDAGALIRWA, M. K., MUWONGA, J., KEELER, C., EMCH, M., LIKWELA, J. L., TSHEFU, A. & MESHNICK, S. R. 2016. Low prevalence of Plasmodium malariae and Plasmodium ovale mono-infections among children in the Democratic Republic of the Congo: a population-based, cross-sectional study. *Malaria Journal*, 15, 350.
- DONDORP, A. M., NOSTEN, F., YI, P., DAS, D., PHYO, A. P., TARNING, J., LWIN, K. M., ARIEY, F., HANPITHAKPONG, W., LEE, S. J., RINGWALD, P., SILAMUT, K., IMWONG, M., CHOTIVANICH, K., LIM, P., HERDMAN, T., AN, S. S., YEUNG, S., SINGHASIVANON, P., DAY, N. P., LINDEGARDH, N., SOCHEAT, D. & WHITE, N. J. 2009. Artemisinin resistance in Plasmodium falciparum malaria. *N Engl J Med*, 361, 455-67.
- DURASINGH, M. T. & COWMAN, A. F. 2005. Contribution of the pfmdr1 gene to antimalarial drug-resistance. *Acta Trop*, 94, 181-90.
- DURU, V., KHIM, N., LEANG, R., KIM, S., DOMERGUE, A., KLOEUNG, N., KE, S., CHY, S., EAM, R., KHEAN, C., LOCH, K., KEN, M., LEK, D., BEGHAIN, J., ARIEY, F., GUERIN, P. J., HUY, R., MERCEREAU-PUIJALON, O., WITKOWSKI, B. & MENARD, D. 2015. Plasmodium falciparum dihydroartemisinin-piperaquine failures in Cambodia are associated with mutant K13 parasites presenting high survival rates in novel piperaquine in vitro assays: retrospective and prospective investigations. *BMC Med*, 13, 305.

- EASTMAN, R. T., DHARIA, N. V., WINZELER, E. A. & FIDOCK, D. A. 2011. Piperaquine resistance is associated with a copy number variation on chromosome 5 in drug-pressured *Plasmodium falciparum* parasites. *Antimicrob Agents Chemother*, 55, 3908-16.
- ECKER, A., LEHANE, A. M., CLAIN, J. & FIDOCK, D. A. 2012. PfCRT and its role in antimalarial drug resistance. *Trends Parasitol*, 28, 504-14.
- EGGLESON, K. K., DUFFIN, K. L. & GOLDBERG, D. E. 1999. Identification and characterization of falcilysin, a metallopeptidase involved in hemoglobin catabolism within the malaria parasite *Plasmodium falciparum*. *J Biol Chem*, 274, 32411-7.
- FAIRHURST, R. M. & DONDORP, A. M. 2016. Artemisinin-Resistant *Plasmodium falciparum* Malaria. *Microbiol Spectr*, 4.
- FEACHEM, R. G. A., CHEN, I., AKBARI, O., BERTOZZI-VILLA, A., BHATT, S., BINKA, F., BONI, M. F., BUCKEE, C., DIELEMAN, J., DONDORP, A., EAPEN, A., SEKHRI FEACHEM, N., FILLER, S., GETHING, P., GOSLING, R., HAAKENSTAD, A., HARVARD, K., HATEFI, A., JAMISON, D., JONES, K. E., KAREMA, C., KAMWI, R. N., LAL, A., LARSON, E., LEES, M., LOBO, N. F., MICAH, A. E., MOONEN, B., NEWBY, G., NING, X., PATE, M., QUINONES, M., ROH, M., ROLFE, B., SHANKS, D., SINGH, B., STALEY, K., TULLOCH, J., WEGBREIT, J., WOO, H. J. & MPANJU-SHUMBUSHO, W. 2019. Malaria eradication within a generation: ambitious, achievable, and necessary. *Lancet*.
- FERRAMOSCA, A. & ZARA, V. 2013. Biogenesis of mitochondrial carrier proteins: molecular mechanisms of import into mitochondria. *Biochim Biophys Acta*, 1833, 494-502.
- FIDOCK, D. A., NOMURA, T., TALLEY, A. K., COOPER, R. A., DZEKUNOV, S. M., FERDIG, M. T., URSOS, L. M., SIDHU, A. B., NAUDE, B., DEITSCH, K. W., SU, X. Z., WOOTTON, J. C., ROEPE, P. D. & WELLEMS, T. E. 2000. Mutations in the *P. falciparum* digestive vacuole transmembrane protein PfCRT and evidence for their role in chloroquine resistance. *Mol Cell*, 6, 861-71.
- FIDOCK, D. A., ROSENTHAL, P. J., CROFT, S. L., BRUN, R. & NWAKA, S. 2004. Antimalarial drug discovery: efficacy models for compound screening. *Nat Rev Drug Discov*, 3, 509-20.
- FOOTE, S. J., KYLE, D. E., MARTIN, R. K., ODUOLA, A. M., FORSYTH, K., KEMP, D. J. & COWMAN, A. F. 1990. Several alleles of the multidrug-resistance gene are closely linked to chloroquine resistance in *Plasmodium falciparum*. *Nature*, 345, 255-8.
- FORTUNE, J. M., PAVLOV, Y. I., WELCH, C. M., JOHANSSON, E., BURGERS, P. M. & KUNKEL, T. A. 2005. *Saccharomyces cerevisiae* DNA polymerase delta: high fidelity for base substitutions but lower fidelity for single- and multi-base deletions. *J Biol Chem*, 280, 29980-7.
- FRANCIS, S. E., SULLIVAN, D. J., JR. & GOLDBERG, D. E. 1997. Hemoglobin metabolism in the malaria parasite *Plasmodium falciparum*. *Annu Rev Microbiol*, 51, 97-123.

- FREEMAN, J. L., PERRY, G. H., FEUK, L., REDON, R., MCCARROLL, S. A., ALTSHULER, D. M., ABURATANI, H., JONES, K. W., TYLER-SMITH, C., HURLES, M. E., CARTER, N. P., SCHERER, S. W. & LEE, C. 2006. Copy number variation: new insights in genome diversity. *Genome Res*, 16, 949-61.
- GALLUP, J. L. & SACHS, J. D. 2001. The economic burden of malaria. *Am J Trop Med Hyg*, 64, 85-96.
- GARCIA, C. R., MARKUS, R. P. & MADEIRA, L. 2001. Tertian and quartan fevers: temporal regulation in malarial infection. *J Biol Rhythms*, 16, 436-43.
- GARDNER, M. J., HALL, N., FUNG, E., WHITE, O., BERRIMAN, M., HYMAN, R. W., CARLTON, J. M., PAIN, A., NELSON, K. E., BOWMAN, S., PAULSEN, I. T., JAMES, K., EISEN, J. A., RUTHERFORD, K., SALZBERG, S. L., CRAIG, A., KYES, S., CHAN, M. S., NENE, V., SHALLOM, S. J., SUH, B., PETERSON, J., ANGIUOLI, S., PERTEA, M., ALLEN, J., SELENGUT, J., HAFT, D., MATHER, M. W., VAIDYA, A. B., MARTIN, D. M., FAIRLAMB, A. H., FRAUNHOLZ, M. J., ROOS, D. S., RALPH, S. A., MCFADDEN, G. I., CUMMINGS, L. M., SUBRAMANIAN, G. M., MUNGALL, C., VENTER, J. C., CARUCCI, D. J., HOFFMAN, S. L., NEWBOLD, C., DAVIS, R. W., FRASER, C. M. & BARRELL, B. 2002. Genome sequence of the human malaria parasite *Plasmodium falciparum*. *Nature*, 419, 498-511.
- GARNHAM, P. C. C. 1996. *Malaria parasites and other haemosporidia.*, London, United Kingdom, Blackwell.
- GENOMES PROJECT, C., ABECASIS, G. R., ALTSHULER, D., AUTON, A., BROOKS, L. D., DURBIN, R. M., GIBBS, R. A., HURLES, M. E. & MCVEAN, G. A. 2010. A map of human genome variation from population-scale sequencing. *Nature*, 467, 1061-73.
- GHORBAL, M., GORMAN, M., MACPHERSON, C. R., MARTINS, R. M., SCHERF, A. & LOPEZ-RUBIO, J. J. 2014. Genome editing in the human malaria parasite *Plasmodium falciparum* using the CRISPR-Cas9 system. *Nat Biotechnol*, 32, 819-21.
- GINSBURG, H., FAMIN, O., ZHANG, J. & KRUGLIAK, M. 1998. Inhibition of glutathione-dependent degradation of heme by chloroquine and amodiaquine as a possible basis for their antimalarial mode of action. *Biochem Pharmacol*, 56, 1305-13.
- GOLDBERG, D. E., SLATER, A. F., BEAVIS, R., CHAIT, B., CERAMI, A. & HENDERSON, G. B. 1991. Hemoglobin degradation in the human malaria pathogen *Plasmodium falciparum*: a catabolic pathway initiated by a specific aspartic protease. *J Exp Med*, 173, 961-9.
- GOLDBERG, D. E., SLATER, A. F., CERAMI, A. & HENDERSON, G. B. 1990. Hemoglobin degradation in the malaria parasite *Plasmodium falciparum*: an ordered process in a unique organelle. *Proc Natl Acad Sci U S A*, 87, 2931-5.
- GREENWOOD, B. M., FIDOCK, D. A., KYLE, D. E., KAPPE, S. H., ALONSO, P. L., COLLINS, F. H. & DUFFY, P. E. 2008. Malaria: progress, perils, and prospects for eradication. *J Clin Invest*, 118, 1266-76.

- GUINET, F., DVORAK, J. A., FUJIOKA, H., KEISTER, D. B., MURATOVA, O., KASLOW, D. C., AIKAWA, M., VAIDYA, A. B. & WELLEMS, T. E. 1996. A developmental defect in *Plasmodium falciparum* male gametogenesis. *J Cell Biol*, 135, 269-78.
- GUPTA, H., MACETE, E., BULO, H., SALVADOR, C., WARSAME, M., CARVALHO, E., MENARD, D., RINGWALD, P., BASSAT, Q., ENOSSE, S. & MAYOR, A. 2018. Drug-Resistant Polymorphisms and Copy Numbers in *Plasmodium falciparum*, Mozambique, 2015. *Emerg Infect Dis*, 24, 40-48.
- HALL, N., PAIN, A., BERRIMAN, M., CHURCHER, C., HARRIS, B., HARRIS, D., MUNGALL, K., BOWMAN, S., ATKIN, R., BAKER, S., BARRON, A., BROOKS, K., BUCKEE, C. O., BURROWS, C., CHEREVACH, I., CHILLINGWORTH, C., CHILLINGWORTH, T., CHRISTODOULOU, Z., CLARK, L., CLARK, R., CORTON, C., CRONIN, A., DAVIES, R., DAVIS, P., DEAR, P., DEARDEN, F., DOGGETT, J., FELTWELL, T., GOBLE, A., GOODHEAD, I., GWILLIAM, R., HAMLIN, N., HANCE, Z., HARPER, D., HAUSER, H., HORNSBY, T., HOLROYD, S., HORROCKS, P., HUMPHRAY, S., JAGELS, K., JAMES, K. D., JOHNSON, D., KERHORNOU, A., KNIGHTS, A., KONFORTOV, B., KYES, S., LARKE, N., LAWSON, D., LENNARD, N., LINE, A., MADDISON, M., MCLEAN, J., MOONEY, P., MOULE, S., MURPHY, L., OLIVER, K., ORMOND, D., PRICE, C., QUAIL, M. A., RABBINOWITSCH, E., RAJANDREAM, M. A., RUTTER, S., RUTHERFORD, K. M., SANDERS, M., SIMMONDS, M., SEEGER, K., SHARP, S., SMITH, R., SQUARES, R., SQUARES, S., STEVENS, K., TAYLOR, K., TIVEY, A., UNWIN, L., WHITEHEAD, S., WOODWARD, J., SULSTON, J. E., CRAIG, A., NEWBOLD, C. & BARRELL, B. G. 2002. Sequence of *Plasmodium falciparum* chromosomes 1, 3-9 and 13. *Nature*, 419, 527-31.
- HAMILTON, W. L., AMATO, R., VAN DER PLUIJM, R. W., JACOB, C. G., QUANG, H. H., THUY-NHIEN, N. T., HIEN, T. T., HONGVANTHONG, B., CHINDAVONGSA, K., MAYXAY, M., HUY, R., LEANG, R., HUCH, C., DYSOLEY, L., AMARATUNGA, C., SUON, S., FAIRHURST, R. M., TRIPURA, R., PETO, T. J., SOVANN, Y., JITTAMALA, P., HANBOONKUNUPAKARN, B., PUKRITTAYAKAMEE, S., CHAU, N. H., IMWONG, M., DHORDA, M., VONGPROMEK, R., CHAN, X. H. S., MAUDE, R. J., PEARSON, R. D., NGUYEN, T., ROCKETT, K., DRURY, E., GONCALVES, S., WHITE, N. J., DAY, N. P., KWIATKOWSKI, D. P., DONDORP, A. M. & MIOTTO, O. 2019. Evolution and expansion of multidrug-resistant malaria in southeast Asia: a genomic epidemiology study. *Lancet Infect Dis*.
- HAPUARACHCHI, S. V., COBBOLD, S. A., SHAFIK, S. H., DENNIS, A. S., MCCONVILLE, M. J., MARTIN, R. E., KIRK, K. & LEHANE, A. M. 2017. The Malaria Parasite's Lactate Transporter PfFNT Is the Target of Antiplasmodial Compounds Identified in Whole Cell Phenotypic Screens. *PLoS Pathog*, 13, e1006180.
- HARINASUTA, T., SUNTHARASAMAI, P. & VIRAVAN, C. 1965. Chloroquine-resistant *falciparum* malaria in Thailand. *Lancet*, 2, 657-60.
- HASENKAMP, S., RUSSELL, K. T. & HORROCKS, P. 2012. Comparison of the absolute and relative efficiencies of electroporation-based transfection protocols for *Plasmodium falciparum*. *Malar J*, 11, 210.

- HAWKING, F. 1970. The clock of the malaria parasite. *Sci Am*, 222, 123-31.
- HAWKING, F., WORMS, M. J. & GAMMAGE, K. 1968. 24- and 48-hour cycles of malaria parasites in the blood; their purpose, production and control. *Trans R Soc Trop Med Hyg*, 62, 731-65.
- HAY, S. I., GUERRA, C. A., TATEM, A. J., NOOR, A. M. & SNOW, R. W. 2004. The global distribution and population at risk of malaria: past, present, and future. *Lancet Infect Dis*, 4, 327-36.
- HAYNES, J. D., DIGGS, C. L., HINES, F. A. & DESJARDINS, R. E. 1976. Culture of human malaria parasites *Plasmodium falciparum*. *Nature*, 263, 767-9.
- HELLER, L. E. & ROEPE, P. D. 2019. Artemisinin-Based Antimalarial Drug Therapy: Molecular Pharmacology and Evolving Resistance. *Trop Med Infect Dis*, 4.
- HEMPELMANN, E. & KRAFTS, K. 2013. Bad air, amulets and mosquitoes: 2,000 years of changing perspectives on malaria. *Malaria Journal*, 12, 232.
- HOGLUND, R. M., WORKMAN, L., EDSTEIN, M. D., THANH, N. X., QUANG, N. N., ZONGO, I., OUEDRAOGO, J. B., BORRMANN, S., MWAI, L., NSANZABANA, C., PRICE, R. N., DAHAL, P., SAMBOL, N. C., PARIKH, S., NOSTEN, F., ASHLEY, E. A., PHYO, A. P., LWIN, K. M., MCGREADY, R., DAY, N. P., GUERIN, P. J., WHITE, N. J., BARNES, K. I. & TARNING, J. 2017. Population Pharmacokinetic Properties of Piperaquine in *Falciparum* Malaria: An Individual Participant Data Meta-Analysis. *PLoS Med*, 14, e1002212.
- HOMEWOOD, C. A., WARHURST, D. C., PETERS, W. & BAGGALEY, V. C. 1972. Lysosomes, pH and the anti-malarial action of chloroquine. *Nature*, 235, 50-2.
- HONMA, H., HIRAI, M., NAKAMURA, S., HAKIMI, H., KAWAZU, S., PALACPAC, N. M., HISAEDA, H., MATSUOKA, H., KAWAI, S., ENDO, H., YASUNAGA, T., OHASHI, J., MITA, T., HORII, T., FURUSAWA, M. & TANABE, K. 2014. Generation of rodent malaria parasites with a high mutation rate by destructing proofreading activity of DNA polymerase delta. *DNA Res*, 21, 439-46.
- HONMA, H., NIIKURA, M., KOBAYASHI, F., HORII, T., MITA, T., ENDO, H. & HIRAI, M. 2016. Mutation tendency of mutator *Plasmodium berghei* with proofreading-deficient DNA polymerase delta. *Sci Rep*, 6, 36971.
- HOSTETLER, J. B., LO, E., KANJEE, U., AMARATUNGA, C., SUON, S., SRENG, S., MAO, S., YEWHALAW, D., MASCARENHAS, A., KWIATKOWSKI, D. P., FERREIRA, M. U., RATHOD, P. K., YAN, G., FAIRHURST, R. M., DURAISINGH, M. T. & RAYNER, J. C. 2016. Independent Origin and Global Distribution of Distinct *Plasmodium vivax* Duffy Binding Protein Gene Duplications. *PLoS Negl Trop Dis*, 10, e0005091.
- HUBSCHER, U., MAGA, G. & SPADARI, S. 2002. Eukaryotic DNA polymerases. *Annu Rev Biochem*, 71, 133-63.
- IMWONG, M., SUWANNASIN, K., KUNASOL, C., SUTAWONG, K., MAYXAY, M., REKOL, H., SMITHUIS, F. M., HLAING, T. M., TUN, K. M., VAN DER PLUIJM, R. W., TRIPURA, R., MIOTTO, O., MENARD, D., DHORDA, M., DAY, N. P. J.,

- WHITE, N. J. & DONDORP, A. M. 2017. The spread of artemisinin-resistant *Plasmodium falciparum* in the Greater Mekong subregion: a molecular epidemiology observational study. *Lancet Infect Dis*, 17, 491-497.
- INOUE, J., SILVA, M., FOFANA, B., SANOGO, K., MARTENSSON, A., SAGARA, I., BJORKMAN, A., VEIGA, M. I., FERREIRA, P. E., DJIMDE, A. & GIL, J. P. 2018. *Plasmodium falciparum* Plasmepsin 2 Duplications, West Africa. *Emerg Infect Dis*, 24.
- ITOH, K., WAKABAYASHI, N., KATOH, Y., ISHII, T., IGARASHI, K., ENGEL, J. D. & YAMAMOTO, M. 1999. Keap1 represses nuclear activation of antioxidant responsive elements by Nrf2 through binding to the amino-terminal Neh2 domain. *Genes Dev*, 13, 76-86.
- JACOB, C. G., ANSBRO, M. R., AMATO, R., KEKRE, M., VONGPROMEK, R., DHORDA, M., AMARATUNGA, C., SRENG, S., SUON, S., MIOTTO, O., FAIRHURST, R. M., WELLEMS, T. E. & KWIATKOWSKI, D. P. 2019. Development of copy number assays for detection and surveillance of piperazine resistance associated plasmepsin 2/3 copy number variation in *Plasmodium falciparum*. *bioRxiv*.
- JANI, D., NAGARKATTI, R., BEATTY, W., ANGEL, R., SLEBODNICK, C., ANDERSEN, J., KUMAR, S. & RATHORE, D. 2008. HDP-a novel heme detoxification protein from the malaria parasite. *PLoS Pathog*, 4, e1000053.
- JANSE, C. J., RAMESAR, J. & WATERS, A. P. 2006. High-efficiency transfection and drug selection of genetically transformed blood stages of the rodent malaria parasite *Plasmodium berghei*. *Nat Protoc*, 1, 346-56.
- JENSEN, J. 1988. In vitro cultivation of malaria parasites. *Erythrocytic stages, Malaria*, 1, 307-347.
- JIANG, F. & DOUDNA, J. A. 2017. CRISPR-Cas9 Structures and Mechanisms. *Annu Rev Biophys*, 46, 505-529.
- JOHNSTON, J. C., SHAHIDI, N. C., SADATSAFAVI, M. & FITZGERALD, J. M. 2009. Treatment outcomes of multidrug-resistant tuberculosis: a systematic review and meta-analysis. *PLoS One*, 4, e6914.
- JOICE, R., NILSSON, S. K., MONTGOMERY, J., DANKWA, S., EGAN, E., MORAHAN, B., SEYDEL, K. B., BERTUCCINI, L., ALANO, P., WILLIAMSON, K. C., DURAISINGH, M. T., TAYLOR, T. E., MILNER, D. A. & MARTI, M. 2014. *Plasmodium falciparum* transmission stages accumulate in the human bone marrow. *Sci Transl Med*, 6, 244re5.
- KAFSACK, B. F., ROVIRA-GRAELLS, N., CLARK, T. G., BANCELLS, C., CROWLEY, V. M., CAMPINO, S. G., WILLIAMS, A. E., DROUGHT, L. G., KWIATKOWSKI, D. P., BAKER, D. A., CORTES, A. & LLINAS, M. 2014. A transcriptional switch underlies commitment to sexual development in malaria parasites. *Nature*, 507, 248-52.

- KAUR, S. D. & SINGH, L. 2017. Identification of Mosquitoes, Nature of Diseases and Treatment in Early Sanskrit Literature. *Indian Journal of History of Science*, 52, 243-250.
- KERANTZAS, C. A. & JACOBS, W. R., JR. 2017. Origins of Combination Therapy for Tuberculosis: Lessons for Future Antimicrobial Development and Application. *MBio*, 8.
- KHIM, N., BOUCHIER, C., EKALA, M. T., INCARDONA, S., LIM, P., LEGRAND, E., JAMBOU, R., DOUNG, S., PUIJALON, O. M. & FANDEUR, T. 2005. Countrywide survey shows very high prevalence of Plasmodium falciparum multilocus resistance genotypes in Cambodia. *Antimicrob Agents Chemother*, 49, 3147-52.
- KIRK, K. 2001. Membrane transport in the malaria-infected erythrocyte. *Physiol Rev*, 81, 495-537.
- KLONIS, N., XIE, S. C., MCCAWE, J. M., CRESPO-ORTIZ, M. P., ZALOUMIS, S. G., SIMPSON, J. A. & TILLEY, L. 2013. Altered temporal response of malaria parasites determines differential sensitivity to artemisinin. *Proc Natl Acad Sci U S A*, 110, 5157-62.
- KOEPFLI, C., NGUITRAGOOL, W., HOFMANN, N. E., ROBINSON, L. J., OME-KAIUS, M., SATTABONGKOT, J., FELGER, I. & MUELLER, I. 2016. Sensitive and accurate quantification of human malaria parasites using droplet digital PCR (ddPCR). *Scientific Reports*, 6, 39183.
- KRAMER, K. J., KAN, S. C. & SIDDIQUI, W. A. 1982. Concentration of Plasmodium falciparum-infected erythrocytes by density gradient centrifugation in Percoll. *J Parasitol*, 68, 336-7.
- KUNJI, E. R. 2004. The role and structure of mitochondrial carriers. *FEBS Lett*, 564, 239-44.
- LAMBROS, C. & VANDERBERG, J. P. 1979. Synchronization of Plasmodium falciparum erythrocytic stages in culture. *J Parasitol*, 65, 418-20.
- LEANG, R., BARRETTE, A., BOUTH, D. M., MENARD, D., ABDUR, R., DUONG, S. & RINGWALD, P. 2013. Efficacy of dihydroartemisinin-piperaquine for treatment of uncomplicated Plasmodium falciparum and Plasmodium vivax in Cambodia, 2008 to 2010. *Antimicrob Agents Chemother*, 57, 818-26.
- LEANG, R., TAYLOR, W. R., BOUTH, D. M., SONG, L., TARNING, J., CHAR, M. C., KIM, S., WITKOWSKI, B., DURU, V., DOMERGUE, A., KHIM, N., RINGWALD, P. & MENARD, D. 2015. Evidence of Plasmodium falciparum Malaria Multidrug Resistance to Artemisinin and Piperaquine in Western Cambodia: Dihydroartemisinin-Piperaquine Open-Label Multicenter Clinical Assessment. *Antimicrob Agents Chemother*, 59, 4719-26.
- LEE, A. H. & FIDOCK, D. A. 2016. Evidence of a Mild Mutator Phenotype in Cambodian Plasmodium falciparum Malaria Parasites. *PLoS One*, 11, e0154166.
- LEE, M. A., TAN, C. H., AW, L. T., TANG, C. S., SINGH, M., LEE, S. H., CHIA, H. P. & YAP, E. P. 2002. Real-time fluorescence-based PCR for detection of malaria parasites. *J Clin Microbiol*, 40, 4343-5.

- LEHANE, A. M. & KIRK, K. 2008. Chloroquine resistance-conferring mutations in *pfprt* give rise to a chloroquine-associated H⁺ leak from the malaria parasite's digestive vacuole. *Antimicrob Agents Chemother*, 52, 4374-80.
- LEROY, D., MACINTYRE, F., ADOKE, Y., OUOBA, S., BARRY, A., MOMBO-NGOMA, G., NDONG NGOMO, J. M., VARO, R., DOSSOU, Y., TSHEFU, A. K., DUONG, T. T., PHUC, B. Q., LAURIJSENS, B., KLOPPER, R., KHIM, N., LEGRAND, E. & MÉNARD, D. 2019. African isolates show a high proportion of multiple copies of the *Plasmodium falciparum* plasmepsin-2 gene, a piperaquine resistance marker. *Malaria Journal*, 18, 126.
- LEVINE, N. D. 1988. Progress in taxonomy of the Apicomplexan protozoa. *J Protozool*, 35, 518-20.
- LEW, V. L., TIFFERT, T. & GINSBURG, H. 2003. Excess hemoglobin digestion and the osmotic stability of *Plasmodium falciparum*-infected red blood cells. *Blood*, 101, 4189-94.
- LI, G. Q., ARNOLD, K., GUO, X. B., JIAN, H. X. & FU, L. C. 1984. Randomised comparative study of mefloquine, qinghaosu, and pyrimethamine-sulfadoxine in patients with *falciparum* malaria. *Lancet*, 2, 1360-1.
- LI, H. & DURBIN, R. 2009. Fast and accurate short read alignment with Burrows-Wheeler transform. *Bioinformatics*, 25, 1754-60.
- LIM, P., ALKER, A. P., KHIM, N., SHAH, N. K., INCARDONA, S., DOUNG, S., YI, P., BOUTH, D. M., BOUCHIER, C., PUIJALON, O. M., MESHNICK, S. R., WONGSRICHANALAI, C., FANDEUR, T., LE BRAS, J., RINGWALD, P. & ARIEY, F. 2009. *Pfmdr1* copy number and artemisinin derivatives combination therapy failure in *falciparum* malaria in Cambodia. *Malaria Journal*, 8, 11.
- LIM, P., DEK, D., TRY, V., EASTMAN, R. T., CHY, S., SRENG, S., SUON, S., MAO, S., SOPHA, C., SAM, B., ASHLEY, E. A., MIOTTO, O., DONDORP, A. M., WHITE, N. J., SU, X. Z., CHAR, M. C., ANDERSON, J. M., AMARATUNGA, C., MENARD, D. & FAIRHURST, R. M. 2013. Ex vivo susceptibility of *Plasmodium falciparum* to antimalarial drugs in western, northern, and eastern Cambodia, 2011-2012: association with molecular markers. *Antimicrob Agents Chemother*, 57, 5277-83.
- LITHANATUDOM, P., WIPASA, J., INTI, P., CHAWANSUNTATI, K., SVASTI, S., FUCHAROEN, S., KANGWANPONG, D. & KAMPUANSAI, J. 2016. Hemoglobin E Prevalence among Ethnic Groups Residing in Malaria-Endemic Areas of Northern Thailand and Its Lack of Association with *Plasmodium falciparum* Invasion In Vitro. *PLoS One*, 11, e0148079.
- LIU, J., ISTVAN, E. S., GLUZMAN, I. Y., GROSS, J. & GOLDBERG, D. E. 2006. *Plasmodium falciparum* ensures its amino acid supply with multiple acquisition pathways and redundant proteolytic enzyme systems. *Proc Natl Acad Sci U S A*, 103, 8840-5.
- LOESBANLUECHAI, D., KOTANAN, N., DE COZAR, C., KOCHAKARN, T., ANSBRO, M. R., CHOTIVANICH, K., WHITE, N. J., WILAIRAT, P., LEE, M. C. S., GAMO, F. J., SANZ, L. M., CHOOKAJORN, T. & KUMPORN SIN, K. 2019.

- Overexpression of plasmepsin II and plasmepsin III does not directly cause reduction in *Plasmodium falciparum* sensitivity to artesunate, chloroquine and piperazine. *Int J Parasitol Drugs Drug Resist*, 9, 16-22.
- LOVETT, S. T. 2011. The DNA Exonucleases of *Escherichia coli*. *EcoSal Plus*, 4.
- LOZANO, S., GAMALLO, P., GONZALEZ-CORTES, C., PRESA MATILLA, J. L., FAIRHURST, R. M., HERREROS, E., AMARATUNGA, C. & RODRIGUES, J. 2018. Gametocytes from K13 Propeller Mutant *Plasmodium falciparum* Clinical Isolates Demonstrate Reduced Susceptibility to Dihydroartemisinin in the Male Gamete Exflagellation Inhibition Assay. *Antimicrob Agents Chemother*, 62.
- LUKENS, A. K., ROSS, L. S., HEIDEBRECHT, R., JAVIER GAMO, F., LAFUENTE-MONASTERIO, M. J., BOOKER, M. L., HARTL, D. L., WIEGAND, R. C. & WIRTH, D. F. 2014. Harnessing evolutionary fitness in *Plasmodium falciparum* for drug discovery and suppressing resistance. *Proc Natl Acad Sci U S A*, 111, 799-804.
- MACKINNON, M. J., LI, J., MOK, S., KORTOK, M. M., MARSH, K., PREISER, P. R. & BOZDECH, Z. 2009. Comparative transcriptional and genomic analysis of *Plasmodium falciparum* field isolates. *PLoS Pathog*, 5, e1000644.
- MAIER, A. G., MATUSCHEWSKI, K., ZHANG, M. & RUG, M. 2019. *Plasmodium falciparum*. *Trends Parasitol*, 35, 481-482.
- MALOY, S. & SCHAECHTER, M. 2006. The era of microbiology: a golden phoenix. *Int Microbiol*, 9, 1-7.
- MANSKE, H. M. & KWIATKOWSKI, D. P. 2009. LookSeq: a browser-based viewer for deep sequencing data. *Genome Res*, 19, 2125-32.
- MANSKE, M., MIOTTO, O., CAMPINO, S., AUBURN, S., ALMAGRO-GARCIA, J., MASLEN, G., O'BRIEN, J., DJIMDE, A., DOUMBO, O., ZONGO, I., OUEDRAOGO, J. B., MICHON, P., MUELLER, I., SIBA, P., NZILA, A., BORRMANN, S., KIARA, S. M., MARSH, K., JIANG, H., SU, X. Z., AMARATUNGA, C., FAIRHURST, R., SOCHEAT, D., NOSTEN, F., IMWONG, M., WHITE, N. J., SANDERS, M., ANASTASI, E., ALCOCK, D., DRURY, E., OYOLA, S., QUAIL, M. A., TURNER, D. J., RUANO-RUBIO, V., JYOTHI, D., AMENGA-ETEGO, L., HUBBART, C., JEFFREYS, A., ROWLANDS, K., SUTHERLAND, C., ROPER, C., MANGANO, V., MODIANO, D., TAN, J. C., FERDIG, M. T., AMAMBUA-NGWA, A., CONWAY, D. J., TAKALA-HARRISON, S., PLOWE, C. V., RAYNER, J. C., ROCKETT, K. A., CLARK, T. G., NEWBOLD, C. I., BERRIMAN, M., MACINNIS, B. & KWIATKOWSKI, D. P. 2012. Analysis of *Plasmodium falciparum* diversity in natural infections by deep sequencing. *Nature*, 487, 375-9.
- MANSON, P. 1894. On the Nature and Significance of the Crescentic and Flagellated Bodies in Malarial Blood. *Br Med J*, 2, 1306-8.
- MANSON, P. 1898. SURGEON-MAJOR RONALD ROSS'S RECENT INVESTIGATIONS on the MOSQUITO-MALARIA THEORY. *Br Med J*, 1, 1575-7.

- MARCHETTI, R. V., LEHANE, A. M., SHAFIK, S. H., WINTERBERG, M., MARTIN, R. E. & KIRK, K. 2015. A lactate and formate transporter in the intraerythrocytic malaria parasite, *Plasmodium falciparum*. *Nat Commun*, 6, 6721.
- MARCHIAFAVA, E., CELLI, A. 1885. Nove ricerche sulla infezione malarica. *Arch. Sci. Med. Torino*, 9, 311-340.
- MARTIN, R. E. & KIRK, K. 2004. The malaria parasite's chloroquine resistance transporter is a member of the drug/metabolite transporter superfamily. *Mol Biol Evol*, 21, 1938-49.
- MARTIN, R. E., MARCHETTI, R. V., COWAN, A. I., HOWITT, S. M., BROER, S. & KIRK, K. 2009. Chloroquine transport via the malaria parasite's chloroquine resistance transporter. *Science*, 325, 1680-2.
- MATHISON, B. A. & PRITT, B. S. 2017. Update on Malaria Diagnostics and Test Utilization. *J Clin Microbiol*, 55, 2009-2017.
- MCFADDEN, G. I. 2012. Plasmodia - don't. *Trends Parasitol*, 28, 306.
- MEISTER, S., PLOUFFE, D. M., KUHEN, K. L., BONAMY, G. M., WU, T., BARNES, S. W., BOPP, S. E., BORBOA, R., BRIGHT, A. T., CHE, J., COHEN, S., DHARIA, N. V., GAGARING, K., GETTAYACAMIN, M., GORDON, P., GROESSL, T., KATO, N., LEE, M. C., MCNAMARA, C. W., FIDOCK, D. A., NAGLE, A., NAM, T. G., RICHMOND, W., ROLAND, J., ROTTMANN, M., ZHOU, B., FROISSARD, P., GLYNNE, R. J., MAZIER, D., SATTABONGKOT, J., SCHULTZ, P. G., TUNTLAND, T., WALKER, J. R., ZHOU, Y., CHATTERJEE, A., DIAGANA, T. T. & WINZELER, E. A. 2011. Imaging of *Plasmodium* liver stages to drive next-generation antimalarial drug discovery. *Science*, 334, 1372-7.
- MENARD, D., CHAN, E. R., BENEDET, C., RATSIMBASOA, A., KIM, S., CHIM, P., DO, C., WITKOWSKI, B., DURAND, R., THELLIER, M., SEVERINI, C., LEGRAND, E., MUSSET, L., NOUR, B. Y., MERCEREAU-PUIJALON, O., SERRE, D. & ZIMMERMAN, P. A. 2013. Whole genome sequencing of field isolates reveals a common duplication of the Duffy binding protein gene in Malagasy *Plasmodium vivax* strains. *PLoS Negl Trop Dis*, 7, e2489.
- MENARD, D. & DONDORP, A. 2017. Antimalarial Drug Resistance: A Threat to Malaria Elimination. *Cold Spring Harb Perspect Med*, 7.
- MESHNICK, S. R. 2002. Artemisinin: mechanisms of action, resistance and toxicity. *Int J Parasitol*, 32, 1655-60.
- MESHNICK, S. R., THOMAS, A., RANZ, A., XU, C. M. & PAN, H. Z. 1991. Artemisinin (qinghaosu): the role of intracellular hemozoin in its mechanism of antimalarial action. *Mol Biochem Parasitol*, 49, 181-9.
- MIAO, J. & CUI, L. 2011. Rapid isolation of single malaria parasite-infected red blood cells by cell sorting. *Nat Protoc*, 6, 140-6.
- MILLER, L. H., ACKERMAN, H. C., SU, X. Z. & WELLEMS, T. E. 2013. Malaria biology and disease pathogenesis: insights for new treatments. *Nat Med*, 19, 156-67.

- MILLER, L. H., BARUCH, D. I., MARSH, K. & DOUMBO, O. K. 2002. The pathogenic basis of malaria. *Nature*, 415, 673-9.
- MILLER, R. L., IKRAM, S., ARMELAGOS, G. J., WALKER, R., HARER, W. B., SHIFF, C. J., BAGGETT, D., CARRIGAN, M. & MARET, S. M. 1994. Diagnosis of *Plasmodium falciparum* infections in mummies using the rapid manual ParaSight-F test. *Trans R Soc Trop Med Hyg*, 88, 31-2.
- MIOTTO, O., ALMAGRO-GARCIA, J., MANSKE, M., MACINNIS, B., CAMPINO, S., ROCKETT, K. A., AMARATUNGA, C., LIM, P., SUON, S., SRENG, S., ANDERSON, J. M., DUONG, S., NGUON, C., CHUOR, C. M., SAUNDERS, D., SE, Y., LON, C., FUKUDA, M. M., AMENGA-ETEGO, L., HODGSON, A. V., ASOALA, V., IMWONG, M., TAKALA-HARRISON, S., NOSTEN, F., SU, X. Z., RINGWALD, P., ARIEY, F., DOLECEK, C., HIEN, T. T., BONI, M. F., THAI, C. Q., AMAMBUA-NGWA, A., CONWAY, D. J., DJIMDE, A. A., DOUMBO, O. K., ZONGO, I., OUEDRAOGO, J. B., ALCOCK, D., DRURY, E., AUBURN, S., KOCH, O., SANDERS, M., HUBBART, C., MASLEN, G., RUANO-RUBIO, V., JYOTHI, D., MILES, A., O'BRIEN, J., GAMBLE, C., OYOLA, S. O., RAYNER, J. C., NEWBOLD, C. I., BERRIMAN, M., SPENCER, C. C., MCVEAN, G., DAY, N. P., WHITE, N. J., BETHELL, D., DONDORP, A. M., PLOWE, C. V., FAIRHURST, R. M. & KWIATKOWSKI, D. P. 2013. Multiple populations of artemisinin-resistant *Plasmodium falciparum* in Cambodia. *Nat Genet*, 45, 648-55.
- MIOTTO, O., AMATO, R., ASHLEY, E. A., MACINNIS, B., ALMAGRO-GARCIA, J., AMARATUNGA, C., LIM, P., MEAD, D., OYOLA, S. O., DHORDA, M., IMWONG, M., WOODROW, C., MANSKE, M., STALKER, J., DRURY, E., CAMPINO, S., AMENGA-ETEGO, L., THANH, T. N., TRAN, H. T., RINGWALD, P., BETHELL, D., NOSTEN, F., PHYO, A. P., PUKRITTAYAKAMEE, S., CHOTIVANICH, K., CHUOR, C. M., NGUON, C., SUON, S., SRENG, S., NEWTON, P. N., MAYXAY, M., KHANTHAVONG, M., HONGVANTHONG, B., HTUT, Y., HAN, K. T., KYAW, M. P., FAIZ, M. A., FANELLO, C. I., ONYAMBOKO, M., MOKUOLU, O. A., JACOB, C. G., TAKALA-HARRISON, S., PLOWE, C. V., DAY, N. P., DONDORP, A. M., SPENCER, C. C., MCVEAN, G., FAIRHURST, R. M., WHITE, N. J. & KWIATKOWSKI, D. P. 2015. Genetic architecture of artemisinin-resistant *Plasmodium falciparum*. *Nat Genet*, 47, 226-34.
- MITCHISON, T. J. 1994. Towards a pharmacological genetics. *Chem Biol*, 1, 3-6.
- MOHAMMED, A., NDARO, A., KALINGA, A., MANJURANO, A., MOSHA, J. F., MOSHA, D. F., VAN ZWETSELAAR, M., KOENDERINK, J. B., MOSHA, F. W., ALIFRANGIS, M., REYBURN, H., ROPER, C. & KAVISHE, R. A. 2013. Trends in chloroquine resistance marker, Pfcrt-K76T mutation ten years after chloroquine withdrawal in Tanzania. *Malar J*, 12, 415.
- MOK, S., ASHLEY, E. A., FERREIRA, P. E., ZHU, L., LIN, Z., YEO, T., CHOTIVANICH, K., IMWONG, M., PUKRITTAYAKAMEE, S., DHORDA, M., NGUON, C., LIM, P., AMARATUNGA, C., SUON, S., HIEN, T. T., HTUT, Y., FAIZ, M. A., ONYAMBOKO, M. A., MAYXAY, M., NEWTON, P. N., TRIPURA, R., WOODROW, C. J., MIOTTO, O., KWIATKOWSKI, D. P., NOSTEN, F., DAY, N. P., PREISER, P. R., WHITE, N. J., DONDORP, A. M., FAIRHURST, R. M. & BOZDECH, Z. 2015. Drug resistance. Population transcriptomics of human malaria parasites reveals the mechanism of artemisinin resistance. *Science*, 347, 431-5.

- MOK, S., IMWONG, M., MACKINNON, M. J., SIM, J., RAMADOSS, R., YI, P., MAYXAY, M., CHOTIVANICH, K., LIONG, K. Y., RUSSELL, B., SOCHEAT, D., NEWTON, P. N., DAY, N. P., WHITE, N. J., PREISER, P. R., NOSTEN, F., DONDORP, A. M. & BOZDECH, Z. 2011. Artemisinin resistance in *Plasmodium falciparum* is associated with an altered temporal pattern of transcription. *BMC Genomics*, 12, 391.
- MOK, S., LIONG, K. Y., LIM, E. H., HUANG, X., ZHU, L., PREISER, P. R. & BOZDECH, Z. 2014. Structural polymorphism in the promoter of *pfmrp2* confers *Plasmodium falciparum* tolerance to quinoline drugs. *Mol Microbiol*, 91, 918-34.
- MOON, R. W., HALL, J., RANGKUTI, F., HO, Y. S., ALMOND, N., MITCHELL, G. H., PAIN, A., HOLDER, A. A. & BLACKMAN, M. J. 2013. Adaptation of the genetically tractable malaria pathogen *Plasmodium knowlesi* to continuous culture in human erythrocytes. *Proc Natl Acad Sci U S A*, 110, 531-6.
- MORRISON, A. & SUGINO, A. 1994. The 3'→5' exonucleases of both DNA polymerases delta and epsilon participate in correcting errors of DNA replication in *Saccharomyces cerevisiae*. *Mol Gen Genet*, 242, 289-96.
- MOURA, P. A., DAME, J. B. & FIDOCK, D. A. 2009. Role of *Plasmodium falciparum* digestive vacuole plasmepsins in the specificity and antimalarial mode of action of cysteine and aspartic protease inhibitors. *Antimicrob Agents Chemother*, 53, 4968-78.
- MUELLER, I., ZIMMERMAN, P. A. & REEDER, J. C. 2007. *Plasmodium malariae* and *Plasmodium ovale*--the "bashful" malaria parasites. *Trends Parasitol*, 23, 278-83.
- MUKHERJEE, A., GAGNON, D., WIRTH, D. F. & RICHARD, D. 2018. Inactivation of Plasmepsins 2 and 3 Sensitizes *Plasmodium falciparum* to the Antimalarial Drug Piperaquine. *Antimicrob Agents Chemother*, 62.
- MUNKONGDEE, T., TANAKULMAS, J., BUTTHEP, P., WINICHAGOON, P., MAIN, B., YIANNAKIS, M., GEORGE, J., DEVENISH, R., FUCHAROEN, S. & SVASTI, S. 2016. Molecular Epidemiology of Hemoglobinopathies in Cambodia. *Hemoglobin*, 40, 163-167.
- MURRAY, C. J., ROSENFELD, L. C., LIM, S. S., ANDREWS, K. G., FOREMAN, K. J., HARING, D., FULLMAN, N., NAGHAVI, M., LOZANO, R. & LOPEZ, A. D. 2012. Global malaria mortality between 1980 and 2010: a systematic analysis. *Lancet*, 379, 413-31.
- MWANZA, S., JOSHI, S., NAMBOZI, M., CHILESHE, J., MALUNGA, P., KABUYA, J. B., HACHIZOVU, S., MANYANDO, C., MULENGA, M. & LAUFER, M. 2016. The return of chloroquine-susceptible *Plasmodium falciparum* malaria in Zambia. *Malar J*, 15, 584.
- NAKATANI, K., ISHIKAWA, H., AONO, S. & MIZUTANI, Y. 2014. Identification of Essential Histidine Residues Involved in Heme Binding and Hemozoin Formation in Heme Detoxification Protein from *Plasmodium falciparum*. *Scientific Reports*, 4, 6137.

- NGOTHO, P., SOARES, A. B., HENTZSCHEL, F., ACHCAR, F., BERTUCCINI, L. & MARTI, M. 2019. Revisiting gametocyte biology in malaria parasites. *FEMS Microbiol Rev*, 43, 401-414.
- NOEDL, H., SE, Y., SCHAECHER, K., SMITH, B. L., SOCHEAT, D., FUKUDA, M. M. & ARTEMISININ RESISTANCE IN CAMBODIA 1 STUDY, C. 2008. Evidence of artemisinin-resistant malaria in western Cambodia. *N Engl J Med*, 359, 2619-20.
- NOSTEN, F., TER KUILE, F., CHONGSUPHAJASIDDHI, T., LUXEMBURGER, C., WEBSTER, H. K., EDSTEIN, M., PHAIPUN, L., THEW, K. L. & WHITE, N. J. 1991. Mefloquine-resistant falciparum malaria on the Thai-Burmese border. *Lancet*, 337, 1140-3.
- ODUOLA, A. M., MILHOUS, W. K., WEATHERLY, N. F., BOWDRE, J. H. & DESJARDINS, R. E. 1988a. Plasmodium falciparum: induction of resistance to mefloquine in cloned strains by continuous drug exposure in vitro. *Exp Parasitol*, 67, 354-60.
- ODUOLA, A. M., WEATHERLY, N. F., BOWDRE, J. H. & DESJARDINS, R. E. 1988b. Plasmodium falciparum: cloning by single-erythrocyte micromanipulation and heterogeneity in vitro. *Exp Parasitol*, 66, 86-95.
- OMARA-OPYENE, A. L., MOURA, P. A., SULSONA, C. R., BONILLA, J. A., YOWELL, C. A., FUJIOKA, H., FIDOCK, D. A. & DAME, J. B. 2004. Genetic disruption of the Plasmodium falciparum digestive vacuole plasmepsins demonstrates their functional redundancy. *J Biol Chem*, 279, 54088-96.
- PALOQUE, L., RAMADANI, A. P., MERCEREAU-PUIJALON, O., AUGEREAU, J. M. & BENOIT-VICAL, F. 2016. Plasmodium falciparum: multifaceted resistance to artemisinins. *Malar J*, 15, 149.
- PAYNE, D. 1987. Spread of chloroquine resistance in Plasmodium falciparum. *Parasitol Today*, 3, 241-6.
- PELLEAU, S., MOSS, E. L., DHINGRA, S. K., VOLNEY, B., CASTERAS, J., GABRYSZEWSKI, S. J., VOLKMAN, S. K., WIRTH, D. F., LEGRAND, E., FIDOCK, D. A., NEAFSEY, D. E. & MUSSET, L. 2015. Adaptive evolution of malaria parasites in French Guiana: Reversal of chloroquine resistance by acquisition of a mutation in pfert. *Proc Natl Acad Sci U S A*, 112, 11672-7.
- PETERS, W. 1970. *Chemotherapy and Drug Resistance in Malaria*, London, Academic Press.
- PETERS, W. 1987. *Chemotherapy and Drug Resistance in Malaria*, London, Academic Press.
- PHILLIPS, M. A., BURROWS, J. N., MANYANDO, C., VAN HUIJSDUIJNEN, R. H., VAN VOORHIS, W. C. & WELLS, T. N. C. 2017. Malaria. *Nat Rev Dis Primers*, 3, 17050.
- PICOT, S., OLLIARO, P., DE MONBRISON, F., BIENVENU, A. L., PRICE, R. N. & RINGWALD, P. 2009. A systematic review and meta-analysis of evidence for

correlation between molecular markers of parasite resistance and treatment outcome in falciparum malaria. *Malar J*, 8, 89.

- PONNUDURAI, T., LEEUWENBERG, A. D. & MEUWISSEN, J. H. 1981. Chloroquine sensitivity of isolates of *Plasmodium falciparum* adapted to in vitro culture. *Trop Geogr Med*, 33, 50-4.
- PRESTON, M. D., CAMPINO, S., ASSEFA, S. A., ECHEVERRY, D. F., OCHOLLA, H., AMAMBUA-NGWA, A., STEWART, L. B., CONWAY, D. J., BORRMANN, S., MICHON, P., ZONGO, I., OUEDRAOGO, J. B., DJIMDE, A. A., DOUMBO, O. K., NOSTEN, F., PAIN, A., BOUSEMA, T., DRAKELEY, C. J., FAIRHURST, R. M., SUTHERLAND, C. J., ROPER, C. & CLARK, T. G. 2014. A barcode of organellar genome polymorphisms identifies the geographic origin of *Plasmodium falciparum* strains. *Nat Commun*, 5, 4052.
- PRICE, R. N., DOUGLAS, N. M. & ANSTEY, N. M. 2009. New developments in *Plasmodium vivax* malaria: severe disease and the rise of chloroquine resistance. *Curr Opin Infect Dis*, 22, 430-5.
- PRICE, R. N., TJITRA, E., GUERRA, C. A., YEUNG, S., WHITE, N. J. & ANSTEY, N. M. 2007. Vivax malaria: neglected and not benign. *Am J Trop Med Hyg*, 77, 79-87.
- PRICE, R. N., UHLEMANN, A. C., BROCKMAN, A., MCGREADY, R., ASHLEY, E., PHAIPUN, L., PATEL, R., LAING, K., LOOAREESUWAN, S., WHITE, N. J., NOSTEN, F. & KRISHNA, S. 2004. Mefloquine resistance in *Plasmodium falciparum* and increased pfmdr1 gene copy number. *Lancet*, 364, 438-447.
- PRICE, R. N., UHLEMANN, A. C., VAN VUGT, M., BROCKMAN, A., HUTAGALUNG, R., NAIR, S., NASH, D., SINGHASIVANON, P., ANDERSON, T. J., KRISHNA, S., WHITE, N. J. & NOSTEN, F. 2006. Molecular and pharmacological determinants of the therapeutic response to artemether-lumefantrine in multidrug-resistant *Plasmodium falciparum* malaria. *Clin Infect Dis*, 42, 1570-7.
- PRYCE, J. & HINE, P. 2019. Pyronaridine-artesunate for treating uncomplicated *Plasmodium falciparum* malaria. *Cochrane Database Syst Rev*, 1, CD006404.
- PUKRITTAYAKAMEE, S., SUPANARANOND, W., LOOAREESUWAN, S., VANIJANONTA, S. & WHITE, N. J. 1994. Quinine in severe falciparum malaria: evidence of declining efficacy in Thailand. *Trans R Soc Trop Med Hyg*, 88, 324-7.
- PULCINI, S., STAINES, H. M., LEE, A. H., SHAFIK, S. H., BOUYER, G., MOORE, C. M., DALEY, D. A., HOKE, M. J., ALTENHOFEN, L. M., PAINTER, H. J., MU, J., FERGUSON, D. J., LLINAS, M., MARTIN, R. E., FIDOCK, D. A., COOPER, R. A. & KRISHNA, S. 2015. Mutations in the *Plasmodium falciparum* chloroquine resistance transporter, PfCRT, enlarge the parasite's food vacuole and alter drug sensitivities. *Sci Rep*, 5, 14552.
- REED, M. B., SALIBA, K. J., CARUANA, S. R., KIRK, K. & COWMAN, A. F. 2000. Pgh1 modulates sensitivity and resistance to multiple antimalarials in *Plasmodium falciparum*. *Nature*, 403, 906-9.
- REILING, S. J. & ROHRBACH, P. 2015. Monitoring PfMDR1 transport in *Plasmodium falciparum*. *Malaria Journal*, 14, 270.

- RIDLEY, R. G. 1998. Malaria: dissecting chloroquine resistance. *Curr Biol*, 8, R346-9.
- RIDLEY, R. G., WHITE, J. H., MCALEESE, S. M., GOMAN, M., ALANO, P., DE VRIES, E. & KILBEY, B. J. 1991. DNA polymerase delta: gene sequences from *Plasmodium falciparum* indicate that this enzyme is more highly conserved than DNA polymerase alpha. *Nucleic Acids Res*, 19, 6731-6.
- ROBINSON, A. J. & KUNJI, E. R. 2006. Mitochondrial carriers in the cytoplasmic state have a common substrate binding site. *Proc Natl Acad Sci U S A*, 103, 2617-22.
- ROCAMORA, F., ZHU, L., LIONG, K. Y., DONDORP, A., MIOTTO, O., MOK, S. & BOZDECH, Z. 2018. Oxidative stress and protein damage responses mediate artemisinin resistance in malaria parasites. *PLoS Pathog*, 14, e1006930.
- ROCK, E. P., MARSH, K., SAUL, A. J., WELLEMS, T. E., TAYLOR, D. W., MALOY, W. L. & HOWARD, R. J. 1987. Comparative analysis of the *Plasmodium falciparum* histidine-rich proteins HRP-I, HRP-II and HRP-III in malaria parasites of diverse origin. *Parasitology*, 95 (Pt 2), 209-27.
- ROSARIO, V. 1981. Cloning of naturally occurring mixed infections of malaria parasites. *Science*, 212, 1037-8.
- ROSENTHAL, P. J. 2013. The interplay between drug resistance and fitness in malaria parasites. *Mol Microbiol*, 89, 1025-38.
- ROSS, L. S., DHINGRA, S. K., MOK, S., YEO, T., WICHT, K. J., KUMPORN SIN, K., TAKALA-HARRISON, S., WITKOWSKI, B., FAIRHURST, R. M., ARIEY, F., MENARD, D. & FIDOCK, D. A. 2018a. Emerging Southeast Asian PfCRT mutations confer *Plasmodium falciparum* resistance to the first-line antimalarial piperazine. *Nat Commun*, 9, 3314.
- ROSS, L. S., LAFUENTE-MONASTERIO, M. J., SAKATA-KATO, T., MANDT, R. E. K., GAMO, F. J., WIRTH, D. F. & LUKENS, A. K. 2018b. Identification of Collateral Sensitivity to Dihydroorotate Dehydrogenase Inhibitors in *Plasmodium falciparum*. *ACS Infect Dis*, 4, 508-515.
- ROSS, R. 1897. On some Peculiar Pigmented Cells Found in Two Mosquitos Fed on Malarial Blood. *Br Med J*, 2, 1786-8.
- RUPRECHT, J. J., HELLAWELL, A. M., HARDING, M., CRICHTON, P. G., MCCOY, A. J. & KUNJI, E. R. 2014. Structures of yeast mitochondrial ADP/ATP carriers support a domain-based alternating-access transport mechanism. *Proc Natl Acad Sci U S A*, 111, E426-34.
- SA, J. M., KASLOW, S. R., KRAUSE, M. A., MELENDEZ-MUNIZ, V. A., SALZMAN, R. E., KITE, W. A., ZHANG, M., MORAES BARROS, R. R., MU, J., HAN, P. K., MERSHON, J. P., FIGAN, C. E., CALEON, R. L., RAHMAN, R. S., GIBSON, T. J., AMARATUNGA, C., NISHIGUCHI, E. P., BREGLIO, K. F., ENGELS, T. M., VELMURUGAN, S., RICKLEFS, S., STRAIMER, J., GNADIG, N. F., DENG, B., LIU, A., DIOUF, A., MIURA, K., TULLO, G. S., EASTMAN, R. T., CHAKRAVARTY, S., JAMES, E. R., UDENZE, K., LI, S., STURDEVANT, D. E., GWADZ, R. W., PORCELLA, S. F., LONG, C. A., FIDOCK, D. A., THOMAS, M. L., FAY, M. P., SIM, B. K. L., HOFFMAN, S. L., ADAMS, J. H., FAIRHURST, R.

- M., SU, X. Z. & WELLEMS, T. E. 2018. Artemisinin resistance phenotypes and K13 inheritance in a *Plasmodium falciparum* cross and Aotus model. *Proc Natl Acad Sci U S A*, 115, 12513-12518.
- SA, J. M., TWU, O., HAYTON, K., REYES, S., FAY, M. P., RINGWALD, P. & WELLEMS, T. E. 2009. Geographic patterns of *Plasmodium falciparum* drug resistance distinguished by differential responses to amodiaquine and chloroquine. *Proc Natl Acad Sci U S A*, 106, 18883-9.
- SACHANONTA, N., CHOTIVANICH, K., CHAISRI, U., TURNER, G. D., FERGUSON, D. J., DAY, N. P. & PONGPONRATN, E. 2011. Ultrastructural and real-time microscopic changes in *P. falciparum*-infected red blood cells following treatment with antimalarial drugs. *Ultrastruct Pathol*, 35, 214-25.
- SANDER, J. D. & JOUNG, J. K. 2014. CRISPR-Cas systems for editing, regulating and targeting genomes. *Nat Biotechnol*, 32, 347-55.
- SAUNDERS, D. L., VANACHAYANGKUL, P., LON, C., PROGRAM, U. S. A. M. M. R., NATIONAL CENTER FOR PARASITOLOGY, E., MALARIA, C. & ROYAL CAMBODIAN ARMED, F. 2014. Dihydroartemisinin-piperaquine failure in Cambodia. *N Engl J Med*, 371, 484-5.
- SAUVAGE, V., AUBERT, D., ESCOTTE-BINET, S. & VILLENA, I. 2009. The role of ATP-binding cassette (ABC) proteins in protozoan parasites. *Mol Biochem Parasitol*, 167, 81-94.
- SCHENONE, M., DANCIK, V., WAGNER, B. K. & CLEMONS, P. A. 2013. Target identification and mechanism of action in chemical biology and drug discovery. *Nat Chem Biol*, 9, 232-40.
- SCHLAGENHAUF, P. 2004. Malaria: from prehistory to present. *Infect Dis Clin North Am*, 18, 189-205, table of contents.
- SCHLITZER, M. 2007. Malaria chemotherapeutics part I: History of antimalarial drug development, currently used therapeutics, and drugs in clinical development. *ChemMedChem*, 2, 944-86.
- SCHUSTER, F. L. 2002. Cultivation of plasmodium spp. *Clin Microbiol Rev*, 15, 355-64.
- SHEARER, F. M., HUANG, Z., WEISS, D. J., WIEBE, A., GIBSON, H. S., BATTLE, K. E., PIGOTT, D. M., BRADY, O. J., PUTAPORNTIP, C., JONGWUTIWES, S., LAU, Y. L., MANSKE, M., AMATO, R., ELYAZAR, I. R., VYTHILINGAM, I., BHATT, S., GETHING, P. W., SINGH, B., GOLDING, N., HAY, S. I. & MOYES, C. L. 2016. Estimating Geographical Variation in the Risk of Zoonotic *Plasmodium knowlesi* Infection in Countries Eliminating Malaria. *PLoS Negl Trop Dis*, 10, e0004915.
- SHEVELEV, I. V. & HÜBSCHER, U. 2002. The 3'-5' exonucleases. *Nature Reviews Molecular Cell Biology*, 3, 364-376.
- SHIFF, C. J., PREMJI, Z. & MINJAS, J. N. 1993. The rapid manual ParaSight-F test. A new diagnostic tool for *Plasmodium falciparum* infection. *Trans R Soc Trop Med Hyg*, 87, 646-8.

- SIDHU, A. B., UHLEMANN, A. C., VALDERRAMOS, S. G., VALDERRAMOS, J. C., KRISHNA, S. & FIDOCK, D. A. 2006. Decreasing pfmdr1 copy number in plasmodium falciparum malaria heightens susceptibility to mefloquine, lumefantrine, halofantrine, quinine, and artemisinin. *J Infect Dis*, 194, 528-35.
- SIM, I. K., DAVIS, T. M. & ILETT, K. F. 2005. Effects of a high-fat meal on the relative oral bioavailability of piperazine. *Antimicrob Agents Chemother*, 49, 2407-11.
- SINHA, A., HUGHES, K. R., MODRZYNSKA, K. K., OTTO, T. D., PFANDER, C., DICKENS, N. J., RELIGA, A. A., BUSHELL, E., GRAHAM, A. L., CAMERON, R., KAFSACK, B. F. C., WILLIAMS, A. E., LLINAS, M., BERRIMAN, M., BILLKER, O. & WATERS, A. P. 2014. A cascade of DNA-binding proteins for sexual commitment and development in Plasmodium. *Nature*, 507, 253-257.
- SISOWATH, C., STROMBERG, J., MARTENSSON, A., MSELLEM, M., OBONDO, C., BJORKMAN, A. & GIL, J. P. 2005. In vivo selection of Plasmodium falciparum pfmdr1 86N coding alleles by artemether-lumefantrine (Coartem). *J Infect Dis*, 191, 1014-7.
- SKINNER, T. S., MANNING, L. S., JOHNSTON, W. A. & DAVIS, T. M. 1996. In vitro stage-specific sensitivity of Plasmodium falciparum to quinine and artemisinin drugs. *Int J Parasitol*, 26, 519-25.
- SMALLEY, M. E. & SINDEN, R. E. 1977. Plasmodium falciparum gametocytes: their longevity and infectivity. *Parasitology*, 74, 1-8.
- SMILKSTEIN, M., SRIWILAIJAROEN, N., KELLY, J. X., WILAIRAT, P. & RISCOE, M. 2004. Simple and Inexpensive Fluorescence-Based Technique for High-Throughput Antimalarial Drug Screening. *Antimicrobial Agents and Chemotherapy*, 48, 1803-1806.
- SNOUNOU, G. & BECK, H. P. 1998. The use of PCR genotyping in the assessment of recrudescence or reinfection after antimalarial drug treatment. *Parasitol Today*, 14, 462-7.
- SPRING, M. D., LIN, J. T., MANNING, J. E., VANACHAYANGKUL, P., SOMETHY, S., BUN, R., SE, Y., CHANN, S., ITTIVERAKUL, M., SIA-NGAM, P., KUNTAWUNGINN, W., ARSANOK, M., BUATHONG, N., CHAORATTANAKAWEE, S., GOSI, P., TA-AKSORN, W., CHANARAT, N., SUNDRAGES, S., KONG, N., HENG, T. K., NOU, S., TEJA-ISAVADHARM, P., PICHYANGKUL, S., PHANN, S. T., BALASUBRAMANIAN, S., JULIANO, J. J., MESHNICK, S. R., CHOUR, C. M., PROM, S., LANTERI, C. A., LON, C. & SAUNDERS, D. L. 2015. Dihydroartemisinin-piperazine failure associated with a triple mutant including kelch13 C580Y in Cambodia: an observational cohort study. *Lancet Infect Dis*, 15, 683-91.
- STANLEY, H. A., LANGRETH, S. G., REESE, R. T. & TRAGER, W. 1982. Plasmodium falciparum merozoites: isolation by density gradient centrifugation using Percoll and antigenic analysis. *J Parasitol*, 68, 1059-67.
- STEPNIEWSKA, K., TAYLOR, W., SIRIMA, S. B., OUEDRAOGO, E. B., OUEDRAOGO, A., GANSANÉ, A., SIMPSON, J. A., MORGAN, C. C., WHITE, N.

- J. & KIECHEL, J.-R. 2009. Population pharmacokinetics of artesunate and amodiaquine in African children. *Malaria Journal*, 8, 200.
- STRAIMER, J., GNADIG, N. F., WITKOWSKI, B., AMARATUNGA, C., DURU, V., RAMADANI, A. P., DACHEUX, M., KHIM, N., ZHANG, L., LAM, S., GREGORY, P. D., URNOV, F. D., MERCEREAU-PUIJALON, O., BENOIT-VICAL, F., FAIRHURST, R. M., MENARD, D. & FIDOCK, D. A. 2015. Drug resistance. K13-propeller mutations confer artemisinin resistance in *Plasmodium falciparum* clinical isolates. *Science*, 347, 428-31.
- STRAIMER, J., LEE, M. C., LEE, A. H., ZEITLER, B., WILLIAMS, A. E., PEARL, J. R., ZHANG, L., REBAR, E. J., GREGORY, P. D., LLINAS, M., URNOV, F. D. & FIDOCK, D. A. 2012. Site-specific genome editing in *Plasmodium falciparum* using engineered zinc-finger nucleases. *Nat Methods*, 9, 993-8.
- SU, X. Z. 2014. Tracing the geographic origins of *Plasmodium falciparum* malaria parasites. *Pathog Glob Health*, 108, 261-2.
- SU, X. Z., LANE, K. D., XIA, L., SA, J. M. & WELLEMS, T. E. 2019. *Plasmodium* Genomics and Genetics: New Insights into Malaria Pathogenesis, Drug Resistance, Epidemiology, and Evolution. *Clin Microbiol Rev*, 32.
- SUBRAMANIAN, S., HARDT, M., CHOE, Y., NILES, R. K., JOHANSEN, E. B., LEGAC, J., GUT, J., KERR, I. D., CRAIK, C. S. & ROSENTHAL, P. J. 2009. Hemoglobin cleavage site-specificity of the *Plasmodium falciparum* cysteine proteases falcipain-2 and falcipain-3. *PLoS One*, 4, e5156.
- SULLIVAN, D. J., JR., GLUZMAN, I. Y., RUSSELL, D. G. & GOLDBERG, D. E. 1996. On the molecular mechanism of chloroquine's antimalarial action. *Proc Natl Acad Sci U S A*, 93, 11865-70.
- SUMMERS, R. L., NASH, M. N. & MARTIN, R. E. 2012. Know your enemy: understanding the role of PfCRT in drug resistance could lead to new antimalarial tactics. *Cell Mol Life Sci*, 69, 1967-95.
- SUTHERLAND, C. J. 2017. Rescuing artemisinin combination therapy in Africa. *Lancet Glob Health*, 5, e8-e9.
- SUTHERLAND, C. J., TANOMSING, N., NOLDER, D., OGUIKE, M., JENNISON, C., PUKRITTAYAKAMEE, S., DOLECEK, C., HIEN, T. T., DO ROSÁRIO, V. E., AREZ, A. P., PINTO, J., MICHON, P., ESCALANTE, A. A., NOSTEN, F., BURKE, M., LEE, R., BLAZE, M., OTTO, T. D., BARNWELL, J. W., PAIN, A., WILLIAMS, J., WHITE, N. J., DAY, N. P. J., SNOUNOU, G., LOCKHART, P. J., CHIODINI, P. L., IMWONG, M. & POLLEY, S. D. 2010. Two Nonrecombining Sympatric Forms of the Human Malaria Parasite *Plasmodium ovale* Occur Globally. *The Journal of Infectious Diseases*, 201, 1544-1550.
- SWAN, M. K., JOHNSON, R. E., PRAKASH, L., PRAKASH, S. & AGGARWAL, A. K. 2009. Structural basis of high-fidelity DNA synthesis by yeast DNA polymerase delta. *Nat Struct Mol Biol*, 16, 979-86.
- SZYMCZAK, A. L., WORKMAN, C. J., WANG, Y., VIGNALI, K. M., DILIOGLOU, S., VANIN, E. F. & VIGNALI, D. A. 2004. Correction of multi-gene deficiency in vivo

using a single 'self-cleaving' 2A peptide-based retroviral vector. *Nat Biotechnol*, 22, 589-94.

- TAKALA-HARRISON, S., CLARK, T. G., JACOB, C. G., CUMMINGS, M. P., MIOTTO, O., DONDORP, A. M., FUKUDA, M. M., NOSTEN, F., NOEDL, H., IMWONG, M., BETHELL, D., SE, Y., LON, C., TYNER, S. D., SAUNDERS, D. L., SOCHEAT, D., ARIEY, F., PHYO, A. P., STARZENGRUBER, P., FUEHRER, H. P., SWOBODA, P., STEPNIIEWSKA, K., FLEGG, J., ARZE, C., CERQUEIRA, G. C., SILVA, J. C., RICKLEFS, S. M., PORCELLA, S. F., STEPHENS, R. M., ADAMS, M., KENEFIC, L. J., CAMPINO, S., AUBURN, S., MACINNIS, B., KWIATKOWSKI, D. P., SU, X. Z., WHITE, N. J., RINGWALD, P. & PLOWE, C. V. 2013. Genetic loci associated with delayed clearance of *Plasmodium falciparum* following artemisinin treatment in Southeast Asia. *Proc Natl Acad Sci U S A*, 110, 240-5.
- TALISUNA, A. O., BLOLAND, P. & D'ALESSANDRO, U. 2004. History, dynamics, and public health importance of malaria parasite resistance. *Clin Microbiol Rev*, 17, 235-54.
- TARNING, J., ASHLEY, E. A., LINDEGARDH, N., STEPNIIEWSKA, K., PHAIPHUN, L., DAY, N. P., MCGREADY, R., ASHTON, M., NOSTEN, F. & WHITE, N. J. 2008. Population pharmacokinetics of piperazine after two different treatment regimens with dihydroartemisinin-piperazine in patients with *Plasmodium falciparum* malaria in Thailand. *Antimicrob Agents Chemother*, 52, 1052-61.
- TARNING, J., LINDEGARDH, N., ANNERBERG, A., SINGTOROJ, T., DAY, N. P., ASHTON, M. & WHITE, N. J. 2005. Pitfalls in estimating piperazine elimination. *Antimicrob Agents Chemother*, 49, 5127-8.
- TEKLEHAIMANOT, A. & MEJIA, P. 2008. Malaria and poverty. *Ann N Y Acad Sci*, 1136, 32-7.
- THAM, J. M., LEE, S. H., TAN, T. M., TING, R. C. & KARA, U. A. 1999. Detection and species determination of malaria parasites by PCR: comparison with microscopy and with ParaSight-F and ICT malaria Pf tests in a clinical environment. *J Clin Microbiol*, 37, 1269-73.
- TILLEY, L., STRAIMER, J., GNADIG, N. F., RALPH, S. A. & FIDOCK, D. A. 2016. Artemisinin Action and Resistance in *Plasmodium falciparum*. *Trends Parasitol*, 32, 682-696.
- TRAGER, W. & JENSEN, J. B. 1976. Human malaria parasites in continuous culture. *Science*, 193, 673-5.
- TSE, E. G., KORSIK, M. & TODD, M. H. 2019. The past, present and future of anti-malarial medicines. *Malaria Journal*, 18, 93.
- TU, Y. 2011. The discovery of artemisinin (qinghaosu) and gifts from Chinese medicine. *Nature Medicine*, 17, 1217-1220.
- VALDERRAMOS, S. G. & FIDOCK, D. A. 2006. Transporters involved in resistance to antimalarial drugs. *Trends Pharmacol Sci*, 27, 594-601.

- VAN DER PLUIJM, R. W., IMWONG, M., CHAU, N. H., HOA, N. T., THUY-NHIEN, N. T., THANH, N. V., JITTAMALA, P., HANBOONKUNUPAKARN, B., CHUTASMIT, K., SAELOW, C., RUNJARERN, R., KAEWMOK, W., TRIPURA, R., PETO, T. J., YOK, S., SUON, S., SRENG, S., MAO, S., OUN, S., YEN, S., AMARATUNGA, C., LEK, D., HUY, R., DHORDA, M., CHOTIVANICH, K., ASHLEY, E. A., MUKAKA, M., WAITHIRA, N., CHEAH, P. Y., MAUDE, R. J., AMATO, R., PEARSON, R. D., GONCALVES, S., JACOB, C. G., HAMILTON, W. L., FAIRHURST, R. M., TARNING, J., WINTERBERG, M., KWIATKOWSKI, D. P., PUKRITTAYAKAMEE, S., HIEN, T. T., DAY, N. P., MIOTTO, O., WHITE, N. J. & DONDORP, A. M. 2019. Determinants of dihydroartemisinin-piperaquine treatment failure in *Plasmodium falciparum* malaria in Cambodia, Thailand, and Vietnam: a prospective clinical, pharmacological, and genetic study. *Lancet Infect Dis*.
- VEIGA, M. I., DHINGRA, S. K., HENRICH, P. P., STRAIMER, J., GNÄDIG, N., UHLEMANN, A.-C., MARTIN, R. E., LEHANE, A. M. & FIDOCK, D. A. 2016a. Globally prevalent PfMDR1 mutations modulate *Plasmodium falciparum* susceptibility to artemisinin-based combination therapies. *Nature Communications*, 7, 11553.
- VEIGA, M. I., DHINGRA, S. K., HENRICH, P. P., STRAIMER, J., GNADIG, N., UHLEMANN, A. C., MARTIN, R. E., LEHANE, A. M. & FIDOCK, D. A. 2016b. Globally prevalent PfMDR1 mutations modulate *Plasmodium falciparum* susceptibility to artemisinin-based combination therapies. *Nat Commun*, 7, 11553.
- VEIGA, M. I., OSORIO, N. S., FERREIRA, P. E., FRANZEN, O., DAHLSTROM, S., LUM, J. K., NOSTEN, F. & GIL, J. P. 2014. Complex polymorphisms in the *Plasmodium falciparum* multidrug resistance protein 2 gene and its contribution to antimalarial response. *Antimicrob Agents Chemother*, 58, 7390-7.
- WALLIKER, D., QUAKYI, I. A., WELLEMS, T. E., MCCUTCHAN, T. F., SZARFMAN, A., LONDON, W. T., CORCORAN, L. M., BURKOT, T. R. & CARTER, R. 1987. Genetic analysis of the human malaria parasite *Plasmodium falciparum*. *Science*, 236, 1661-6.
- WANG, J., ZHANG, C. J., CHIA, W. N., LOH, C. C., LI, Z., LEE, Y. M., HE, Y., YUAN, L. X., LIM, T. K., LIU, M., LIEW, C. X., LEE, Y. Q., ZHANG, J., LU, N., LIM, C. T., HUA, Z. C., LIU, B., SHEN, H. M., TAN, K. S. & LIN, Q. 2015. Haem-activated promiscuous targeting of artemisinin in *Plasmodium falciparum*. *Nat Commun*, 6, 10111.
- WANG, X., MU, J., LI, G., CHEN, P., GUO, X., FU, L., CHEN, L., SU, X. & WELLEMS, T. E. 2005. Decreased prevalence of the *Plasmodium falciparum* chloroquine resistance transporter 76T marker associated with cessation of chloroquine use against *P. falciparum* malaria in Hainan, People's Republic of China. *Am J Trop Med Hyg*, 72, 410-4.
- WASSMER, S. C. & GRAU, G. E. 2017. Severe malaria: what's new on the pathogenesis front? *Int J Parasitol*, 47, 145-152.
- WASSMER, S. C., TAYLOR, T. E., RATHOD, P. K., MISHRA, S. K., MOHANTY, S., AREVALO-HERRERA, M., DURAISINGH, M. T. & SMITH, J. D. 2015.

Investigating the Pathogenesis of Severe Malaria: A Multidisciplinary and Cross-Geographical Approach. *Am J Trop Med Hyg*, 93, 42-56.

- WEATHERALL, D. J. & CLEGG, J. B. 2001. Inherited haemoglobin disorders: an increasing global health problem. *Bull World Health Organ*, 79, 704-12.
- WEISS, G. E., GILSON, P. R., TAECHALERTPAISARN, T., THAM, W. H., DE JONG, N. W., HARVEY, K. L., FOWKES, F. J., BARLOW, P. N., RAYNER, J. C., WRIGHT, G. J., COWMAN, A. F. & CRABB, B. S. 2015. Revealing the sequence and resulting cellular morphology of receptor-ligand interactions during *Plasmodium falciparum* invasion of erythrocytes. *PLoS Pathog*, 11, e1004670.
- WELLEMS, T. E. & HOWARD, R. J. 1986. Homologous genes encode two distinct histidine-rich proteins in a cloned isolate of *Plasmodium falciparum*. *Proc Natl Acad Sci U S A*, 83, 6065-9.
- WELLEMS, T. E. & HOWARD, R. J. 1995. *Recombinant DNA clone containing a genomic fragment of PfHRP-II gene from Plasmodium falciparum*. USA patent application. Dec. 19, 1995.
- WELLEMS, T. E. & PLOWE, C. V. 2001. Chloroquine-resistant malaria. *J Infect Dis*, 184, 770-6.
- WELLEMS, T. E., WALKER-JONAH, A. & PANTON, L. J. 1991. Genetic mapping of the chloroquine-resistance locus on *Plasmodium falciparum* chromosome 7. *Proc Natl Acad Sci U S A*, 88, 3382-6.
- WERNSDORFER, W. H. & PAYNE, D. 1991. The dynamics of drug resistance in *Plasmodium falciparum*. *Pharmacol Ther*, 50, 95-121.
- WHITE, N. J. 2004. Antimalarial drug resistance. *J Clin Invest*, 113, 1084-92.
- WHITE, N. J. 2008. Qinghaosu (artemisinin): the price of success. *Science*, 320, 330-4.
- WILLIAMS, J. L. 1999. Stimulation of *Plasmodium falciparum* gametocytogenesis by conditioned medium from parasite cultures. *Am J Trop Med Hyg*, 60, 7-13.
- WILSON, C. M., SERRANO, A. E., WASLEY, A., BOGENSCHUTZ, M. P., SHANKAR, A. H. & WIRTH, D. F. 1989. Amplification of a gene related to mammalian *mdr* genes in drug-resistant *Plasmodium falciparum*. *Science*, 244, 1184-6.
- WILSON, C. M., VOLKMAN, S. K., THAITHONG, S., MARTIN, R. K., KYLE, D. E., MILHOUS, W. K. & WIRTH, D. F. 1993. Amplification of *pfmdr 1* associated with mefloquine and halofantrine resistance in *Plasmodium falciparum* from Thailand. *Mol Biochem Parasitol*, 57, 151-60.
- WITKOWSKI, B., DURU, V., KHIM, N., ROSS, L. S., SAINTPIERRE, B., BEGHAIN, J., CHY, S., KIM, S., KE, S., KLOEUNG, N., EAM, R., KHEAN, C., KEN, M., LOCH, K., BOUILLON, A., DOMERGUE, A., MA, L., BOUCHIER, C., LEANG, R., HUY, R., NUEL, G., BARALE, J. C., LEGRAND, E., RINGWALD, P., FIDOCK, D. A., MERCEREAU-PUIJALON, O., ARIEY, F. & MENARD, D. 2017. A surrogate marker of piperazine-resistant *Plasmodium falciparum* malaria: a phenotype-genotype association study. *Lancet Infect Dis*, 17, 174-183.

- WITKOWSKI, B., KHIM, N., CHIM, P., KIM, S., KE, S., KLOEUNG, N., CHY, S., DUONG, S., LEANG, R., RINGWALD, P., DONDORP, A. M., TRIPURA, R., BENOIT-VICAL, F., BERRY, A., GORGETTE, O., ARIEY, F., BARALE, J. C., MERCEREAU-PUIJALON, O. & MENARD, D. 2013. Reduced artemisinin susceptibility of Plasmodium falciparum ring stages in western Cambodia. *Antimicrob Agents Chemother*, 57, 914-23.
- WOHLRAB, H. 2009. Transport proteins (carriers) of mitochondria. *IUBMB Life*, 61, 40-6.
- WONGSRICHANALAI, C. & MESHNICK, S. R. 2008. Declining artesunate-mefloquine efficacy against falciparum malaria on the Cambodia-Thailand border. *Emerg Infect Dis*, 14, 716-9.
- WOOTTON, J. C., FENG, X., FERDIG, M. T., COOPER, R. A., MU, J., BARUCH, D. I., MAGILL, A. J. & SU, X. Z. 2002. Genetic diversity and chloroquine selective sweeps in Plasmodium falciparum. *Nature*, 418, 320-3.
- WORLD HEALTH ORGANIZATION 2001. Antimalarial Drug Combination Therapy. Report of a WHO Technical Consultation.
- WORLD HEALTH ORGANIZATION 2015. Guidelines for the Treatment of Malaria. In: EDITION, R. (ed.) *Guidelines for the Treatment of Malaria*. Geneva.
- WORLD HEALTH ORGANIZATION 2017a. P. falciparum hrp2/3 gene deletions. Malaria Policy Advisory Committee Meeting (22–24 March 2017, background document for Session 7); (date accessed 21 July 2019).
- WORLD HEALTH ORGANIZATION 2017b. Status report on artemisinin and ACT resistance: artemisinin and artemisinin-based combination therapy resistance.
- WORLD HEALTH ORGANIZATION 2018. World Malaria Report 2018.
- WU, B., RAMBOW, J., BOCK, S., HOLM-BERTELSEN, J., WIECHERT, M., SOARES, A. B., SPIELMANN, T. & BEITZ, E. 2015. Identity of a Plasmodium lactate/H(+) symporter structurally unrelated to human transporters. *Nat Commun*, 6, 6284.
- WU, Y., SIFRI, C. D., LEI, H. H., SU, X. Z. & WELLEMS, T. E. 1995. Transfection of Plasmodium falciparum within human red blood cells. *Proc Natl Acad Sci U S A*, 92, 973-7.
- WUNDERLICH, J., ROHRBACH, P. & DALTON, J. P. 2012. The malaria digestive vacuole. *Front Biosci (Schol Ed)*, 4, 1424-48.
- WWARN 2019. K13 Genotype-Phenotype Study Group: Association of mutations in the Plasmodium falciparum Kelch13 gene (Pf3D7_1343700) with parasite clearance rates after artemisinin-based treatments-a WWARN individual patient data meta-analysis. *BMC Med*, 17, 1.
- YAYON, A., CABANTCHIK, Z. I. & GINSBURG, H. 1984. Identification of the acidic compartment of Plasmodium falciparum-infected human erythrocytes as the target of the antimalarial drug chloroquine. *EMBO J*, 3, 2695-700.